Pulmonary Arterial Hypertension: Role of miRNAs in Animal Models and Pathological Samples.

Paola Caruso MSc. (Hons)

Thesis submitted for the degree of Doctor of Philosophy to the University of Glasgow

Institute of Cardiovascular and Medical Sciences
College of Medical, Veterinary and Life Sciences
University of Glasgow

January 2012

Declaration

I declare that this thesis has been written entirely by myself and is a record of research performed by myself with the exception of *in situ* experiments, performed in collaboration with Dr. Ruifang Lu, si*BMP2 in vitro* experiment, conducted in collaboration with Dr. Paul D. Upton and evaluation of the percentage of remodelled vessels in miR-21 KO mice, performed by Dr. Yvonne Dempsie. No contents of this thesis have been previously submitted for a Higher Degree. All research was performed at the Institute of Cardiovascular and Medical Sciences, College of Medical, Veterinary and Life Sciences, University of Glasgow, under the supervision of Professor Andrew H Baker, Professor Margaret R. MacLean and Professor Nicholas W Morrell.

Paola Caruso

January 2012

Acknowledgments

First of all, I would like to thank my supervisors Prof. Andrew H. Baker, Prof. Margaret R. MacLean and Prof. Nicholas W. Morrell for their expertise and guidance during these years. I would also like to acknowledge British Heart Foundation for financial support of this project.

A big thank you to all the members of the Andrew Baker, Margaret MacLean and Nicholas Morrell research groups, I own you so much that I do not know who to start with. In particular, a special thank you to Dr. Robert McDonald and Dr. Laura Denby for sharing with me their experience and knowledge during my whole PhD and to Dr. Ruifang Lu for introducing me to northern blot and *in situ* hybridization. A huge thanks also to Dr. Ian Morecroft, Yvonne Dempsie, Kevin White and Margaret Nilsen for all your help, support and advice for the *in vivo* work and to Paul Upton, Lu Long, and Mark Southwood for the priceless help with the experiments involving the TGF-*beta* signaling and the analysis of the lung sections. Every other person working in these labs should be mentioned and thanked here for the help and kindness I received. I really hope one day I'll be able to give back at least a part of what I've received.

A special thank you to all the friends I met during this fantastic experience, starting with those amazing girls who have been so "lucky" to share the office with me during the "relaxing" moments of my writing up, Adyani Redzuan, Stacy Wood, Jennifer McLachlan and Helen Chick. Thanks for sharing with me the ups and downs, the laughs, the tears and all the "I'll never manage to finish this!!" moments. I already miss you so much!

Finally, I'm afraid part of this acknowledgement must be in Italian, being this a big part of what I am and also a big part of my experience in Glasgow. Voglio quindi ringraziare con tutto il cuore le persone fantastiche conosciute in questa città e diventate in breve tempo parte essenziale del mio quotidiano, Manù, Fabio, Ilenia, Laura, Antonio e Gianluca, per le risate, le liti furiose, i momenti pazzi e anche quelli

dolorosi, niente di quello che ho passato sarebbe stato lo stesso se non lo avessi condiviso con tutti voi, siamo una famiglia un po' strampalata forse, ma proprio per questo davvero speciale. Non voglio chiaramente escludere quegli amici che rappresentano il mio passato e le mie radici, il tempo mi ha provato che la distanza non può indebolire certi rapporti. Quindi Nadia, Ambra, Francesca, Romi, mi sento davvero onorata di avervi nella mia vita. Per concludere, un abbraccio e un ringraziamento immenso alla mia famiglia, per l'affetto e l'appoggio incondizionato. Se è vero che la famiglia è colei che ti cresce e ti protegge finchè non sei forte abbastanza da andarti a conquistare il tuo pezzetto di mondo credo che la missione non potesse essere compiuta in modo migliore.

Table of Contents

List of Figures

List of Tables

List of Publications

1. **Caruso P.**, Dempsie Y., Stevens H., McDonald RA., Long L., Lu R., White K., Mair K., Southwood M., Upton P., Xin M., Van Rooij E., Olson E., Morrell NW., MacLean MR. and Baker AH. A role for microRNA-145 in the development of pulmonary arterial hypertension: Evidence from mouse models and patient samples. Paper submitted to Circulation Research.

2. Cherubini G., Naim V., **Caruso P.**, Burla R., Bogliolo M., Cundari E., Benihoud K., Saggio I. and Rosselli F. The FANC pathway is activated by adenovirus infection and promotes viral replication-dependent recombination. Nucleic Acids Res. 2011 Mar 17

3. **Caruso P.**, MacLean MR., Khanin R., McClure J., Soon E., Southwood M., McDonald RA., Greig JA., Robertson KE., Masson R., Denby L., Dempsie Y., Long L., Morrell NW. and Baker AH. Dynamic changes in lung miRNA profiles during the development of pulmonary hypertension due to chronic hypoxia and monocrotaline. Arteriosclerosis, Thrombosis, and Vascular Biology, 2010 Apr; 30(4):716-23. Epub 2010 Jan 28.

4. **Caruso P.**, Burla R., Piersanti S., Cherubini G., Remoli C., Martina Y., Saggio I. Prion expression is activated by Adenovirus 5 infection and affects the adenoviral cycle in human cells. Virology. 2009 Mar 15; 385(2):343-50. Epub 2009 Jan 12.

Posters and Presentations

1. **Caruso P.**, Dempsie Y., Stevens H., McDonald RA., Long L., Lu R., White K., Mair K., Southwood M., Upton P., Xin M., Van Rooij E., Olson E., Morrell NW., MacLean MR. and Baker AH. A role for microRNA-145 in the development of pulmonary arterial hypertension: Evidence from mouse models and patient samples. ESC 2011 international conference, Paris, France.

2. **Caruso P**.,MacLean MR.,Khanin R.,McClure J.,Soon E.,Southwood M.,McDonald R., Robertson K.,Denby L.,Dempsie Y.,Long L., Morrell NW. and Baker AH. Dynamic changes in lung microRNA profiles during the development of pulmonary hypertension due to chronic hypoxia and monocrotaline. ATS 2010 international conference, New Orleans, LA, USA.

3. **Caruso P**., Burla R., Martina Y., Piersanti S., Remoli C., Saggio I. (September 2007) Adenovirus-induced activation of the human prion. FISV 2007, IX annual congress, Riva del Garda, Italy

4. Burla R., **Caruso P**., Piersanti S., Remoli C., Cundari E., Saggio I. (September 2007) Knock down of ATM and ATR induces p53 displacement from centrosomes in human primary cells. FISV 2007, IX annual congress, Riva del Garda, Italy

5. Cherubini G., Burla R., **Caruso P.**, Benihoud K., Cundari E., Saggio I. and Rosselli F. (October 8 - 11, 2007) Adenovirus: a new tool to understand the role of FANCD2 in replication. Nineteenth Annual Fanconi Anemia Scientific Symposium, Westin Michigan Avenue, Chicago, IL

6. Cherubini G., Burla R., **Caruso P**., Benihoud K., Cundari E., Saggio I. and Rosselli F. (October 4-5, 2007) Adenovirus induces FANCD2 activation to help viral replication. Early Steps of the Virus life Cycle: Molecular and Cellular Insights. Institut pasteur, Paris, France

Awards

1. ATS International Trainee Travel Award.

Definitions/Abbreviations

* strand	Passenger strand/non functional
3' UTR	3 prime untranslated region
ACE	Angiotension Converting Enzyme
ADARB1	Adenosine deaminase, RNA-specific, B1
AGO	Argonaute Protein
Alk1	Activin receptor-like kinase 1
Alk5	Activin receptor-like kinase 5
ANOVA	Analysis of variance
APES	3-amino-propyltriethoxysaline
ARE	AU-rich element
ATP	Adenosine triphosphate
AU	Arbitrary units
BMPR1A	Bone morphogenetic protein receptor 1A
BMPR1B	Bone morphogenetic protein receptor 1B
BMPR2	Bone morphogenetic protein receptor 2
BMPs	Bone morphogenetic proteins
bp	Base pairs
BSA	Bovine serum albumin
CCB	Calcium channel blocker
cDNA	Complementary deoxyribonucleic acid
cGMP	Cyclic guanosine monophosphate
CLL	Chronic lymphocytic leukemia
co-Smads	Common-mediator Smad
Ct	Cycle threshold
CTEPH	Chronic thromboembolic pulmonary hypertension
DCL1	Dicer-like protein 1
DEPC	Diethylpyrocarbonate
DGCR8	DiGeorge syndrome critical region 8
DIG	Digoxigenin
DMEM	Dulbeccos modified Eagle medium
DMSO	Dimethyl sulphoxide
DNA	Deoxyribonucleic acid
dNTPs	Deoxynucleoside triphosphates
dsRBD	Double-stranded RNA binding domain
dsRNA	Double-stranded RNA
DTT	Dithiotheitol
ECL	Chemiluminescence
EDTA	Ethylenediaminetetracetic acid
ET-1	Endothelin-1
ETA	Endothelin A receptor
ETB	Endothelin B receptor
Exp5	Exportin-5
FCS	Fetal calf serum
FDA	Food and Drug Administration
GAPDH	Glyceraldehyde 3-phosphate dehydrogenase
HEPES	4-(2-hydroxyethyl)-1-piperazineethanesulfonic acid

HIV	Human immunodeficiency virus
HP1A	Heterochromatin protein 1A
HPAECs	Human Pulmonary Artery Endothelial Cells
HPAFs	Human Pulmonary Artery Fibroblasts
HPAH	Heritable pulmonary arterial hypertension
HPASMCs	Human pulmonary artery smooth muscle cells
HR	Heart rate
HRP	Horseradish peroxidase
hsa	Homo sapiens
HYL1	HYPONASTIC LEAVES1
ID1	Inhibitor of DNA binding-1
IPAH	Idiopathic pulmonary arterial hypertension
I-Smads	Inhibitory Smads
KCNJ6	Potassium inwardly-rectifying channel, subfamily J, member 6
kDa	KiloDalton
KLF4	Kruppel-like factor 4
KLF5	Kruppel-like factor 5
KO	Knock-out
LNAs	Locked nucleotides
LV	Left ventricle
LV+S	Left ventricle plus septum
M	Molar
MCTP	monocrotaline pyrrole
MEF2	Myocyte enhancer factor-2
miRISC	miRNA-Induced silencing complex
miRNA	Micro ribonucleic acid (microRNA)
miRNPs	micro-ribonucleoproteins
mM	Milli molar
mmu	Mus musculus
mPAP	Mean pulmonary arterial pressure
mRNA	Messenger ribonucleic acid
mSAP	Mean systemic arterial pressure
Myocd	Myocardin
MyoD	Myogenic differentiation factor
NBF	neutral-buffered formalin
NCASP	Nuclear factor of activated T-cells 5
nM	Nanomolar (nanomoles per litre)
NO	Nitric oxide
nt	Nucleotide
NYHA	New York Heart Association
PA	Pulmonary artery
PABP	Poly A binding protein
PACT	Protein activator of PKR
PAECs	Pulmonary artery endothelial cells
PAFs	Pulmonary artery fibroblasts
PAH	Pulmonary arterial hypertension
PAI1	Plasminogen activator inhibitor type 1
PAP	Pulmonary artery pressure
Pasha	Partner of Drosha
PASMCs	Pulmonary artery smooth muscle cells

PAZ	Piwi-Argonaute-Zwille
P-bodies	Processing-bodies
PBS	Phosphate buffered saline
PCH	Pulmonary capillary hemangiomatosis
PCR	Polymerase Chain Reaction
PDCD4	Programmed cell death protein 4
PDE-5	Phosphodiesterase type 5
PDGF	Platelet derived growth factor
PFA	Paraformaldehyde
PGI2	Prostacyclin
piRISC	piRNA-induced silencing complex
piRNAs	PIWI-interacting RNAs
piwiRNA	P-element-induced wimpy testis RNA
PMSF	Phenylmethylsulfonylfluoride
pol-II	polymerase-II
pol-III	polymerase-III
PPAR-gamma	peroxisome proliferator-activated receptor gamma
PPHN	Persistent pulmonary hypertension of the newborn
PPP2R5E	Protein phosphatase 2, regulatory subunit B (B56), epsilon isoform
pre-miRNA/pre-miR	Preliminary miRNA
pri-miRNA/pri-miR	Primary miRNA
PTEN	Phosphatase and tensin homologue
PVOD	Pulmonary veno-occlusive disease
PVR	Pulmonary vascular resistance
Ran-GTP	RAs-related Nuclear protein-Guanosine-5'-triphosphate
RBPSUH	Recombining binding protein suppressor of hairless (Drosophila)
RdRP	RNA-dependent RNA polymerase
RHC	Right heart catheterization
RIIID	RNAse III domain
RISC	RNA induced silencing complex
RITS	RNA-induced transcriptional gene silencing
RNA	Ribonucleic acid
RNAi	RNA interference
rno	Rattus norvegicus
RNP	Ribonucleoprotein
ROC	Receptor operated calcium channel
ROCK	Rho-kinase
RPAFs	Rat pulmonary artery fibroblasts
RPASMCs	Rat pulmonary artery smooth muscle cells
rRNAs	Ribosomal RNAs
R-smads	Receptor-activated smads
RT	Room Temperature
RV	Right ventricle
RV/LV+S	Ratio of right ventricle to left ventricle plus septum
RVH	Right ventricular hypertrophy
RVP	Right ventricular pressure
SAP	Systemic arterial pressure
SDS	Sodium dodecyl sulphate
SDS-PAGE	Sodium dodecyl sulphate polyacrylamide gel electrophoresis

SEM	Standard error of the mean
SERT	Serotonin transporter
SERT+	Mice over-expressing SERT
SILAC	Stable isotope labelling with amino acids in cell culture
siRNA	Short Interfering ribonucleic acid
SLC6A4	Serotonin transporter gene
SMC	Smooth muscle cell
snoRNAs	Small nucleolar RNAs
snRNAs	Small nuclear RNAs
Spry1	sprouty homologue 1
SRF	Serum response factor
sRVP	Systolic right ventricular pressure
stRNAs	Short temporal RNAs
TACC1	Transforming, acidic coiled-coil containing protein 1
TBE	Tris/Borate/EDTA
TEs	Transposable elements
TGF-beta	Transforming growth factor beta
TGFBR1	Transforming growth factor, beta receptor 1
TGFBRAP1	Transforming growth factor, beta receptor associated protein 1
Tm	Melting temperature
TNRC6A	Trinucleotide repeat containing 6a
TPH1	Tryptophan hydroxylase 1
TRBP	TAR RNA-binding protein
tRNAs	Transfer RNAs
U	Unit
UTR	Untranslated Region
V	Volt
v/v	Volume/volume
VEGF	Vascular endothelial growth factor
VGCCs	Voltage-gated calcium channels
VSMC	Vascular smooth muscle cell
WT	Wild-type
YWHAZ	Tyrosine 3-monooxygenase/tryptophan 5-monooxygenase activation protein, zeta polypeptide
µM	Micromolar (micromoles per litre

Abstract

Pulmonary arterial hypertension (PAH) is a disease of the small pulmonary arteries (PAs), characterized by an increase in pulmonary arterial pressure and vascular remodelling leading to a progressive increase in pulmonary vascular resistance. The consequence of vascular obliteration is right heart failure and high mortality. Germline mutations in the gene coding for the bone morphogenetic protein (BMP) type-2 receptor (*BMPR2*), a receptor for the transforming growth factor (TGF)-beta super-family, have been identified in approximately 70% of patients with the heritable form of PAH (HPAH). Moreover, *BMPR2* expression is markedly reduced in PAH cases in the absence of mutations in this gene (idiopathic PAH, IPAH). In pulmonary artery smooth muscle cells (PASMCs) mutations in *BMPR2* are associated with an abnormal growth response to BMPs and TGF-*beta*. In endothelial cells (PAECs), these mutations increase the susceptibility of cells to apoptosis. The absence of *BMPR2* mutations in some families and in the majority of IPAH cases suggests that further pathological mechanisms still need to be identified. The serotonin system has also been implicated in both experimental and human PAH. In fact, an additional genetic risk factor for the development of this pathology has been identified in the serotonin transporter (SERT), dysregulated in IPAH patients. Mice over-expressing SERT (SERT+ mice) exhibit PAH and exaggerated hypoxia-induced PAH.

Although different advanced PAH therapies are currently available, they can only provide a symptomatic relief, and mortality rates remain high. Therefore, the identification of novel therapeutic approaches for the treatment of this pathology is urgently required.

MicroRNAs (miRNAs) are a class of small, endogenous and non-coding RNAs able to negatively regulate gene expression by targeting specific messenger RNAs (mRNAs) and inducing their degradation or translational repression. These non-coding sequences are transcribed from endogenous loci as long precursors, converted in single-stranded molecules of approximately 20 nucleotides after a series of enzymatic maturation steps. miRNAs carry out their activity in association with the RNA-induced silencing complex (RISC), interacting with the 3’ untranslated region (3’UTR) of specific

target mRNAs which they bind with imperfect complementarity. Several recent studies have assessed the direct role of miRNAs in vascular inflammation and in the development of cardiovascular pathologies. The aim of this project was to investigate the role of miRNAs in the development of PAH.

In Chapter 3, two distinct and well established rat models (hypoxic and monocrotaline) of PAH were used to determine the regulation of miRNAs during disease initiation and progression. We demonstrate time and insult-dependent changes in a specific group if miRNAs and this dysregulation was also confirmed *in vitro* in rat and human PA cells exposed to chronic hypoxia. Moreover, the stimulation of rat cells with TGF-*beta* and BMP4 mimicked the alteration of miRNA expression observed *in vivo*. An analysis of the expression level of the main enzymes involved in miRNA maturation (i.e. Dicer, Drosha, DGCR8 and Exp5) revealed the significant down-regulation of Dicer in response to chronic hypoxia both *in vivo* and *in vitro*, suggesting that the manipulation of this enzyme could re-establish a normal miRNA expression level in pathological samples. We also identified selective targets altered in response to miRNA dysregulation, suggesting the possibility of future interventional studies.

In Chapter 4 the specific role of miR-143 and miR-145 in the development of PAH was evaluated. We report the significant up-regulation of these miRNAs in WT mice exposed to chronic hypoxia and that genetic ablation of miR-145 is protective against the development of PAH (with no effects on miR-143 expression), assessed via measurement of systolic right ventricular pressure (sRVP), pulmonary vascular remodelling and right ventricular hypertrophy (RVH). miR-145 KO has also an effect on the expression of specific targets, including kruppel-like factor 4 and 5 (KLF4 and 5), which are regulators of smooth muscle proliferation and differentiation. Further, both miR-143 and miR-145 are up-regulated in mice heterozygous for a *BMPR2* mutation. In human tissues we confirm the elevated expression of the miR-143/145 cluster observed in hypoxic mice in pathological samples compared with unaffected controls, suggesting a conserved regulation of these miRNAs in the two species. The study described in this chapter is the first to report a critical role for miR-145 in the development of PAH *in vivo*.

Finally, in Chapter 5 a preliminary study focused on miR-21 regulation and function on PAH development is shown. An analysis of the expression of this miRNA in WT mice revealed its up-regulation in response to chronic hypoxia, whereas the genetic ablation of miR-21 induced an exaggerated hypoxia-induced PAH phenotype. However, the analysis of human pathological samples showed a reduced expression of this miRNA in comparison with unaffected controls, suggesting its differential regulation in hypoxic mice and patients, although the differences observed between the animal and the human pathology could be the cause of this different phenothipe. The identification of dysregulated targets in both the species will give more informations about the effect of miR-21 alteration in the development of PAH.

In summary, the results presented in this thesis support a role for defined miRNAs in the development of PAH, both in animal models and patients. Whether this specific alteration of selective miRNAs can be used as a novel therapeutical approach still need to be evaluated, but represent an attractive possibility to assess in the longer term.

1. Introduction

1.1 The Pulmonary Circulation

1.1.1 General Structure and Organization of the Circulatory System

The pulmonary circulation comprises the passage of blood from the heart to the lung, and back to the heart again. In particular, the right atrium of the heart receives through the superior (upper) and inferior (lower) vena cava all the blood de-oxygenated during its transit in the systemic circulation. This blood reaches then the right ventricle and is pumped into the pulmonary artery, travelling through the lungs. The pulmonary artery is the only artery of the body that carries deoxygenated blood, and it begins at the anterior base of the right ventricle. It then bifurcates into two branches, the right and the left pulmonary arteries, which deliver the de-oxygenated blood to the lungs, located in two cavities on either side of the heart. The right and the left lung are both divided into lobes by interlobular fissures. In particular, the left lung is characterized by a superior and inferior lobe, both supplied with a branch of the left pulmonary artery, whereas the right lung is divided into three lobes, superior, middle and inferior, all supplied with a branch of the right pulmonary artery. The main function of the pulmonary circulation is to deliver the whole cardiac output to the anatomic sites of gas exchange, located at the level of the terminal alveoli, named terminal respiratory units or acini (Murray 2010). The large surface area within the alveolar region guarantees an efficient oxygenation of the blood, which leaves the lungs and returns to the left atrium of the heart through pulmonary veins, to be then distributed to the body through the systemic circulation. Most branches of the pulmonary artery lie side by side with branches of the bronchial tree, whereas pulmonary veins are isolated structures which normally lie distant from pulmonary arteries and bronchi (Murray 2010).

All the branches originated from the main pulmonary artery can be numerically categorized using the diameter-defined Strahler ordering system (Jiang, Kassab et al. 1994; Huang, Yen et al. 1996). This system defines as “order 1” vessels the most peripheral pulmonary arteries and the order number of the confluent vessel is

increased by 1 when two vessels of the same order meet, until the main pulmonary artery is reached. 15 different orders have been identified in this way, and specific characteristics can be assigned to different groups of orders. For example, large proximal pulmonary arteries (orders 15-13), which lie next to cartilage-containing bronchi, are characterized by an elastic wall, whereas the more distal peripheral pulmonary arteries (orders 13-4) have muscular walls, as a consequence of increased smooth muscle and decreased elastic laminae in the tunica media. It is important to note that these orders of arteries can be defined muscular in comparison with the main branches of the pulmonary artery, and therefore within the pulmonary circulation, but appear substantially less muscularized than their counterparts in the systemic circulation. This layer of smooth muscle cells is decreased even further in the precapillary arteries (orders 4-1), mainly composed of a thin endothelial cell layer to facilitate gas exchange (Hislop and Reid 1978; Murray 2010).

Pulmonary arterial walls are composed of three different layers or “tunics”, named intima, media and adventitia. Distinct cell types can be identified in each tunic. The tunica intima represents the innermost layer of a pulmonary artery, and it is composed by a single layer of pulmonary artery endothelial cells (PAECs). Being directly in contact with the blood flow, PAECs undoubtedly exert a relevant modulating influence on the response of the pulmonary circulation to different stimuli via the release of several mediators, including nitric oxide (NO), endothelin-1 (ET-1) and prostacyclin (Aaronson, Robertson et al. 2002). The tunica media is the middle coat of an artery and is made up of smooth muscle cells and elastic tissue. Multiple phenotypically distinct smooth muscle cell populations have been identified in this layer (Frid, Moiseeva et al. 1994). Pulmonary artery smooth muscle cells (PASMCs) are able to produce a contractile response when stimulated, and they can therefore regulate arterial tone and blood pressure. The tunica adventitia represents the last and outermost layer of a pulmonary blood vessel, and it is mainly composed of pulmonary artery fibroblasts (PAFs). An increasing volume of studies indicates that this layer is a critical regulator of vessel wall function in health and disease. In fact, in response to environmental stresses such as hypoxia, PAFs are characterized by a variety of functional changes, including cell proliferation and secretion of factors able to influence vascular tone and wall structure (Stenmark, Fagan et al. 2006).

1.1.2 Main Functions of the Pulmonary Circulation

As already mentioned, the main and most essential function of the pulmonary circulation is to determine the re-oxygenation of the poorly oxygenated blood deriving from the systemic circulation. The pulmonary artery begins as a single trunk at the anterior base of the right heart, but then it divides into a right and a left branch which in turn originate thousands of arterioles, and finally hundreds of millions of alveolar capillaries. The volume of blood which can go across these capillaries at one time is only about 75 ml, but the total surface area of the capillaries is 70 m^2. Also the alveolar area has a similar surface available for gas exchange (Comroe 1966). However, several additional functions can be assigned to the pulmonary circulation. First of all, it accomplishes the important function of retaining fine particles present in mixed venous blood, preventing these from entering the systemic circulation (Comroe 1966). It also acts as a physical barrier against those thrombi which are formed in the systemic venous circulation, again preventing their passage to the systemic circulation. In fact, there are many more pulmonary capillaries than are needed for effective gas exchange in resting man and some of these can be sacrificed to protect the rest of the circulation from occlusions which may induce an infarction (Comroe 1966). Moreover, pulmonary vessels, normally containing about 600 ml of blood, represents an important reservoir that can supply blood to fill the heart and maintain a normal output after a trauma (Comroe 1966).

1.1.3 Pulmonary Vascular Resistance and Blood Flow

Vascular resistance is defined as the resistance to flow that must be overcome to push blood across the circulatory system. In particular, a systemic and a pulmonary vascular resistance (SVR and PVR respectively) can be identified. During fetal life, oxygenation of the blood occurs mainly via the placenta, and only 8-10% of the total cardiac output flows through the pulmonary circulation, characterized by an high PVR to divert away blood from the lungs (Hislop and Pierce 2000). This is due to the relatively small lumen and thick muscle walls of the pulmonary arteries observed at this stage. However, immediately after birth, when exposure to atmospheric oxygen fully dilates the pulmonary circulation, a decrease in wall thickness occurs, with a consequent drop in

PVR, and 100% of the cardiac output can flow across the lungs. In the adult, the pulmonary circulation can be therefore considered a high-flow, but low-resistance and low-pressure system in comparison with the systemic circulation. In fact, the mean pulmonary arterial pressure (mPAP) is substantially lower than the corresponding mean systemic arterial pressure (mSAP), being the first around 15 mmHg and the second 93 mmHg (Morgan, Lauri et al. 2004). Considering that small changes in the diameter of a blood vessel can significantly affect blood flow and PVR, it is not surprising that uncontrolled cell growth and vascular remodelling are the main cause of the sustained increased in PAP observed in several cardiovascular pathologies.

1.1.4 Passive and Active Regulation and Distribution of the Blood Flow

The lung of a normal healthy person can be divided into three zones characterized by a different blood flow, determined by different relative values of pulmonary arterial (P_a), pulmonary venous (P_v) and alveolar (P_A) pressure. A passive uneven blood flow distribution can therefore be identified in the pulmonary circulation, gravity-dependent and influenced by the site-entry of the pulmonary arteries in the lung, localized in the mid-portion of the organ. In particular, zone 1 identifies the upper portion of the lung, where the blood flow is extremely low since P_A is greater than both P_v and P_a ($P_A > P_a > P_v$), with a consequent collapse of the vasculature (Figure 1-1). In zone 2, localized in the medium part of the lung, P_a is the greatest among the three pressures, but P_A still exceeds P_v ($P_a > P_A > P_v$) (Figure 1-1). The blood flow is therefore higher, but still not at its maximum level, although modest increases in arterial pressure can determine the recruitment of more vessels into the pulmonary circulation. The lowest part of the lung is identified as zone 3, where both P_a and P_v are higher than P_A ($P_a > P_v > P_A$), determining a constant distention of the vessels and a high blood flow (Hughes 1975) (Figure 1-1).

Pulmonary arterial pressure is also deeply influenced by an active regulation of the blood flow. In fact, several factors, including sympathetic nerves, humoral mechanisms and respiratory gases can act on the PASMC contraction, determining in this way changes on the PVR (Barnes and Liu 1995).

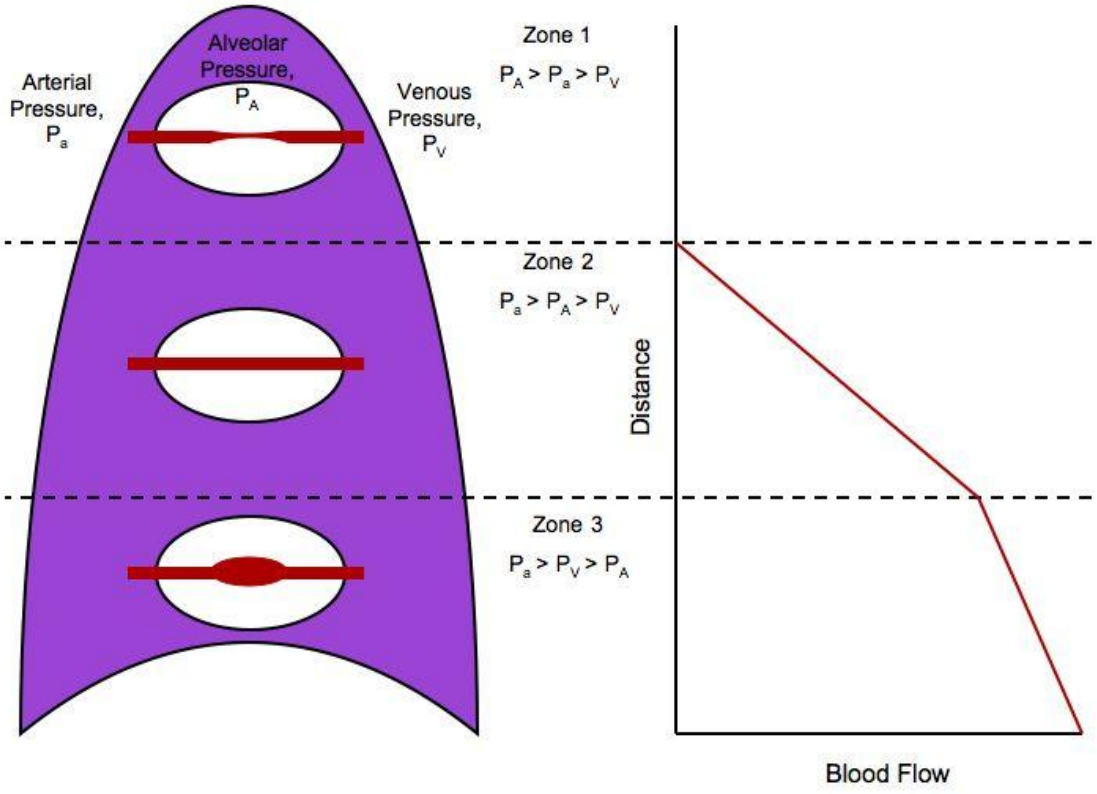

Figure 1-1 Passive, gravity-dependent blood flow distribution through the lung. The lung of an healthy adult can be divided in three different zones, characterized by different relative values of pulmonary arterial pressure (Pa), pulmonary venous pressure (Pv) and alveolar pressure (PA), resulting in a different blood flow. Reported from University of Michigan Medical School,
http://creativecommons.org/licenses/by/3.0/deed.en

1.1.5 Hypoxic Pulmonary Vasoconstriction

Hypoxic pulmonary vasoconstriction (HPV) is an adaptive response to alveolar hypoxia that consent the redistribution of blood from poorly oxygenated areas to better ventilated lung segments by an active process of vasoconstriction. This process determines a more efficient blood re-oxygenation, and involves mainly the small resistance arteries (McCulloch, Kempsill et al. 2000). HPV is an intrinsic mechanism of the pulmonary vasculature, since the vasodilator effect of hypoxia on the systemic vasculature has been previously reported (Gregor and Janig 1977). PASMCs have been identified as the cell type responsible for monitoring the O_2 concentration in the vasculature, since HPV occurs in presence or in absence of the endothelium (Marshall and Marshall 1992), although different studies reported a prolonged contractile response of PASMCs in response to hypoxia only in presence of a functional endothelium (Holden and McCall 1984; Archer, Wu et al. 2004). It is well accepted that an elevation of the internal Ca^{2+} concentration in these cells is an early and critical element leading to HPV. However, the mechanism and the vasoactive mediators responsible for this process are still under investigation. The best documented hypothesis suggests that hypoxia could induce the inhibition of voltage-gated K^+ channels (Kv channels), causing the depolarization of the PASMC membrane and the consequent Ca^{2+} entry via voltage-dependent L-type channels (McMurtry, Davidson et al. 1976). According with this theory, Kv channel inhibition would be determined by a decrease in the intracellular concentration of H_2O_2, due to a reduction in mitochondrial electron transport induced by the lack of O_2. Considering the main role of mitochondria in O_2 consumption and energy generation, they would represent an ideal candidate for O_2 sensing, and several studies have supported this hypothesis (Mauban, Remillard et al. 2005; Moudgil, Michelakis et al. 2005), although others have reported an hypoxia-mediated increase of the levels of H_2O_2 and other reactive oxygen species (ROS) in HPV, suggesting the existence of an alternative mechanism that still needs to be investigated (Waypa and Schumacker 2005).

1.2 Pulmonary Arterial Hypertension

1.2.1 Clinical Presentation and Classification

Pulmonary arterial hypertension (PAH) is a disease of the small pulmonary arteries (PAs), characterized by vasoconstriction and vascular remodeling leading to a progressive increase in pulmonary vascular resistance (PVR), resulting in right ventricular hypertrophy and dilatation (Rich, Dantzker et al. 1987; Gaine and Rubin 1998). The consequence of vascular obliteration is right heart failure and high mortality (Eddahibi, Morrell et al. 2002; Jeffery and Morrell 2002). PAH is normally diagnosed if mean pulmonary arterial pressure (mPAP) is higher than 25 mm Hg at rest. It is a rare disease that affects approximately two or three individuals per million per year.

Transthoracic echocardiogram is usually the first diagnostic test performed in case of suspected PAH. This test can give an evaluation of the systolic right ventricular pressure (sRVP), right chamber dimension and RV function. The diagnosis is then normally confirmed with the measurement of the pulmonary haemodynamics and cardiac output, obtained through right heart catheterization (RHC). An early diagnosis of PAH is very important since prognosis without treatment is poor, with a median survival time of 2.8 years (D'Alonzo, Barst et al. 1991). However, the symptoms of this disease, including shortness of breath, fatigue and syncope, are often non-specific in the early stages of this disease, and may be attributed to stress or anxiety. For this reason, diagnosis can be often delayed. For a correct identification of this condition, particular attention should be given to previous medical conditions, drug use and family history. According to the last National Pulmonary Hypertension Audit Report, the mean age of the diagnosed patients is 56 years and the ratio of females to males is 1.9:1 (NCASP, First Annual Report of the National Audit of Pulmonary Hypertension 2010). After diagnosis, the clinical severity of PAH can be classified using the New York Heart Association (NYHA) classification for heart failure symptoms, characterized by 4 functional classes based on the patient's ability to function. In particular, class I patients are still asymptomatic and in an early stage of the disease, while class IV patients are substantially limited in their physical activity (Nauser and Stites 2001)

(Table 1-1). This classification is very important for the identification of the best available treatment for the patient. Another useful marker of disease severity includes the 6-minute walk test, used to undertake a functional assessment of exercise capacity. In particular, this test can reveal decreased exercise tolerance in PAH patients (Miyamoto, Nagaya et al. 2000). Clinical manifestations of the disease are fairly consistent among PAH patients, regardless of its etiology (Simonneau, Galie et al. 2004; Voelkel and Cool 2004). In particular, HPAH and IPAH have a similar clinical course and a survival rate although recent reports suggest that HPAH has an earlier onset and more severe hemodynamic impairment at diagnosis (Sztrymf, Coulet et al. 2008).

The first classification of PAH, based on the pathophysiological mechanisms and the therapeutic options available at the time, was proposed in 1973 by the World Health Organization. Since then, there have been a series of modifications to reflect the new findings in the last few years. According to the latest classification, formulated during the 4th World Symposium on PAH held in 2008 in Dana Point, California, PAH can be subcategorized into i) idiopathic (IPAH), when the disease is sporadic and cannot be correlated with a family history or with an identified risk factor, ii) heritable (HPAH), when it occurs in a familial context and/or it is associated with a germline mutation, iii) drug- and toxin-induced, iv) associated with a known risk factor, including a congenital heart disease or HIV infection, and finally v) persistent pulmonary hypertension of the newborn (PPHN) (Rosenkranz and Erdmann 2008; Simonneau, Robbins et al. 2009). This classification also includes other forms of PH, subcategorized into pulmonary veno-occlusive disease (PVOD) and/or pulmonary capillary hemangiomatosis (PCH), pulmonary hypertension owing to left heart disease, pulmonary hypertension owing to lung disease and/or hypoxia and chronic thromboembolic pulmonary hypertension (CTEPH) (Table 1-2) (Rosenkranz and Erdmann 2008; Simonneau, Robbins et al. 2009).

Functional Assessment of Patients with Pulmonary Hypertension	
Class I	Patients with pulmonary hypertension but without resulting limitation of physical activity. Ordinary physical activity does not cause undue dyspnea or fatigue, chest pain or near syncope.
Class II	Patients with pulmonary hypertension resulting in slight limitation of physical activity. These patients are comfortable at rest, but ordinary physical activity causes undue dyspnea or fatigue, chest pain or near syncope.
Class III	Patients with pulmonary hypertension resulting in marked limitation of physical activity. These patients are comfortable at rest, but less than ordinary physical activity causes undue dyspnea or fatigue, chest pain or near syncope.
Class IV	Patients with pulmonary hypertension resulting in inability to perform any physical activity without symptoms. These patients manifest signs of right heart failure. Dyspnea and/or fatigue may be present at rest, and discomfort is increased by any physical activity.

Table 1-1 New York Heart Association (NYHA) classification of functional status in patients with pulmonary hypertension.

Updated Clinical Classification of Pulmonary Hypertension (Dana Point, 2008)
1. Pulmonary arterial hypertension (PAH)
1.1. Idiopathic PAH
1.2. Heritable
1.2.1. BMPR2
1.2.2. ALK1, endoglin (with or without hereditary hemorrhagic telangiectasia)
1.2.3. Unknown
1.3. Drug- and toxin-induced
1.4. Associated with
1.4.1. Connective tissue diseases
1.4.2. HIV infection
1.4.3. Portal hypertension
1.4.4. Congenital heart diseases
1.4.5. Schistosomiasis
1.4.6. Chronic hemolytic anemia
1.5 Persistent pulmonary hypertension of the newborn
1'. Pulmonary veno-occlusive disease (PVOD) and/or pulmonary capillary hemangiomatosis (PCH)
2. Pulmonary hypertension owing to left heart disease
2.1. Systolic dysfunction
2.2. Diastolic dysfunction
2.3. Valvular disease
3. Pulmonary hypertension owing to lung diseases and/or hypoxia
3.1. Chronic obstructive pulmonary disease
3.2. Interstitial lung disease
3.3. Other pulmonary diseases with mixed restrictive and obstructive pattern
3.4. Sleep-disordered breathing
3.5. Alveolar hypoventilation disorders
3.6. Chronic exposure to high altitude
3.7. Developmental abnormalities
4. Chronic thromboembolic pulmonary hypertension (CTEPH)
5. Pulmonary hypertension with unclear multifactorial mechanisms
5.1. Hematologic disorders: myeloproliferative disorders, splenectomy
5.2. Systemic disorders: sarcoidosis, pulmonary Langerhans cell histiocytosis: lymphangioleiomyomatosis, neurofibromatosis, vasculitis
5.3. Metabolic disorders: glycogen storage disease, Gaucher disease, thyroid disorders
5.4. Others: tumoral obstruction, fibrosing mediastinitis, chronic renal failure on dialysis

Table 1-2 Current WHO clinical classification of pulmonary hypertension, Dana Point 2008. *BMPR2*, bone morphogenetic protein receptor type 2; ALK1, activin receptor like kinase-1, HIV, human immunodeficiency virus.

1.2.2 PAH Pathobiology

PAH is characterized by structural alterations of the small, peripheral arteries of the lung (Figure 1-2). A marked increase in vasocostriction is considered an important initiating factor responsible for the development of PAH, mainly due to endothelial cell dysfunction. In fact, in healthy subjects one of the main functions of the pulmonary endothelium is the maintenance of a low and stable PVR through a balance between vasodilator (mainly prostacyclin and nitric oxide (NO)) and vasoconstrictor (including endothelin-1 and serotonin) release. In contrast, it has been shown that in PAH patients, endothelial cells lose their capacity to preserve the normal vascular tone and start to produce more vasoconstrictors and less vasodilator/antiproliferative mediators, thereby shifting this balance, resulting in an elevation of PVR (Giaid and Saleh 1995; Tuder, Cool et al. 1999; Eddahibi, Humbert et al. 2001; Davies and Morrell 2008). The second step of the disease is characterized by an abnormal proliferation of pulmonary artery fibroblasts (PAFs), pulmonary artery smooth muscle cells (PASMCs) and pulmonary artery endothelial cells (PAECs) leading to vascular remodelling, considered the hallmark of PAH (Hassoun, Mouthon et al. 2009). A direct consequence of vascular remodelling is the narrowing and eventually the obliteration of the vessel lumen, leading to a further increase in PVR (Humbert, Morrell et al. 2004; Tuder, Abman et al. 2009). If this persists, the increased workload of the heart causes a compensatory hypertrophy of the right ventricle (RVH), and eventually right ventricular failure. The latter is the main cause of mortality in PAH patients (Guglin and Khan 2010).

Although vascular remodelling is characterized by an increased level of cell proliferation, PAECs apoptosis has been observed in early stages of the process. This temporary reduction in EC number may stimulate PASMCs through their exposure to circulating mitogenic factors (Sakao, Tatsumi et al. 2009). Moreover, enhanced apoptosis of PAECs may create the conditions for the selection of apoptosis-resistant cells with increased growth potential. This hypothesis is consistent with the observation that few apoptotic cells have been identified in the remodeled vessels of patients with severe PAH (Ameshima, Golpon et al. 2003). Also, Masri et al. reported that PAECs isolated from IPAH patients exhibit a hyper-proliferative potential, with

decreased susceptibility to apoptosis (Masri, Xu et al. 2007). Since bone morphogenetic proteins (BMPs, section 1.2.4.1) can reduce *in vitro* apoptosis of PAECs (Hirose, Hosoda et al. 2000), the impaired BMP signaling due to mutations in the *BMPR2* gene, observed in 80% of cases of HPAH (section 1.2.4.1), could explain this initial cell apoptosis (Sakao, Tatsumi et al. 2009). As already mentioned, dysfunction of PAECs can directly alter the balance between proliferation and apoptosis in PASMCs, since several vasoconstrictive agents, vasodilators and growth factors produced by PAECs, which act upon PASMCs proliferation and differentiation in healthy conditions, are dysregulated in PAH patients (Davies and Morrell 2008). Also, PASMCs isolated from PAH patients express decreased expression and function of potassium ion channels, inducing membrane depolarization and a subsequent cytosolic intake of calcium. This can not only further enhances vasoconstriction, but stimulates PASMCs migration and proliferation (Yuan, Aldinger et al. 1998; Mandegar and Yuan 2002; Pozeg, Michelakis et al. 2003). As a result, smooth muscle hyperplasia and thickening is typically observed in mild class II-III PAH vessels (Rubin 1999; Sakao, Tatsumi et al. 2009). In particular, one of the main histopathological features common to all forms of PAH is the accumulation of cells expressing smooth muscle specific alpha-actin (SMA) in peripheral pulmonary arteries (Figure 1-3). This includes the appearance of SMA-positive cells in the neointima, characterized by the presence of a conspicuous extracellular matrix, and the extension of SMA-positive cells into precapillary pulmonary arterioles that are normally devoid of smooth muscle (Mandegar, Fung et al. 2004). Also numerous macrophages can be identified within intimal lesions (Atkinson, Stewart et al. 2002). The cellular processes responsible for the muscularization of this distal part of the PA are not clear, but these observations suggest a central role for PASMCs in the development of PAH.

Plexiform lesions represent an extreme example of vascular remodelling and can be usually observed in severe PAH patients. These lesions can normally develop just distal to bifurcation sites of small pulmonary arteries (≈ 50-300 μm) predominantly as a result of PAECs hyper-proliferation, and cause the obliteration of the arterial lumen (Tuder, Groves et al. 1994) (Figure 1-3). This abnormal and uncontrolled growth of endothelial cells can be considered a neoplastic-like event. In 2003 Ameshima and colleagues reported the decreased expression of the peroxisome proliferator-activated

receptor (PPAR)-gamma, a tumor suppressor gene, in the plexiform lesions of patients with severe PAH (Ameshima, Golpon et al. 2003). PPAR-gamma has anti-proliferative, pro-apoptotic and anti-inflammatory functions, and it has been reported to inhibit angiogenesis (Chinetti, Griglio et al. 1998; Jiang, Ting et al. 1998; Tsubouchi, Sano et al. 2000). Inflammatory cells (including T-, B-lymphocytes and macrophages) have been identified in the surrounding area of plexiform lesions (Humbert, Morrell et al. 2004; Hassoun, Mouthon et al. 2009; Pullamsetti, Savai et al. 2011).

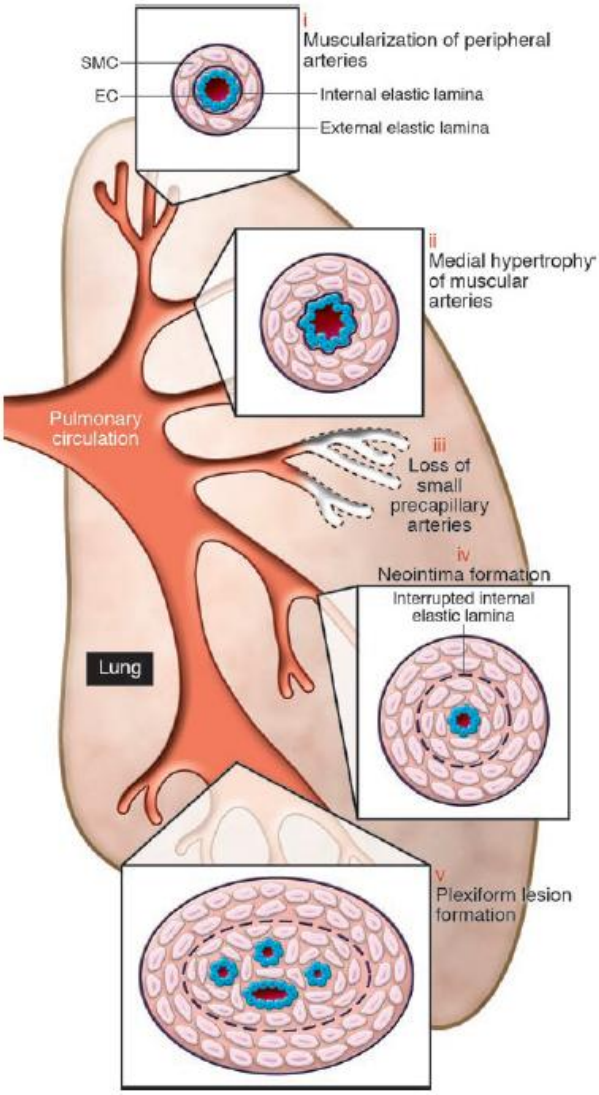

Figure 1-2 Pathobiology of PAH. The cartoon illustrates the structural alterations associated with PAH in comparison with normal pulmonary circulation. They include: (i) abnormal muscularization of distal precapillary arteries, (ii) medial thickening of large pulmonary muscular arteries, (iii) loss of precapillary arteries, (iv) neointimal formation and (v) formation of plexiform lesions in these vessels. Reported from (Rabinovitch 2008).

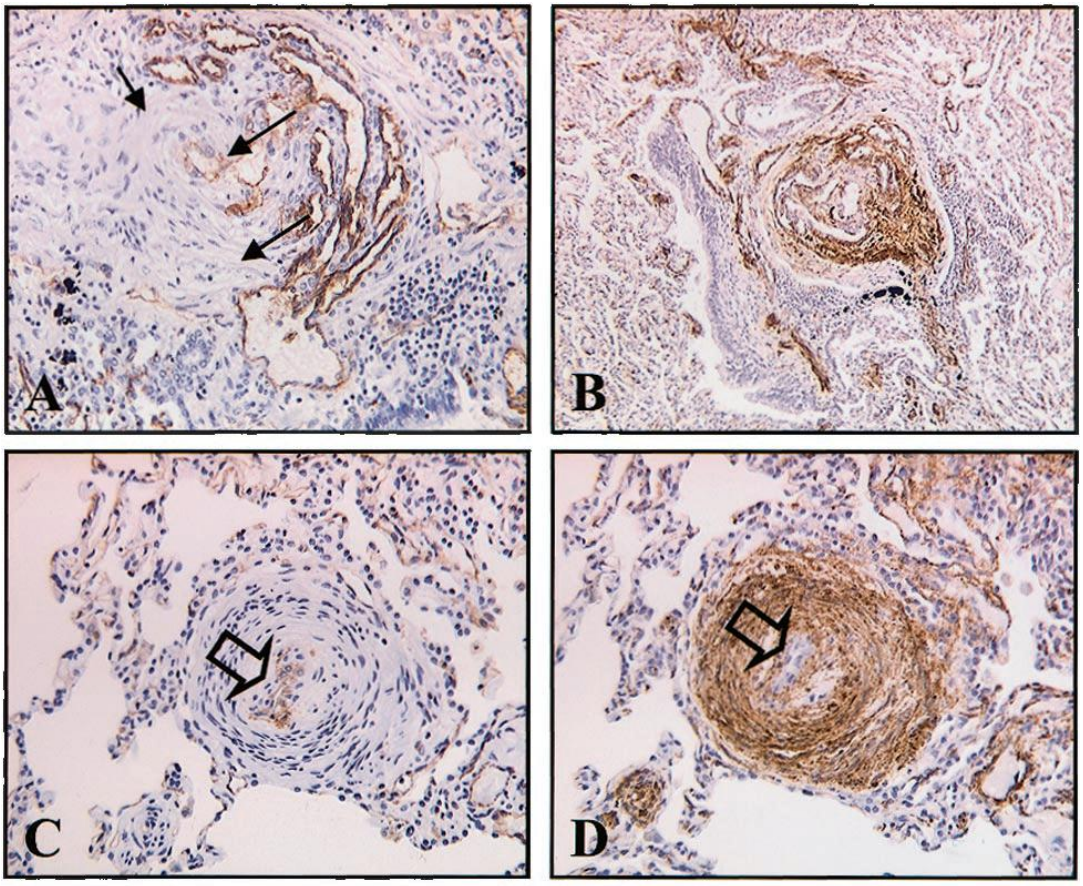

Figure 1-3 Histopathological changes associated with human PAH. Positive immunostaining of endothelial marker CD31 is identified in plexiform lesions (A), whereas supporting stroma is positive for alpha-smooth muscle actin (alpha-SMA) (B). In concentric intimal lesions, a single layer of PAECs is detected adjacent to vascular lumen (C, arrow) while concentric layers of PASMCs are identified in the vascular wall (D). Adapted from (Atkinson, Stewart et al. 2002).

1.2.3 PAH Animal Models

Numerous animal models for the study of PAH are currently available. In particular, the chronic hypoxic and the monocrotaline injury model have been abundantly used in the last decade for the investigation of the PAH pathobiology. However, different models have been also introduced in the last years.

1.2.3.1 Chronic Hypoxic Animals

Hypobaric hypoxia is often used to induce PAH in a wide variety of animal species. This model is very reproducible, although differences can be observed between different species and strains (Figure 1-4). Rats and mice are the species most commonly exposed to chronic hypoxia to conduct PAH studies. In rats, 2 weeks of hypoxia can induce a moderate PAH characterized by a doubling of mRVP and a significant RVH, with a rare right ventricle failure. In particular, the muscularization of the small, non-muscular arteries of the pulmonary vasculature is observed relatively rapidly, followed by their increased medial and adventitial thickening (Meyrick and Perkett 1989). It has also been reported that sustained hypoxia can induce a pulmonary artery-specific inflammatory response (Burke, Frid et al. 2009). In mice, the vascular remodelling induced by the exposure to chronic hypoxia is minimal and less evident than in rats, but it is possible to observe the muscularization of the non-muscular vessels and a poor medial thickening (Firth, Mandel et al. 2010) (Figure 1-4). Adventitial thickening and fibrosis of proximal pulmonary arteries has also been reported (Estrada and Chesler 2009). However, both in mice and rats, the disease is reversible when normoxia is restored.

1.2.3.2 Monocrotaline-Induced PAH

The pneumotoxic alkaloid monocrotaline can be used to generate an animal model of PAH. Its capacity to induce the progressive development of PAH after ingestion in several animal species was reported more than 40 years ago (Kay, Harris et al. 1967). In particular, this toxin must be activated in the liver by specific oxidases to form the monocrotaline pyrrole (MCTP), able to induce PAH. A single subcutaneous or

intraperitoneal injection can induce, by an unknown mechanism, pulmonary vascular remodelling, RVH and elevated mPAP over a period of one to two weeks (Hessel, Steendijk et al. 2006). The accumulation of mononuclear inflammatory cells in the adventitia of the small intra-acinar vessels has also been reported (Wilson, Segall et al. 1989). This treatment is most commonly used in rats, whereas in mice a monocrotaline-induced PAH can be observed only after the injection of the active MCTP, since the precursor is not metabolized in the liver. However, injection of active MCTP is highly variable and rarely used (Dumitrascu, Koebrich et al. 2008). The ingestion of monocrotaline can also induce liver and kidney damage (Roth, Dotzlaf et al. 1981). Monocrotaline injury is severe but not irreversible. In fact, the disease can be prevented and in some case treated with several agents (Cowan, Heilbut et al. 2000; Baber, Deng et al. 2007; Csiszar, Labinskyy et al. 2009; Hsu, Ko et al. 2009). In particular, it is interesting to note that some agents implicated in the development of PAH in humans can attenuate or treat the disease in the monocrotaline model, including dexfenfluramine (Mitani, Mutlu et al. 2002).

Since hypoxic and monocrotaline-injected animals do not represent a perfect model for PAH, several alternatives have been considered in recent years. In consideration of the association between mutations in the *BMPR2* gene and this disease (Section 1.2.4.1), PAH development in heterozygous mice (*BMPR2*+/-) has been evaluated. Long et al. studied 8 weeks old *BMPR2*+/- animals and observed a normal mPAP at rest. An additional factor such has serotonin was required to observe a significant increase in mPAP (Long, MacLean et al. 2006). However, West et al. recently reported that 9 weeks old mice over-expressing a truncating mutation in the *BMPR2* gene tail domain (R899X) developed elevated right ventricular systolic pressures (RVSP), associated with extensive pruning, muscularization of small pulmonary vessels, and development of large structural pulmonary vascular changes, approximately one-third of the time in normoxic conditions (West, Harral et al. 2008). Since *BMPR2* homozygous KO is lethal in mice, a conditional KO could represent in the future an interesting option to evaluate.

Based on the concept that vascular endothelial growth factor (VEGF) has a crucial role in endothelial cell differentiation, researchers assessed the effect of the inhibition of VEGF signaling in animals exposed to chronic hypoxia. They observed that the VEGF

receptor inhibitor Sugen 5416 could induce severe and irreversible PAH in chronic hypoxic rats. In particular several pieces of evidence showed not only the persistence, but also a further progression of the disease even after the removal of the hypoxic stimulus (Taraseviciene-Stewart, Kasahara et al. 2001). These mice present occlusive neointimal lesions, elevated mPAP and vascular smooth muscle/endothelial cells hyperproliferation, and represent for this reason a new interesting option for the investigation of PAH (Figure 1-5).

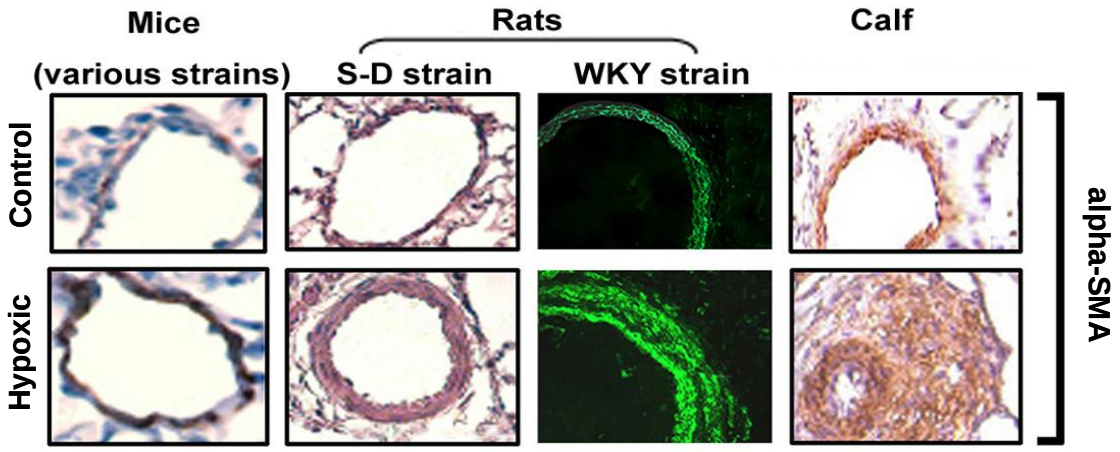

Figure 1-4 Effect of hypoxia on the pulmonary vasculature of mice, rats and calf. Hypoxia-induced vascular remodelling varies significantly among species, with minimal changes in mice and marked changes in neonatal calves. Adapted from (Stenmark, Meyrick et al. 2009).

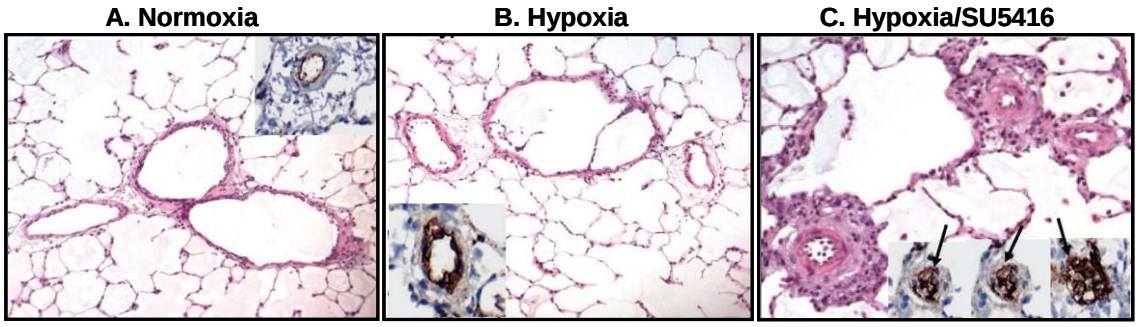

Figure 1-5 Occlusive neointimal lesions in rats treated with Sugen 5416 and chronic hypoxia. Compared with normoxic rats (A), rats exposed to hypoxia alone display only mild lung vascular remodelling (B). In contrast, hypoxia/SU-5416-exposed rats show marked vascular remodelling with medial wall thickening and endothelial cell hyper-proliferation (C, inserts). Adapted from (Stenmark, Meyrick et al. 2009).

1.2.4 Genetic Basis of Pulmonary Arterial Hypertension

1.2.4.1 TGF-beta Super-Family and BMPR2 Involvement in PAH

The transforming growth factor beta (TGF-*beta*) super-family is one of the most evolutionarily conserved signal transduction pathways in the animal kingdom, composed by secreted polypeptides that activate cellular responses during growth and differentiation (Eickelberg and Morty 2007). More than 60 members of this family have been identified so far, with 30-40 proteins encoded by the human genome (Feng and Derynck 2005). This group includes three TGF-*beta* isoforms, five activins and at least eight different bone morphogenetic proteins (BMPs), able to signal through cell surface by binding specific type I (e.g. TGF-*beta* receptor 1, TGFBR1 (also named Alk5), activin receptor-like kinase 1, Alk1, BMP receptor 1A and 1B, BMPR1A and BMPR1B) and type II receptors (e.g. TGF-*beta* receptor 2, TGFBR2, and BMP receptor 2, BMPR2). In particular, both the receptor types are trans-membrane serine/threonine kinases that form homodimers at the cell surface in the absence of ligands but have heteromeric affinity for each other. Ligand binding induces the formation of a receptor complex composed by two homodimers (one composed by type I receptors and one made of type II receptors), followed by the transphosphorylation of the type I receptors by the constitutively active type II receptors (Figure 1-6 and Figure 1-7) (Feng and Derynck 2005). Active type I receptors can then phosphorylate the receptor-associated cytoplasmic effector molecules of the TGF-*beta* signaling, represented by the Smad proteins. Three sub-groups of Smad proteins have been identified: receptor-activated smads (R-smads), common-mediator Smad (co-Smads) and antagonistic or inhibitory Smads (I-Smads) (Figure 1-6) (Derynck and Zhang 2003; Shi and Massague 2003; Feng and Derynck 2005). When ligand binds the receptor complex, type I receptors recruits and phosphorylate R-Smads (i.e. TGFBR1 activates Smad2 and Smad3 after the interaction with a TGF-*beta* isoform, while Alk1, BMPR1A and BMPR1B activate Smad1, Smad5 and Smad8 via binding with a BMP ligand, (Figure 1-6 and Figure 1-7) leading to their conformational change and dissociation from the receptor. After the activation two R-Smads interact with a co-Smad (called Smad4) and translocate into the nucleus, where they act as transcription factors regulating genes that modulate cell proliferation and apoptosis (Figure 1-6) (Derynck and Zhang 2003;

Shi and Massague 2003). Since different combinations of type I and type II receptors can be formed (Figure 1-7), it is interesting to note that the same ligand can induce different signaling responses depending on the composition of the activated receptor complex. The I-Smad group is represented by Smad6 and Smad7 and it is able to interfere with the intracellular transmission of the signal. These proteins can in fact associate with type I receptors blocking R-Smad recruitment and activation (Hayashi, Abdollah et al. 1997; Imamura, Takase et al. 1997). Since Smad1 and Smad5 induce Smad6 whereas Smad3 stimulates Smad7 expression, both the TGF-*beta* and the BMP signaling are subdued to an inhibitory feedback loop. One of the main transcriptional targets of BMP signaling is the inhibitor of DNA binding family of proteins (id1-4) (Hollnagel, Oehlmann et al. 1999), characterized by the ability to bind with an high affinity helix-loop-helix transcription factors and inhibit their binding to target DNA (Sun, Copeland et al. 1991; Ruzinova and Benezra 2003). This function confers to id proteins an important role in cell differentiation and proliferation (Lasorella, Uo et al. 2001; Peng, Kang et al. 2004).

TGF-*beta* signaling has been implicated in the regulation of ECs and SMCs proliferation and differentiation during angiogenesis. Several *in vivo* studies show that depletion of different components of this super-family leads to abnormal formation of the vascular plexus and decreased vessel wall integrity. In particular, mice depleted for Alk1, TGFBR1 or TGFBR2 die during mid-gestation due to impaired vascular development (Goumans and Mummery 2000; Carvalho, Itoh et al. 2007).

TGF-*beta* can regulate ECs proliferation and migration via interaction with Alk1 or TGFBR1. In fact, TGF-*beta*/TGFBR1 signaling inhibits ECs proliferation and migration through the phosphorylation of Smad2/3 and the subsequent activation of plasminogen activator inhibitor type 1 (PAI1), a negative regulator of EC migration (Deng, Curriden et al. 1996; Goumans, Valdimarsdottir et al. 2002; Goumans, Valdimarsdottir et al. 2003). On the contrary, TGF-*beta*/Alk1 signaling has been shown to stimulate EC migration and proliferation via activation of Smad1/5 and their target id1 (Goumans, Valdimarsdottir et al. 2002; Goumans, Valdimarsdottir et al. 2003). However, Alk1 interaction with a different ligand, BMP9, induces the opposite effect (David, Mallet et al. 2007). Also BMP4 and BMP6 promote EC proliferation and migration via Smad1/5/8 phosphorylation (Suzuki, Montagne et al. 2008).

TGF-*beta* can also stimulate vascular SMCs differentiation by activating a large set of SMC differentiation marker genes (Owens 2007). TGF-*beta* also induces inhibition of cellular growth via a TGFBR1-mediated Smad3 activation (Feinberg, Watanabe et al. 2004). Also BMPs have an effect on SMCs activation state. BMP2 stimulates SMCs migration, while BMP7 inhibits their growth and maintain their differentiated state and BMP4 can induce their apoptosis via a caspase8/9-dependent mechanism (Lagna, Nguyen et al. 2006; Hansmann, de Jesus Perez et al. 2008).

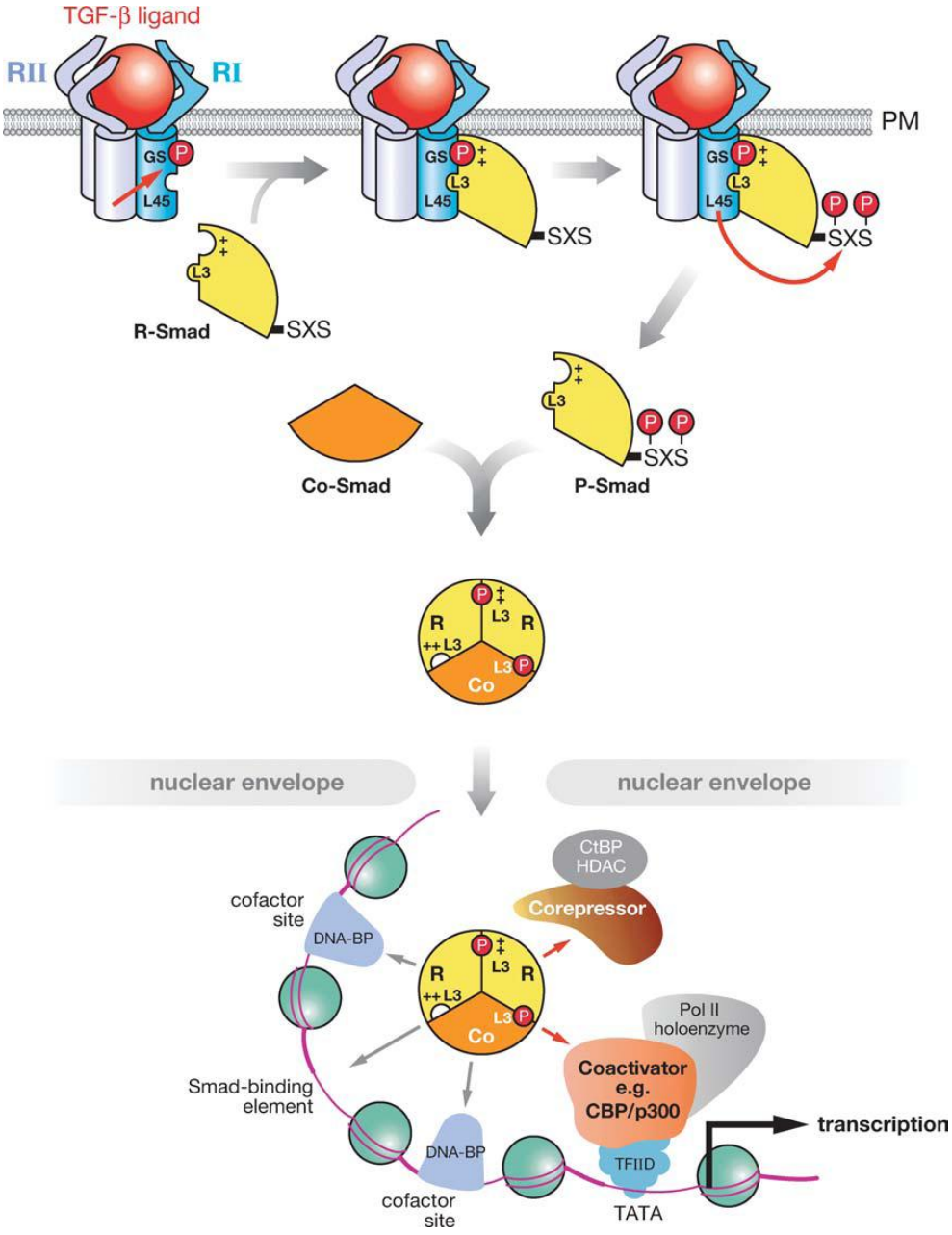

Figure 1-6 The TGF-beta signaling pathway. Ligands of the TGF-beta super-family first bind to the type II or type I homodimers stabilizing them in a tetrameric complex, in which type II receptors phosphorylate type I receptors. Following receptor activation, R-Smads are recruited to the receptor complex and phosphorylated. Phosphorylated Smads (P-Smads) then form a trimeric complex with Smad4 and translocate into the nucleus, where they interact with DNA to regulate transcription factor expression. Reported from (Feng and Derynck 2005).

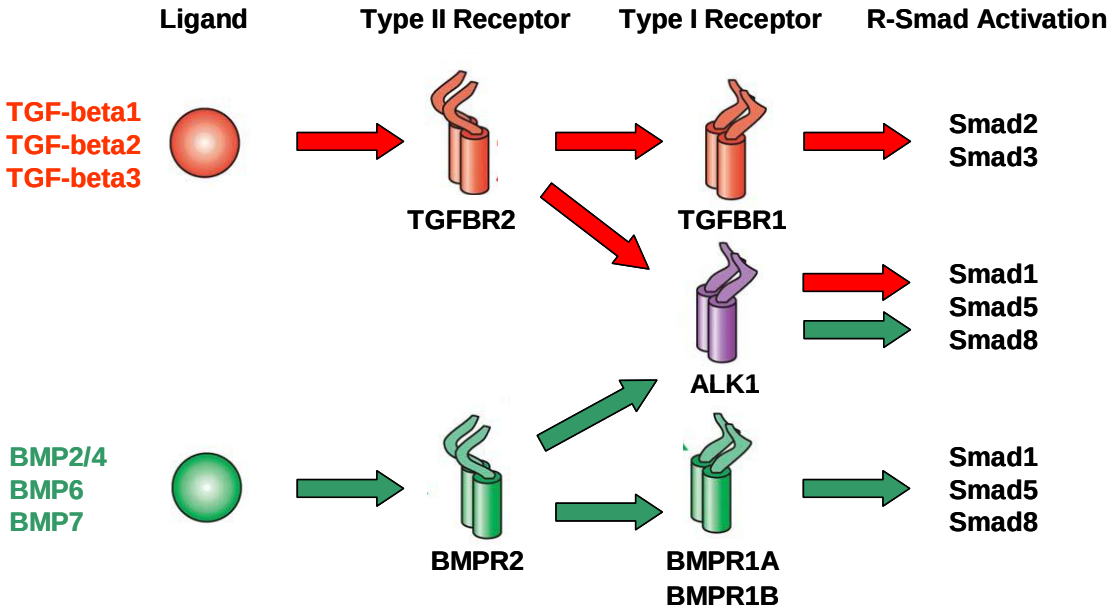

Figure 1-7 Heteromeric combinations of TGF-*beta* super-family receptors. Specific combinations of type II-type I heterotetramers able to bind TGF-beta ligands at the cell surface are indicated. Subsequent activation of R-Smads is shown on the right. Adapted from (Feng and Derynck 2005).

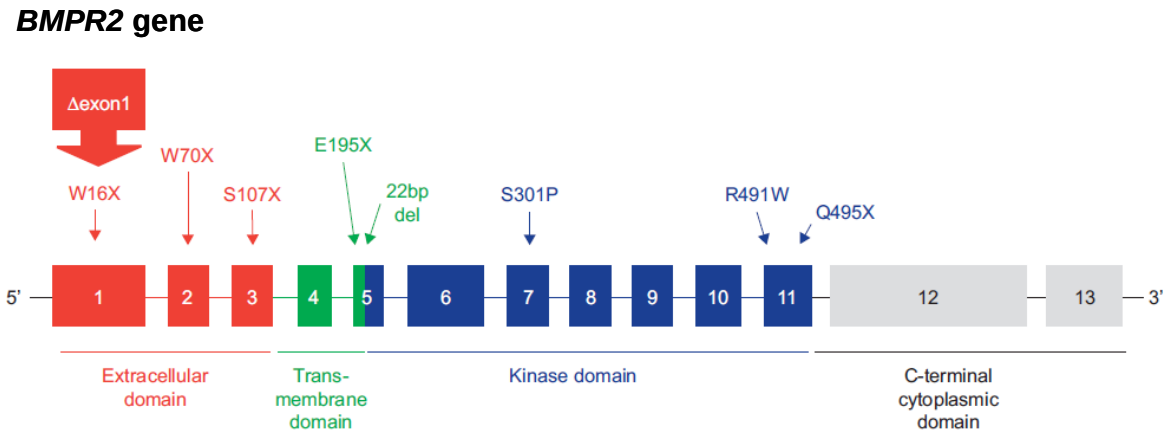

Figure 1-8 Schematic representation of *BMPR2* functional domains. A range of *BMPR2* mutations observed in patients, indicating the nature of amino acid substitution or nonsense mutations (X) are showed. Adapted from (Dewachter, Adnot et al. 2009).

Mutations in the gene coding for the type II receptor *BMPR2* are associated with the development of HPAH. In fact, mutations in this gene have been identified in more than 70% of families characterized by affected members (Machado, Aldred et al. 2006), and also 15-40% of patients with IPAH are carriers of similar mutations (Thomson, Machado et al. 2000). It has been estimated that the risk of developing PAH for someone carrying a *BMPR2* mutation is 10^5 higher in comparison with non-carriers (Morrell 2010). These mutations segregate with an autosomal dominant pattern of inheritance, but the penetrance of the phenotype is remarkably low, with only 20-30% of carriers actually developing HPAH (Newman, Wheeler et al. 2001; Newman, Trembath et al. 2004). This low penetrance suggests the existence of some type of "second hit", of genetic or environmental nature (Morrell 2010). The *BMPR2* gene is 190 Kb long and contains 13 exons and a big 90 Kb first intron with frequent repetitive sequences (Johnson, Vnencak-Jones et al. 2009) (Figure 1-8). More than 200 different mutations, dispersed across the whole gene, have been described so far. The majority of them (approximately 70%) are frame-shift and nonsense mutations, resulting in aberrant transcripts degraded by the nonsense-mediated decay system (NMD), a surveillance system specifically evolved to eliminate those messenger RNA (mRNA) sequences containing premature termination codons (Kuzmiak and Maquat 2006; Machado, Aldred et al. 2006; Li, Dunmore et al. 2010). Thus, haploinsufficiency for *BMPR2* seems to represent the main risk factor for HPAH development. Also, it is interesting to notice that the low penetrance of the *BMPR2* mutations could be at least partially explained with the fact that the NMD system is not 100% efficient (Kuzmiak and Maquat 2006; Eickelberg and Morty 2007). In the lung vasculature, *BMPR2* is mainly expressed in PAECs and at a lower lever in PASMCs and PAFs. It is important to notice that the expression of this gene is reduced in the pulmonary vasculature of HPAH patients carrying a mutation but also in IPAH patients in whom no mutation have been identified, suggesting a central role of *BMPR2* in the pathogenesis of this pathology also in non-carriers (Morrell 2010). Moreover, a reduced phosphorylation of Smad1/Smad5 has been shown in patients harboring *BMPR2* mutation and one study demonstrated increased activation of Smad2 in these category of PAH patients, supporting the hypothesis that *BMPR2* reduction is able to significantly dysregulate the down-stream signaling pathway both via TGF-*beta* isoforms and BMP proteins (Richter, Yeager et al. 2004; Yang, Long et al. 2005). Since BMPR2 transduce the signal to R-Smads by binding BMP proteins, several groups analyzed the effect of BMP stimulation

on pulmonary vascular cells. In primary cells obtained from unaffected controls, the response of PASMCs to BMP ligands is related to the site of origin of cells. In fact, BMP stimulation of PASMCs harvested from the main or lobar pulmonary arteries (derived from neural crest) (Beall and Rosenquist 1990) inhibits cell proliferation and may induce apoptosis (Zhang, Fantozzi et al. 2003; Yang, Long et al. 2005), while in contrast, in cells isolated from peripheral arteries (1 to 2 mm diameter, mainly formed by vasculogenesis within the developing lung mesenchyme) (Hall, Hislop et al. 2000) BMPs stimulate proliferation. In healthy conditions, PAECs proliferate and migrate in response to BMPs. This proliferation is mediated by Smad1/Smad5 activation and id proteins induction (Valdimarsdottir, Goumans et al. 2002). BMPs can also protect PAECs from apoptosis (Teichert-Kuliszewska, Kutryk et al. 2006). These specific responses observed in normal cells suggest that a critical reduction in BMPR2-mediated BMP signaling may promote the increased PAECs apoptosis observed initially in the pathology (section 1.2.2), stimulating PASMCs through their exposition to circulating mitogenic factors and creating the conditions for the selection of apoptosis-resistant cells with increased growth potential (section 1.2.2). In addition, PASMCs located in the underlying media, exposed to the high doses of TGF-*beta* released as a consequence of PAECs apoptosis, would be characterized by an exaggerated growth response due to their impaired Smad1/Smad5 signaling (Morrell 2010), explaining the exaggerated PASMCs proliferation observed in PAH patients. Further studies will be necessary to validate this hypothesis both *in vivo* and *in vitro*.

Several studies analyzed the effects of an increased *BMPR2* expression in rat models of PAH. In monocrotaline rats, adenoviral-mediated *BMPR2* over-expression, obtained via airway delivery, did not prevent monocrotaline-induced PAH (McMurtry, Moudgil et al. 2007), whereas a very recent study shows that vascular delivery of an adenovirus expressing *BMPR2* attenuates monocrotaline-induced PAH (Reynolds, Holmes et al. 2011). In hypoxic rats a targeted gene delivery of *BMPR2* to the pulmonary vascular endothelium significantly reduced RVP and RVH (McMurtry, Moudgil et al. 2007; Reynolds, Xia et al. 2007).

Because of the enhanced TGF-*beta* signaling observed in IPAH patients (Richter, Yeager et al. 2004) and in monocrotaline-induced rat PAH (Long, Crosby et al. 2009), the effect of TGFBR1 blocking has been evaluated in rats. Three different studies showed

beneficial effects of TGFBR1 inhibition on PAH development and progression (Long, Crosby et al. 2009).

1.2.4.2 Serotonin and SERT Involvement in PAH

The serotonin system has also been involved in the pathobiology of PAH. In particular, the "serotonin hypothesis of PAH" was formulated for the first time in 1960s, and then proposed again the 1980s, after the observation that obese patients treated with appetite suppressants such as aminorex and dexfenfluramine had an increased risk of developing PAH (Abenhaim, Moride et al. 1996; Kramer and Lane 1998). Both aminorex and dexfenfluramine are in fact serotonin transporter (SERT) substrate and are able to increase the extracellular concentration of serotonin (Rothman, Ayestas et al. 1999). Further studies focused on the role of serotonin in PAH revealed its capacity to induce proliferation of both PAFs and PASMCs and to promote vasoconstriction and remodelling of the pulmonary vasculature (MacLean, Herve et al. 2000; Welsh, Harnett et al. 2004). Moreover, it has been observed that PASMCs isolated from PAH patients proliferate faster than normal cells in response to serotonin, and elevated levels of serotonin itself can be detected in affected patients (Eddahibi, Humbert et al. 2001).

Since tryptophan hydroxylase 1 (Tph1) is the rate-limiting enzyme in the synthesis of serotonin in the periphery, its expression level in PAH patients has been evaluated. Analysis of lung tissue and PAECs revealed an increased expression of Tph1 in IPAH patients in comparison with unaffected controls (MacLean, Herve et al. 2000). Also, hypoxia-induced increases in RVP and vascular remodelling are ablated in Tph1 deficient mice, suggesting a central role for serotonin synthesis in the development of hypoxia-induced PAH (Morecroft, Dempsie et al. 2007).

Several studies identified the SERT coding gene (named solute carrier family 6 member 4, *SLC6A4*) as another genetic risk factor for PAH development. SERT is an integral membrane protein that belongs to the Na^+/Cl^- family of transporters and it is able to transport serotonin across the membrane using Na^+ concentration gradient as driving force. The promoter region of SLC6A4 is characterized by the presence of repetitive elements of varying length, with a common allele composed of 14 repeats (short variant, S) and another common allele composed of 16 repeated elements (long

variant, L). The L allele results in a higher expression of SERT with a consequent increased uptake activity. In a study based on the analysis of a small cohort of IPAH patients, a high percentage (65%) of patients homozygous for the L allele was identified, suggesting the involvement of SERT enhanced expression in PAH development (Eddahibi, Humbert et al. 2001). Also, a predominance of the L allele variant has been associated with exaggerated PAH in patients with chronic obstructive lung disease and with an increased RVP in patients affected by heart failure (Eddahibi, Chaouat et al. 2003). However, subsequent studies based on larger cohorts of PAH patients failed to confirm these findings, although affected patients with the L allele may present an earlier onset of the pathology (Willers, Newman et al. 2006). It is also important to note that an increased expression of the *SLC6A4* gene has been observed in IPAH patients, with no correlation with the genotype (Eddahibi, Humbert et al. 2001). Several *in vivo* studies suggested an involvement of SERT in PAH pathobiology. In fact, mice over-expressing SERT (SERT+) exhibit an enhanced RVP and vascular remodelling, and develop an exaggerated PAH in response to hypoxia (MacLean, Deuchar et al. 2004). A targeted over-expression of SERT in PASMCs induces a similar effect in mice (Guignabert, Izikki et al. 2006). On the contrary, mice deficient for SERT expression are less susceptible to hypoxia-induced PAH and the pharmacological inhibition of SERT via citalopram attenuates the severity of hypoxia-induced PAH in WT and SERT+ mice (Eddahibi, Hanoun et al. 2000; Morecroft, Pang et al. 2010). Since SERT+ mice show high expression levels of Rho kinase (ROCK), involved in cellular proliferation and migration, and also an increased ROCK-dependent vascular remodelling, it has been suggested that serotonin could promote cell proliferation via activation of the ROCK pathway (Liu, Ren et al. 2009; McMurtry, Abe et al. 2010; Connolly and Aaronson 2011). Also, in the previously mentioned Long et al. study (section), animals heterozygous for *BMPR2* expression (*BMPR2*+/-) exhibited a significant increase in RVP only after serotonin infusion, suggesting that serotonin could represent the “second hit” required to uncover a PAH phenotype in case of BMPR2 haploinsufficiency (Long, MacLean et al. 2006).

1.2.5 Treatment Options

Through the 1980s, PAH prognosis was very poor, with only 30% of survivors after 3 years from the diagnosis. However, over the last decade, several new therapies for the treatments of PAH have been introduced, with the intent to improve the hemodynamics, the functional NYHA class and the exercise capacity of the patients. The next sections will summarize these treatments (Figure 1-9), but it is important to remember that although they can substantially improve symptoms and quality of life, they do not treat PAH directly, and patient survival still remains poor.

1.2.5.1 Calcium Channel Blockers

Calcium channel blockers (CCB), also called calcium antagonists, are a class of drugs able to slow down the rate at which calcium passes through voltage-gated calcium channels (VGCCs) in cardiac muscle and blood vessels. This decreases the intracellular concentration of calcium, leading to cellular hyper-polarization and reduction in muscle contraction. In particular, in blood vessels a decrease in calcium results in less contraction of the vascular smooth muscle and therefore in an increase in arterial diameter inducing vasodilatation. In 1991/1992, Rich et al. reported that the use of CCB could dramatically improve the survival in PAH patients. However, this positive effect was characteristic of those patients showing a favorable response to acute administration of a vasodilator, tested during right heart catheterization (Rich and Kaufmann 1991; Rich, Kaufmann et al. 1992). In Rich studies, acute vasodilator response was assessed through the administration of an high dose of CCB (Rich and Kaufmann 1991; Rich, Kaufmann et al. 1992), but subsequent studies documented that such a treatment could result in serious adverse effects, especially in non-responders (Sitbon, Humbert et al. 1998; Sitbon, Humbert et al. 2005). Different agents are therefore recommended for the evaluation of the pulmonary vasoresponsiveness, including inhaled nitric oxide (NO), intravenous adenosine and epoprotenol (Galie, Ussia et al. 1995; Sitbon, Humbert et al. 1998; Badesch, Champion et al. 2009). A pulmonary vasodilator test is considered positive when it is possible to observe a decrease in the mPAP of at least 10 mm Hg to reach an absolute value of 40 mm Hg or less without a decrease in cardiac output. Unfortunately, such a response is observed

only in 10% of patients with PAH and only half of them normally experience long-term benefits after CCB administration, suggesting that other factors can influence the efficacy of this treatment (Sitbon, Humbert et al. 2005; Montani, Savale et al. 2010). In case of negative test, the administration of CCB can result in systemic hypotension, worsening right heart failure and death (Partanen, Nieminen et al. 1993; Galie, Torbicki et al. 2004), and this treatment is never recommended for patients with severe PAH because of the potential high mortality rate observed in this group (Sitbon, Humbert et al. 2005).

1.2.5.2 Prostanoids

Prostacyclin (PGI2) is a natural prostanoid (prostanoids are a group of complex fatty acids) produced by the vascular endothelium. It is a potent vasodilator able to reduce PVR and it has also antiplatelet aggregator properties. Moreover, it attenuates VSMC proliferation through signal transduction following ligand binding to its receptor (Shirotani, Yui et al. 1991). Several studies reported that a deficiency in prostacyclin production may contribute to the pathogenesis of PAH (Christman, McPherson et al. 1992; Tuder, Cool et al. 1999; Humbert, Morrell et al. 2004).

Intravenous epoprostenol was the first prostacyclin analogue approved by the Food and Drug Administration (FDA) for the treatment of severe PAH in 1995 and it is still used with NYHA class III and class IV patients (Badesch, Abman et al. 2004; Badesch, Abman et al. 2007). Data obtained from different clinical trials show that a continuous intravenous infusion of epoprostenol can significantly improve the 6-minute walk test results and the quality of life of patients reducing the mPAP and the PVR (Rubin, Mendoza et al. 1990; Barst, Rubin et al. 1996; Badesch, Tapson et al. 2000). However, this is an expensive therapy (Highland, Strange et al. 2003), also complicated by the need of a continuous administration (obtained via a central venous catheter) due to its very short half-life (≈ 3 min). Any interruption of the infusion can result in severe rebound PAH. Epoprostenol administration should be avoided in case of concomitant use of antiplatelet agents or anticoagulants, which could increase the risk of bleeding, or with medications that lower blood pressure. Common adverse effects include jaw pain, diarrhea, flushing, nausea and headaches.

Treprostinil is another prostacyclin analogue and its use has been approved in 2002 for the treatment of NYHA class II-IV PAH. Data obtained from the first clinical trial demonstrated that treprostinil administration can substantially improve the 6-minute walk test result, the dyspnea fatigue rating and pulmonary hemodynamics including mPAP and PVR (Simonneau, Barst et al. 2002). Having a longer half-life than epoprostenol (≈3 hours), it can be administrated by subcutaneous infusion, eliminating the need for a surgically inserted central venous catheter, with a consequent reduction of infection and thrombosis. However, this kind of infusion often induces in patient injection-site pain and erythema and also the same adverse effects of epoprostenol can be observed (Simonneau, Barst et al. 2002). For this reason, this therapy is normally reserved for patients with a severe disease that result refractory to oral therapies (Badesch, Abman et al. 2004).

Iloprost is the last synthetic analogue of prostacyclin approved by FDA for the treatment of severe PAH (Badesch, Abman et al. 2004). It can be administered by inhalation and represents for this reason an attractive option for PAH patients. However, the first clinical trials showed a reduced efficacy in comparison with epoprostenol and treprostinil, suggesting a potential role for iloprost as an adjunctive agent (Hoeper, Schwarze et al. 2000; Olschewski, Simonneau et al. 2002; Opitz, Wensel et al. 2005). The adverse effects of this therapy include cough, headache, flushing and jaw pain but also syncope, tachycardia, pneumonia and dyspnea.

1.2.5.3 Endothelin Receptor Antagonists

Endothelins are a class of strong vasoconstrictors mainly produced by endothelial cells that play a central role in vascular homeostasis. Endothelin-1 (ET-1) is the most abundantly expressed isoform in the pulmonary circulation and it is over-expressed in the plasma and the lung of PAH patients (Giaid, Yanagisawa et al. 1993). It has been shown that an increase in the expression of this peptide not only results in vasoconstriction, but can induce an abnormal growth of endothelial cells, smooth muscle cells and fibroblasts and inhibit the apoptosis of smooth muscle and endothelial cells (Shichiri, Kato et al. 1997; Jankov, Kantores et al. 2006). ET-1 interacts with two different G protein-coupled receptors, named ET_A and ET_B. ET_A is expressed in smooth muscle cells and fibroblasts (Evans, Cobban et al. 1999), while ET_B is abundant

in endothelial and smooth muscle cells (Hori, Komatsu et al. 1992). Both the receptors are involved in smooth muscle cells contraction and proliferation (McCulloch, Docherty et al. 1996; Davie, Haleen et al. 2002), but ET_B also mediates the release of vasodilators and antiproliferative factors including prostacyclins and NO from endothelial cells (Fukuroda, Nishikibe et al. 1992; Dupuis, Goresky et al. 1996). Consequently, a selective blockade of the ET_A receptor has been suggested as a potential therapeutic agent for the treatment of PAH, and studies conducted with animal models of PAH showed that such a treatment result in a 25% reduction of the severity of the pathology (Black, Mata-Greenwood et al. 2003). Controversially, another study demonstrated that a combined blockage of both the receptors can better antagonize the ET-1-induced vasoconstriction (Sato, Oka et al. 1995), suggesting that more studies will be necessary to identify the best strategy. At the moment, three endothelin receptor antagonists (ERAs) are in clinical use: bosentan, effective in the inhibition of both ET_A and ET_B, sitaxsentan and ambrisentan, selective for the ET_A receptor (Badesch, Feldman et al. 2011; Klinger, Oudiz et al. 2011; Sandoval, Torbicki et al. 2011).

Bosentan is an orally active ERA indicated for the treatment of class III-IV PAH. Clinical trials completed so far showed that a bosentan-based therapy can significantly decrease PVR and improve the exercise capacity (Rubin, Badesch et al. 2002; Galie, Hinderliter et al. 2003; McLaughlin, Sitbon et al. 2005). The most common side effects of bosentan are represented by headache, dizziness, flushing and syncope, but also an abnormal hepatic function has been observed (Rubin, Badesch et al. 2002).
Both ambrisentan and sitaxsentan are ERAs specific for ET_A with a longer half-life than bosentan, which allows once a day dosing. Data obtained from the first clinical trials report encouraging improvements in hemodynamics and exercise capacity, but their efficacy is still under evaluation (Girgis, Frost et al. 2007; Oudiz, Galie et al. 2009).

1.2.5.4 Phosphodiesterase Type 5 Inhibitors

Phosphodiesterases are a super-family of enzymes involved in the hydrolysis of cyclic nucleotides, and have a specific tissue distribution. In particular, phosphodiesterase type 5 (PDE-5) is selectively expressed in the lung and it is implicated in endothelial dysfunction because of its capacity to inactivate cyclic guanosine monophosphate

(cGMP), the second messenger of the NO pathway in the pulmonary vasculature (Moncada and Higgs 1993; Wharton, Strange et al. 2005). Different studies reported an increased *PDE-5* gene expression and activity in PAH patients, resulting in an impaired antiproliferative and vasodilating effect of endogenous NO (Badesch, Abman et al. 2004; Corbin, Beasley et al. 2005). As we mentioned in section 1.2.5.1, inhaled NO is recommended for acute vasodilator testing, but its therapeutic use in the treatment of PAH is limited by its very short half-life. For this reason, PDE-5 inhibitors have been tested instead as therapeutic agents. In particular, sildenafil, an orally active highly specific PDE-5 inhibitor (already used in the treatment of erectile dysfunction) was approved by the FDA in 2005. Its use is recommended in patients with mild to moderate symptoms (Michelakis, Tymchak et al. 2002; Tantini, Manes et al. 2005; Ghofrani, Osterloh et al. 2006). The clinical trials conducted so far show the capacity of sildenafil to improve exercise tolerance and RVH (Bhatia, Frantz et al. 2003; Michelakis, Tymchak et al. 2003; Sastry, Narasimhan et al. 2004). Also, experiments conducted with rats demonstrated an increased percentage of survivals in monocrotaline-induced PAH (Schermuly, Kreisselmeier et al. 2004) and an *in vitro* study showed that this treatment can efficiently reduce PASMCs proliferation induced by platelet-derived growth factor (Tantini, Manes et al. 2005). Wilkins et al. study compared the efficacy of sildenafil versus bosentan as first-line therapy for PAH, showing a comparable effect of the two treatments (Wilkins, Paul et al. 2005). In comparison with other treatments (i.e. prostanoids), Phosphodiesterase type 5 inhibitors are less expensive and therefore more affordable for patients. However, not only common side effects of sildenafil use (including headache, flushing, palpitations and back pain) have been observed, but also death due to worsening PAH, to pulmonary embolism or myocardial infarction has been reported with low frequency (Galie, Ghofrani et al. 2005; Wilkins, Paul et al. 2005).

1.2.5.5 Combined Therapy

Considering that none of the therapies reported in the previous sections represent a definitive “cure” for PAH, the use of a combination therapy is at the moment attractive. Several efficacy studies have been conducted or are in process (Humbert, Barst et al. 2004; Kayser 2005; Paul, Gibbs et al. 2005; Hoeper, Leuchte et al. 2006;

Mathai, Girgis et al. 2007), but the most efficacious combination for specific subgroups of patients still need to be evaluated.

Lung transplantation represents at this time the only “cure” for PAH, and it is reserved for those patients unable to respond to other therapies.

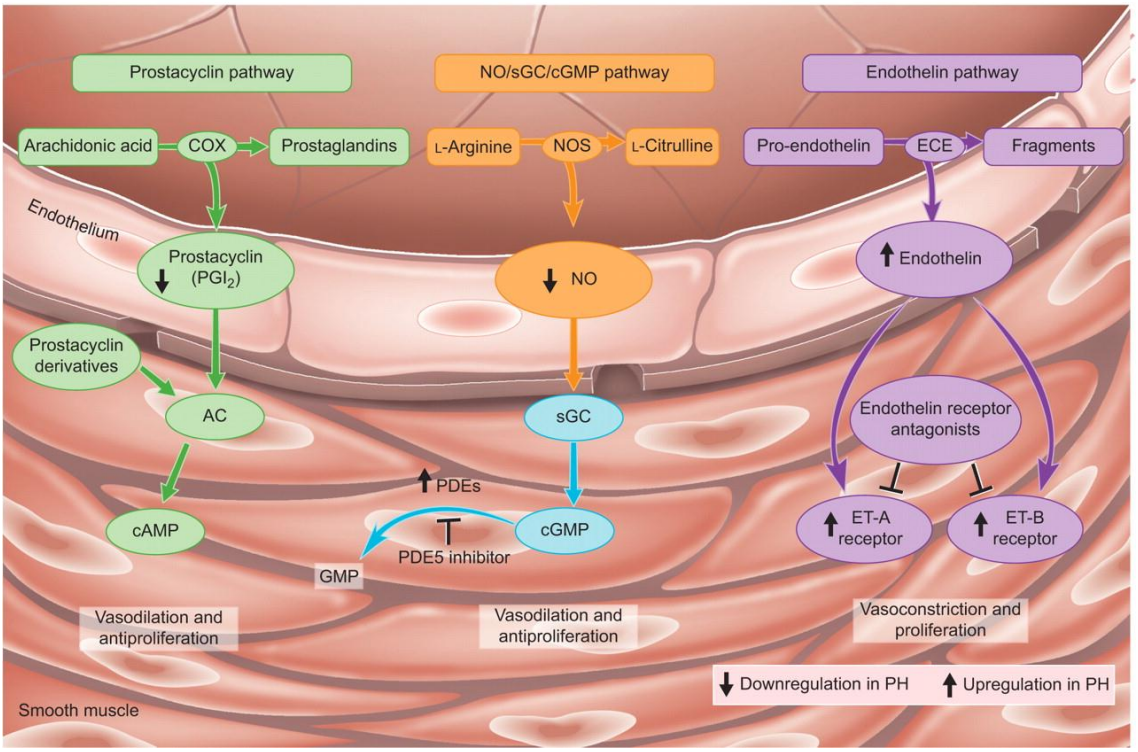

Figure 1-9 Major molecular pathways for PAH which are currently approved for medical treatments. Reported from (Ghofrani and Grimminger 2009; Humbert 2010).

1.3 Non Coding RNAs

At the beginning of this century it was generally thought that the amount of DNA in a genome correlated with the complexity of an organism. In fact, the human genome is about 30 times bigger than that of simpler organism such as *Caenorhabditis elegans* or *Drosophila melanogaster*, and 250 times bigger than that of the yeast Saccharomyces cerevisiae (Griffiths-Jones 2007). For this reason many geneticists predicted that the human genome should contain around 100,000 protein-coding genes (Roest Crollius, Jaillon et al. 2000), assuming that such a substantial quantity of DNA could explain the differences between a human and a roundworm in term of quantity of proteins that could be produced. However, the human genome consists approximately of 25,000 protein-coding genes, only a few thousand more than worms or flies (Griffiths-Jones 2007; Taft, Pheasant et al. 2007). Moreover, the analysis of the genome of our closest relative, the chimpanzee, showed that almost 30% of all the orthologous proteins encoded in human and in this primate are identical, without any correlation between proteins number/structure and complexity of the species (Watanabe, Fujiyama et al. 2004). This paradox, known as G-value paradox (Hahn and Wray 2002; Taft, Pheasant et al. 2007), remained without any explanation for years, and the non-coding portion of the genome, representing in the most evolved organisms the vast majority, was named “junk DNA” or “transcriptional noise”. However over the past decade it has been observed that the percentage of the genome coding for proteins decreases linearly with the biological complexity, starting with almost 90% in prokaryotes, decreasing to almost 68% in yeast, almost 25% in nematodes and 17% in insect, and reaching 1% in mammals (Taft, Pheasant et al. 2007; Costa 2008). Therefore many researchers started to analyse more in detail this “junk” portion of the genome, identifying several different classes of small non-coding RNAs essential for many vital functions. They includes transfer RNAs (tRNAs), responsible for the transport of specific amino acids to the ribosomes during protein translation (RajBhandary and Kohrer 2006; Soll and RajBhandary 2006), ribosomal RNAs (rRNAs), identified in the small and the large subunits of ribosomes (Nissen, Hansen et al. 2000; Beringer and Rodnina 2007; Rodnina, Beringer et al. 2007), spliceosomal RNAs (also called small nuclear RNAs, snRNAs), part of the spliceosome complex and therefore involved in mRNA splicing (Padgett, Grabowski et al. 1986), and small nucleolar RNAs (snoRNAs), responsible for guiding a series of site-specific post-transcriptional modifications of the

other classes (Smith and Steitz 1997). However, the most abundant and studied class of small non-coding RNAs is represented by small silencing RNAs, including PIWI-interacting RNAs (piRNAs), small interfering RNAs (siRNAs) and microRNAs (miRNAs), all able to inhibit specifically gene expression through complementary recognition of RNA targets.

1.3.1 Piwi-Interacting RNAs

piRNAs are 24-32 nucleotides long non-coding RNAs obtained from single-stranded (ss) RNA precursors mainly transcribed from specific intergenic repetitive elements called piRNA clusters (Siomi, Sato et al. 2011). They have been identified in the germ line of several animal species, where their main role is to silence transposable elements (TEs) (Malone and Hannon 2009), genomic parasites able to move from site to site in the genome by insertion or transposition potentially disrupting coding genes of the host organism (Kazazian 2004). To protect the integrity of the genome, these short RNAs associate with PIWI proteins, germline-specific members of the Argonaute family, to form an active piRNA-induced silencing complex (piRISC), able to silence specific target RNA sequences (Girard, Sachidanandam et al. 2006). In fact, like other members of the Argonaute family (Section 1.3.3.6), PIWI proteins exhibit endonuclease activity and can therefore cleave target TEs that are complementary to the guide piRNA (Brennecke, Aravin et al. 2007; Gunawardane, Saito et al. 2007). It has been hypothesized that the piRISC could also guide the de novo methylation machinery to specific TE loci (Kuramochi-Miyagawa, Watanabe et al. 2008), and even direct heterochromatin protein 1A (HP1A) localization to target sequences to induce their conversion to heterochromatin (Brower-Toland, Findley et al. 2007), however further investigation will be necessary to validate these theories.

1.3.2 Short Interfering RNAs

siRNAs are 20-25 nt long perfectly complementary duplexes able to bind specific mRNA targets and silence them. They were identified for the first time in the 1990's after the observation that in plants transgenes identical to host genes can sometimes cause silencing of both the transgene and the homologous endogenous gene through the formation of aberrant double stranded (ds) RNAs, a phenomenon named co-

supression (Napoli, Lemieux et al. 1990; van der Krol, Mur et al. 1990; Hamilton and Baulcombe 1999). In the same period a similar discovery was made in animals, when Guo et al. injected antisense ss-RNAs into *Caenorhabditis elegans* to down regulate specific genes, discovering that surprisingly the long dsRNA used as a negative control could reduce efficiently the expression of their gene of interest (Guo and Kemphues 1995; Fire, Xu et al. 1998). SiRNAs can be experimentally introduced in the cell as synthetic dsRNAs or can be virally derived (exogenous siRNAs), but they can also derive from more extended dsRNAs obtained from bidirectional transcription at a single locus or complementary transcripts produced from distinct loci in the nucleus (endogenous siRNAs), as reported in mouse and in *Drosophila melanogaster* (Chung, Okamura et al. 2008; Czech, Malone et al. 2008; Ghildiyal, Seitz et al. 2008; Okamura, Chung et al. 2008; Tam, Aravin et al. 2008; Watanabe, Totoki et al. 2008). Another source of endogenous dsRNAs, found in the yeast Saccharomyces pombe, in plants and in *Caenorhabditis elegans* is transcription from an RNA-dependent RNA polymerase (RdRP) (Herr, Jensen et al. 2005; Xie and Qi 2008; Grewal 2010). These long endogenous transcripts are then processed by the class III RNase III enzyme Dicer (Section 1.3.3.6) in a shorter ds and loaded onto different effector ribonucleoprotein (RNP) complexes, able to mediate different small RNA functions including mRNA cleavage and translational repression (mediated by the RNA-induced silencing complex, RISC (Section 1.3.3.6), but also regulation of chromatin structure (mediated by the RNA-induced transcriptional gene silencing, RITS, complex) (Grewal 2010). In fact, in association with the Argonaute protein Ago1, the chromodomain protein Chp1 and the self-associated adaptor protein Tas3, siRNAs can target specific pericentromeric regions of Saccharomyces pombe inducing formation of heterochromatin (Reinhart and Bartel 2002; Volpe, Schramke et al. 2003; Verdel, Jia et al. 2004).

1.3.3 miRNAs

1.3.3.1 Discovery

The first miRNA was identified in 1993, when two different groups of researchers discovered in *Caenorhabditis elegans* a short RNA transcript, named lin-4, able to inhibit the expression of another gene, lin-14, by binding to its 3'untranslated region

(UTR) (Lee, Feinbaum et al. 1993; Wightman, Ha et al. 1993). This discovery was considered a nematode idiosyncrasy until 2000, when a second RNA with such a function was characterized. It was named let-7 and it was reported to be able to repress *lin-41*, *lin-14*, *lin-28*, *lin-42*, and *daf-12* expression during specific stages of development of *Caenorhabditis elegans* (Reinhart, Slack et al. 2000). Since let-7 was soon found to be conserved in many species (Pasquinelli, Reinhart et al. 2000), the ability of short non-coding RNAs to silence target genes started to be considered a wider phenomenon, and the interest on this kind of gene regulation grew rapidly. However, in consideration of the role of these short RNAs in developmental timing, they were first named short temporal RNAs (stRNAs), and the term microRNA (miRNA) was not introduced until 2001 (Lagos-Quintana, Rauhut et al. 2001).

Over the last decade, the number of miRNA publications and registered new sequences in miRBase (Section 1.3.3.2) have grown exponentially (miRBase 17, released in April 2011, contains 16772 entries representing hairpin precursor miRNAs, expressing 19724 mature miRNA products, in 153 species), testifying the enormous importance of these small sequences in the current research world.

1.3.3.2 Nomenclature

miRNA nomenclature, sequence data, annotation and predicted targets are collected in the miRNA database, called miRBase (Griffiths-Jones, Grocock et al. 2006; Griffiths-Jones, Saini et al. 2008; Griffiths-Jones 2010). In particular, names have been assigned by the miRBase registry based on a strict convention established by prominent miRNA researchers with the aim to prevent duplication (Ambros, Bartel et al. 2003).

miRNAs are named using the prefix “miR” (while the precursor hairpins are labeled “mir”) and an identifying number, assigned sequentially when the discovery of a new miRNA is described in a manuscript accepted for publication and it is therefore included in miRBase (Griffiths-Jones, Grocock et al. 2006). Each miRNA also have a 3 or 4 letter prefix to designate its species, such as “hsa” for human (*Homo sapiens*) or “mmu” for mouse (*Mus musculus*) sequences (Griffiths-Jones, Grocock et al. 2006; Griffiths-Jones, Saini et al. 2008). MiRNAs with identical sequences in different species are normally given the same number, while miRNAs that differ only in one or two positions in the same organism present a lowercase letter as suffix (e.g. rno-miR-19a

and rno-miR-19b). These miRNAs are considered members of the same family (Griffiths-Jones, Grocock et al. 2006). When identical mature miRNAs are coded by distinct loci, they are given numbered suffixes (e.g. dme-miR-281-1 and dme-miR-281-2). After miRNA identification and the first manuscripts about their activity, it was generally believed that only one strand of the mature miRNA could interact with its targets. However, now we know that (rarely) both strands can be incorporated in the RISC complex (Section 1.3.3.6) and regulate gene expression (Guo and Lu 2010; Yang, Phillips et al. 2011). Since these two complementary mature miRNAs originated from the same precursors contain different (but complementary) seed sequences, they have also been named in a different way. When one single strand is less active than the other, it is distinguished by an asterisk (e.g. hsa-miR-21 and hsa-miR21*) and it is named passenger strand (the other strand, normally included in the miRISC complex, is named guide strand), while when the two single stranded mature miRNAs are equally active on targets (or when their relative expression levels are not known) they are named with the same number followed by the name of the hairpin arm from which they are originated (-3'p for the 3'arm and -5'p for the 5'arm, e.g. rno-miR-10a-3p and rno-miR-10a-5p).

MiRNA coding genes are also named using the same 3 or 4 letter prefix and the same identifying number, but in capital letters or italics according to the conventions of the organism (for example, mir-1 in *Caenorhabditis elegans* and *Drosophila melanogaster*, MIR-156 in *Arabidopsis thaliana*).

1.3.3.3 Biogenesis: miRNA Transcription

MiRNAs are initially transcribed as long transcripts (their length can vary between few hundreds and several thousands of nucleotides), known as pri-miRNAs. The majority of these precursors contains cap structures and a poly(A) tail, and can therefore be classified as class II genes, transcribed by polymerase-II (pol-II), along with all protein-coding genes and specific non-coding genes including U1, U2, U4 and U5 snRNAs (Lee, Kim et al. 2004). However, over 20% of human miRNAs, including those located in the chromosome 19 miRNA cluster (C19MC), resides within repetitive elements such as Alu repeats and were reported to be therefore transcribed from their polymerase-III (pol-III) promoters (Borchert, Lanier et al. 2006). However Bortolin-Cavaillé et al.

recently questioned this hypothesis suggesting that C19MC miRNAs would be originated instead from a non-protein-coding Pol-II (and not Pol-III) transcript (Bortolin-Cavaille, Dance et al. 2009).

miRNAs can be localized within introns of known coding genes (intronic) or between clusters of genes (intergenic) (Schanen and Li 2011) (Figure 1-10). Intronic miRNAs can be transcribed from the host gene promoter, while intergenic miRNAs are normally derived from independent transcription units (Lee, Jeon et al. 2002; Bartel 2004). Unfortunately, very little is still known about the promoter structure and the transcriptional regulation of these miRNAs, but the characterization of the promoter of the miRNA gene cluster miR-23a ≈27a ≈24-2 showed that this region lacks the TATA box, the initiator element, the down-stream promoter element (DPE) and the TFIIB recognition element (BRE), all essential for messenger RNA (mRNA) transcription (Lee, Kim et al. 2004).

Pri-miRNAs are characterized by the presence of stem and loop structures, with imperfect complimentary regions. This precursor can encode a single miRNA (monocistronic unit) or several miRNAs (polycistronic unit) (Figure 1-10). All the miRNAs generated from the same polycistronic unit are members of the same cluster, transcriptionally regulated in the same way (Bartel 2004).

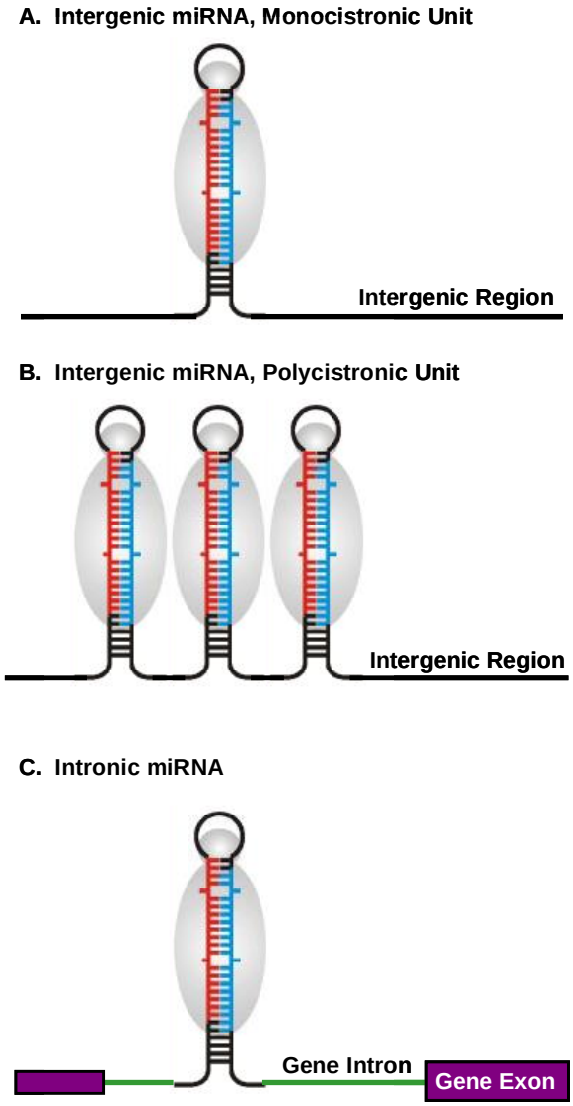

Figure 1-10 miRNA gene models. Canonical miRNA genes can be found in intergenic regions as independent transcriptional units, where they can encode for one (A) or several miRNAs (B), or they can be localized in introns of host genes (C), where they may be transcribed independently or as part of host gene transcripts.

1.3.3.4 Biogenesis: the Drosha/DGCR8 Complex in Primary miRNA Processing

MiRNA maturation begins in the nucleus with cleavage of the pri-miRNA to release a 60-70 nt long stem loop intermediate called pre-miRNA (Figure 1-11). This step is mediated by Drosha, a 160 kDa Class II type RNase III enzyme able to cleave the pri-miRNA in an asymmetric way to leave a 5' phosphate and a 2 nt 3' overhang. This also facilitates the other steps of miRNA maturation since protruding 3' ends are recognized more efficiently by Exportin 5 and Dicer (Lee, Ahn et al. 2003; Lund, Guttinger et al. 2004).

RNase III proteins are dsRNA-specific endonucleases able to cut both sides of a RNA helix and they are grouped into three classes based on their domain organization (Han, Lee et al. 2004). Class one proteins contain one RNAse III domain (RIIID) and one ds-RNA binding domain (dsRBD). They can be found in yeast and bacteria. Class II enzymes like Drosha have two RNase III catalytic sites with a dsRBD, both required for pri-miRNA processing. In addition, Drosha also has a proline-rich domain and arginine/serine-rich domain at the N terminus, which is important in protein-protein interactions (Figure 1-12) (Tsunetsugu-Yokota and Yamamoto 2010). Drosha homologs can be found only in animals. Class III proteins include Dicer, which will be described in detail in a separate section (section 1.3.3.6). In a first moment Drosha was only known for being implicated in pre-ribosomal RNA processing (Wu, Xu et al. 2000), but in 2003 its role in miRNA maturation was made clear by the observation that its depletion in cultured cells resulted in the dramatic accumulation of pri-miRNAs (Lee, Ahn et al. 2003) with a very low detection of mature miRNAs. One year after that, the mode of action of this step of miRNA maturation was better understood with the identification of a complex, termed microprocessor, containing Drosha and the dsRNA binding protein DGCR8 (also known in *Drosophila melanogaster* as Pasha, partner of Drosha) (Denli, Tops et al. 2004; Gregory, Yan et al. 2004; Han, Lee et al. 2004). This is an evolutionary conserved protein which has two dsRBDs and a WW domain containing two conserved tryptophan (W) residues, known to interact with proline-reach peptides such as the N-terminal domain of Drosha (Gregory, Yan et al. 2004) (Figure 1-12). DGCR8 is a 120 kDa protein and it is one of the 30 genes in the chromosomal region 22q11.2 whose heterozygous deletion result in the DiGeorge syndrome, a disease

characterized by congenital heart defects, immunodeficiency and developmental and behavioural problems (Gregory and Shiekhattar 2005). Its role in miRNA processing is to recognize the substrate and bind the base of the pri-miRNA hairpin, positioning Drosha in the right position to cleave the pri-miRNA stem at a distance of 11 base pairs (bp) from the junction between the dsRNA stem and the flanking ssRNA regions (Han, Lee et al. 2006) (Figure 1-13).

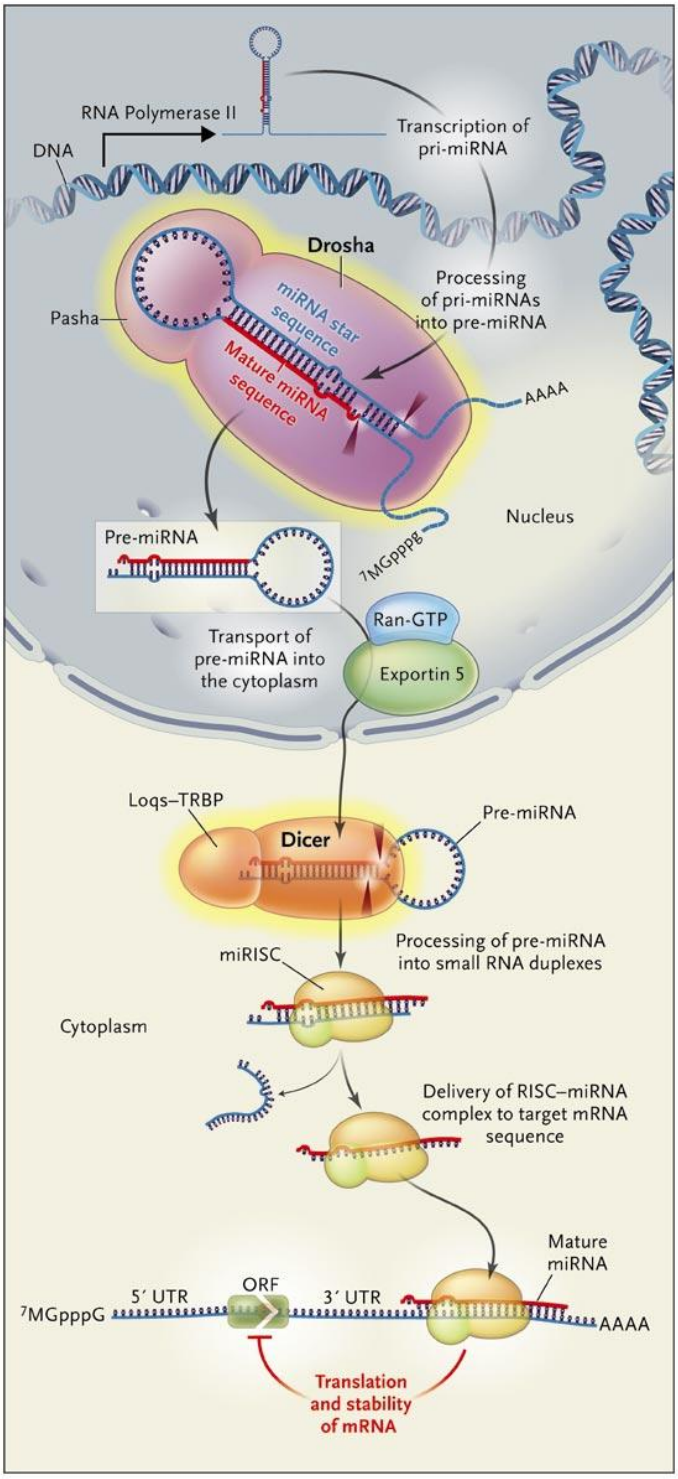

Figure 1-11 miRNA biogenesis. The primary transcripts of miRNAs, called pri-miRNAs, are transcribed as individual miRNA genes, from introns of protein-coding genes, or from polycistronic transcripts. The RNase Drosha further processes the pri-miRNA into 70–100 nucleotides, hairpin-shaped precursors, called pre-miRNA, which are exported from the nucleus by exportin 5. In the cytoplasm, the pre-miRNA is cleaved by Dicer into a miRNA:miRNA* duplex. Assembled into the RISC, the mature miRNA negatively regulates gene expression by either translational repression or mRNA degradation.

Obtained from http://eugenemaster.wordpress.com/what-is-microrna/

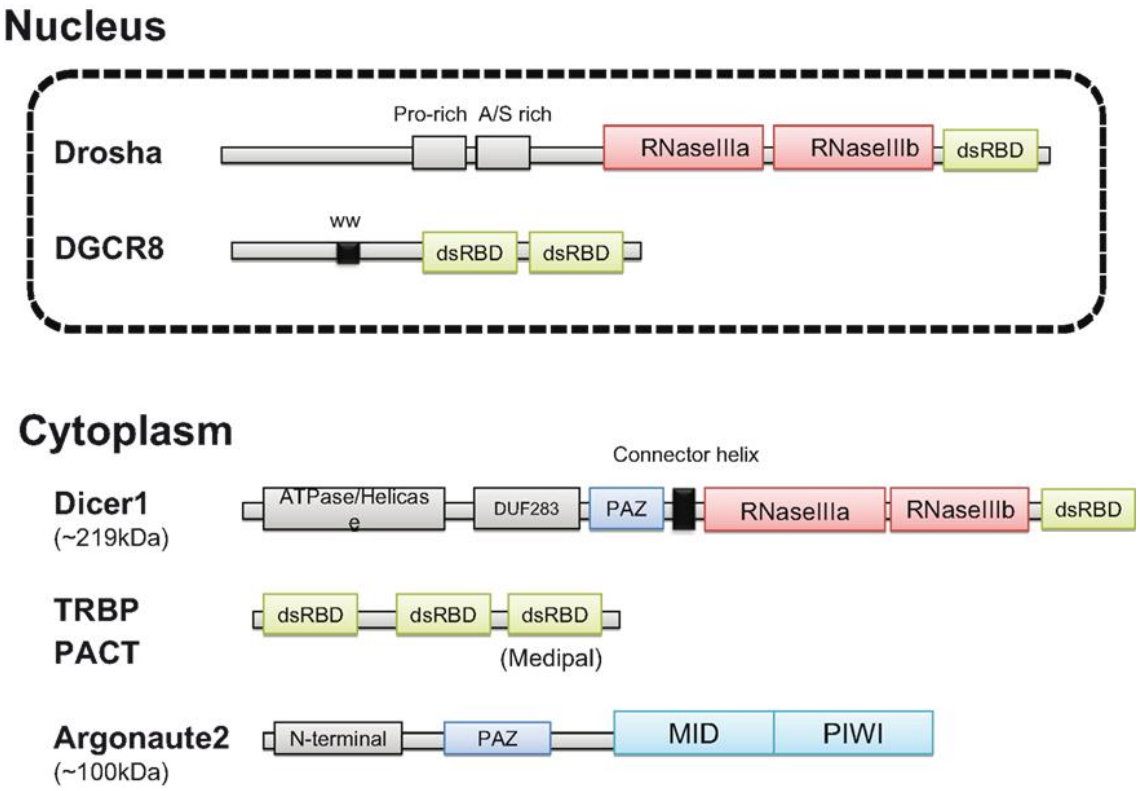

Figure 1-12 Structure of the miRNA processing enzymes. The common domains are indicated in the same colour. See the text for further details about the function of each domain. Reported from (Tsunetsugu-Yokota and Yamamoto 2010).

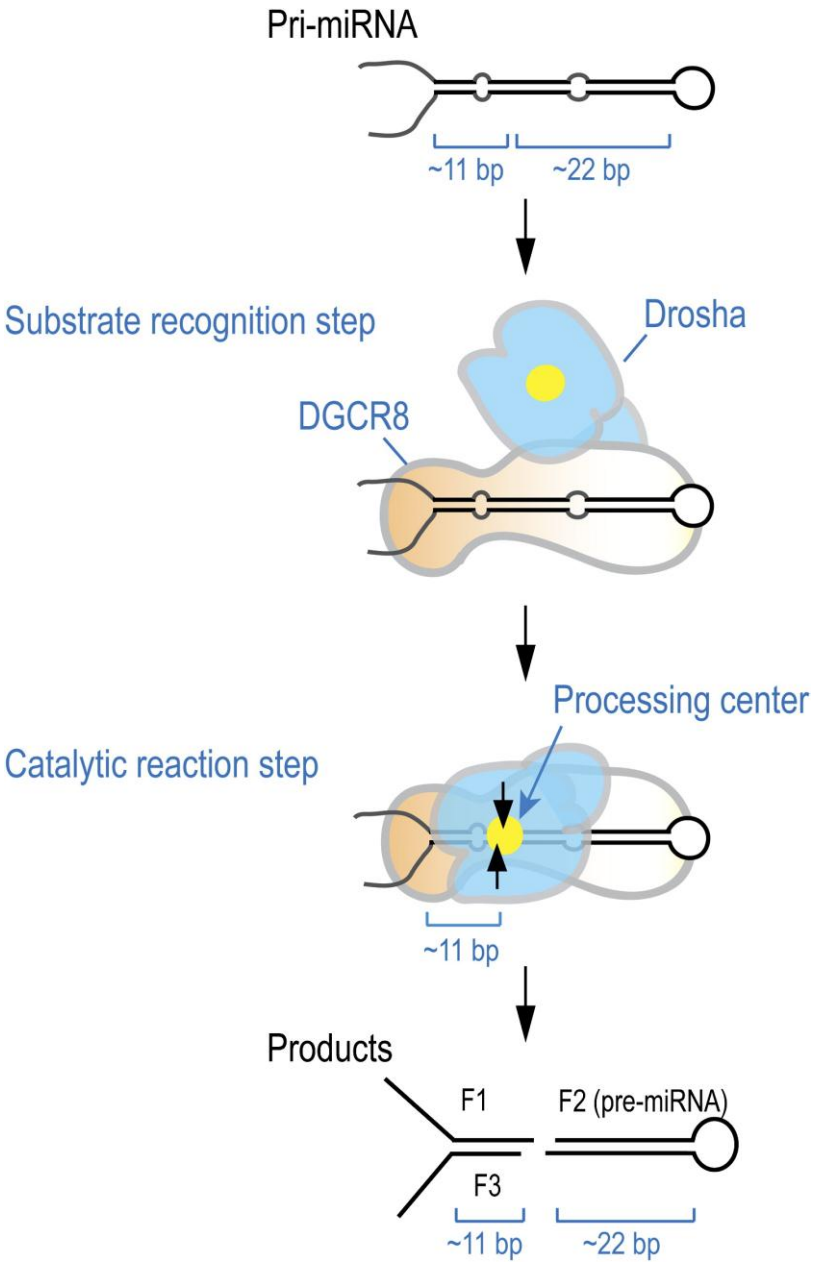

Figure 1-13 DGCR8 role in Pri-miRNA processing. DGCR8 can recognize the Pri-miRNA substrate and anchor Dicer in the right position. The processing centre (yellow circle) of Drosha is placed then at ≈11 bp from the basal segments. Adapted from (Han, Lee et al. 2006).

As already mentioned, no homologous proteins to Drosha can be found in plants, where this stage of miRNA biogenesis seem to be different (Chen 2009; Voinnet 2009). In fact, both the pri-to-pre-miRNA conversion and mature miRNA processing are made in plants by DCL1, a nuclear Dicer-like protein, together with the ds-RNA-binding protein HYPONASTIC LEAVES1 (HYL1) and the C2H2-zinc finger protein SERRATE (SE). The mature miRNA duplex is then methylated by the RNA methyltransferase HEN1 and the miRNA is loaded into an AGO1 complex (Figure 1-14) (Chen 2009; Voinnet 2009).

Recent studies show that pri-miRNA processing might be a co-transcriptional process. In fact, in intronic miRNAs, Drosha is able to process the miRNA precursor before the intron is excised. Thus, miRNA maturation and mRNA splicing might be coordinated mechanisms (Kim and Kim 2007; Kim, Han et al. 2009) (Figure 1-15A).

In 2007 a new class of small intronic hairpins was identified first in *Drosophila melanogaster* and *Caenorhabditis elegans* (Okamura, Hagen et al. 2007; Ruby, Jan et al. 2007) and then also in mammalian (Berezikov, Chung et al. 2007). They were named mirtrons. These small RNA precursors are characterized by the presence of introns and flanking exonic sequences and their nuclear biogenesis can bypass Drosha cleavage, requiring instead the splicing machinery and the lariat-debranching enzyme (Ldbr) (Okamura, Hagen et al. 2007). The pre-mirtron so generated can be exported to the cytoplasm by Exportin-5 (Section 1.3.3.5) and cleaved by Dicer (Section 1.3.3.6), generating an active miRNA (Okamura, Hagen et al. 2007) (Figure 1-15B).

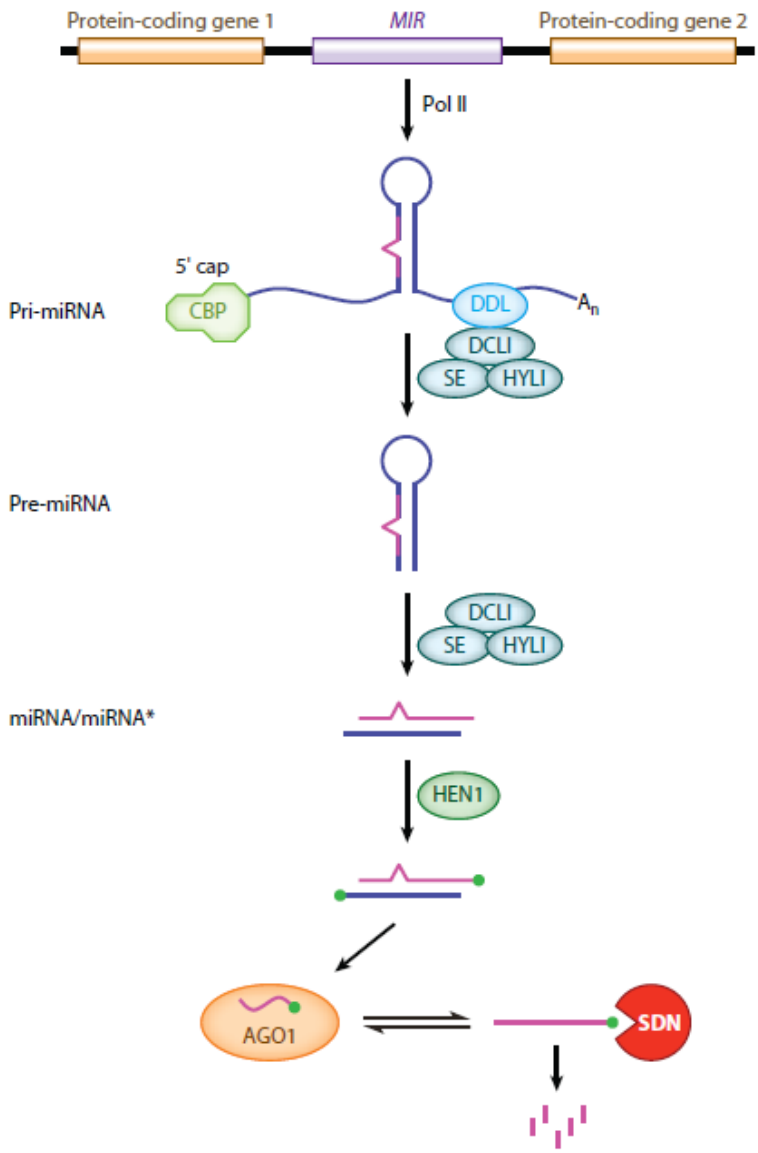

Figure 1-14 miRNA biogenesis in plants. As in animals, a miRNA is transcribed in the nucleus in a long pri-miRNA. However, no homologous proteins to Drosha can be found in plants, and this precursor is then processed by DCL1 together with HYL1 and SE. The mature miRNA duplex is then methylated by HEN1 and loaded into an AGO1 complex. See the text for further details. Reported from (Chen 2009).

A. Canonical intronic miRNA processing (Dicer-mediated)

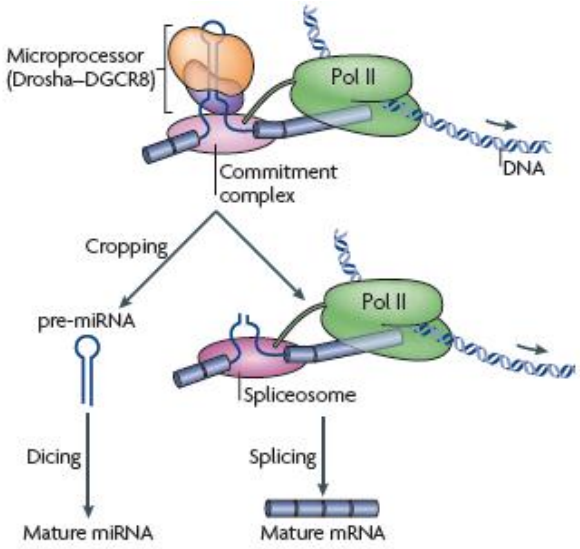

B. mirtron processing (Dicer-independent)

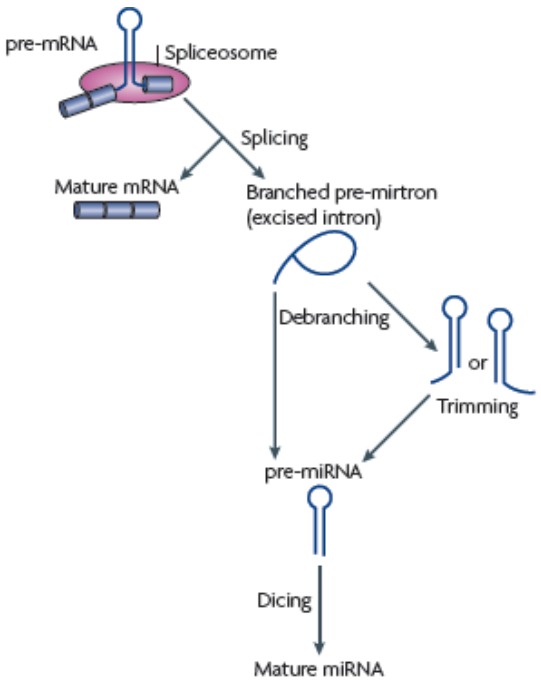

Figure 1-15 Maturation of canonical intronic miRNAs and mirtrons. (A) Canonical intronic miRNAs are processed by Drosha. In particular, this enzyme might be recruited together with the spliceosome complex and process the miRNA precursor before the intron is excised. On the contrary, non canonical pre-mirtrons are produced from spliced introns and debranching (B). This mechanism is mediated by Ldbr and bypasses the Drosha-processing step. Reported from (Kim, Han et al. 2009).

1.3.3.5 Biogenesis: Exportin-5 Mediates the Nuclear Export of Pre-miRNAs

Pre-miRNAs processed by Drosha and DGCR8 are then exported to the cytoplasm where the last steps of miRNA maturation take place. This nuclear export is efficiently mediated by Exportin-5 (Exp5), a member of the karyopherin family of nucleo-cytoplasmic transport factors (Yi, Qin et al. 2003) (Figure 1-13).

Several members of this family are involved in the nuclear export of non-coding RNAs, including tRNAs, snRNAs and rRNAs (Lei and Silver 2002; Cullen 2003), and Exp5 in particular can also mediate the export of adenovirus VA1 and tRNAs (Lee, Jiko et al. 2011). All these receptors possess a RanGTP-binding site (Ran is a GTPase enzyme), and the RanGTP gradient across the nuclear envelope is used as an energy source (Bohnsack, Czaplinski et al. 2004). Exp5 binds efficiently RanGTP and the pre-miRNA in the nucleus to form a hetero-trimeric complex and pass through the nuclear pore (Yi, Qin et al. 2003; Zeng and Cullen 2004; Wang, Xu et al. 2011) (Figure 1-16). Then, once in the cytoplasm, the Ran-GTP is hydrolysed to Ran-GDP resulting in the release of the pre-miRNA, further processed by Dicer. It is interesting to notice that Exp5 binding requires a ›14 bp RNA stem with a base-paired 5'and a short 3' overhang (Gwizdek, Ossareh-Nazari et al. 2003; Zeng and Cullen 2004) (Figure 1-16), while it shows a weak interaction with extended-pre-miRNAs that give incorrect mature miRNAs after Dicer processing *in vitro* (Lund, Guttinger et al. 2004; Zeng and Cullen 2004).

As expected, antibodies directed against Exp5 block pre-miRNA export decreasing its cytoplasmic concentration (Bohnsack, Czaplinski et al. 2004), but this doesn't result in pre-miRNA accumulation in the nucleus, suggesting that this miRNA precursor is relatively unstable (Bohnsack, Czaplinski et al. 2004; Zeng and Cullen 2004).

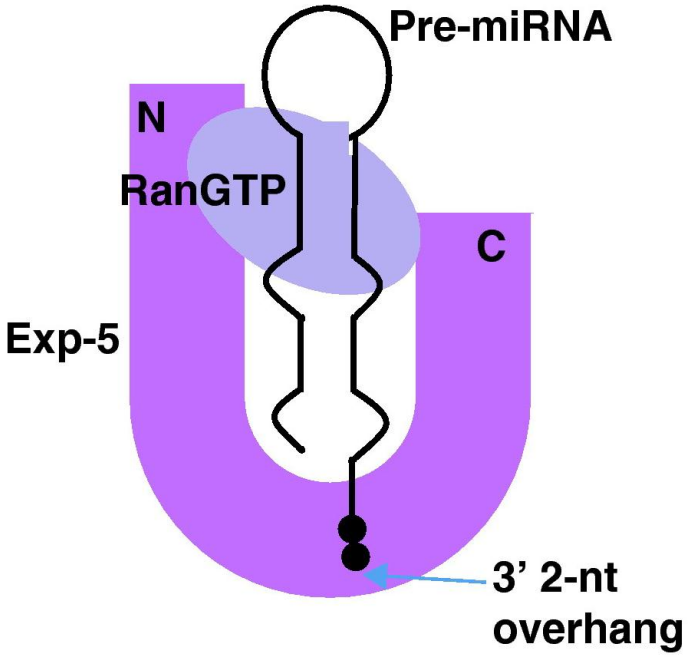

Figure 1-16 Schematic representation of Exp-5:RanGTP:pre-miRNA. Adapted from (Lee, Jiko et al. 2011).

1.3.3.6 Biogenesis: Cytoplasmic Processing and miRISC

Once exported to the cytoplasm, the pre-miRNA is loaded into the RISC (RNA Induced Silencing Complex) Loading Complex (RLC) (Figure 1-13 and Figure 1-17). The core of this complex is represented by the RNase III enzyme Dicer, TAR RNA-binding protein (TRBP), protein activator of PKR (PACT) and an Argonaute protein (AGO). This complex processes the pre-miRNA and selects the guide strand of the obtained ds mature miRNA to direct target-miRNA interaction (Gregory, Chendrimada et al. 2005).

As every typical class III RNase III enzyme, Dicer is characterized by the presence of two RNase III domains, one dsRBD, a DUF283 (domain of unknown function) and a PAZ (Piwi-Argonaute-Zwille) domain in the middle and a helicase/ATPase domain at the N-terminus (Figure 1-14). The PAZ domain binds specifically to the 3' two nucleotide overhang structure of the pre-miRNA (Song, Liu et al. 2003), anchoring the enzyme on the miRNA precursor with the right orientation allowing in this way its cleavage at a fixed distance from that end. The dsRNA generated by Dicer is normally 21 to 25 nucleotides (nt) long and contains a miRNA guide strand and a passenger strand. It has been shown in *Drosophila melanogaster* that loss of function mutations in this enzyme prevent the conversion of the pre-miRNA in its mature form (Lee, Nakahara et al. 2004), and double Knock-out (KO) mice die in early stages of development (Bernstein, Kim et al. 2003), proving its fundamental role in miRNA biogenesis. Moreover, it has been demonstrated the presence of a physical interaction of Dicer with Argonaute 2 (AGO2), responsible for the miRNA mediated post-transcriptional gene silencing, suggesting a role for this enzyme not only in miRNA maturation, but also in the formation of the RISC complex (Gregory, Chendrimada et al. 2005). In consideration of these evidences it is not surprising that Dicer levels are kept strictly under control in the cell, but it is interesting to observe that this regulation is miRNA mediated. In fact it has been reported that the let-7 miRNA family, and in particular let-7d, is able to regulate Dicer expression, constituting in this way a negative feedback loop, since Dicer is involved in let-7 maturation (Tokumaru, Suzuki et al. 2008).

Both the dsRNA-binding proteins TRBP and PACT have similar structures, with three dsRBDs that directly interact with each other and with Dicer (Figure 1-14). They do not have a direct role in miRNA processing like Dicer, but they both play a role in the

recruitment of the pre-miRNA and in the RISC assembly. In fact, their depletion only reduces the efficiency of miRNA maturation (Grishok, Pasquinelli et al. 2001; Haase, Jaskiewicz et al. 2005; Lee, Hur et al. 2006)

After the cleavage of the pre-miRNA, the 22 nt duplex miRNA remains associated with RISC, and the complex identifies the guide strand (Figure 1-13 and Figure 1-17). The mechanism behind miRNA unwinding, probably ATP-dependent, and the recruitment of the right strand is still largely unknown. However, the selection of a specific strand could be at least partially explained by the thermodynamic properties of the two ends of the duplex. In fact, the strand with a less stable 5' end (often due to the presence of uracils) is the one that is normally incorporated in the active RISC complex and represent the guide strand, while the passenger strand is degraded (Khvorova, Reynolds et al. 2003; Schwarz, Hutvagner et al. 2003). Another theory states that the two strands can be distinguished using their nucleotide sequence and secondary structure (Ahmed, Ansari et al. 2009). However, both the strands of the duplex are sometimes functional and can be incorporated in the RISC complex to target different mRNAs, as it has been recently described (Packer, Xing et al. 2008).

The active RISC complex forms with the selected ss mature miRNA the miRNA-induced silencing complex (miRISC), also called micro-ribonucleoproteins (miRNPs) complex (Filipowicz, Bhattacharyya et al. 2008) (Figure 1-13 and Figure 1-17). The main protein of the complex is again a member of the Argonaute family. This highly conserved family of proteins is characterized by a PAZ domain, which binds to the 3' end of guide RNA (Wang, Sheng et al. 2008; Jinek and Doudna 2009), a MID domain which provides a binding pocket for the 5'-phosphate end of the miRNA (Boland, Tritschler et al. 2010), and a PIWI domain, similar to RNase H, with endonuclease activity (also named "slicer" activity) (Jinek and Doudna 2009) (Figure 1-14). In humans there are 4 different Argonaute proteins (named AGO 1-4), and even if all of them show the same affinity to miRNAs, only AGO2 has endonuclease activity (Liu, Carmell et al. 2004; Meister, Landthaler et al. 2004) and can therefore cleave a target mRNA. However, if there is not perfect complementarity between the miRNA and the target, the mRNA may be physically unreachable by the active "slicer" domain of AGO2, resulting instead in mRNA destabilization or translational repression. Because of the low degree of complementarity observed in animals, it was suggested that translational repression is

more prevalent in animals than in plants (Rhoades, Reinhart et al. 2002; Jones-Rhoades, Bartel et al. 2006; Bartel 2009). The reason why a specific member of the AGO family is recruited in the active miRISC complex instead of the others still need to be clarified.

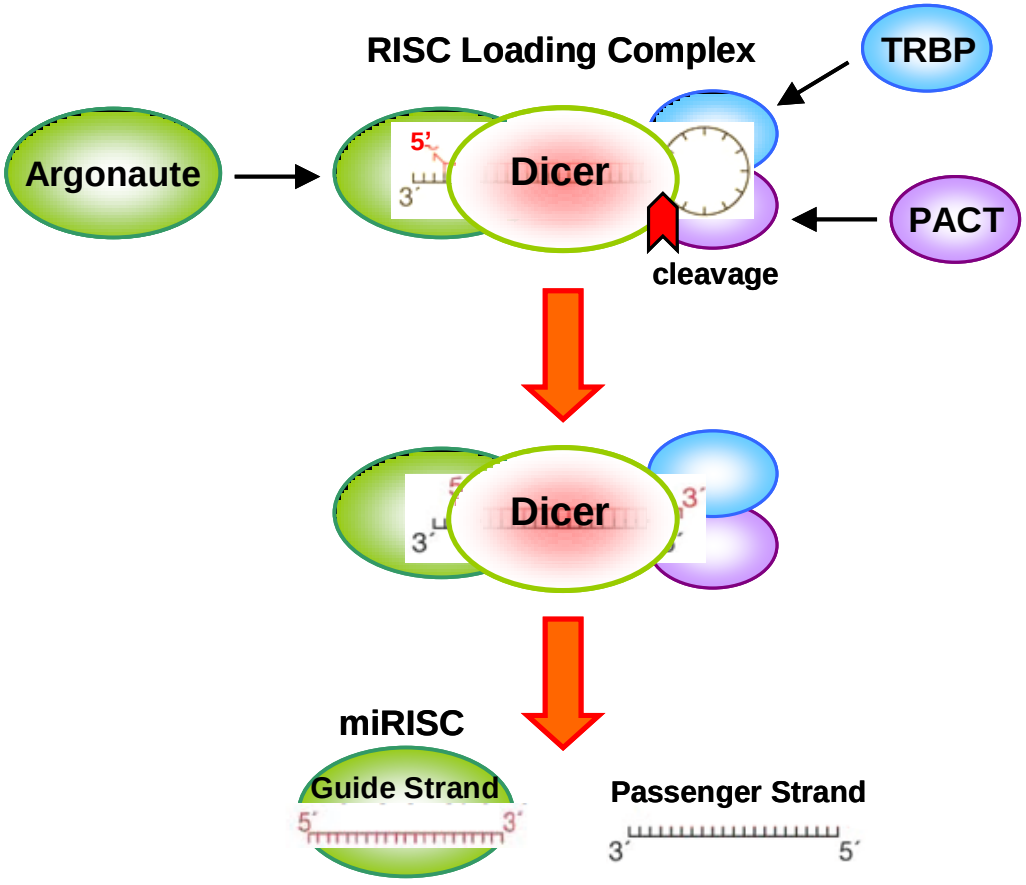

Figure 1-17 Cytoplasmic miRNA processing, RISC loading complex and miRISC. After export to the cytoplasm, pre-miRNA associates with the endonuclease Dicer and several other regulatory proteins, such as TRBP and PACT and a member of the Argonaute family. Dicer mediated cleavage results in production of about 20-nt-long miRNA/miRNA* duplex. After processing, the guide strand of the miRNA/miRNA* duplex is incorporated into the miRNA-induced silencing complex (miRISC), whereas the passenger strand (miRNA*) is degraded. In some cases, also the passenger strand may be included in the miRISC to function as mature miRNA.

1.3.3.7 miRNA-Mediated Gene Silencing

The most important part of a miRNA in its interaction with a mRNA target is the 5' portion. This has been hypothesize for the first time after the observation that in the 3'UTR of the target gene lin-14 there is a "core element" of complementarity to the 5' region of the lin-4 miRNA (Wightman, Ha et al. 1993), and the theory was confirmed when it became clear that residues 2-8 of miRNAs are the most conserved among homologous metazoan miRNAs (Lewis, Shih et al. 2003; Lim, Glasner et al. 2003). This miRNA portion was called "seed sequence" since it mediates target binding, and the introduction of mismatches in this core region can inhibit initial target recognition even if there is perfect complementarity elsewhere (Doench and Sharp 2004; Brennecke, Stark et al. 2005). Mostly miRNAs target sites located in the 3'UTR of a target gene, often in multiple copies (Jackson and Standart 2007).

A large number of bioinformatics databases can predict miRNA:mRNA interaction (i.e. TargetScan, EMBL, PicTar and Mirnada) using several criteria including stringent seed pairing, site number, site accessibility and overall predicted pairing stability (Bartel 2009). MiRNA target prediction in mammals show that about one third of genes might be miRNA regulated and each miRNA can regulate an overage of 100-200 target genes (Lewis, Burge et al. 2005; Lim, Lau et al. 2005). Moreover, different miRNAs can act in a cooperative way to regulate the same target, creating a miRNA network more difficult to figure out.

The mechanism behind miRNA ability to silence gene expression is still quite controversial. Two main models have been proposed, each of them supported by several evidences: mRNA degradation or mRNA translation repression. Moreover, both the initiation and the post initiation steps of translation have been identified as potential target of mRNA activity. Next sections summarize the experimental evidences supporting each model.

1.3.3.8 miRNA Activity: Inhibition of Translation Initiation

The hypothesis that miRNAs could block translation at some point of the initiation step was formulated for the first time in 2005, when Pillai et al. studied the activity of

endogenous let-7a in HeLa cells using a luciferase construct with three bulged target sites for this miRNA in its 3' UTR (Pillai, Bhattacharyya et al. 2005). 48 h after transfection they observed an 80-90% reduction in luciferase expression, but the mRNA abundance was decreased only of a 20%, suggesting that protein translation was somehow inhibited (Pillai, Bhattacharyya et al. 2005). Analyzing a sucrose gradient of polysome, they also observed the target mRNA in the same fraction of the 40s small ribosomal subunit, the first recruited during ribosome assembling, strongly suggesting an inhibition of the transcription initiation (Pillai, Bhattacharyya et al. 2005). The same result was obtained one year later in a study focused on miR-122 repression of the endogenous cationic amino acid transporter-1 in HuH7 cells (Bhattacharyya, Habermacher et al. 2006). Moreover, the Pillai et al. study showed that an active luciferase repression was obtained only in presence of a 7-methylguanosine (m^7GpppG)-capped polyadenylated target mRNA, while uncapped targets where completely resistant (Pillai, Bhattacharyya et al. 2005). This result was further investigated by Humphreys et al. in a study showing that not only uncapped mRNAs, but also nonpolyadenylated targets could not be efficiently repressed (Humphreys, Westman et al. 2005). They hypothesized that miRNA could block translation interfering with the formation of the "closed loop", a structure assumed by the mRNA to facilitates translation (Lomakin, Hellen et al. 2000; Kahvejian, Svitkin et al. 2005) and formed by the interaction of poly(A) binding proteins (PABPs), bound to the mRNA tail, with eIF (eukaryotic initiation factor) proteins, associated with the m^7GpppG-cap (Figure 1-18) (Humphreys, Westman et al. 2005). This theory was supported by the discovery that AGO2 is able to bind directly the m^7GpppG-cap with its MID region (Figure 1-19), homologous with a domain of the cap-binding eIF (eIF4E), antagonizing in a competitive way the interaction between the target mRNA and eIF4E (Kiriakidou, Tan et al. 2007). However this result has been recently challenged by two different manuscript (Eulalio, Huntzinger et al. 2008; Kinch and Grishin 2009), and for this reason this model will require further validations.

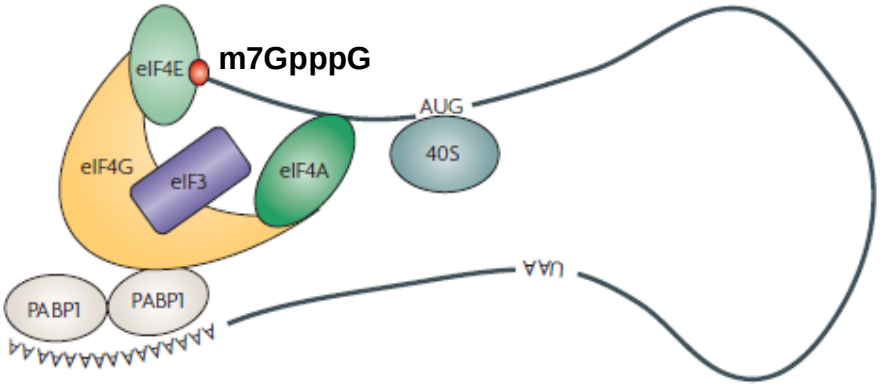

Figure 1-18 Schematic representation of the "closed loop". In this structure, PABPs, bound to the mRNA tail, interact with eIF proteins, associated with the m7GpppG-cap, to facilitate translation. Reported from (Filipowicz, Bhattacharyya et al. 2008).

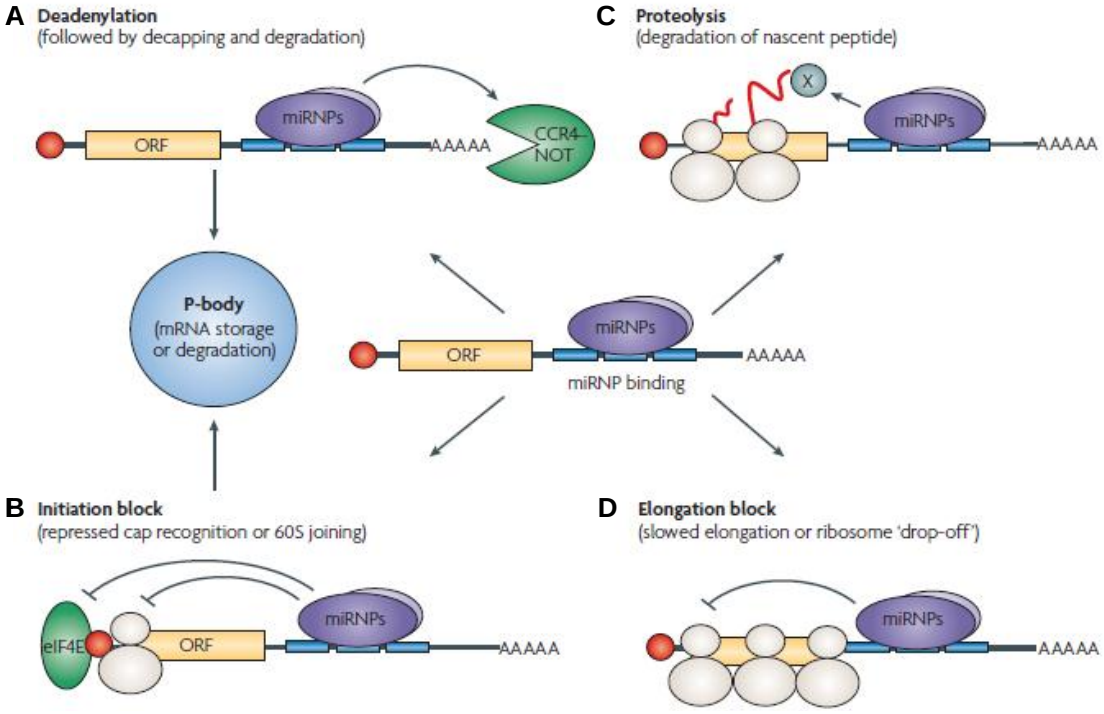

Figure 1-19 Possible mechanisms of the microRNA-mediated post-transcriptional gene regulation. After binding the 3'UTR of the target gene, a miRNA can induce deadenylation and decay of target (A), blocking of the translation initiation step (B), proteolytic cleavage of nascent polypeptides (C) or blocking of the translation elongation step (D). mRNAs repressed by deadenylation or at the translation-initiation stage are moved to P-bodies for either degradation or storage. Reported from (Filipowicz, Bhattacharyya et al. 2008).

1.3.3.9 miRNA Activity: Inhibition of Translation after Initiation

The first evidences of a possible miRNA-mediated inhibition of mRNA translation at some point after initiation were reported for the first time by Olsen et al., in a study focused on lin-4, the first discovered miRNA (Olsen and Ambros 1999). They observed that in the L2 and L3 larval stages of *Caenorhabditis elegans* development, when the expression of this miRNA is at its maximum, the amount of the target protein LIN-28 is reduced of a 90%, while the abundance of its mRNA is essentially unchanged (Olsen and Ambros 1999). For this reason they validated the hypothesis of a translational repression. However, when they analyzed a sucrose gradient of polysomes at L2-L3 stage, they identified the repressed lin-28 mRNA in the same fraction as in L1 extracted polysomes (when it is actively translated), suggesting that in both cases this mRNA is associated with active ribosomes and then active translation is already in progress when protein expression is inhibited (Olsen and Ambros 1999). Similar evidences were also obtained in 293T cells transfected with a luciferase construct with 6 bulged sites for let-7a in its 3'UTR (Petersen, Bordeleau et al. 2006). Cosedimentation of several miRNAs with polysomes has been considered a further confirmation of this theory (Kim, Krichevsky et al. 2004; Nelson, Hatzigeorgiou et al. 2004). A more detailed model was proposed by Petersen at al., suggesting that miRNAs could promote the premature termination of protein translation by inducing the dissociation of the ribosome from the mRNA (ribosome "drop-off") (Petersen, Bordeleau et al. 2006) (Figure 1-19). However, they failed to detect any nascent protein chain, introducing the hypothesis that miRNAs could also recruit specific protease to degrade newly synthesized peptides (Nottrott, Simard et al. 2006; Petersen, Bordeleau et al. 2006) (Figure 1-19).

1.3.3.10 miRNA Activity: Target mRNA Degradation

miRNA are often able to affect substantially the expression of their target despite marginal changes in the abundance of their mRNA are observed (Olsen and Ambros 1999; Pillai, Bhattacharyya et al. 2005). For this reason, for several years it was concluded that miRNA ability to regulate gene expression was only due to its capacity to interfere with mRNA translation. However, in the last years different publications reported a substantial decrease of target mRNA levels due to changes in miRNA

expression (Giraldez, Mishima et al. 2006; Rehwinkel, Natalin et al. 2006; Guo, Ingolia et al. 2010). First of all, repetition of some of the experiments originally performed in *Caenorhabditis elegans* (Olsen and Ambros 1999; Seggerson, Tang et al. 2002) surprisingly showed that lin-4 and let-7 are both able to promote extensive degradation of lin-14, lin-28 and lin-41 target mRNAs (Bagga, Bracht et al. 2005; Valencia-Sanchez, Liu et al. 2006). In addition, microarray analysis of mRNAs extracted from HeLa cells showed that expression of the brain-specific miR-124 and the muscle-specific miR-1 results in changes in the abundance of subsets of 100 to 200 different mRNAs in each case (Lim, Lau et al. 2005). miRNAs can induce such a decrease in mRNA abundance mediating the acceleration of target mRNA degradation through deadenylation followed by decapping (Behm-Ansmant, Rehwinkel et al. 2006; Schmitter, Filkowski et al. 2006; Wu, Fan et al. 2006; Wu, Thivierge et al. 2010) (Figure 1-19). In particular, deadenylation is able to destabilize a mRNA through disruption of the "closed loop" already described in section 1.3.3.8 (Figure 1-18), while decapping results in the degradation of the body of the mRNA by 5'-3' exonuclease activity (Behm-Ansmant, Rehwinkel et al. 2006; Schmitter, Filkowski et al. 2006; Wu, Fan et al. 2006).

AGO proteins, miRNAs and target mRNAs accumulate and can be detected in cytoplasmic foci known as P-bodies, or processing bodies (Liu, Valencia-Sanchez et al. 2005). These foci are composed by several different proteins, always including enzymes involved in mRNA decapping and decay (Sheth and Parker 2003). P-bodies are able to move within the cell cytoplasm, and can fluctuate in size and number. For example, inhibition of translation initiation can induce their increase in size and number, suggesting that only ribosomes-free mRNAs can localize to P-bodies (Brengues, Teixeira et al. 2005). In fact, it has been shown that mRNAs, and in particular mRNA decay intermediates are required for P-bodies integrity (Teixeira, Sheth et al. 2005). Thus, deadenylated mRNAs are internalized into P-bodies and therefore degraded (Kulkarni, Ozgur et al. 2010). However, entry of a mRNA into P-bodies not always leads to its degradation. This reversibility has been showed for the cationic amino acid transporter (CAT-1) mRNA, regulated by miR-122. In normal conditions miR-122 is able to reduce CAT-1 expression by a 65%, and both this miRNA and CAT-1 mRNA can be detected in P-bodies. However, if cells are amino acid starved, the mRNA cannot be longer detected in these loci, with a rapid increase in the amount

of CAT-1 protein (Bhattacharyya, Habermacher et al. 2006). This mRNA release requires a particular AU-rich element (ARE) in its 3'UTR, and the presence of the ARE binding protein HuR (Bhattacharyya, Habermacher et al. 2006). P-bodies can therefore be considered temporary repository for untranslated mRNAs, increasing the ability of miRNAs to finely regulate gene expression.

All the evidences presented in the previous sections suggest that mRNA degradation and inhibition of translation both contribute to miRNA-mediated gene silencing, and probably the relative importance of each mechanism is different in different systems and cell types.

1.3.3.11 miRNA Turnover

Considering the involvement of miRNAs in regulation of gene expression, it is not a surprise that their turnover is finely regulated too. First of all, during miRNA maturation only one of the two strands of the short RNA is preserved, the guide strand, while the passenger strand is normally rapidly degraded. It has been suggested that AGO proteins can stabilize the strand required for gene silencing, leading to degradation of the non-targeting strand (Kai and Pasquinelli 2010).

Very little it is known at the moment about miRNA half-life and degradation. However, decay of mature miRNAs in animals seem to be mediated by the 5´-to-3´ exoribonuclease XRN2, known as Rat1p in plants (Chatterjee and Grosshans 2009). Also 3´-to-5´ exoribonucleases have been identified in mammals, but their involvement in miRNA turnover still needs to be evaluated (Kai and Pasquinelli 2010). Several type of post-transcriptional modification can alter miRNA stability, including 3' methylation in plants with some evidences emerging in animals too, a mechanism able to block the addition of uracil (U) residues associated with miRNA degradation, and 3' adenylation in mammals and plants. This has been reported in particular for miR-122, a miRNA abundantly expressed in the liver and important in Hepatitis C, stabilized by the addition of an extra A to its end (Kai and Pasquinelli 2010). Alterations in the expression/stability of miRNAs are often associated with the development of different pathologies.

1.3.3.12 Effect of miRNA Dysregulation

1.3.3.12.1 miRNAs and Cancer

Cancer is nowadays considered the leading cause of death in the developed world, and even if several treatments are now available depending upon the specific type of malignancies, they are often damaging for the rest of the body (i.e. chemotherapy, radiation therapy) and not always effective for all the patients. In order to evaluate miRNA role in tumor development and growth, during the last years many groups of researchers focused their attention on alterations of non-coding sequences in cancer. Interestingly, several studies showed evidences of a global repression of miRNAs in different malignancies (Calin, Ferracin et al. 2005; Lu, Getz et al. 2005; Calin and Croce 2006; Cummins, He et al. 2006; Yanaihara, Caplen et al. 2006; Zhang, Volinia et al. 2008). The causes for this down-regulation are multifactorial and can involve each step of miRNA biogenesis. For example, a reduced expression of Dicer has been observed in lung cancer and adenocarcinoma (Karube, Tanaka et al. 2005; Chiosea, Jelezcova et al. 2007), while more recently Melo et al. identified mutations in the gene coding for Exp5 (XPO5) within different cancer cell lines harboring microsatellite instability (Melo, Moutinho et al. 2010). Re-introduction of a wild type form of the gene in these cells resulted in the up-regulation of several miRNAs previously repressed (Melo, Moutinho et al. 2010). Moreover, transcriptional factors can contribute to the down-regulation of specific miRNAs, including miR-17-92 cluster, regulated by the oncogene c-Myc (amplified in several types of human tumors) (O'Donnell, Wentzel et al. 2005; Chang, Yu et al. 2008).

One of the first evidences of an involvement of miRNA dysregulation in cancer was presented in 2002 by Calin et al. They showed that two miRNAs, miR-15a and miR-16-1, transcribed in cluster from human chromosome 13, are down-regulated in 68% of patients with chronic lymphocytic leukemia (CLL) (Calin, Dumitru et al. 2002). Further analysis demonstrated that this cluster can efficiently regulate the expression of Bcl2, an apoptosis regulator protein, and an increase in miR-15a/16-1 expression can lead cells to apoptosis (Cimmino, Calin et al. 2005).

Even if the majority of miRNAs is down-regulated in cancer, different examples of selective miRNA up-regulation have been reported as well. In breast cancer, an elevation in miR-103/107 expression has been associated with high metastatic phenotype, due to a functional targeting of Dicer (Martello, Rosato et al. 2010), while in lung cancer miR-21 up-regulation results in the silencing of different tumor suppression factors including PDCD4. A targeted deletion of miR-21 significantly reduces *in vivo* lung tumorigenesis (Hatley, Patrick et al. 2010).

The examples presented in this section show clearly that miRNAs can alter biological processes involved in cancer development. However, further studies will be necessary to evaluate if the manipulation of these short non-coding RNAs can be used to treat this complex disease.

1.3.3.12.2 miRNAs and Cardiovascular Diseases

The importance of miRNAs in cardiovascular development was demonstrated for the first time in mice, after the observation that a selective deletion of Dicer or DGCR8 coding genes in myocardial and vascular cells leads to a lethal phenotype (Chen, Murchison et al. 2008; Rao, Toyama et al. 2009). Despite that, no specific miRNA ablation has been found to be fully lethal in rodents, suggesting a redundancy in miRNA function. A thorough analysis of miRNA expression in the cardiovascular system revealed the existence of a relatively small group of miRNAs highly expressed in the heart, including miR-1, let-7, miR-133, miR-126-3p, miR-143, miR-30c and miR-22 (Lagos-Quintana, Rauhut et al. 2002). Between them, miR-1 was the first miRNA implicated in heart development, and together with the related miR-133, it shows a cardiac- and skeletal muscle-specific expression. miR-1 and miR-133 are transcribed from a common bicistronic precursor, and they are encoded from multiple, highly conserved loci in the genome. In particular, in the cardiac muscle they expression is regulated by serum response factor (SRF) and myocardin (Myocd) (Zhao, Samal et al. 2005), while in skeletal muscles they are controlled by myogenic differentiation factor (MyoD) and the myocyte enhancer factor-2 (MEF2) (Chen, Mandel et al. 2006; Rao, Kumar et al. 2006; Liu, Williams et al. 2007). This suggests an important role for transcription factors in the tissue-specific expression of miRNAs within the

cardiovascular system, composed by multiple cell lineages that must present peculiar physiological, electric and anatomic properties for a correct functionality of each region of the heart. Although many groups investigated the role of miR-1 and miR-133, their function is still unclear. For example, they have been shown to act synergistically to promote mesoderm differentiation of embryonic stem (ES) cells (Ivey, Muth et al. 2008), while in cultured myoblasts, miR-1 promotes differentiation and miR-133 induces proliferation (Chen, Mandel et al. 2006).

Considering the involvement of miRNAs in the development of a normal heart, it is not a surprise that miRNA expression is specifically altered in heart diseases. An example of this is represented by cardiac hypertrophy, characterized by an extensive remodelling of the heart. In fact, a significant up-regulation in miR-195 expression has been identified in human and mouse hypertrophic hearts, and a further increase in the expression of this miRNA leaded to heart failure in mice within 2 weeks of birth (van Rooij, Sutherland et al. 2006). Also, transgenic over-expression of miR-208a in the heart was sufficient to induce hypertrophic growth in mice (van Rooij, Sutherland et al. 2007; Callis, Pandya et al. 2009).

miR-21 has been identified as a target for heart failure, being increased selectively in cardiac fibroblasts extracted from the failing heart. In particular, miR-21 regulates the ERK–MAP kinase signaling pathway through inhibition of sprouty homologue 1 (*Spry1*), and *in vivo* silencing of this miRNA leads to an attenuation of cardiac dysfunction (Thum, Gross et al. 2008).

miRNA dysregulation has also been reported in cardiac fibrosis, a dysfunction induced by an inappropriate secretion of extracellular matrix from cardiac fibroblasts. A substantial down-regulation of miR-29 was observed in affected tissues, suggesting a potential beneficial effect of the up-regulation of this miRNA (van Rooij, Sutherland et al. 2008).

Finally, also angiogenesis, responsible for the adequate blood supply to the tissues, is affected by miRNA dysregulation. First of all, Dicer deficiency is lethal in mice, leading to abnormalities in the development of the blood vessel network (Kuehbacher, Urbich et al. 2007). In particular, 3 miRNAs (miR-21, miR-143 and miR-145) have been

implicated in the last years in vascular smooth muscle cell (VSMC) differentiation and proliferation, acting on specific targets. Cheng et al. reported that miR-21 (more information about it will be reported in chapter 5), is up-regulated in vessels during neointima lesion formation and is able to increase VSMC proliferation and reduce apoptosis *in vitro*. Two main targets of this miRNA have been involved so far in this process, the tumor suppressor gene PTEN (Phosphatase and tensin homolog) (Ji, Cheng et al. 2007) and PDCD4 (Programmed cell death protein 4) (Zhang 2009). On the other hand, miR-143 and miR-145 (described in details in chapter 4) are selectively expressed in VSMCs of arterial walls, and they have been recently presented as novel biomarkers and modulators of VSMC phenotype (Cheng, Liu et al. 2009). Their targets include Kruppel-like factor 4 and 5 (KLF4 and KLF5), and also the angiotensin-converting enzyme (ACE), all implicated in the effect of miR-143 and miR-145 on VSMCs behavior (Boettger, Beetz et al. 2009; Cheng, Liu et al. 2009; Cordes, Sheehy et al. 2009). Two different studies reported a dedifferentiated state of VSMCs in miR-143/miR-145 deficient mice (Boettger, Beetz et al. 2009; Elia, Quintavalle et al. 2009), and a decreased blood pressure was observed in these animals, due to a reduced contractile ability of the vessels (Boettger, Beetz et al. 2009; Xin, Small et al. 2009). However, while Boettger et al. observed a substantial neointima lesion formation in miR-143/miR-145 KO mice (Boettger, Beetz et al. 2009), Xin et al. reported a reduced neointima formation after carotid artery ligation in the same mouse model (Xin, Small et al. 2009), suggesting that further studies will be necessary to better understand the role of these miRNAs in VSMC differentiation and angiogenesis.

1.3.3.12.3 miRNAs as Biomarkers

An early detection of cancer is often crucial to improve treatment outcomes. For this reason, during the last few years a big effort has been placed in the identification of novel, easily accessible, non-invasive biomarkers.

The possibility to extract and analyze miRNAs from body fluids including serum was shown for the first time in 2008 (Lawrie, Gal et al. 2008). The analysis of these short non-coding RNAs proved their capacity to resist to harsh treatments such as boiling, low/high pH and freeze-thaw cycles and also to resist to Rnase A digestion (Chen, Ba et

al. 2008; Gilad, Meiri et al. 2008; Mitchell, Parkin et al. 2008). Although the origin of cell-free miRNAs is still unclear, two theories have been formulated. The first theory suggests that tissue injury could lead to a passive release of miRNAs in the body fluids. This has been observed for miR-208, normally expressed selectively in the heart, but detected also in the serum after a heart injury (Ji, Takahashi et al. 2009). The second theory derives from the recent observation that mRNAs and miRNAs can be transported from a cell to another within microvesicles known as exosomes to regulate gene expression (van Niel, Porto-Carreiro et al. 2006; Valadi, Ekstrom et al. 2007). This hypothesis could explain the reason why cell free miRNAs are protected against Rnase activity.

While in healthy individuals cell free miRNA levels stay stable in the serum (Chen, Ba et al. 2008; Mitchell, Parkin et al. 2008), selective dysregulations have been identified in specific malignancies. For example, high levels of miR-21 have been detected in the serum of patients with B-cell lymphoma (Lawrie, Gal et al. 2008), while analysis of serum from leukemia patients showed a substantial reduction in miR-92a detection (Tanaka, Oikawa et al. 2009). A significant dysregulation of circulating miRNAs has also been detected in early stage colon cancer patients, suggesting that these new biomarkers could become very important for the detection of tumors when they are still clinically asymptomatic (Huang, Huang et al. 2010). More recently, dysregulation of specific miRNAs has been observed in the serum of patients affected by cardiomyopathy (i.e. miR-1 and miR.133a) and cardiovascular diseases such as coronary artery disease (i.e. miR-133a, miR.208a and miR-92a) suggesting that circulating miRNAs could become important biomarkers for the diagnosis of cardiovascular pathologies and heart failure (Fichtlscherer, De Rosa et al. 2010; Kuwabara, Ono et al. 2011).

Unfortunately, miRNA extraction from serum is still technically challenging, mainly due to the low concentration of circulating miRNAs often observed in fluids. In fact, several miRNAs are extremely low concentrated in serum, and the extracted material results therefore difficult to quantify (Chen, Ridzon et al. 2005). Moreover, due to the absence of validated endogenous controls, the normalization of Real-Time PCR analysis of these cell-free miRNAs is often a critical issue. Several studies selected miR-16 as the most appropriate endogenous control because of its stable and widespread expression in

many tissues and in serum (Wang, Chen et al. 2009; Heneghan, Miller et al. 2010), but its dysregulation in specific malignancies has been reported too (Lodes, Caraballo et al. 2009), suggesting that an improvement in circulating miRNAs extraction and analysis is still needed.

1.3.3.12.4 miRNA-Based Therapies

In the previous sections we have described the deep involvement of miRNAs in post-transcriptional gene regulation and we have reported several examples of miRNA dysregulation in severe pathologies. Despite that, the specific role of most miRNAs is still unclear. Loss of function studies have always been considered very helpful to improve our knowledge about a genomic sequence, however generating genetic KOs for specific miRNAs is often difficult, in particular for those non-coding sequences expressed from multiple genomic loci or coded in the intronic region of a gene. For this reason, alternative strategies have been developed in the last few years to regulate post-transcriptionally a miRNA.

The first strategy developed to efficiently repress the activity of a miRNA requires the use of ss-antisense oligonucleotide (ASOs) complementary to the miRNA sequence and therefore able to sequester it (Figure 1-20). Multiple steps of miRNA maturation can be targeted in this way, with the design of ASOs directed against the Pri-, the Pre- or the mature miRNA of interest (Esau 2008). Several modifications to protect ASOs against nuclease degradation and to improve affinity for the target miRNA have been tested, including 2' sugar or 2'fluoro modifications (Esau 2008). DNA oligonucleotides containing locked nucleotides (LNAs) have also been shown to efficiently inhibit miRNA activity. In particular, these LNA/DNA mixmer can form highly stable and sequence specific duplexes with their targets due to their higher melting temperature (Tm) (Orom, Kauppinen et al. 2006). A third class of oligonucleotides used for miRNA silencing is then represented by the "antagomiRs", cholesterol-conjugated single-stranded RNA analogues complementary to a miRNA target (Krutzfeldt, Rajewsky et al. 2005). All these sequences can be efficiently transfected *in vitro* but also intravenous (i.v.) (Krutzfeldt, Rajewsky et al. 2005) or intraperitoneally (i.p.) (Esau 2008) injected *in vivo* for miRNA silencing. The efficiency of ASOs has also been demonstrated *in vivo*

when delivered to the lung by inhalation (Duan, Chan et al. 2005). Alternatively, a stable loss of function can be achieved by virus-mediated transfer (Scherr, Venturini et al. 2007).

A different strategy has been recently developed to efficiently silence entire miRNA seed families through the use of competitive inhibitors called “miRNA sponges”. These competitive inhibitors are represented by transgene sequences expressed from a strong promoter and containing multiple, tandem binding sites to a miRNA of interest in their 3’UTR (Ebert, Neilson et al. 2007). These chemically synthesized RNAs can be expressed transiently from transfected plasmids or stably inserted in the genome by lentiviral vectors (Gentner, Schira et al. 2009). Since the binding sites can interact efficiently only with the seed sequence, all the miRNAs sharing the same seed region will be efficiently sequestered by the sponge. Alternatively, combinations of seed binding sites for two or more miRNAs of interest can be cloned in the 3’UTR of the transgene for a multiple silencing effect (Ebert, Neilson et al. 2007). The existence of natural endogenous miRNA sponges able to fine-tune the activity of a miRNA was first showed in plants and recently also in mammalian (Franco-Zorrilla, Valli et al. 2007; Ebert and Sharp 2010; Poliseno, Salmena et al. 2010).

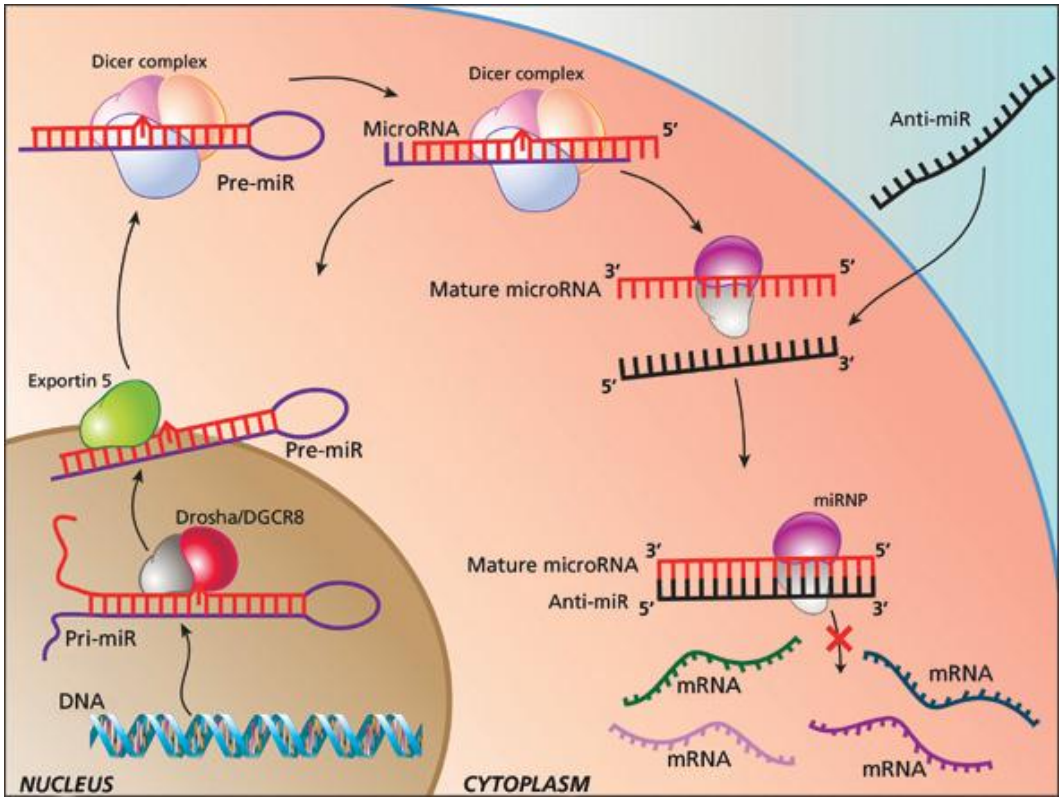

Figure 1-20 ASOs pharmacologically modulate microRNAs activity. The antisense oligonucleotide (black) binds the mature microRNA (red), blocking its function within the cell. Obtained from PharmTech (http://pharmtech.findpharma.com/pharmtech/article/).

1.4 Aims

The principle research aim of this work was to investigate the role of miRNAs in the development of PAH. This may offer insight into the pathobiology and the genetic basis of PAH, generating the possibility of new treatments. This was evaluated through investigation of the following experimental study aims:

- *In vivo* and *in vitro* characterisation of global miRNA expression profile in two different rat models of PAH and identification of specific miRNAs potentially involved in the development of the pathology;

- *In vivo* analysis of the effects of the genetic ablation of specific miRNAs (i.e. miR-145 and miR-21) in the development of PAH;

- Evaluation of the role of the TGF-*beta* superfamily on miRNA regulation via in vitro TGF-*beta*/BMP4 stimulations and BMPR2 manipulation.

2. Materials and methods

2.1 Chemicals

All chemicals, unless otherwise stated, were obtained from Sigma-Aldrich (Poole, UK) and were of the highest grade obtainable. All cell culture reagents were obtained from Gibco (Invitrogen, Paisley, UK) unless otherwise indicated. Dulbecco's calcium and magnesium free phosphate buffered saline (PBS) was obtained from Lonza (Lonza Group Ltd, Basel, Switzerland). All oligonucleotides were obtained from MWG-Biotech (Edersberg, Germany).

2.2 Cell Culture

All tissue culture work was performed using a biological safety class II vertical laminar flow cabinet in sterile conditions. Cell lines were grown as a monolayer, maintained in the appropriate cell culture media (described below in detail) and incubated at 37°C in a 5% CO_2 atmosphere. Cells were routinely passaged when monolayer cell growth reached 90% confluency, to prevent cell growth arrest via contact inhibition. Briefly, cells were washed twice in PBS and incubated in a minimal volume of trypsin-EDTA at 37°C, 5% CO_2 for approximately 5 min in order to detach cells. The action of trypsin-EDTA was inhibited by the addition of an equal volume of media containing fetal calf serum (FCS). Cells were harvested by centrifugation at 500 × g for 5 min and resuspended in fresh media for passaging or plating.

2.2.1 Isolation and Culture of Primary Rat Pulmonary Artery Fibroblasts

Rat pulmonary artery fibroblasts (RPAFs) were extracted from male Wistar rats (specific pathogen free, Harlan UK Ltd, 6 weeks old; 300-400g) using the technique of Freshney as previously described (Peacock, Dawes et al. 1992). Cells were maintained in Dulbecco's modified Eagle medium (DMEM) containing 10% (v/v) FCS,

supplemented with penicillin/streptomycin (100 U/ml and 100 μg/ml respectively) and L-glutamine (27 mg/ml) and used at passage 4.

2.2.2 Isolation and Culture of Primary Rat Pulmonary Artery Smooth Muscle Cells

Rat pulmonary artery smooth muscle cells (RPASMCs) were derived from small precapillary pulmonary arterioles using an iron oxide magnetic separation method, as previously described (Sobolewski, Jourdan et al. 2004). Cells were maintained in DMEM containing 10% (v/v) FCS, supplemented with penicillin/streptomycin (100 U/ml and 100 μg/ml respectively) and used at passage 4.

2.2.3 Primary Culture of Human Pulmonary Artery Endothelial Cells

Human Pulmonary Artery Endothelial Cells (HPAECs) were obtained from Lonza (Lonza Group Ltd, Basel, Switzerland) and cultured by following the supplier's instructions. Briefly, cells were maintained in EGM®-2 Endothelial Cell Growth Medium-2 (Lonza Group Ltd, Basel, Switzerland) containing 2% (v/v) FCS, supplemented with penicillin/streptomycin (100 U/ml and 100 μg/ml respectively) and used at passage 3.

2.2.4 Primary Culture of Human Pulmonary Artery Fibroblasts

Human Pulmonary Artery Fibroblasts (HPAFs) were obtained from ScienCell (Carlsbad, CA, USA). Cells were cultured by following the Supplier's instructions. They were maintained in Fibroblast Medium (ScienCell, Carlsbad, CA, USA) containing 2% (v/v) FCS and supplemented with penicillin/streptomycin (100 U/ml and 100 μg/ml respectively). Cells were used at passage 3.

2.2.5 Isolation and Culture of Primary Human Pulmonary Artery Smooth Muscle Cells

Human pulmonary artery smooth muscle cells (HPASMCs) were kindly provided by Prof N.W Morrell, University of Cambridge, UK. They were explanted from peripheral arteries as previously described (Yang, Long et al. 2005). Smooth muscle cell lines were obtained from 4 patients with PAH known to harbour a mutation in *BMPR2*. These included: 1 patient with a mutation in the kinase domain of *BMPR2* in which arginine is substituted for cysteine at position 347 (C347R); 1 patient with a missense mutation in the cytoplasmic tail of *BMPR2*, leading to a serine in place of asparagine at position 903 (N903S); 1 patient with a truncating mutation at amino acid position 9 (W9X) and 1 patient with a truncating mutation at amino acid position 899 (R899X). Three further PASMC preparations were obtained from macroscopically normal lung biopsies excised from non-PAH donors as unaffected controls. Cells were cultured as previously described (Yang, Long et al. 2005). Briefly, cells were maintained in DMEM containing 10% (v/v) FCS, supplemented with 2 mM L-glutamine and penicillin/streptomycin (100 U/ml and 100 μg/ml respectively) and used at passage 4.

2.2.6 Cell Freezing/Thawing

Cells were harvested as described in Section 2.2 and then resuspended in 1 ml of Cryopreservation Medium (DMEM containing 10% (v/v) FBS and 10% (v/v) dimethyl sulphoxide (DMSO) for RPAFs, RPASMCs and HPASMCs. EGM®-2 Endothelial Cell Growth Medium-2 containing 2% (v/v) FBS and 10% (v/v) DMSO for HPAECs). The resuspended cells were placed in a 2 ml cryo-preservation vial and left on ice for 1 h followed by a -80°C freezer overnight. The cryo-preservation vials were then transferred in liquid nitrogen for long term storage. Frozen cells were removed from liquid nitrogen and thawed rapidly in a water bath at 37°C, then transferred in a 15 ml centrifuge tube containing the appropriate pre-warmed cell culture media (as specified above). The tubes were centrifuged at 500 × g for 5 min to pellet the cells and remove the DMSO. Cells were then resuspended in 10 ml of fresh growth media and seeded onto T-25 flasks. The following day they were placed in fresh media.

2.2.7 Growth of cells in a hypoxic environment

A humidified temperature-controlled incubator (LEEC model GA156; Colwick, Nottingham, UK) was used as a hypoxic chamber. This incubator allows control of internal oxygen levels between 0 and 21% while CO_2 level is simultaneously controlled at 5%. For the experiments of chapter 3, RPAF, RPASMCs, HPAFs and HPAECs were transferred to 6-well plates at approximately 80% confluence and kept in 5% oxygen for 24 h before extracting total RNA for checking miRNAs expression level.

2.2.8 TGF-beta and BMP4 RPASMCs stimulation

Passage 4 RPASMCs were cultured in 6-well plates in the appropriate growth media (as specified in Section 2.2.2). After 24 h the media was replaced with 0.1% FCS media and cells incubated for a further 24 h. Wells were then incubated with 1 ng/ml of TGF-beta (R&D Systems**,** Minneapolis, MN, USA) or 10 ng/ml of BMP4 (R&D Systems**,** Minneapolis, MN, USA) or with DMEM containing 0.1% FCS as a negative control. Total RNA was extracted after 5 and 24 h of stimulation and stored for TaqMan® Real-Time PCR analysis of miRNA expression.

2.2.9 Down-regulation of BMPR2 expression with a si sequence

PASMCs were seeded in 6-well plates (1.5 x 10^5 cells/well) and grown for two days in DMEM/10% FBS. Prior to transfection, PASMCs were incubated in Optimem I for 3 h. PASMCs were transfected with a final concentration of 10 nM siRNA (Dharmacon™ On-TARGETplus siRNA for *BMPR2*, or siControl Nontargeting Pool, Perbio Science UK Ltd) in complex with DharmaFECT1™ (4ml/well) diluted in Optimem I. The Dharmafect was incubated in half the final volume (200 μl for 1 well) of Optimem I for 5 min followed by addition of Optimem I (200 μl for 1 well) containing 10X final concentration of the relevant siRNA, making the siRNA at 5X final concentration. The mix was incubated for 20 min at room temperature to allow lipoplexes to form. The Transfection mix (400 μl/well) was dropped onto cells in fresh Optimem I (1.6ml/well), ensuring full coverage of the well. Cells were incubated with the complexes for 4 h at 37°C, followed by replacement with DMEM/10% FBS for 24h. RNA was extracted after 72 h.

2.3 Development of hypoxia-induced PAH in rats and mice

The development of hypoxia-induced PAH was obtained in rats and mice using a hypobaric hypoxic chamber. Following acclimatization, mice were exposed to 550 mbar for a continuous period of 14 days and rats up to 21 days. As a consequence of atmospheric depressurization from ≈ 1000 mbar (ambient room pressure) to 550 mbar, oxygen availability is decreased from 21% O_2 to 10% O_2, inducing the development of PAH. Temperature (21-23 °C) and relative humidity (30-50%) were maintained within a normal range and all the animals were re-housed with clean bedding and food/water every week.

2.4 Animals, treatments and tissue collection

For the rat study of chapter 3, WT male Sprague-Dawley rats (6-7 weeks old; 250-300 g) were used throughout. All protocols and surgical procedures were approved by the local animal care committee and performed under the project license held by Dr Nicholas W. Morrell (University of Cambridge, UK). For the induction of PAH due to chronic hypoxia, groups of rats were maintained in a normobaric hypoxic chamber (as described in the previous paragraph) for up to 21 days. In the monocrotaline model, animals received a single subcutaneous injection of monocrotaline (60 mg/kg). To characterize miRNAs expression in PAH, animals were sacrificed at 2, 7 and 21 days immediately after the rats were anesthetized (intramuscular ketamine 75 mg/kg and zylazine 6mg/kg). Rats were exsanguinated and the lungs were removed and snap frozen in liquid nitrogen for further analysis.

For the experiments based on *BMPR2* mutated mice in chapter 4 and chapter 5 (Sections 4.2.6 and 5.2.4), mice harbouring a heterozygous truncating mutation in *BMPR2* were used to further determine the regulation of miR-143, miR-145 and miR-21 and kindly provided by Dr Nicholas W. Morrell (University of Cambridge, UK). These mice, similar to previously described R899X transgenic mice (West, Harral et al. 2008) develop spontaneous pulmonary hypertension. Lung tissue was harvested from R899X+/- mice (strain C57BL/6J, 6 months of age, 25 to 30 g body weight) and WT littermates for miR-143, miR-145 and miR-21 expression and for *in situ* hybridization

studies. Animal experiments were reviewed and approved by the local animal care committee and performed under the project license held by Dr Nicholas W. Morrell (University of Cambridge, Cambridge, UK). To assess miRNA expression level, animals were sacrificed with an injection of Euthatal (Chemindustry, Monrovia, CA, USA). The solution is administered at the rate of 1 ml per 1.4 Kg body weight (≈ 150 mg/Kg body weight). Then the thoracic cavity was opened to expose heart and lung, isolated after the excision of the carotid. Lungs were dissected out and snap frozen in liquid nitrogen for RNA extraction or fixed in 10% (v/v) neutral-buffered formalin (NBF, 10% (v/v) formalin, 33 mMol/L NaH_2PO_4, 45 mMol/L Na_2HPO_4) for three days, under gentle agitation and then embedded in paraffin for histological analysis.

For the miR-145 KO mouse study of chapter 4 and the miR-21 KO mouse study of chapter 5, mice were generated as previously described (Xin, Small et al. 2009; Patrick, Montgomery et al. 2010) and kindly provided by Dr Olson (University of Texas Southwestern Medical Center, Dallas, Texas, USA). All the experiments were reviewed and approved by the local animal care committee in Glasgow, UK, and performed under the project license held by Prof. Margaret R MacLean (University of Glasgow, UK), Licence No. 60/3773. Briefly, the genomic region coding for the pre-miR-145 or the pre-miR-21 was replaced with a neomycin resistance cassette flanked by loxP sites through homologous recombination. The neomycin resistance cassette was then removed by breeding these mice with mice expressing the Cre transgene. Homozygous aged matched miR-145-/- (or miR-21-/-) female mice or WT matching controls (strain C57BL6J/129SVEV, 8 weeks of age, 25 to 30 g body weight) were exposed to chronic hypoxia for 14 days (as described in section 2.3) or maintained in normoxic conditions and analyzed at 10 weeks of age. To assess vascular remodelling and miRNA/target expression, animals were sacrificed with an injection of Euthatal (Chemindustry, Monrovia, CA, USA) and the lung isolated as previously described in this section. The extralobar branch of the pulmonary artery (PA) was excised from its insertion into heart and lungs and snap frozen in liquid nitrogen. Lungs, hearts, kidneys, brains and spleens were collected and snap frozen in liquid nitrogen or fixed in 10% (v/v) neutral-buffered formalin (NBF, 10% (v/v) formalin, 33 mMol/L NaH_2PO_4, 45 mMol/L Na_2HPO_4) for three days, under gentle agitation and then embedded in paraffin for histological analysis.

2.5 Assessment of PAH

2.5.1 Haemodynamic Measurements

The induction of general anaesthesia was performed via exposure to 3% (v/v) isoflurane supplemented with O_2. Mice were immediately weighed and 1-2% (v/v) isoflurane continuously administered via a facemask to maintain general anaesthesia. General anaesthesia was confirmed by the absence of a hind-limb and tail reflex. These reflexes were also routinely assessed throughout surgery. Following confirmation of general anaesthesia, both right ventricular pressure (RVP) and systemic arterial pressure (SAP) were measured.

2.5.2 Right Ventricular Pressure Measurement

RVP was measured via a transdiaphragmatic approach. The continuous measurement of RVP was assessed via a heparinised saline-filled calibrated 25-gauge needle attached to an Elcomatic E751A pressure transducer connected to a MP100 data acquisition system (BIOPAC Systems Inc, Santa Barbra, USA). Briefly, the anterior sternum was exposed removing a portion of skin from the ventral chest. The 25-gauge needle was then advanced through the mid-portion of the sternum, into the abdomen. A negative pressure reading was obtained in consequence of the entry into the diaphragm, then the needle was advanced directly into the right ventricle via puncture through the right ventricular free wall. This was confirmed by the characteristic pressure waveform typically observed inside the right ventricle (Figure 2-1). From this recording, kept stable for up to 20 min, systolic RVP (sRVP) was deduced and used as an index of PAH.

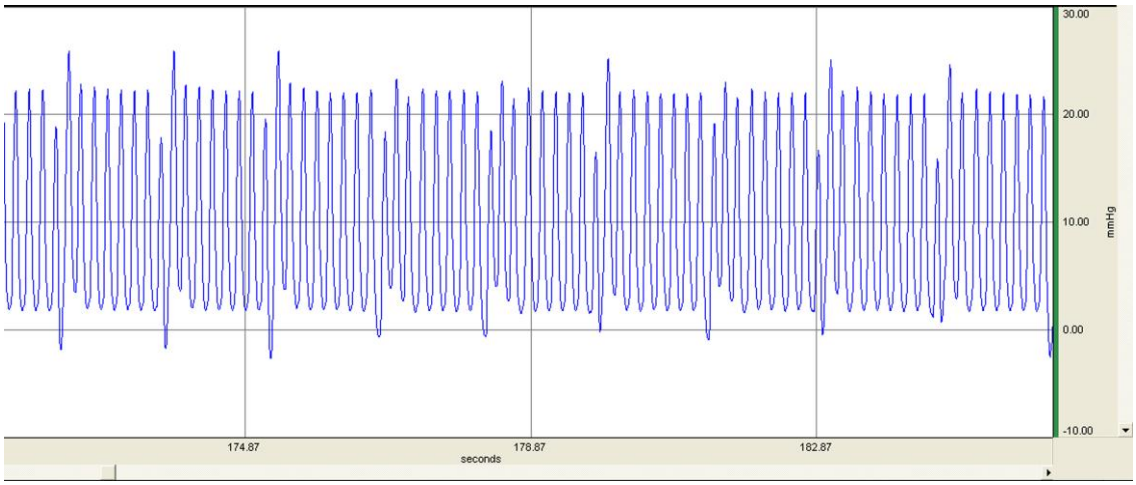

Figure 2-1 Representative recording of right ventricular pressure. Representative measurement of right ventricular pressure in mice. Y-axis expressed in mmHg.

2.5.3 Systemic Arterial Pressure Measurement

Systemic Arterial Pressure (SAP) was measured via cannulation of the left common carotid artery. Briefly, the trachea was exposed via skin incision through the ventral neck. Lateral blunt dissection was performed through the muscle lying inferior to the trachea. The left common carotid artery is typically positioned ≈ 2 mm lateral (left) and less than 1 mm posterior to the trachea. The artery was carefully separated from both the vagus nerve and the recurrent laryngeal nerve. Distal suture (7-0 silk non-braided) was used for isolation of the artery and an arterial clip positioned at the most proximal arterial segment to temporarily occlude blood flow through the lumen. Following incision through the arterial wall, a heparinised saline-filled polypropylene cannula (Harvard Apparatus, Boston, USA) was proximally inserted 4-5 mm into the lumen and secured using suture. As for the RVP measurement, the systemic arterial cannula was also attached to an Elcomatic E751A pressure transducer connected to a MP100 data acquisition system (BIOPAC Systems Inc, Santa Barbra, USA) allowing the recording of the SAP (Figure 2-2). Following measurement of RVP and SAP, mice were killed by cervical dislocation.

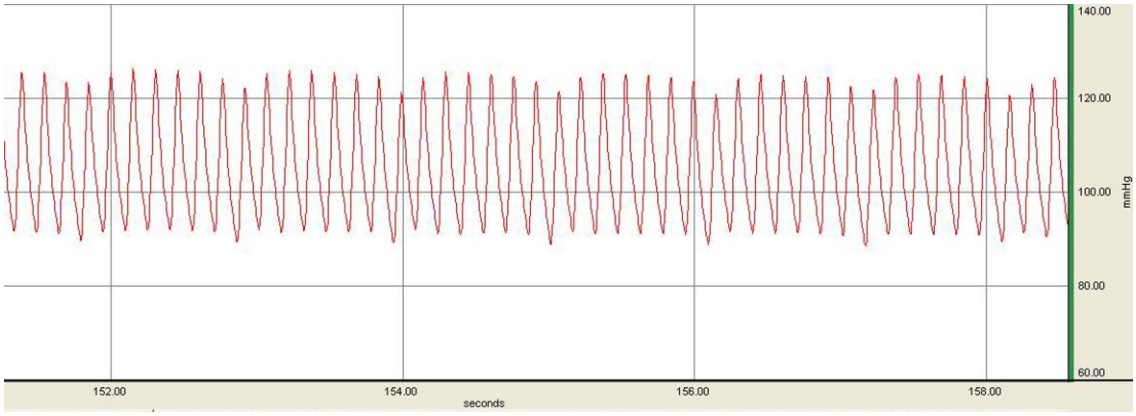

Figure 2-2 Representative recording of systemic arterial pressure. Representative measurement of systemic arterial pressure in mice. Y-axis expressed in mmHg.

2.5.4 Right Ventricular Hypertrophy Measurement

The atria, large blood vessels and pericardial fat were dissected free from the ventricles. The right ventricular free wall (RV) was dissected from the left ventricle plus septum (LV+S) and both were weighted in order to assess right ventricular hypertrophy (RVH). The ratio RV/LV+S has been used as an index of PAH (MacLean, Deuchar et al. 2004; Morecroft, Pang et al. 2010).

2.5.5 Pulmonary Vascular Remodelling Assessment

Three 5 µm sagittal sections of lung were elastic-Van Gieson stained and microscopically assessed for the muscularisation of pulmonary arteries (<80 µm external diameter) in a blinded fashion. The presence of double elastic laminae allowed the individuation of the remodelled arteries. Lung sections from 5 mice for each group were analyzed. Approximately 150 arteries from each sagittal lung section were assessed. This was expressed as a percentage of pulmonary vascular remodelling

(remodelled vessels/total pulmonary vessels x 100 = % pulmonary vascular remodelling).

2.6 DNA extraction from mouse tissue

In order to verify the genotype of miR-145 (or miR-21) KO mice used in chapter 4 (or chapter 5), genomic DNA was isolated from tissue samples using the QIAamp DNA Mini Kit (Qiagen, CA, USA) following the manufacturer's instructions. Briefly, mouse ear clips were placed in 200 μl SDS-containing lysis buffer with proteinase K and incubated overnight at 55°C. 200 μl of ethanol were added to the samples, mixed and then loaded onto a QIAamp Spin Column. Samples were centrifuged for 1 minute at 6000 x g to adsorb the DNA onto the silica-gel membrane of the spin column. The spin column was washed with buffers AW1 and AW2 and then DNA was eluted in 50 μl of deionised water by centrifugation at 6000 x g for 1 minute. The concentration of DNA in each sample was quantified using the NanoDrop ND-1000 Spectrophotometer (Nano-Drop Technologies, Wilmington, DE, USA) as described in detail in Section 2.8.2.

2.7 Polymerase Chain Reaction (PCR)

The absence in the genome of the DNA sequence coding for pre-miR-145 or pre-miR-21 in the KO mice was assessed by PCR, a technique used to amplify a DNA sequence using two oligonucleotides that are complementary to the 3' (three prime) ends of each of the sense and anti-sense strand of the DNA target, generating millions of copies. In particular, during a first step DNA is heated to break all the hydrogen bonds and separate the two DNA strand, after that it is cooled down to consent the annealing of the primer and then heated again for the elongation step obtained through the action of a thermostable DNA polymerase. The final step is the re-annealing of the new DNA strands. This steps are repeated several times (30 to 40 generally) in order to amplify the DNA template. In this case, specific oligonucleotides allowed the amplification of a sequence flanking the pre-miR coding region of each miRNA of interest, absent in the KO mice. If the analyzed animal is a KO, the amplified DNA

fragment will have a different size than a WT, depending by the strategy used for creating the KO, previously described (Xin, Small et al. 2009; Patrick, Montgomery et al. 2010). In particular, for miR-145 samples, a 145 bp fragment was obtained for the WT animals and a 200 bp for the mutants, while for miR-21 samples, a 469 bp fragment was obtained for the WT animals and a 330 bp for the mutants (Figure 2-3and Figure 2-4). For each sample analyzed, 5 ng of DNA were incubated with a mix containing 5 µl of 5X Go Taq Flexi Buffer (Promega, Southampton, UK), 3 mM $MgCl_2$, 400 nM forward and reverse primers (sequence and annealing temperature are indicated in Table 2-1) and 0.6 U of Taq DNA polymerase (Promega, Southampton, UK). Reactions were then incubated in a 96-well plate at 95°C for 2 min (denaturation), following by 35 cycles of 95°C for 15 s (amplification), 62°C or 61°C (for miR-21 or miR-145 KO mice respectively) for 35 s (annealing) and 72°C for 30 s (extension). PCR products were analyzed in an agarose gel (Figure 2-3 and Figure 2-4). Briefly, A 1% (w/v) agarose gel for miR-21 KO samples (or 2% for miR-145 KO samples) was prepared in 1X Tris/Borate/EDTA (TBE, 10 mM Tris, 10 mM boric acid, 10 mM EDTA, pH 8.3) containing ethidium bromide (10 ng/ml). Samples were subjected to electrophoresis at 80V for 1 h alongside a DNA ladder (100 bp or 1 Kb as indicated, Promega, Southampton, UK).

PCR Primers	Sequence		Melting Point
miR-145	Forward	GCACGTGCTGAAGGCATCTCTC	59°C
	Reverse	GGGTGGGAGGGAGACAGATCC	60°C
miR-21	Forward	GGGCGTCGACCCGGCTTTAACAGGTG	66°C
	Reverse	GGGCGTCGACGATACTGCTGCTGTTACCAAG	67°C

Table 2-1 Oligo nucleotides used for PCR reactions.

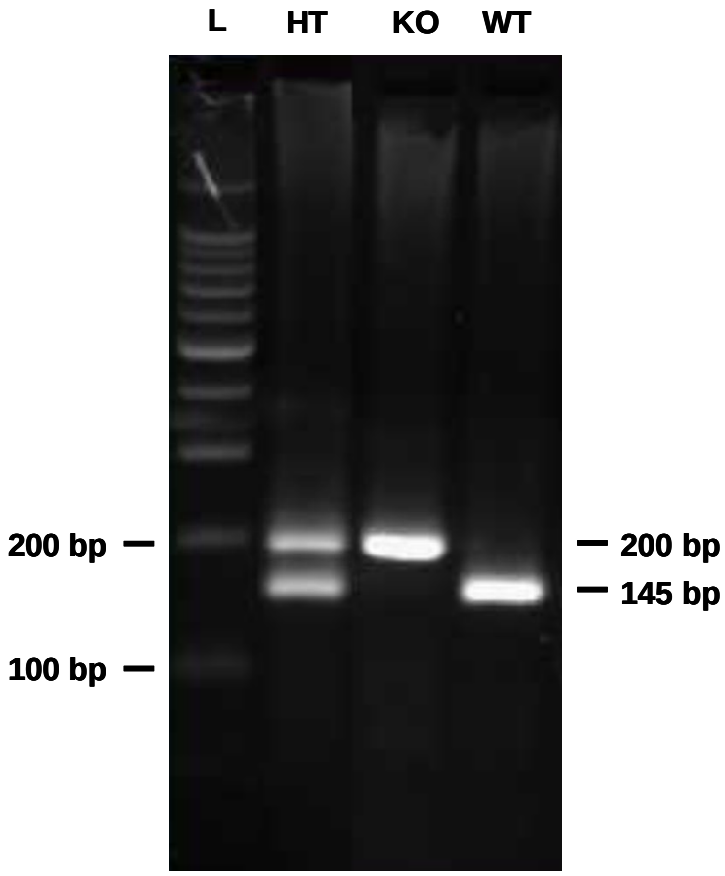

Figure 2-3 Representative PCR showing the specific fragments amplified from heterozygous (HT), miR-145 KO or WT mice. In the first lane the fragments of the 100 bp DNA ladder are shown (L).

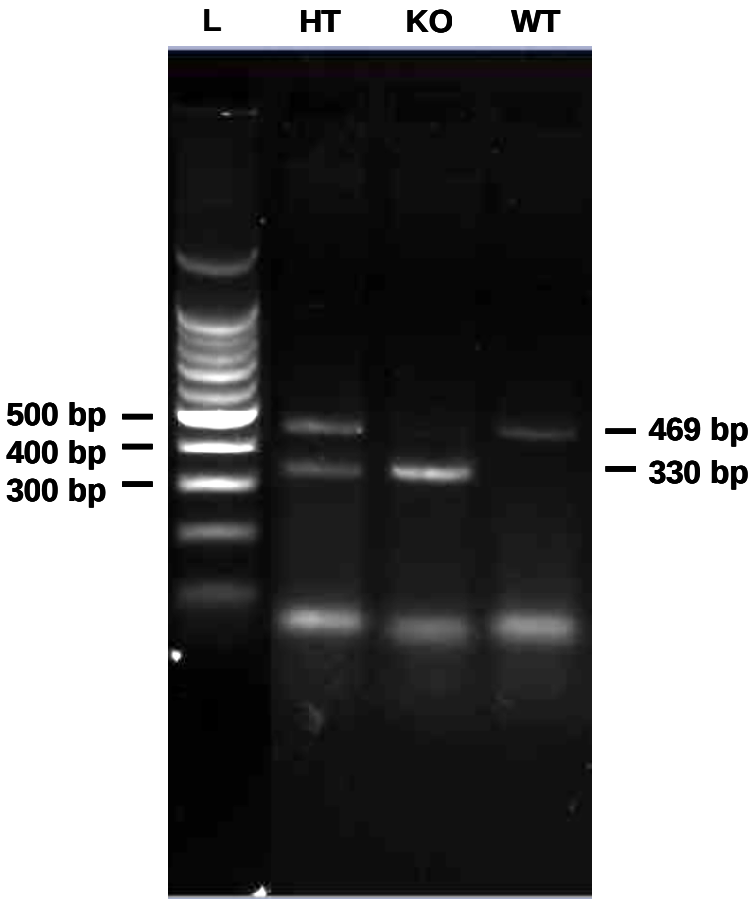

Figure 2-4 Representative PCR showing the specific fragments amplified from heterozygous (HT), miR-21 KO or WT mice. In the first lane the fragments of the 100 bp DNA ladder are shown.

2.8 Total RNA extraction from frozen tissues, PASMCs, PAFs, PAECs and human serum

Total RNA (including miRNAs) from tissues and cells was obtained using the miRNeasy kit (Qiagen, Hilden, Germany). In particular for the extraction from frozen tissues, 700 μl of QIAzol Lysis Reagent (Qiagen, Hilden, Germany) were added to each sample while it was still frozen, and the tissue were disrupted using the TissueLyser system (Qiagen, Hilden, Germany) by rapid agitation in the presence of a 5 mm tungsten carbide bead (Qiagen, Hilden, Germany) for 4 cycles of 30 s each at 20 Hz. After that the homogenates were carefully transferred to a fresh 1.5 ml centrifuge tube. The addition of 140 μl of chloroform allowed RNA separation from DNA and proteins in an upper phase after a 15 min centrifugation at 12,000 x g at 4°C. 500 μl of ethanol were then added in order to facilitate RNA binding to the column and the samples were loaded into RNeasy spin columns and centrifuged at 8,000 x g for 15 s. The RNA bounded to the column was then washed 3 times (1X with 700 μl of RWT buffer and 2X with 500 μl of RPE buffer) and finally eluted with 40 μl of Diethylpyrocarbonate (DEPC) treated water. DEPC is a strong inhibitor of RNases and avoid RNA degradation. Samples were stored at -80°C.

For RNA extraction from cells the same protocol was used with the exception of the first step. 700 μl of QIAzol Lysis Reagent (Qiagen, Hilden, Germany) were added directly to the 6-well plates used for the experiments. The solution was then collected in a micro centrifuge tube for each sample.

2.8.1 DNAse treatment

In order to eliminate the genome DNA contamination the DNAse 1, amplification grade (Sigma-Aldrich, Poole, UK) was used following the manufacturer's instructions. Briefly, 4 μl of 10X reaction buffer were added to the purified RNA, previously eluted in 40 μl of DEPC water as described above in detail. Then 2 μl of amplification grade DNAse I (1 U/μl) were added to each sample and the reaction was incubated for 15 min at RT. 1 unit of amplification grade DNAse I completely digests 1 μg of plasmid DNA to

oligonucleotides in 10 min at 37°C. Re-suspended stop solution was then added to each sample (0.1 volumes) and incubated for 19 min at 70°C to inactivate the DNase I. Heating also denatures RNA secondary structure, so the RNA can be used directly in reverse transcription reaction. After the treatment, the RNA was stored at -80°C in order to prevent degradation.

2.8.2 RNA quantification and quality assessment

Total RNA was quantified using the NanoDrop ND-1000 Spectrophotometer (Nano-Drop Technologies, Wilmington, DE, USA). This instrument is able to calculate the concentration of a nucleic acid exposing a sample to ultraviolet light at 260 nm, and measuring the light that passes through the sample. The more light is absorbed by the sample, the higher is the nucleic acid concentration. In particular, the correlation between the amount of light absorbed and the nucleic acid concentration is calculated using the Beer–Lambert law as follows:

$$c = A/(\varepsilon \times l)$$

Where:

c = nucleic acids concentration

A = absorbance

ε = molar absorptivity

l = length of solution the light passes through

The molar absorptivity is a measurement of how strongly a chemical species absorbs light at a given wavelength (260 nm in this case), and it is an intrinsic property of the species. For nucleic acids, the ε used values are 50 ng/μl for double-stranded DNA, 33 ng/μl for single-stranded DNA and 40 ng/μl for RNA.

For assessing RNA quality, absorbance of the RNA samples was quantified at 260 and 280 nm, and the 260/280 ratio was calculated. The samples showed a 260/280 ratio ≥ 1.9, which was assumed as an indicator of RNA purity. In order to further determine RNA quality, when enough RNA was extracted from tissues or cells, agarose gel electrophoresis was used. RNA samples (700 ng) and 1 kb DNA marker plus 6X loading buffer (0.02% bromophenol blue, 0.02% xylene cyanole and 2.5% glycerol, Promega, Southampton, UK) were loaded onto a 1% (w/v) agarose gel in 1X Tris/Borate/EDTA

(TBE) (10 mM Tris, 10 mM boric acid, 10 mM EDTA, pH 8.3) and ethidium bromide (10 ng/mL). Gels were electrophoresed at a constant voltage of 80/90 V with TBE as a running buffer and visualized under UV light (260 nm). This allows the visualization of 28S and 18S ribosomal RNA (rRNA) as two separate bands (Figure 2-5).

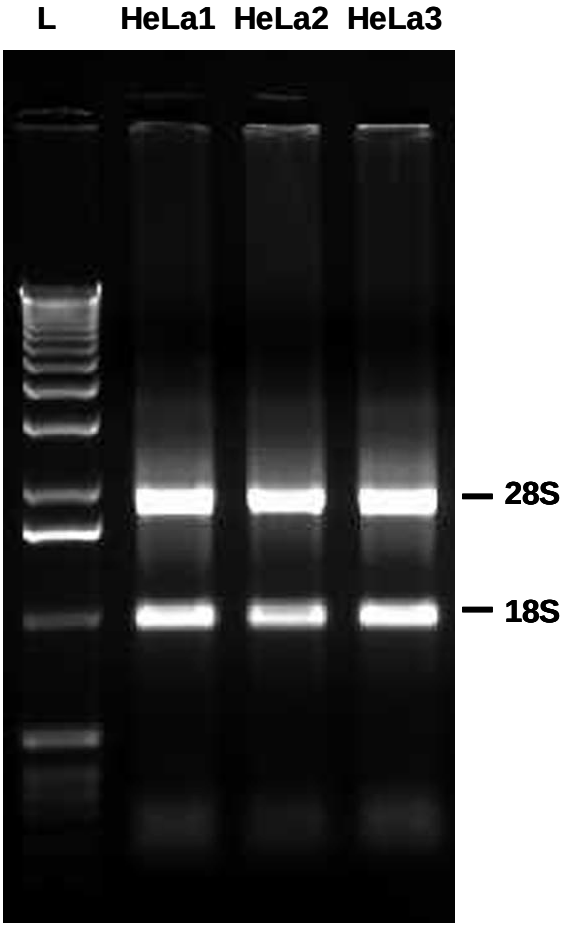

Figure 2-5 Example of an RNA gel. Total RNA was extracted in triplicate from HeLa cells. 1 µg was loaded in each well.

2.8.3 Reverse transcription

Complementary DNA (cDNA) specific for each miRNA was synthesized from total RNA using stem-loop reverse transcription primers according to the TaqMan® MicroRNA Assay protocol (Chen, Ridzon et al. 2005) (Applied Biosystems, Foster city, CA, USA). The assays specific for each miRNA and control are shown in Table 2-2. Each reaction contained 5 ng of extracted total RNA, 50 nM stem-looped RT primer, 0.75 μl of 10X RT buffer, 0.25 mM each of deoxyribonucleotide triphosphates (dNTPs), 0.5 μl of 50 U/μl Multiscribe reverse transcriptase and 0.095 μl of 20 U/μl RNase inhibitor. The 15 μl reactions were incubated in a 96-well plate for 30 min at 16°C (preannealing), 30 min at 42°C (reverse transcription), 5 min at 85°C (reverse transcription inactivation) and then stored at -20°C.

Total cDNA for gene expression analysis was obtained from total RNA using the SuperScript II Reverse Transcriptase (Invitrogen, Paisley, UK). Briefly, 1 μg of RNA from each sample to reverse transcribe was diluted in DEPC treated water up to a final volume of 10 μl and denatured at 70°C for 10 min. In the meantime, a master mix reaction was made up in 10 μl according to the following recipe: 4 μl of 5X SuperScript II buffer (Invitrogen, Paisley, UK), 200 U of SuperScript II RT (Invitrogen, Paisley, UK), 3 μg of random hexamer primers (Invitrogen, Paisley, UK), 20 U of RNase inhibitor (Promega, Southampton, UK), 0.125 mM each of dNTPs mixture, nuclease free water up to 10 μl. After the denaturation step the master mix was added to each sample to give a final reaction volume of 20 μl. Cycling conditions were the following: 10 min at 25°C (preannealing), 30 min at 48°C (reverse transcription), 5 min at 95°C (reverse transcription inactivation). cDNA was stored at -20°C.

Assay	Mature miRNA Sequence	Product Code
miR-21	UAGCUUAUCAGACUGAUGUUGA	000397
miR-22	AAGCUGCCAGUUGAAGAACUGU	000398
miR-30c	UGUAAACAUCCUACACUCUCAGC	000419
miR-143	UGAGAUGAAGCACUGUAGCUC	002249
miR-145	GUCCAGUUUUCCCAGGAAUCCCU	002278
miR-451	AAACCGUUACCAUUACUGAGUU	001141
miR-322	AAACAUGAAGCGCUGCAACA	001059
let-7f	UGAGGUAGUAGAUUGUAUAGUU	000382
let-7a	UGAGGUAGUAGGUUGUAUAGUU	000377
let-7d	AGAGGUAGUAGGUUGCAUAGUU	002283

Assay	Control Sequence	Product Code
U87	ACAATGATGACTTATGTTTTTGCCGTTTAC CCAGCTGAGGGTTTCTTTGAAGAGAGAAT TTAAGACTGAGC	001712
U6	GTGCTCGCTTCGGCAGCACATATACTAAA ATTGGAACGATACAGAGAAGATTAGCATG GCCCCTGCGCAAGGATGACACGCAAATTC GTGAAGCGTTCCATATTTT	001973
Rnu-48	GATGACCCCAGGTAACTCTGAGTGTGTCG CTGATGCCATCACCGCAGCGCTCTGACC	001006

Table 2-2 TaqMan® probes used for miRNA reverse transcription and Real-Time PCR.

2.9 Two-channel microarray experiment

For the microarray assay showed in Chapter 3, total RNA extracted from control, hypoxic and monocrotaline-treated rats was sent to LC sciences (Houston, Texas, USA) for a two-channel microarray experiment. 5 μg of each RNA sample were used. For shipping, 0.1 volume of 3 M NaOAc (pH 5.2) and 3 volumes of 100% ethanol were added, mixed and placed in RNase-free 1.5 ml tubes. The samples were packed in dry ice for shipping. Figure 2-6 gives a design of the miRNA microarray study investigating PAH in the rat. Each circle represents a "condition", with each hypoxia treatment being in red and each monocrotaline treatment in blue. Each arrow represents a two-channel microarray experiment. For the experiment, the RNA was labeled with a fluorescent dye then hybridized overnight onto a microfluidic chip containing complementary probes for 723 human miRNAs and other RNA controls. The chip was imaged using a GenePiz 4000B laser scanner and digitized using Array-Pro image analysis software. Raw data matrix was then subtracted from the background matrix. To assess the statistical significance of intergroup differences, rank products were used (Breitling, Armengaud et al. 2004). Significance was assessed using the false discovery rate multiple testing correction method (Reiner, Yekutieli et al. 2003), with a false discovery rate cutoff of 5%.

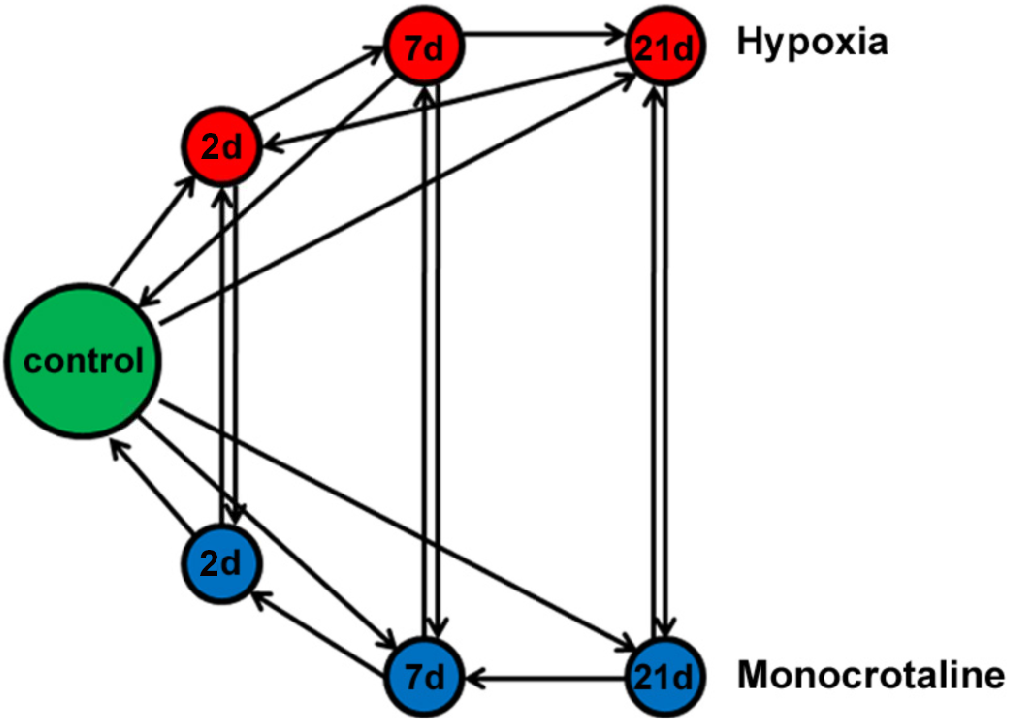

Figure 2-6 Design of the miRNA microarray study investigating PAH in hypoxic or monocrotaline-exposed rats. Each circle represents an animal group (minimum n = 5/group), with each hypoxia treatment being in red and each drug treatment in blue. The control group is represented in green. Each arrow shows a two-channel microarray experiment.

2.10 TaqMan® Quantitative Real-Time PCR analysis of mature, pre- and pri- miRNAs and mRNAs

For the Real-Time PCR step, amplification was carried out using TaqMan® MicroRNA (Chen, Ridzon et al. 2005) or mRNA specific primers (Table 2-2 and Table 2-3) (Applied Biosystems, Foster city, CA, USA) on the Applied Biosystems 7900 HT real-time PCR system. The 10 μl reaction included 0.7-2 μl of template cDNA, 5 μl of 2X TaqMan® Universal PCR Master Mix or SYBR® Green PCR Master Mix (Applied Biosystems, Foster city, CA, USA), 0.5 μl of 20X concentrated FAM or VIC labeled probe for Pri/mature-miRNA or gene expression analysis (Applied Biosystems, Foster city, CA, USA) or 4 pmol of forward and reverse oligos of Pre-miRNA detection, nuclease-free water up to 10 μl. The quantity of template cDNA to use in each experiment was carefully chosen according to the expression level of the specific miRNA/mRNA, in order to have cycle threshold (Ct) values in a range of 20-30. In fact, with Ct values smaller than 20, the fluorescence (that is a measure of the expression level of the transcript of interest) is so high that the identification of differences between samples is not precise, while vice versa, in case of Ct values too low, the consistency of the result can be difficult to determine. Reactions were incubated in a 384-well optical plate at 95°C for 10 min (denaturation), following by 40 cycles of 95°C for 15 s (amplification) and 60°C for 1 minute (annealing). U87, U6, RNU-48 and GAPDH were used as endogenous controls for rat miRNAs, mouse miRNAs, human miRNAs and mRNAs respectively. Ct values were exported directly into EXCEL worksheets for analysis and the relative quantification was made using the $2^{-\Delta\Delta Ct}$ method (Livak and Schmittgen 2001; Cikos, Bukovska et al. 2007). Briefly, the Ct values, defined as the number of cycles it takes for a sample to reach the level where the rate of amplification is the greatest during the exponential phase, were obtained for every miRNA/gene and for the correspondent endogenous control. The ΔCt value was calculated using the equation:
[miRNA/mRNA ΔCt = miRNA/mRNA Ct − control Ct].

The fold change for every miRNA/mRNA expression was finally obtained from the formula $2^{-\Delta\Delta CT}$, where the $\Delta\Delta$CT value was the difference between the control group ΔCT and every other stimulated/mutated group ΔCT values. The value of $2^{-\Delta\Delta CT}$ for the control group was 1. Each experiment was run in triplicate and results are presented as

the mean + standard deviation of the sample. To assess the statistical significance of intergroup differences, student's *t* tests, one-way or two-way ANOVA were performed as specified.

Assay	Species	Amplicon Lenght	Product Code
Kcnj6	Rat	70	Rn00755103_m1
Nfat5	Rat	65	Rn01762487_m1
Ppp2r5e	Rat	68	Rn01769637_m1
Tacc1	Rat	100	Rn01478432_m1
Tnrc6a	Rat	61	Rn01163358_m1
Ywhaz	Rat	104	Rn00755072_m1
Adarb1	Rat	92	Rn00563671_m1
Tgfbr1	Rat	86	Rn00562811_m1
TGFBR1	Human	73	Hs00610320_m1
Tgfbrap1	Rat	71	Rn01437728_m1
Rbpsuh	Rat	113	Rn01457013_g1
Gapdh	Rat	174	Rn01775763_g1
GAPDH	Human	93	Hs02758991_g1
Gapdh	Mouse	107	Mm99999915_g1
Smad4	Mouse	71	Mm03023996_m1
Smad5	Mouse	159	Mm03024001_g1
Klf4	Mouse	77	Mm00516104_m1
Klf5	Mouse	140	Mm00456521_m1

Assay	Species	Amplicon Lenght	Product Code
Pri-miR-21	Human	101	Hs03302625_pri

PCR Primers	Sequence		Species
Pre- miR-145	Forward	CACCTTGTCCTCACGGTCCA	Human
	Reverse	AACCATGACCTCAAGAACAG	
Pre- miR-143	Forward	GCGCAGCGCCCTGTCTCCCA	Human
	Reverse	GCTGCAGAACAACTTCTCTC	
Pre- miR-21	Forward	TGTCGGGTAGCTTATCAGAC	Human
	Reverse	TGTCAGACAGCCCATCGACT	

Table 2-3 TaqMan® probes used for gene expression/Pri-miRNA Real-Time PCR and oligos used for SYBR® Green-based Real-Time PCR analysis.

2.11 Northern blot analysis

In order to detect and visualize miR-145, miR-143 or miR-21 in mouse and human samples, northern blotting assays were performed. Briefly, 2 μg (for miR-21 detection) or 3 μg (for miR-143 and miR-145 detection) of mouse or human total RNA mixed with 5X loading dye (Sigma-Aldrich, Poole, UK) were denatured at 90°C for 5 min and then separated on a 15% TBE-Urea gel (Invitrogen, Paisley, UK) at 150 V for approximately 1 h in running buffer (Invitrogen, Paisley, UK) and transferred to an uncharged nylon membrane, Hybond-NX (Amersham Bioscience UK Ltd, Buckingham, UK) using a trans-blot semi-dry system (Bio-Rad Laboratories, Hemel Hempstead, UK) at 10 V for 1 h and 30 min. After this step, the membrane was EDC-UV cross-linked for 1 h at 60°C in a cross-linking solution composed of 122.5 μl of 1-methylhymidazole (Sigma-Aldrich, Poole, UK), 0.3 g of EDC (1-ethyl-3-(3-dimethylaminopropyl) carbodiimide, Sigma-Aldrich, Poole, UK) and DEPC-treated water up to 12 ml. Pre-hybridization was carried out at 55°C for 30 min with hybridization buffer (50% (v/v) de-ionized formamide, 5X SSPE, 5X Denhardt's solution, 0.1% (v/v) SDS, and 2 mg of heat-denatured herring sperm DNA). Then 25 pmol of miR-21, miR-145, miR-143 or U6 miRCURY LNA™ Detection probe, 5`-digoxigenin (DIG) labeled (Exiqon, Denmark), were added over night at the same pre-hybridization temperature. Following hybridization, the membrane was washed 30 min at 50°C with the low stringency wash solution (Invitrogen, Paisley, UK) followed by a 30 min wash with the high stringency wash solution (Invitrogen, Paisley, UK) and a 5 min wash in a washing buffer composed of 0.1 M maleic acid, 0.15 M NaCl pH 7.5 and 0.3% (v/v) of Tween 20. After that, the membrane was blocked for 30 min in blocking solution (1% (w/v) blocking reagent, Roche Diagnostics, West Sussex, UK, in maleic acid) with shaking and incubated 30 min with an anti-DIG antibody (Roche Diagnostics, West Sussex, UK) diluted 1:5000 in the same blocking solution at RT. Then, the membrane was washed two times for 15 min with the wash buffer followed by 5 min incubation with the detection buffer (0.1 M Tris-HCl) with shaking. The CDP Star Chemiluminescent Substrate (Sigma-Aldrich, Poole, UK) was used to detect the presence of the miRNA of interest on the membrane. miRNA quantification was performed with the Scion Image software (www.scioncorp.com): band intensities of the miRNA of interest were established and normalized to the relative U6 signal.

2.12 Prediction of potential miRNAs targets

In order to identify a list of targets for miR-21, miR-22, miR-30c, miR-451 and miR-322 (Chapter 3) and miR-145 (Chapter 4), we screened 3'UTRs of mRNAs for the seeds of the miRNAs of interest. The seed is the Watson-Crick consecutive pairing between mRNAs and the miRNA at positions 2-7 counted from its 5'end. It has recently been demonstrated that the seed in 3'UTRs is the primary motif associated with miRNA-mediated regulation (Selbach et al, 2008). All seed-based prediction algorithms have the highest overlap with pulsed SILAC data, and the accuracy was only topped by three methods that use evolutionary conservation (PicTar, TargetScanS, Diana). However, the false-positive rate of this target prediction method is still around 40%. In addition, multiple non-conserved seeds, in particular those located at optimal distances of less than 40 nt (Grimson et al, 2007; Selbach et al, 2008) seem to exert the same effect as single conserved seeds (R. Khanin, unpublished observations). Therefore, in this work we opted to simply search for seeds for a miRNA of interest in 3'UTRs of rat, mouse or human mRNAs (downloaded from USCS Genome Browser http://genome.ucsc.edu/). In particular, for miR-21, miR-22 and miR-30c we focused on those targets with multiple seeds for one or two miRNAs. Using the same criteria, we also generated a preliminary list for miR-451/miR-322 targets in order to compare the proteins potentially regulated by the down-regulated and the up-regulated miRNAs of chapter 3. These lists were then used for identifying those targets potentially both regulated in a significant way and involved in the pathology.

2.13 Protein extraction

Rat and mouse lung tissues were homogenated using the TissueLyser system (Qiagen, Hilden, Germany) by rapid agitation in the presence of a 5 mm tungsten carbide bead (Qiagen, Hilden, Germany) for 4 cycles of 30 s each at 20 Hz in lysis buffer containing 150 mM NaCl, 50 mM Tris HCl pH 7.4, 1 mM EDTA, 1% (v/v) triton X 100, 1 mM phenylmethylsulfonylfluoride (PMSF), 0.25% (w/v) Na-deoxycholate, and 1X Roche Complete Protease Inhibitor Cocktail Tablets (Roche Diagnostics, West Sussex, UK). The homogenates were sonicated for 30 s and incubated 20 min on ice. Lysed tissues were

centrifuged at 14,000 rpm at 4°C for 15 min and the supernatant containing protein was then transferred to a fresh 1.5 ml centrifuge tube and stored at -20°C.

2.13.1 Protein quantification

The protein content was determined using the bicinchoninic acid (BCA) Protein Assay Kit (Pierce, Rockford, IL, USA) according to the manufacturer's instructions. Briefly, a standard curve was generated using the following BSA dilutions: 2000 μg/ml, 1500 μg/ml, 1000 μg/ml, 750 μg/ml, 500 μg/ml, 250 μg/ml, 125 μg/ml and 25 μg/ml. In a 96-well plate, 200 μl of working reagent were added to 25 μl of each sample or standard in duplicate, and the plate was then covered to protect from light and incubated at 37°C for 30 min. After that the plate was cooled to RT and the absorbance from each well was read at 560 nm using a Wallac Victor^2 plate reader (Wallac, Turku, Finland). The concentration of each sample was then obtained according to the linear equation based on the standard curve generated from the analysis of the standards absorbance.

2.13.2 Western Blot Analysis

In order to determine the expression level of TGFBR1 in control and 7 day monocrotaline rat lung (Chapter 3, Section 3.2.9), and of KLF4 and KLF5 in WT and miR-145 KO mice (Chapter 4, Section 4.2.4), sodium dodecyl sulphate polyacrylamide gel electrophoresis (SDS-PAGE) and western blotting were performed. To separate TGFBR1, which is 56 KDa, KLF4 and KLF5, which are both 50 KDa, reducing conditions and a 12% polyacrylamide gel (containing 40% (v/v) polyacrylamide (30%), 11.25 mM Tris pH 8.8, 0.1% (v/v) SDS, 300 μl ammonium persulphate (APS) and 30 μl N,N,N′,N′-tetramethylethylenediamine (TEMED)) were used. 20 μg for TGFBR1 and 50 μg for KLF4 and KLF5 of total proteins were mixed with an equal volume of 2X reducing loading dye (125 mM Tris pH 6.8, 4% (v/v) SDS, 10% (v/v) glycerol, 0.006% (v/v) bromophenol blue, 2% (v/v) β-mercaptoethanol). Samples were heated at 95°C for 5 min before the gel was loaded. 40 μl of rainbow ladder (Amersham Bioscience UK Ltd, Buckingham, UK) were also added to the gel as a marker of protein size. Samples were electrophoresed at 200 V in running buffer (0.025 M Tris-HCl, 0.2 M glycine, 0.001 M

SDS) for approximately 3 h. Proteins were transferred onto Hybond-P membrane (Amersham Bioscience UK Limited, Buckingham, UK) overnight at 0.9 mAmps at 4°C in transfer buffer (0.025 M Tris, 0.2 M glycine, 20% (v/v) methanol, 0.01% (v/v) SDS). The membranes were then blocked in TBS-T (150 mM NaCl, 50 mM Tris, 0.1% (v/v) Tween-20) + 10 % (w/v) fat-free milk powder (blocking buffer) for 1 h with shaking. After blocking, the filter was incubated with a rabbit polyclonal anti-TGFBR1, anti-KLF4 or anti-KLF5 antibody (Abcam, Cambridge, UK) diluted 1:750 for TGFBR1 detection and 1:500 for KLF4 and KLF5 detection in blocking buffer for 3 h at RT with shaking. After that, the filter was washed twice in TBS-T for 5 min. The membrane was then incubated with a horseradish peroxidase (HRP) secondary antibody (dilution 1:1000, goat anti-rabbit Abcam, Cambridge, UK) in blocking buffer for 1 h at RT and then washed four times in blocking buffer for 15 min at RT followed by two 15 min washes with TBS-T. The ECL Western Blotting detection kit (Amersham Bioscience UK Ltd, Buckingham, UK) was used to detect the presence of the protein of interest on the membrane. Equal sample loading was verified by stripping the blot in stripping buffer (100 mM 2-mercaptoethanol, 2% (v/v) SDS, 62.5 mM Tris-HCL pH6.8) at 50°C for 30 min with occasional agitation, washing it two times, 10 min each, in TBS-T with agitation, and then reprobing it with an anti-beta-actin antibody (Abcam, Cambridge, UK) for TGFBR1 and an anti-GAPDH antibody (Abcam, Cambridge, UK) for KLF4 and KLF5. Protein quantification was performed with the Scion Image software (www.scioncorp.com): band intensities of the protein of interest were established and normalized to the relative beta-actin or GAPDH signal.

2.14 Histology

Tissues were excised and immediately fixed in 10% (v/v) neutral-buffered formalin (NBF, 10% (v/v) formalin, 33 mMol/L NaH_2PO_4, 45 mMol/L Na_2HPO_4) for three days, under gentle agitation. Formalin-fixed tissues were then paraffin-embedded. For *in situ* and immunohistochemistry experiments, single tissue sections with 3 and 5 µm thickness respectively were mounted onto sialanised glass slides. Slides were baked at 65°C for 3 h, then at 40°C overnight. For haematoxylin and eosin and elastic Vann Gieson staining, 5 µm sections were cut and mounted onto non sialanised slides. Slides were then left overnight at RT to dry.

2.14.1 Slide silinisation

Blank glass slides were placed in a solution of 2% 3-amino-propyltriethoxysaline (APES) in 100% acetone for 30 s. Slides were then rinsed in acetone for 10 s, followed by two 5 min rinses in deionised water before being left to air dry overnight at 37°C.

2.14.2 Immunohistochemistry

Rat, mouse and human lungs were fixed as described in details in the previous section. After deparaffinization with two 7 min washes in Histoclear (Thermo Fisher Scientific, UK), sections were rehydrated by passing through an alcohol gradient 100%, 95% and 70% ethanol for 7 min each and washed in deionised water for 5 min. Following hydration, antigen retrieval was performed by the incubation of lung sections in boiling 0.1 M/L Sodium citrate pH 8.0 for 30 min. Sections were then cooled to RT. Slides were then immersed in 3% (v/v) H_2O_2 in PBS for 30 min at RT to block endogenous peroxidase activity. After that, they were washed twice in deionised water for 5 min and incubated with a blocking solution (10% (v/v) normal goat serum, 5% (w/v) bovine serum albumin (BSA) in PBS) for 1 h in a humidified chamber to reduce non-specific background staining. Sections were then incubated with rabbit anti-TGFBR1 antibody (Abcam, Cambridge, UK), mouse monoclonal antibody against alpha-smooth muscle actin (anti-SMA, DaKo, Clone 1A4, High Wycombe, UK), or isotype matched mouse IgG nonimmune control (DaKo, High Wycombe, UK), in 5% (w/v) BSA and 10% (v/v) normal goat serum in PBS overnight at 4°C in a humidified chamber. Slides were washed three times in PBS for 5 min each. Sections were then incubated with appropriate biotinylated secondary antibody (DaKo, High Wycombe, UK) diluted 1:200 in 5% (w/v) BSA and 10% (v/v) normal goat serum in PBS, and then with horseradish peroxidase-labelled Extravidin^{TM} (Sigma-Aldrich, Poole, UK) diluted 1:200 in 1% (w/v) BSA in PBS. Color was developed using 3.3 diaminobenzidine-nickel and the nuclei were counterstained with Mayer's haematoxylin.

2.14.3 In situ hybridization for detection of miRNA localization

For the detection of miR-143 and miR-145 in mouse lung, sections were rehydrated with histoclear and graded concentrations of ethanol as previously described. Slides were then boiled for 10 min within 10 mM sodium citrate pH 6.0, cool to RT, incubated with 10 μg/ml proteinase K at 37°C for 15 min and finally fixed in 4% paraformaldehyde (PFA) for 10 min at RT in order to allow probe-miRNA interaction. Following antigen retrieval, slides were incubated with hybridisation buffer (50% (v/v) formamide, 4X SSC, 2.5X Denhadrt's solution, 2.5 mg/ml salmon DNA, 0.6 mg/ml yeast tRNA, 0.025% (v/v) SDS and 0.1% (w/v) blocking reagent) at 60°C for 1 h followed by a 60°C overnight incubation with 40 nM of miR-143, miR-145 or scramble miRCURY LNA™ Detection probe, 5`-DIG labeled (Exiqon, Denmark) in the same buffer. Immunodetection was performed blocking the sections in 1% (w/v) blocking reagent in PBS and 10% (v/v) FCS for 1 h at RT followed by a 4°C overnight incubation with an anti-DIG antibody (Roche Diagnostics, West Sussex, UK) diluted 1:1000. Slides were then incubated with 0.1 M Tris pH 9.0 for 5 min. In order to stain miR-143 or miR-145, BM purple solution AP substrate (Roche Diagnostics, West Sussex, UK) was added to each section and left at RT for 3 days.

2.14.4 Haematoxylin and eosin staining

After deparaffinization and rehydration of slides (described above in details), slides were stained in Harris haemotoxylin for 2 min, washed in running tap water for 5 min and then placed in eosin for two min in order to counterstain nuclei. After that, sections were washed again for 5 min in running tap water. Slides were dehydrated using increasing concentrations of ethanol (75%, 95% and 100%) for 7 min each and then cleared by two 7 min washes in histoclear. Sections were then mounted in Histomount. Nuclei appeared blue/purple whereas cytoplasm was stained pink.

2.14.5 Elastin Van Gieson Stain

After deparaffinization and rehydration (described above in details), slides were incubated in 0.5% (w/v) $KMnO_4$ for 5 min and then rinsed in running tap water.

Sections were then decolorized in 1% (w/v) oxalic acid for 2-3 min and washed again in running tap water. After that, slides were rinsed in 95% ethanol and stained in elastic stain for 2 h. The stain in excess was removed rinsing again the sections in 95% ethanol and washing them in running tap water. The counterstain was obtained placing the slides in Van Gieson for 30 s. Sections were then dehydrated as described above and mounted in Histomount. Elastic fibers appeared in black, collagen in deep red, while cytoplasm, muscles and fibrin in yellow.

2.15 Statistical analysis

Statistical analysis was performed using Prism 4.0 Graph Pad software. All results are expressed as mean ± standard error of the mean (SEM). Data were analyzed using a two-way ANOVA followed by Bonferroni's post-hoc test, one-way ANOVA followed by Bonferroni's post-hoc test or unpaired *t*-test as appropriate, and described in Figure legends.

3. Dynamic Changes in Lung MicroRNA Profiles During the Development of Pulmonary Hypertension Due to Chronic Hypoxia and Monocrotaline

3.1 Introduction

Pulmonary arterial hypertension (PAH) is a complex disorder characterized by the obstructive remodeling of pulmonary arteries (PAs) leading to a progressive elevation in pulmonary arterial pressure and subsequent right heart failure and death (Rich, Dantzker et al. 1987). The elevation in pulmonary arterial pressure is due to adventitial, medial and intimal thickening that results from fibroblast, smooth muscle and endothelial cells proliferation (Chapter 1, Section 1.2.2).

Familial PAH is associated with diverse heterozygous mutations in the gene encoding bone morphogenic protein-receptor 2 (*BMPR2*), involved in cartilage and bone growth and repair (Lane, Machado et al. 2000), and has been shown to be related to mutations in the activin-receptor kinase-like 1 (*ALK1*) gene (Harrison, Flanagan et al. 2003) in some severe forms of the pathology. Moreover, reductions in the expression level of *BMPR2* and BMP type 1A receptor (*BMPR1A*) and a dysfunctional Smad1/5 signaling have been observed in PASMCs isolated from patients with idiopathic PAH, supporting the theory of a critical involvement of the TGF-*beta* super-family in the pathobiology of PAH (Chapter 1, Section 1.2.4.1).

In order to study in detail the characteristics and the development of this pathology, different animal models can be used (although each of them presents similarities with the human disease but also limitations, Chapter 1, Section 1.2.3) (Stenmark, Meyrick et al. 2009). In particular, exposure to hypoxia in mice and rats or injection with the toxin monocrotaline all lead to the development of pulmonary arterial changes correlated with PAH, including remodeling and elevation in pulmonary arterial pressure (Wilson, Segall et al. 1992; Brusselmans, Compernolle et al. 2003; Stenmark, Fagan et al. 2006; Stenmark, Meyrick et al. 2009). The signaling and gene expression downstream of BMP and TGF-*beta* receptors in the two rat models have been recently characterized in detail (Morty, Nejman et al. 2007; Long, Crosby et al. 2009). In particular, the analysis of wild type (WT) animals exposed to chronic hypoxia or treated with a single injection

of monocrotaline for 2, 7 or 21 days showed a reduced BMP and enhanced TGF-*beta* signaling. Moreover, hypoxic and monocrotaline-treated animals showed a down-regulation of *BMPR2*, suggesting the involvement of this pathway in the pathology (Long, Crosby et al. 2009) (Chapter 1, Section 1.2.4.1).

miRNAs are small non coding transcripts of 16–29 nt that regulate gene expression post-transcriptionally by targeting mRNAs (Ambros 2004; Jackson and Standart 2007). Approximately 30% of all the human genes are suggested to be regulated by miRNAs (Lewis, Burge et al. 2005) and, importantly, a single miRNA is able to target potentially hundreds of proteins involved in different pathways within a given cell (Boyd 2008) (Chapter 1, Section 1.3). miRNA involvement in many critical cellular process including apoptosis, differentiation and proliferation suggests their potential implication in the development and progression of several pathologies (Croce 2009; Condorelli, Latronico et al. 2010; Varol, Konac et al. 2010; Qin and Zhang 2011; Small and Olson 2011). In cancer, many recent studies have reported distinct miRNA signatures in cancer cells (Ambs, Prueitt et al. 2008; Lujambio, Calin et al. 2008; Yang, Kong et al. 2008) (Chapter 1, Section 1.3.3.12.1). In the heart and vasculature, miRNAs are associated with remodeling and development of hypertrophy and failure (Rao, Toyama et al. 2009; Topkara and Mann 2011; van Almen, Verhesen et al. 2011) (Chapter 1, Section 1.3.3.12.2).

Here, in order to evaluate the involvement of miRNAs in the development of PAH in the monocrotaline and the hypoxic rat models, the lung tissue dissected from the same rats analyzed in the Long et al. study (Long, Crosby et al. 2009) was assessed by miRNA profiling. *In vitro* experiments confirmed the dysregulation of a specific group of miRNAs after treatment with chronic hypoxia. The analysis of mice exposed to hypoxia and human samples obtained from affected patients confirmed miRNA dysregulation in pathological samples from both animal models and PAH patients.

3.2 Results

3.2.1 Global miRNA Profiling of the Lungs of Hypoxia- and Monocrotaline-Exposed Rats

Total RNA (including miRNAs) was isolated from the whole lung of control rats and rats subjected to hypoxia or monocrotaline and harvested at 2, 7 and 21 days post insult. Hemodynamic studies conducted by Prof. Nicholas W. Morrell and his group in Cambridge (Long, Crosby et al. 2009) had already demonstrated the development of PAH in these animals, as described in the introduction of this chapter. In order to verify the involvement of specific miRNAs in the hypoxic- and the monocrotaline induced PAH, the expression level of 350 miRNAs in the lung was investigated using a two-channel microarray experiment. This allowed us to identify their expression signature during the first stages of pathogenesis in both hypoxic- and monocrotaline-induced PAH. In particular, the microarray was designed to allow comparison between time points and also comparison of miRNAs regulated between each injury (Chapter 2, Figure 2.7).

We confirmed the prominent expression of miR-195 and miR-200c in rat lung of control animals (Table 3-1), consistent with the previous identification of these miRNAs as the only lung specific miRNAs (Wang, Weng et al. 2007). Poorly expressed miRNAs were excluded from the analysis, even if they were significantly altered when statistically assessed, since the obtained results were considered not reliable enough when the obtained signal was too low. Moreover, a low absolute expression value for a nucleotidic sequence in a microarray often results in its undetectable expression in a TaqMan® Real-Time PCR assay, making the validation of the microarray result very difficult. For these reasons and in consideration of the relatively high number of miRNAs identified as dysregulated in the samples and characterized by more elevated expression levels, potentially interesting miRNAs, detected with absolute values lower than 500 AU (arbitrary unit), were excluded from the next steps of the project as recommended by LC Sciences (Houston, Texas, USA). This group of miRNAs included miR-204, down-regulated in PAH-affected animal models and human patients, and very recently implicated in the development of PAH. This miRNA acts through a direct

modulation of SRC homology region 2 domain-containing phosphatase-2 (SHP2), an activator of the proto-oncogene tyrosine- protein kinase Src (Courboulin, Paulin et al. 2011). We analyzed miRNA regulation considering both time-fold variation and statistically significant differences between either the hypoxic or monocrotaline groups compared to the control group. This analysis revealed the dysregulation of ~8% of the assessed miRNAs. Within this group, ~80% of miRNAs were down-regulated and ~20% showed an up-regulation. Expression levels of miR-322, miR-451, miR-21, miR-22, miR30c, let-7f and let-7a were the most significantly altered (Table 3-2) and were, therefore, selected for further analysis.

	CTR	H day 2	H day 7	H day 21	M day 2	M day 7	M day 21
rno-miR-195	3,035	2,974	3,329	2,616	3,005	3,044	2,434
	2,962	3,345	2,374	3,850	2,531	2,999	2,270
	3,819	2,504	3,368	4,377	3,693	3,024	1,688
	2,968	3,258	3,127	3,804	3,879	2,323	3,730
	3,077	3,050	2,925	2,822	3,251	2,931	1,975
	2,512	**3,026**	**3,025**	**3,494**	**3,272**	**2,864**	**2,419**
	3,062	**147**	**181**	**333**	**241**	**137**	**352**
	173						

	CTR	H day 2	H day 7	H day 21	M day 2	M day 7	M day 21
rno-miR-200c	1,028	1,193	1,670	1,252	1,147	1,516	1,118
	1,200	902	2,894	894	942	1,335	1,285
	1,691	1,260	1,382	1,439	1,116	1,009	1,051
	1,249	467	815	1,203	1,018	1,327	1,096
	975	911	1,058	690	1,473	926	1,423
	1,629	**947**	**1,564**	**1,096**	**1,384**	**1,223**	**1,195**
	1,295	**140**	**363**	**134**	**91**	**110**	**70**
	123						

Table 3-1 Absolute levels of miR-195 and miR-200c during the progression of PAH. All the absolute intensities are shown, with the mean values in black bold and SEM in red bold at the end of each column (n = 5 or 6/group). To assess the statistical significance of intergroup differences, rank products were used but no significant differences were identified.

		CTR	H day 2	H day 7	H day 21	M day 2	M day 7	M day 21
rno-miR-451	Mean	467	1,528	996	1,539	1,008	1,335	479
	SEM	77	181	174	415	207	201	84
	p-value		**2.50E-04**	**1.40E-02**	**5.67E-03**	**1.39E-02**	**1.53E-03**	
rno-miR-322	Mean	1,066	1,109	931	834	832	210	241
	SEM	133	154	216	242	138	37	288
	p-value						**7.02E-05**	**9.44E-03**
rno-miR-21	Mean	1,686	1,262	1,340	2,243	1,276	367	2,881
	SEM	302	265	504	471	266	63	241
	p-value		**1.65E-02**	**2.44E-02**			**1.27E-03**	
rno-miR-22	Mean	333	720	638	680	570	1,107	666
	SEM	92	135	199	56	159	61	85
	p-value		**4.50E-02**		**4.55E-02**		**5.48E-03**	**3.46E-02**
rno-miR-30c	Mean	4,085	4,285	3,181	2,673	4,120	3,300	2,918
	SEM	346	408	438	341	209	179	124
	p-value				**2.61E-02**			**2.20E-02**
rno-let-7f	Mean	8,290	7,094	8,257	6,035	7,401	2,560	6,359
	SEM	355	1271	1026	1457	1253	217	887
	p-value						**1.00E-04**	
rno-let-7a	Mean	9,747	8,573	10,983	8,370	8,926	4,038	8,414
	SEM	534	1347	1277	1508	1262	262	506
	p-value						**1.01E-05**	

Table 3-2 Expression levels of selected miRNAs in the two-channel microarray study. Mean raw values and SEM for miRNAs up- and down-regulated in PAH rats are shown. To assess the statistical significance of intergroup differences, rank products were used. Significant P-values are shown.

3.2.2 Validation of miRNA Dysregulation

In order to validate the microarray analysis, the expression level of miR-322, miR-451, miR-21, miR-22, miR30c, let-7f and let-7a, selected as described above, plus a control miRNA that was not altered in the lungs of treated male animals compared to controls (miR-145) were analyzed by TaqMan® Real-Time PCR in the total RNA used in the microarray study. As expected, and in agreement with the profiling data, mir-145 levels were not altered under either condition (Figure 3-1). In contrast, miR-451, miR-322, let-7f, miR-21, miR-22 and miR-30c were significantly altered following induction of PAH (Figure 3-1). In particular, miR-451 expression showed a substantial up-regulation in the lung of male rats exposed to hypoxia, and reached a maximum in 7 days monocrotaline rats. MiR-322 was significantly up-regulated just 7 days after the injury for both the models before returning back to control levels by day 21. miR-22 presented opposite trends in the two models resulting in maximal down-regulation after 21 days in hypoxic conditions and 2 days after a monocrotaline injection. MiR-21 and miR-30c showed a significant down-regulation in the monocrotaline and in the hypoxic model alone, respectively (Figure 3-1). Let-7f expression was down-regulated in both the models at early time points in the hypoxic model (2 and 7 days after induction of hypoxia) and later time points in the monocrotaline model (21 days after the injection), while let-7a showed a significant down-regulation only 21 days after monocrotaline injection (Figure 3-1).

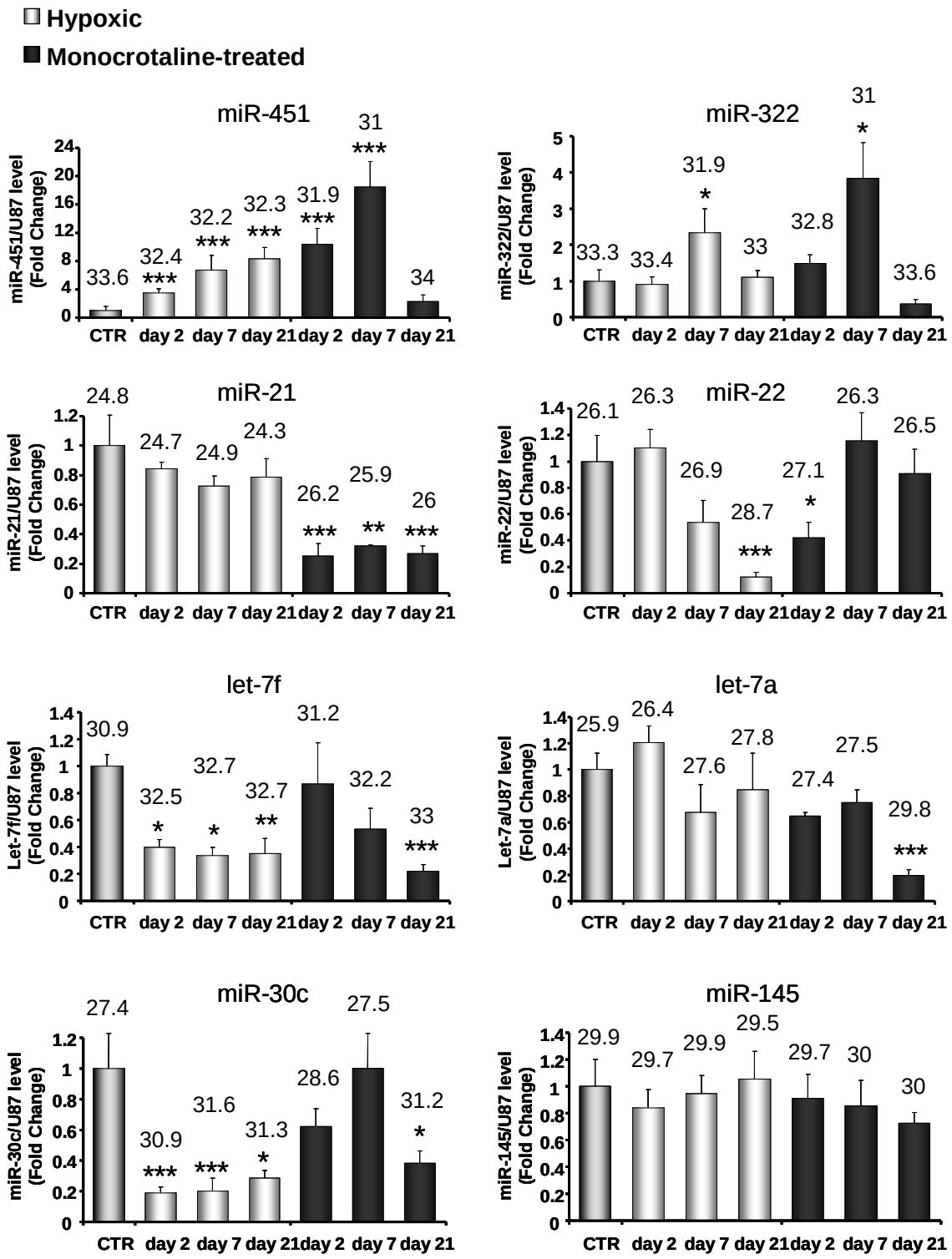

Figure 3-1 Validation of miRNA dysregulation. TaqMan® Real-Time PCR analysis of hypoxic and monocrotaline-injected rats after 2, 7, and 21 days of exposure. Total RNA was extracted from hypoxic (light grey bars) or monocrotaline-injected (black bars) male rats at the age of 6 weeks and analyzed in triplicate. Results were normalized to U87 values and expressed as relative fold change, with an arbitrary value of 1 assigned to the control (CTR) group. Raw Ct values for the target miRNAs are indicated above each column. Data are expressed as mean ± SEM and analysed by two way ANOVA followed by Bonferroni's post-hoc test. *P<0.05, **P<0.01, ***P<0.001 compared to control rats. N = 5/group.

3.2.3 Analysis of the miR-17–miR-92a Cluster in the Monocrotaline and the Hypoxic Rat Models

The expression level of the miR-17–miR-92a cluster (miR-17, miR-19b, miR-20a, and miR-92) was quantified in hypoxic and monocrotaline treated rats, in consideration of its recently described involvement in the regulation of *BMPR2* (Brock, Trenkmann et al. 2009). In particular, a screening based on a computational algorithm (TargetScan, www.targetscan.org) identified several miRNAs encoded by the cluster as potential regulators of the gene, and the ectopic over-expression of miR-17/92 resulted in a strong reduction of the BMPR2 protein (Brock, Trenkmann et al. 2009). For this reason, taking account of the high number of false positive and false negative results of this type of experiment and of the higher precision of the real-time PCR technique (Chapter 2, Section 2.10), a TaqMan® Real-Time PCR validation of the miRNAs included in this cluster was performed despite the microarray analysis showed no significant changes between control animals and hypoxic/monocrotaline-injected mice (Table 3-3). MiR-18a and miR-19a were not assessed because they showed very low expression on the array (lower than 100 AU) (Houston, Texas, USA). TaqMan® Real-Time PCR validations showed a up-regulation of miR-17, miR-19b, miR-20a, and miR-92 in the samples (Figure 3-2), consistent with the Brock et al. study, even if it is important to notice that miR-17 and miR-20a, described as direct regulators of *BMPR2* in the paper, resulted up-regulated only in the monocrotaline model (Figure 3-2).

	CTR	H day 2	H day 7	H day 21	M day 2	M day 7	M day 21
rno-miR-17	180	234	161	130	217	249	225
	184	164	338	201	260	246	272
	197	169	227	155	160	194	278
	214	323	352	184	158	314	175
	169	308	202	232	172	242	218
	250	**240**	**256**	**180**	**193**	**249**	**234**
	199	**34**	**38**	**18**	**20**	**19**	**19**
	12						
rno-miR-18a	29	21	28	16	8	28	23
	23	13	23	28	20	37	41
	16	26	30	25	25	21	30
	19	35	32	40	30	30	21
	22	31	25	24	18	16	40
	28	**25**	**27**	**27**	**20**	**26**	**31**
	23	**4**	**2**	**4**	**4**	**4**	**4**
	2						
rno-miR-19a	12	11	15	7	9	27	12
	12	33	17	12	11	16	17
	10	8	9	23	16	16	12
	9	39	14	21	17	10	14
	13	13	14	11	15	8	23
	16	**21**	**14**	**15**	**14**	**15**	**15**
	12	**6**	**1**	**3**	**1**	**3**	**2**
	1						
rno-miR-20a	268	272	241	216	239	284	264
	236	175	235	219	272	233	353
	214	257	263	300	238	267	281
	276	271	277	210	220	247	212
	216	302	316	108	225	252	248
	259	**255**	**330**	**211**	**239**	**257**	**272**
	245	**21**	**15**	**31**	**9**	**9**	**23**
	11						
rno-miR-19b	94	109	156	118	138	203	44
	83	14	90	199	194	80	113
	80	132	73	161	170	218	67
	39	479	51	102	166	79	141
	56	251	181	121	109	158	76
	100	**223**	**110**	**140**	**155**	**148**	**88**
	75	**68**	**25**	**18**	**15**	**30**	**17**
	10						
rno-miR-92a	418	487	519	500	490	438	509
	573	371	1,294	401	391	390	268
	922	524	708	380	454	415	392
	531	337	599	372	413	316	451
	553	507	453	249	670	444	553
	405	**445**	**715**	**380**	**484**	**401**	**435**
	567	**38**	**151**	**40**	**50**	**23**	**50**
	77						

Table 3-3 Absolute levels of miR-17/92 cluster in the two-channel microarray study. All the absolute intensities are shown, will the mean values in black bold and SEM in red bold at the end of each column (n = 5 or 6/group). To assess the statistical significance of intergroup differences, rank products were used but no significant differences were identified.

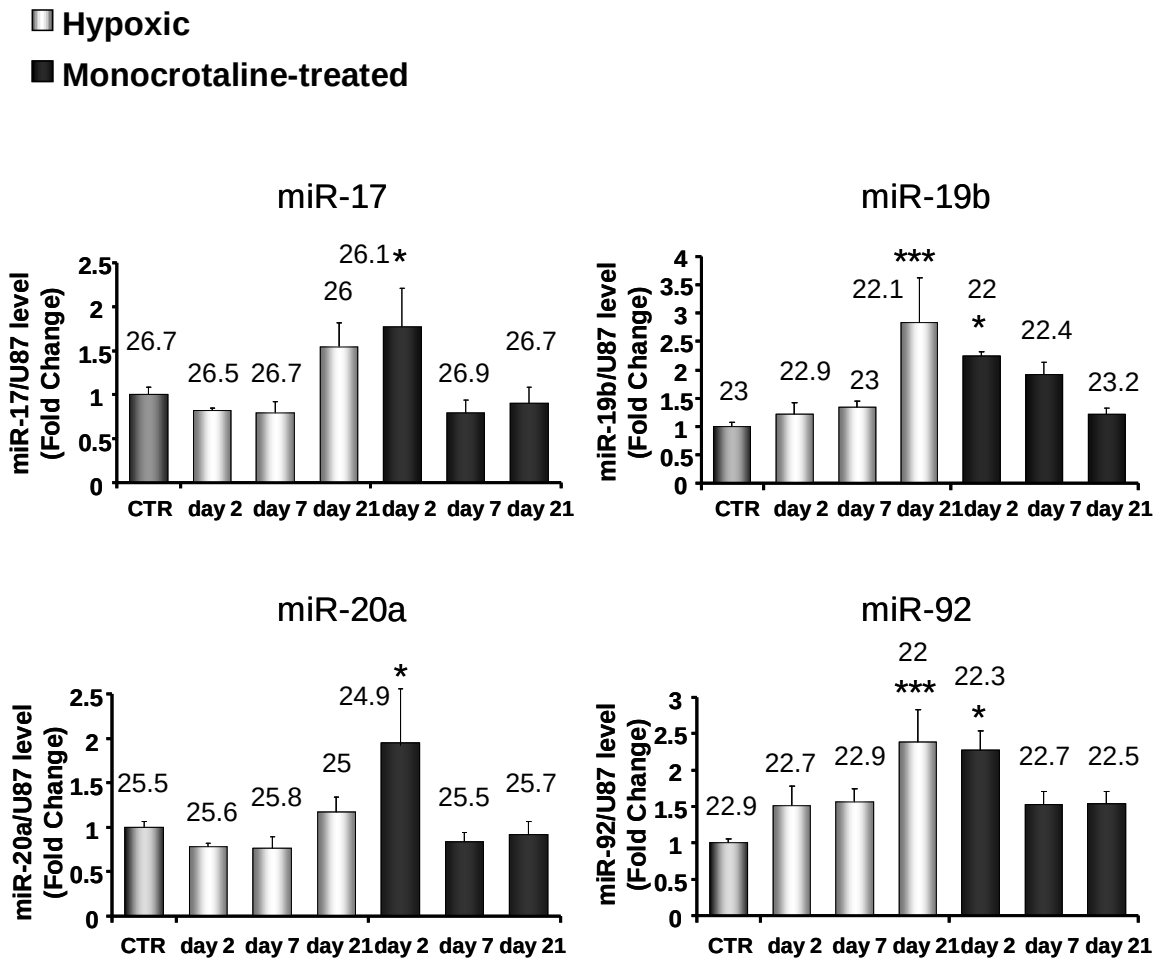

Figure 3-2 TaqMan® Real-Time PCR analysis of the miR-17/92 cluster in hypoxic and monocrotaline-treated rats. Total RNA was extracted from the lung of hypoxic (light grey bars) or monocrotaline-injected (black bars) six weeks old male rats. Time points and samples were tested in triplicate. Results were normalized to U87 values and expressed as relative fold change, with an arbitrary value of 1 assigned to the control group. Raw Ct values for the target miRNAs are indicated above each column. Data are expressed as mean ± SEM and analysed by two way ANOVA followed by Bonferroni's post-hoc test. *P<0.05, ***P<0.001 compared to CTR rats. N = 5/group.

3.2.4 In Vitro Validation of miRNAs Expression Level

As next step, the expression level of the dysregulated miRNA group, identified in the microarray study and validated by TaqMan® Real-Time PCR, was assessed in *in vitro* models of hypoxic injury to determine whether the hypoxic insult *in vitro* paralleled the effect of miRNA profiles *in vivo*. For this purpose, total RNA was extracted from normoxic and 24 h hypoxic rat PAFs and rat PASMCs and analyzed by TaqMan® Real-Time PCR for miRNA levels (Figure 3-3A and B). The inability to isolate PAECs from rat PAs did not allow us to analyze this cell type under the same experimental conditions. From the analysis of the data, miR-451 was slightly up-regulated, although this was not significant, in hypoxic PASMCs but undetectable in PAFs (Figure 3-3A and B). MiR-322, the only other up-regulated miRNA of our group of interest, showed a significant dysregulation in PASMCs, suggesting a potential involvement of both these miRNAs in the cellular changes resulting from a hypoxic insult in this pulmonary artery cell type (Figure 3-3A). On the other hand, the expression pattern for the down-regulated miRNAs of the group was quite similar to the *in vivo* analysis. In PAFs, miR-22, let-7f, and miR-30c were significantly down-regulated, whereas let-7a was not down-regulated and miR-21 showed a similar expression level in both normoxic and hypoxic cells (Figure 3-3B). It is important to remember that miR-21 showed a significant down-regulation *in vivo* only in the monocrotaline model, while no changes in miR-21 expression could be detected after exposure to hypoxia in male rats. In PASMCs, both miR-22 and miR-30c showed a significant down-regulation, whereas miR-21, let-7a and let-7f did not show altered expression after hypoxic treatment (Figure 3-3A). Thus in general the exposure of rat PAFs and PASMCs to hypoxia *in vitro* correlated with the changes in miRNAs observed *in vivo*.

3.2.5 Analysis of Genes Critical for miRNA Biogenesis in Rat Models of PAH

mRNA levels for genes critical to miRNA biogenesis (i.e. Dicer, Drosha, DGCR8, and Exp5, Chapter 1, Sections 1.3.3.4-1.3.3.6) were assessed by TaqMan® Real-Time PCR analysis in the same experimental samples used for miRNA analysis. In particular, *GAPDH* was chosen as housekeeping gene for the normalization of the genes of interest after the evaluation of its stability in hypoxic conditions. In fact, different studies reported in the past the capacity of hypoxia to induce up-regulation of *GAPDH* in different systems (Graven, Troxler et al. 1994; Zhong and Simons 1999). However, more recent studies proved that this dysregulation cannot be observed in several types of malignancies including human hepatocellular carcinoma, mouse hepatoma, human colon cancer and glioblastoma (Said, Hagemann et al. 2007; Said, Polat et al. 2009). In our experiments *GAPDH* didn't show any significant change under hypoxic conditions (Figure 3-4) and was therefore selected as housekeeping gene. The stability of the selected housekeeping gene has been evaluated in every TaqMan® Real-Time PCR performed in this and in the next result chapters (data not shown). Interestingly, *in vivo* exposure to hypoxia induced a marked and sustained decrease in lung mRNA level of Dicer (Figure 3-5A). Monocrotaline injury showed a significant effect on Dicer expression only 21 days post-injection (Figure 3-5A). We also quantified Dicer, Drosha, DGCR8, and Exp5 mRNA expression in 24 h hypoxic rat PAFs. *In vitro*, Dicer expression was significantly down-regulated by hypoxia (Figure 3-5B). Considering the important role played by Dicer in the maturation of a miRNA from its pre-form to its mature and active form (Murchison and Hannon 2004; Tijsterman and Plasterk 2004; Macrae, Zhou et al. 2006) (Chapter 1, Section 1.3.3.6), the significant down-regulation of this factor is consistent with the high number of down-regulated miRNAs identified in this study. It is also interesting to notice the differential response of Dicer to hypoxia and monocrotaline injection, consistent with the differences in pathogenesis observed between these two models (Meyrick and Perkett 1989; Wilson, Segall et al. 1989; Hessel, Steendijk et al. 2006; Firth, Mandel et al. 2010) (Chapter 1, Section 1.2.3).

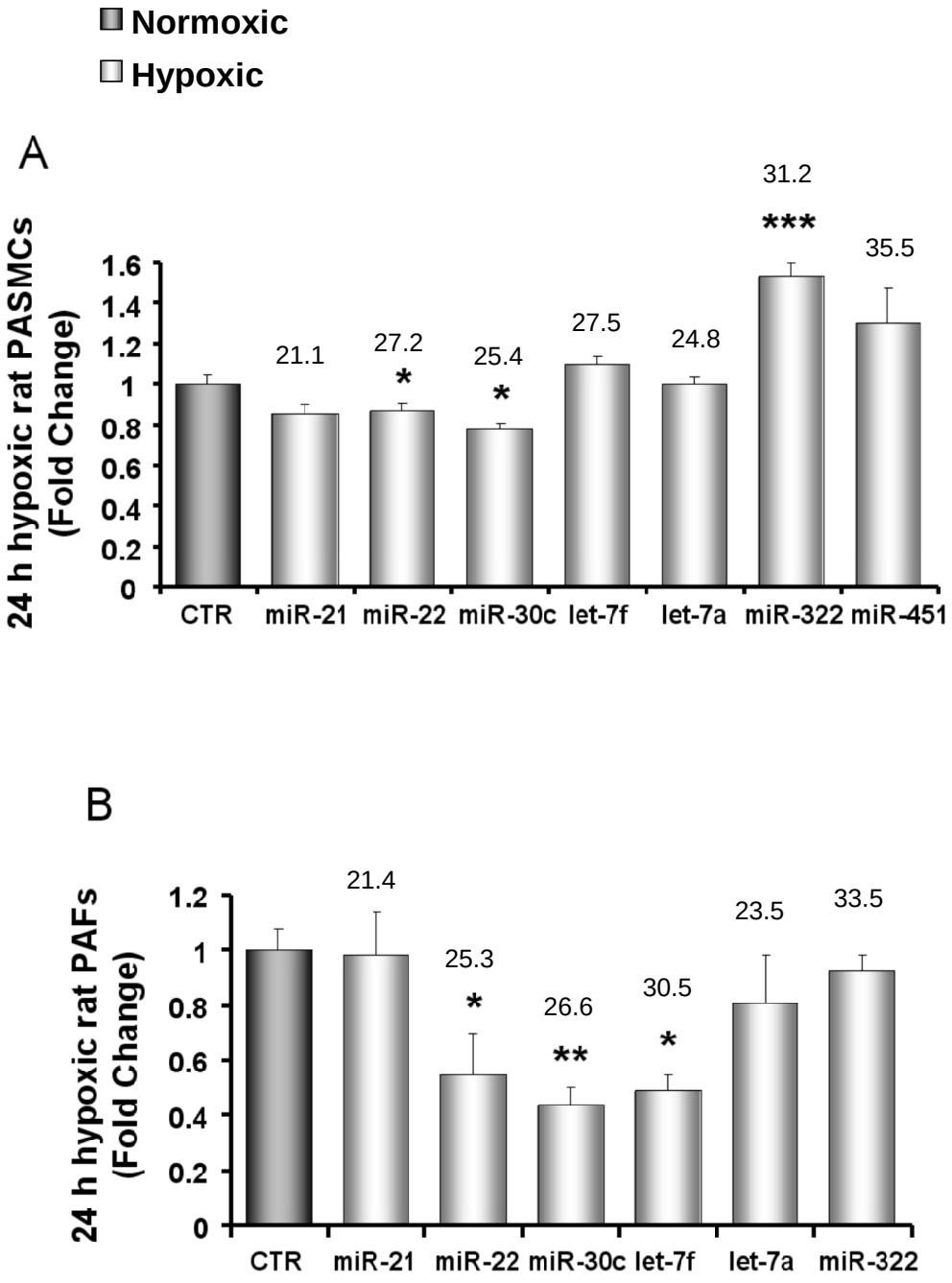

Figure 3-3 miRNA expression is regulated by hypoxia *in vitro*. TaqMan® Real-Time PCR analysis of hypoxic rat PASMCs (A) and PAFs (B) showing the expression level of miR-21, miR-22, miR-30c, let-7f, let-7a, miR-322 and miR-451 after 24 h of hypoxic conditions. These experiments were performed with total RNA extracted from both the control (CTR, dark grey bar) and the hypoxic cells (light grey bars) and tested in triplicate. Results were normalized to U87 values and expressed as relative fold change, with an arbitrary value of 1 assigned to the CTR group. Raw Ct values for the target miRNAs are indicated above each column. Data are expressed as mean ± SEM and analysed by unpaired t-test. *P<0.05, **P<0.01, ***P<0.001 compared to CTR rats. N = 4/group.

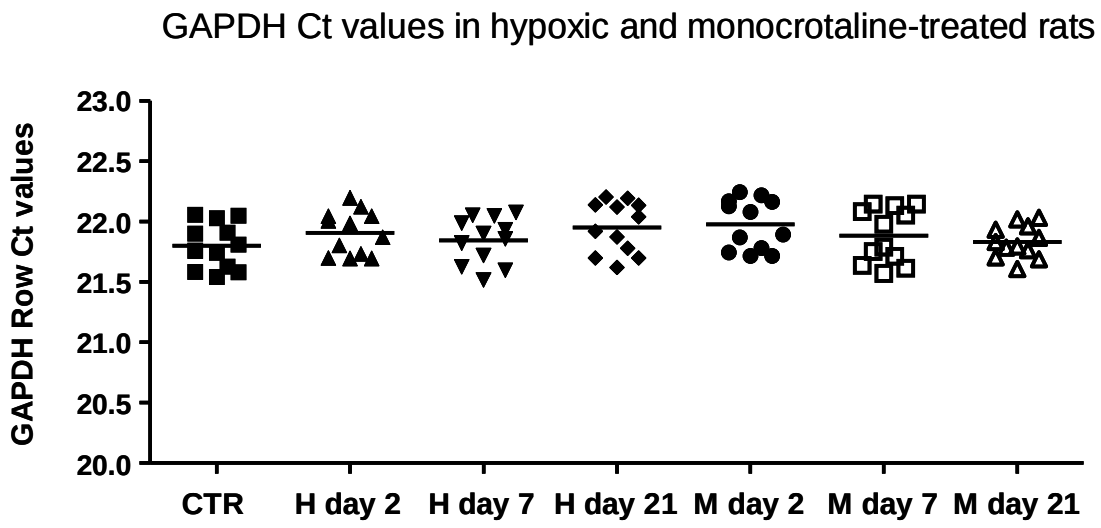

Figure 3-4 GAPDH row Ct values in hypoxic and monocrotaline-treated rats in comparison with untreated rats (CTR). GAPDH expression level was evaluated in hypoxic and monocrotaline-treated rats and compared with untreated animals in order to assess weather hypoxia can induce its expression as previously reported. Raw data are indicated for each sample analyzed in triplicate by TaqMan® Real-Time PCR, with a lane representing the mean value for each group.

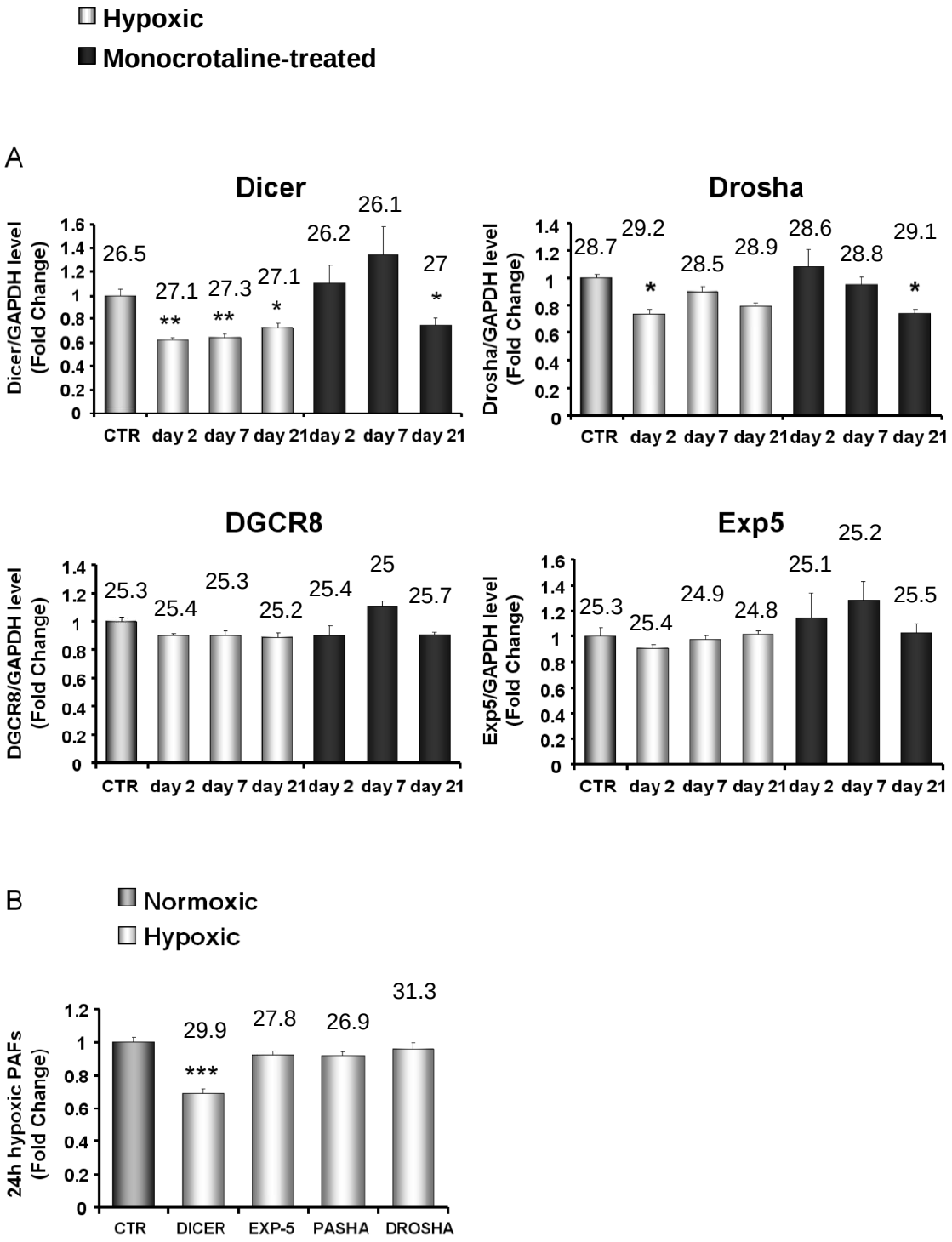
Hypoxic
Monocrotaline-treated
A
Dicer
Dicer/GAPDH level (Fold Change)
26.5
27.1
27.3
27.1
26.2
26.1
27
CTR day 2 day 7 day 21 day 2 day 7 day 21
Drosha
Drosha/GAPDH level (Fold Change)
28.7
29.2
28.5
28.9
28.6
28.8
29.1
CTR day 2 day 7 day 21 day 2 day 7 day 21
DGCR8
DGCR8/GAPDH level (Fold Change)
25.3
25.4
25.3
25.2
25.4
25
25.7
CTR day 2 day 7 day 21 day 2 day 7 day 21
Exp5
Exp5/GAPDH level (Fold Change)
25.3
25.4
24.9
24.8
25.1
25.2
25.5
CTR day 2 day 7 day 21 day 2 day 7 day 21
B
Normoxic
Hypoxic
24h hypoxic PAFs (Fold Change)
29.9
27.8
26.9
31.3
CTR DICER EXP-5 PASHA DROSHA

Figure 3-5 *In vivo* and *in vitro* expression level of Dicer, Exp5, Drosha, and DGCR8 in hypoxic and monocrotaline-treated rats. (A) TaqMan® Real-Time PCR analysis of hypoxic and monocrotaline-injected male rats after 2, 7, and 21 days of exposure. Total RNA was extracted from hypoxic (light gray bars) or monocrotaline-injected (black bars) rats at the age of 6 weeks (N = 4/group), and tested in triplicate. Results were normalized to GAPDH values and expressed as relative fold change, with an arbitrary value of 1 assigned to the control (CTR) group. (B) TaqMan® Real-Time PCR analysis of hypoxic rat PAFs showing the expression level of Dicer, Exp5, DGCR8, and Drosha after 24 h of exposure. This experiment was performed with total RNA extracted from CTR and hypoxic cells (n = 4/group). Results were normalized to GAPDH values. Raw Ct values for the target genes are indicated above each column. Data are expressed as mean ± SEM and analyzed by: (A) two way ANOVA followed by Bonferroni's post-hoc test. *P<0.05, **P<0.01 compared to CTR rats, or (B) unpaired t-test. ***P<0.001 compared to CTR rats.

3.2.6 Assessment of let-7d Expression Level in Hypoxic and Monocrotaline-Treated Rats and in Hypoxic Rat Cells

Considering that Dicer, despite its role in miRNA biogenesis (Murchison and Hannon 2004; Tijsterman and Plasterk 2004; Macrae, Zhou et al. 2006), can itself be the target of specific miRNAs, we decided to assess the expression of let-7d, identified as a miRNA regulator of Dicer expression (Tokumaru, Suzuki et al. 2008) (Chapter 1, Section 1.3.3.6), in the two analyzed rat models of PAH and in 24 h hypoxic rat PAFs. TaqMan® Real-Time PCR analysis of the samples revealed a significant up-regulation of this miRNA in hypoxic conditions both *in vivo* and *in vitro* (Figure 3-6A and B). Monocrotaline-injection led to an altered let-7d expression but only after 2 days of treatment, with normal levels detected 7 and 21 days after the injury (Figure 3-6A and B).

3.2.7 Effects of TGF-beta and BMP4 Stimulations on miRNA Expression in Rat PASMCs

The significant down-regulation occurring in Dicer expression after both a hypoxic and a monocrotaline injury (even if with different timing) correlates well with the down-regulation observed in specific miRNAs, but cannot explain the substantial up-regulation characteristic of miR-451 in both the models. A recent study demonstrates the existence of functional binding sites for SMAD3 (GTCTGGCCT) and SMAD4 (GTCTAGTCT) in the upstream region of this miRNA, suggesting that miR-451 may be activated by the SMAD pathway (Gal, Pandi et al. 2008). Long et al. study (Long, Crosby et al. 2009) showed an increased expression of phospho-SMAD3 in the monocrotaline model, where miR-451 levels reached an up-regulation of 20 times (Figure 3-1). To further evaluate miR-451 regulation, we exposed rat PASMCs to TGF-*beta* and BMP4. First of all we assessed the mRNA expression level of plasminogen activator inhibitor-1 (*PAI1*) and inhibitor of DNA binding-1 (*ID1*), main targets of the TGF-*beta* and the BMP signaling respectively (Miyazono and Miyazawa 2002; ten Dijke, Korchynskyi et al. 2003; Otsuka, Agah et al. 2006; Otsuka, Stempien-Otero et al. 2007; Diebold, Kraicun et al. 2008; Samarakoon and Higgins 2008), in order to verify the efficiency of the stimulation (Figure 3-7A and B). Next, we quantified by TaqMan® Real-Time PCR miR-

451 expression in the samples. Both agonists induced miR-451 levels significantly after 5 h of stimulation (Figure 3-8A). Notably, values returned to the unstimulated level by 24 h (Figure 3-8A). For a better understanding of the role of the TGF-*beta* super-family in the dysregulation of our miRNAs of interest, we also quantified the expression level of miR-21, miR-22, miR-30c, let-7f, let-7a and miR-322 after stimulation. Both TGF-*beta* and BMP4 stimulations induced the same profile of dysregulation we observed in hypoxic and monocrotaline-treated male rats. In fact, all the miRNAs down-regulated *in vivo* (miR-21, miR-22, miR-30c, let-7f and let-7a) were down-regulated after the TGF-*beta* stimulation, however miRNAs were up-regulated after the treatment with BMP4, in agreement with the reduced *BMP* signaling observed in Long et al. *in vivo* analysis (Long, Crosby et al. 2009) (Figure 3-8B and C). On the contrary miR-322, up-regulated in hypoxic and monocrotaline treated rats, showed no up-regulation after the TGF-*beta* stimulation, and a remarkably reduced expression after the BMP4 treatment, this again in correlation with our *in vivo* observations (Figure 3-8B and C).

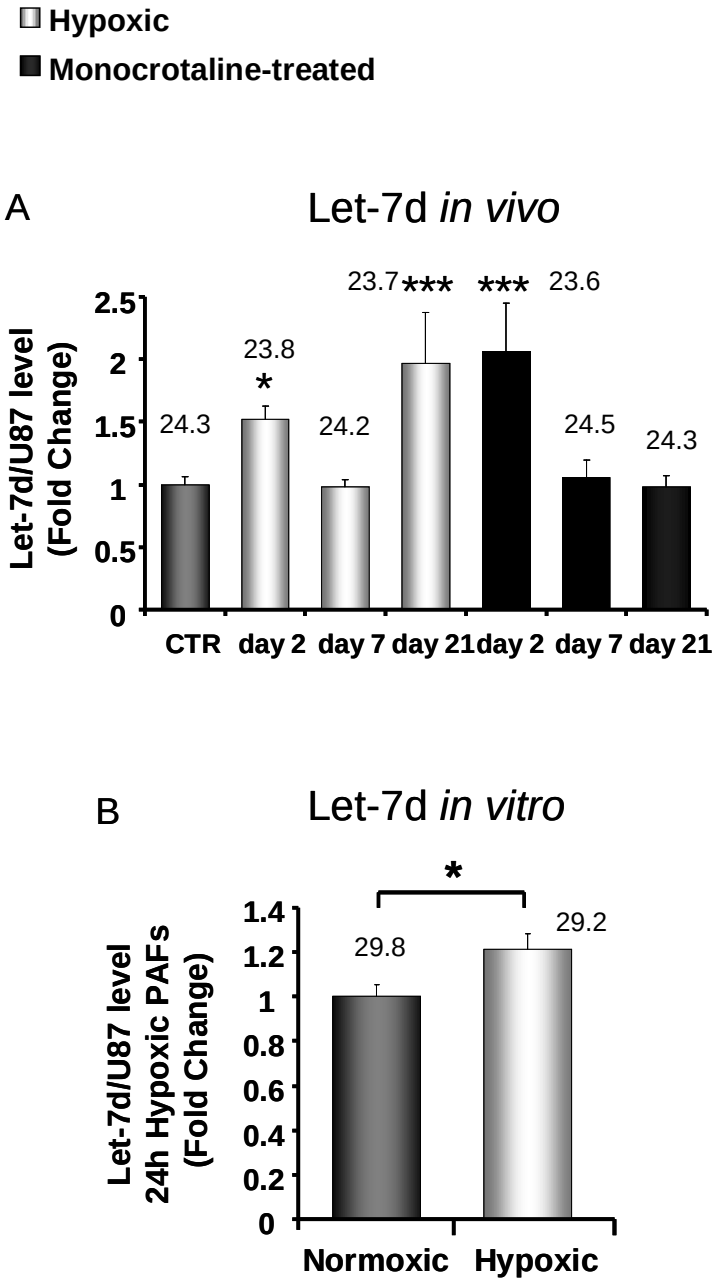

Figure 3-6 Assessment of let-7d expression *in vivo* and *in vitro*. TaqMan® Real-Time PCR analysis of total RNA extracted from the lung of hypoxic/monocrotaline-treated male rats (A, N = 5/group) and rat 24 h hypoxic PAFs (B, N = 6/group) showing let-7d expression. Samples were tested in triplicate. Results were normalized to U87 values and expressed as relative fold change, with an arbitrary value of 1 assigned to the CTR and normoxic group respectively. Raw Ct values for the target miRNAs are indicated above each column. For statistical analysis: (A) Data are expressed as mean ± SEM and analyzed by two way ANOVA followed by Bonferroni's post-hoc test. *P<0.05, ***P<0.001 compared to CTR rats; (B) Data were analyzed using an unpaired t-test. *P<0.05 compared to normoxic samples.

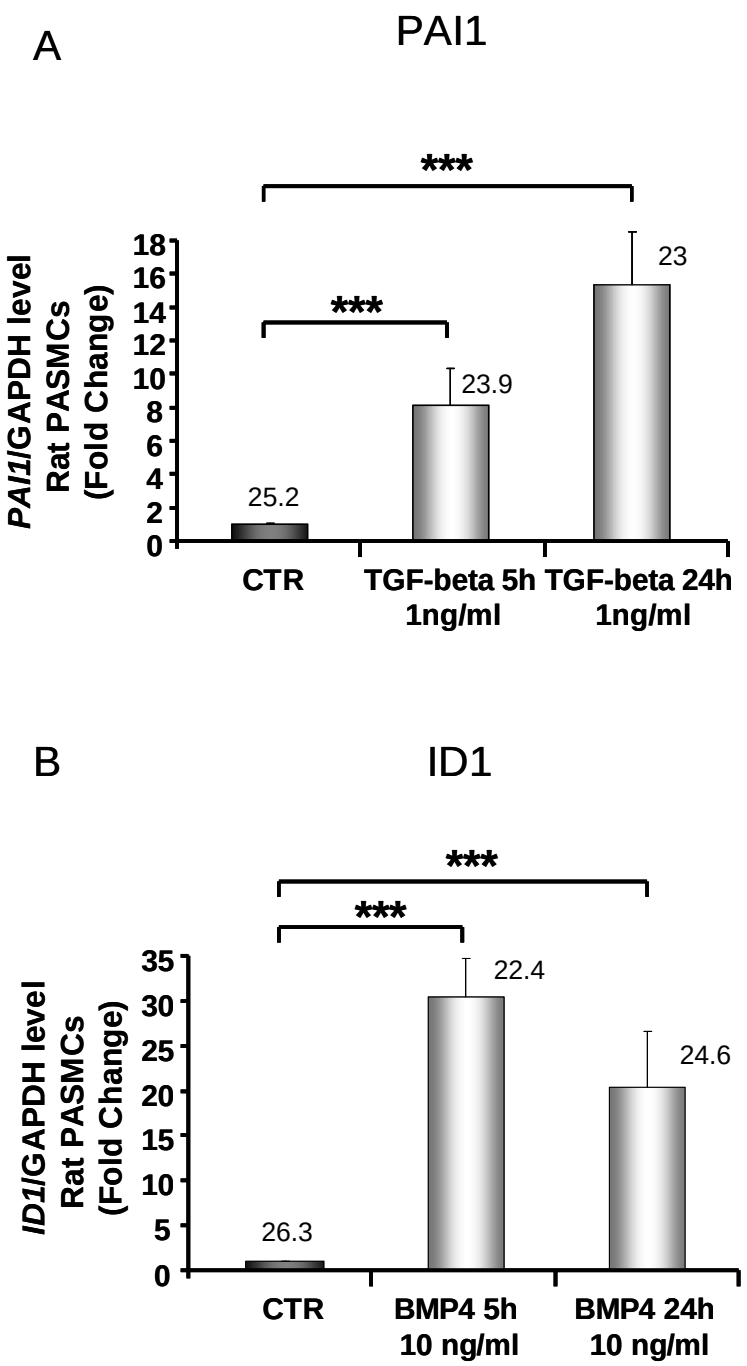

Figure 3-7 Analysis of PAI1 (A) and ID1 (B) expression in TGF-*beta* and BMP4 stimulated rat PASMCs. TaqMan® Real-Time PCR of total RNA extracted from passage 4 PASMCs stimulated with the two agonists for 5 and 24 h. Samples were tested in triplicate. Results were normalized to GAPDH values and expressed as relative fold change, with an arbitrary value of 1 assigned to the CTR group (unstimulated cells). Raw Ct values for the target genes are indicated above each column. Data are expressed as mean ± SEM and analyzed by one way ANOVA followed by Bonferroni's post-hoc test. ***P<0.001 compared to CTR rats. N = 3/group.

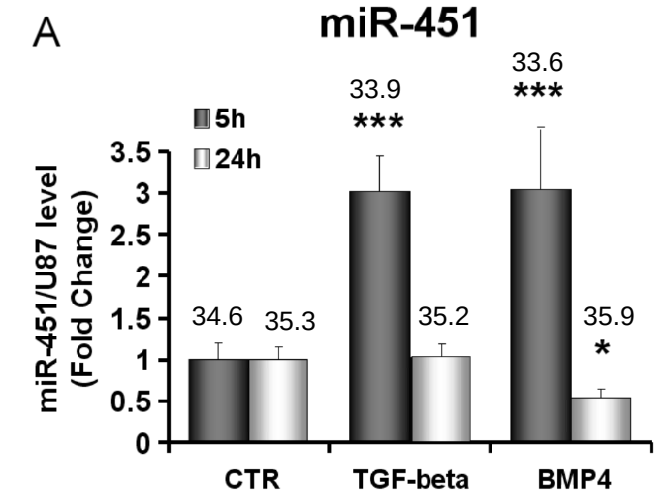
A
miR-451
5h
24h
miR-451/U87 level (Fold Change)
3.5
3
2.5
2
1.5
1
0.5
0
34.6
35.3
33.9
***
35.2
33.6
***
35.9
*
CTR
TGF-beta
BMP4

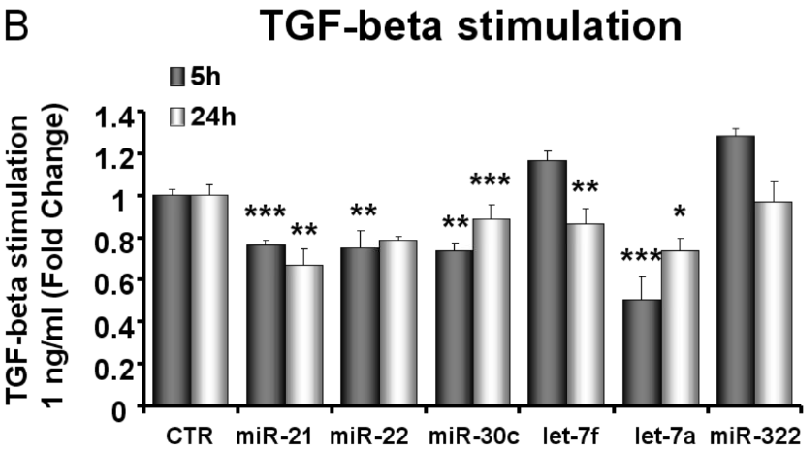
B
TGF-beta stimulation
5h
24h
TGF-beta stimulation 1 ng/ml (Fold Change)
1.4
1.2
1
0.8
0.6
0.4
0.2
0
***
**
**
**
***
**
***
*
CTR
miR-21
miR-22
miR-30c
let-7f
let-7a
miR-322

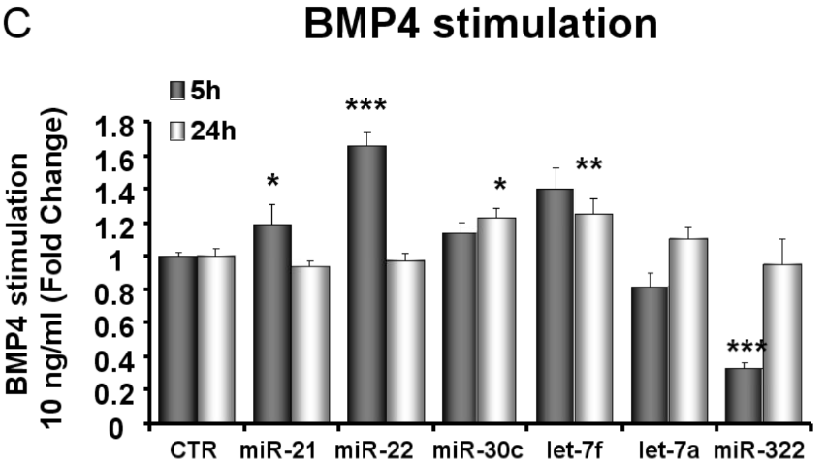
C
BMP4 stimulation
5h
24h
BMP4 stimulation 10 ng/ml (Fold Change)
1.8
1.6
1.4
1.2
1
0.8
0.6
0.4
0.2
0
*
***
*
**
***
CTR
miR-21
miR-22
miR-30c
let-7f
let-7a
miR-322

Figure 3-8 TGF-*beta*/BMP4 stimulation can induce the significant dysregulation of miR-451, miR-322, miR-21, miR-22, miR-30c, let-7a and let-7f in PASMCs. Passage 4 rat PASMCs were stimulated and total RNA extracted after 5 and 24 h of stimulation from both nontreated and stimulated cells. Each sample was analyzed in triplicate by TaqMan® Real-Time PCR for testing miR-451 (A) and miR-21, miR-22, miR-30c, let-7f, let-7a and miR-322 (B and C) expression level. Results were normalized to U87 values and expressed as relative fold change, with an arbitrary value of 1 assigned to the CTR group. For miR-451 expression, Raw Ct values for the target miRNA are indicated above each column. For the other miRNAs in graphs B and C, raw Ct values are the following: graph B: miR-21= 19.9, 20.6 (5 and 24h respectively); miR-22= 26.3, 26.9; miR-30c= 23.9, 23.5; let-7f= 26.4, 26.9; let-7a= 24.7, 24.2; miR-322= 29.8, 30.5. Graph C: miR-21= 19.9, 20.5 (5 and 24h respectively); miR-22= 25.6, 26.4; miR-30c= 24, 24.5; let-7f= 26.6, 26; let-7a= 24.7, 25; miR-322= 32.4, 30.2. Data are expressed as mean ± SEM and analyzed by one way ANOVA followed by Bonferroni's post-hoc test. *P<0.05, **P<0.01, ***P<0.001 compared to CTR rats. N = 3/group.

3.2.8 Prediction of Potential miRNA Targets

In order to identify a list of targets for our miRNAs of interest, the 3' UTRs of mRNAs was screened for the 6-mer seeds of the miRNAs of interest as described in details in Chapter 2 (Section 2.12). Following specific criteria (e.g. high number of seed sites located at short distance to each other, good site accessibility) we generated a list of targets for the down-regulated miRNAs miR-21, miR-22 and miR-30c, the three miRNAs with the same profile of dysregulation (i.e. reduction) sharing the higher number of targets (Table 3-4). We also generated a preliminary list for miR-451 and miR-322 targets (Table 3-5). However, this list was characterized by a very high number of targets, but all with a low number of seeds (no more than 1 or 2), making it difficult to identify the best predicted targets to shortlist. For this reason, we decided to focus our attention on miR-21, miR-22 and miR-30c targets for the validation. Nevertheless it is important to notice that certain targets could be identified in both the lists (marked in lilac in Table 3-5), thus adding additional complexity. In particular, 4 targets were included in the group of those targets selected for further analysis for the down-regulated miRNAs because matching all the criteria (*KCNJ6*, *NFAT5, YWHAZ* and *TACC1*, see below for more details), including multiple number of seeds for more than one miRNA of the group and short distance between the seed sequences.

Target name	Target of	Target function
KCNJ6	miR-22 and miR-30c	potassium inwardly-rectifying channel, subfamily J, member 6
PPP2R5E	miR-21 and miR-22	protein phosphatase 2, regulatory subunit B(B56), epsilon isoform
NFAT5	miR-22 and miR-30c	nuclear factor of activated T-cells 5
TACC1	miR-21 and miR-30c	transforming, acidic coiled-coil containing protein 1
TGFBR1	miR-21 and miR-22	transforming growth factor, beta receptor 1
TGFBRAP1	miR-21 and miR-22	transforming growth factor, beta receptor associated protein 1
ADARB1	miR-22	adenosine deaminase, RNA-specific, B1
RBPSUH	miR-21	recombining binding protein suppressor of hairless (Drosophila)
TNRC6A	miR-30c	trinucleotide repeat containing 6a
YWHAZ	miR-30c	tyrosine 3-monooxygenase/tryptophan 5-monooxygenase activation protein, zeta polypeptide

Table 3-4 Predicted targets for the three down-regulated miRNAs miR-21, miR-22 and miR-30c.

Target name	Also target of	Target function
ANKFY1		ankyrin repeat and FYVE domain containing 1
ANKS1A		ankyrin repeat and sterile alpha motif domain containing 1A
BCL9		B-cell CLL/lymphoma 9
CYBRD1		cytochrome b reductase 1
DHX37		DEAH (Asp-Glu-Ala-His) box polypeptide 37
DISP2		dispatched homolog 2 (Drosophila)
ELK4		ELK4, ETS-domain protein (SRF accessory protein 1)
FBXO21		F-box protein 21
GLS		glutaminase
GRM2		glutamate receptor, metabotropic 2
KCNJ6	**Mir-22 and miR-30c**	**potassium inwardly-rectifying channel, subfamily J, member 6**
KCNK5		potassium channel, subfamily K, member 5
KIAA0174		KIAA0174
MGAT4B		mannosyl (alpha-1,3-)-glycoprotein beta-1,4-N-acetylglucosaminyltransferase, isozyme B
MOBKL1B		MOB1, Mps One Binder kinase activator-like 1B (yeast)
NFAT5	**Mir-22 and miR-30c**	**nuclear factor of activated T-cells 5, tonicity-responsive**
PATL1		protein associated with topoisomerase II homolog 1 (yeast)
PDZD8		PDZ domain containing 8
PLXNC1		plexin C1
PMEPA1		prostate transmembrane protein, androgen induced 1
PPM1L		protein phosphatase 1 (formerly 2C)-like
RAB22A	**Mir-22 and miR-30c**	**RAB22A, member RAS oncogene family**
RCAN2		regulator of calcineurin 2
RGD1561661		similar to Ferritin light chain (Ferritin L subunit)
SAR1A		SAR1 homolog A (S. cerevisiae)
SLC11A2		solute carrier family 11 (proton-coupled divalent metal ion transporters), member 2
SLC12A2		solute carrier family 12 (sodium/potassium/chloride transporters), member 2
SLC25A22		solute carrier family 25 (mitochondrial carrier: glutamate), member 22
SNX11		sorting nexin 11
SNX27		sorting nexin family member 27
TACC1	**Mir-21 and miR-30c**	**transforming, acidic coiled-coil containing protein 1**
TGFA		transforming growth factor, alpha
TPCN1		two pore segment channel 1
UBE2K	**Mir-21 and miR-22**	**ubiquitin-conjugating enzyme E2K (UBC1 homolog, yeast)**
UBE4A		ubiquitination factor E4A (UFD2 homolog, yeast)
UNC5C		unc-5 homolog C (C. elegans)
ZBTB39		zinc finger and BTB domain containing 39
ZNF592		zinc finger protein 592

Table 3-5 Predicted targets for the two up-regulated miRNAs miR-451 and miR-322.

3.2.9 Analysis of miR-21, miR-22, and miR-30c Targets in Hypoxic and Monocrotaline-Treated Lungs

Based on the targets identified in (Table 3-4), we performed TaqMan® Real-Time PCR validations on the same sample set used for miRNA profiling (Figure 3-9). In general, a number of the predicted genes, but not all, were regulated as expected. For example, *KCNJ6* (G protein-activated inward rectifier potassium channel 2, inward-rectifier type potassium channel) mRNA levels were significantly enhanced after both hypoxia- and monocrotaline induced injuries (Figure 3-9). MiR-21 was only down-regulated in monocrotaline-induced injury. Likewise, *TACC1* (transforming acidic coiled-coil-containing protein 1, its function is not precisely known but it is suspected to play a role in carcinogenesis and to regulate mRNA processing) (Conte, Charafe-Jauffret et al. 2002), which has predicted targets for miR-21 and miR-30c, was only up-regulated in the monocrotaline-treated lungs (Figure 3-9). Serine/threonine-protein phosphatase 2A regulatory subunit epsilon isoform (*PPP2R5E*) was up-regulated only after monocrotaline-induced injury, again perhaps indicative of miR-21 regulation. Similarly, transforming growth factor *beta* receptor 1 (*TGFBR1*, serine/threonine protein kinase), transforming growth factor, *beta* receptor associated protein 1 (TGFBRAP1, it associates with inactive heteromeric TGF-*beta* receptor complexes and is released upon activation of signalling) and nuclear factor of activated T-cells 5 (*NFAT5*, transcription factor that regulates the expression of genes involved in the osmotic stress) (Aramburu, Drews-Elger et al. 2006), targets of miR-22/miR-21 and miR-22/miR-30c respectively, showed significant up-regulation selectively in the monocrotaline model (Figure 3-9). The up-regulation of *YWHAZ* (14-3-3 protein zeta/delta, able to interact with TPH1, the rate-limiting enzyme in the biosynthesis of serotonin) (Ichimura, Uchiyama et al. 1995; Winge, McKinney et al. 2008) and *TNRC6A* (trinucleotide repeat-containing gene 6A protein) characteristic only of the monocrotaline-treated rats could be indicative of a significant role of miR-30c in gene regulation after injury (Figure 3-9). Although the dysregulation of several targets correlates well with miRNA dysregulation, some of them seem to be regulated in a different way. RBPSUH (recombining binding protein suppressor of hairless, it is the DNA-binding component of the transcription complex regulated by Notch signaling) for example, target of miR-21, is down-regulated in the hypoxic model. As mentioned in

the previous section, 4 of the validated targets (*KCNJ6*, *NFAT5, YWHAZ* and *TACC1)* can also be identified in the list of miR-322 and miR-451 potentially regulated proteins, suggesting that the action of these miRNAs, up-regulated in both the models, could "balance" the action of miR-21, miR-22 and miR-30c and explain, at least partially, why the expression of these targets does not completely match with the dysregulation of the down-regulated miRNAs. Considering the relevant role of the TGF-*beta* super-family in pulmonary vascular SMC signaling in PAH (Richter, Yeager et al. 2004; Dewachter, Adnot et al. 2009; Morrell, Adnot et al. 2009; Morrell 2010; Morrell 2010) (Chapter 1, Section 1.2.4.1), we decided to select *TGFBR1* for further analysis. To validate the up-regulation of the target at the protein level, we quantified by western blot analysis the expression of TGFBR1 in monocrotaline day 7-treated and untreated male rats. The signal obtained from 4 samples for each group showed a significant up-regulation of this protein in monocrotaline-treated rats (Figure 3-10A and B). Moreover, on day 7, we also localized *TGFBR1* protein in paraffin sections from control and monocrotaline-treated rat lungs with immunohistochemistry assays. Again, this experiment showed *TGFBR1* up-regulation in the monocrotaline model 7 days after initiation of treatment (Figure 3-10C).

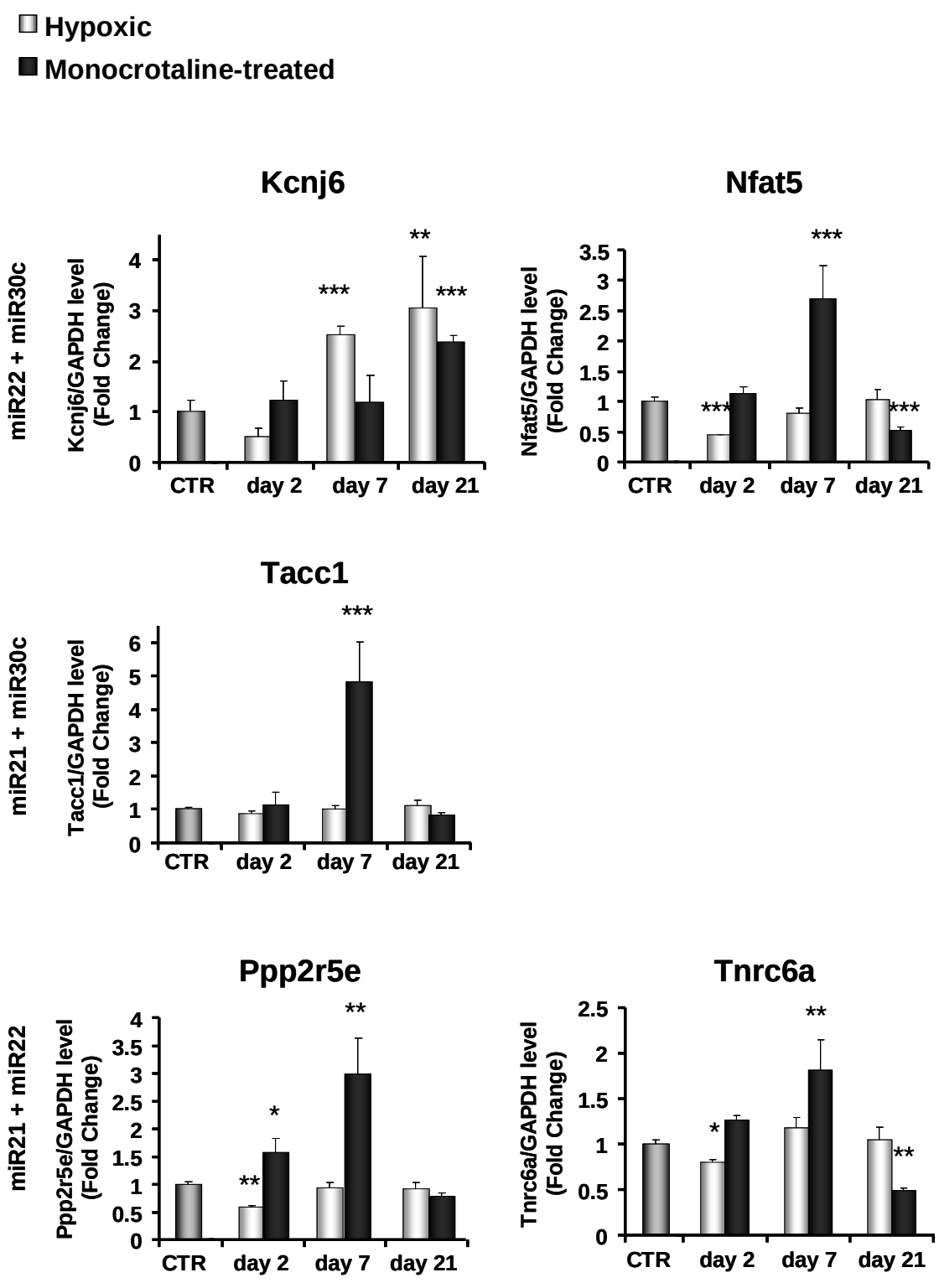
Hypoxic
Monocrotaline-treated
Kcnj6
miR22 + miR30c
Kcnj6/GAPDH level (Fold Change)
CTR
day 2
day 7
day 21
Nfat5
Nfat5/GAPDH level (Fold Change)
Tacc1
miR21 + miR30c
Tacc1/GAPDH level (Fold Change)
Ppp2r5e
miR21 + miR22
Ppp2r5e/GAPDH level (Fold Change)
Tnrc6a
Tnrc6a/GAPDH level (Fold Change)

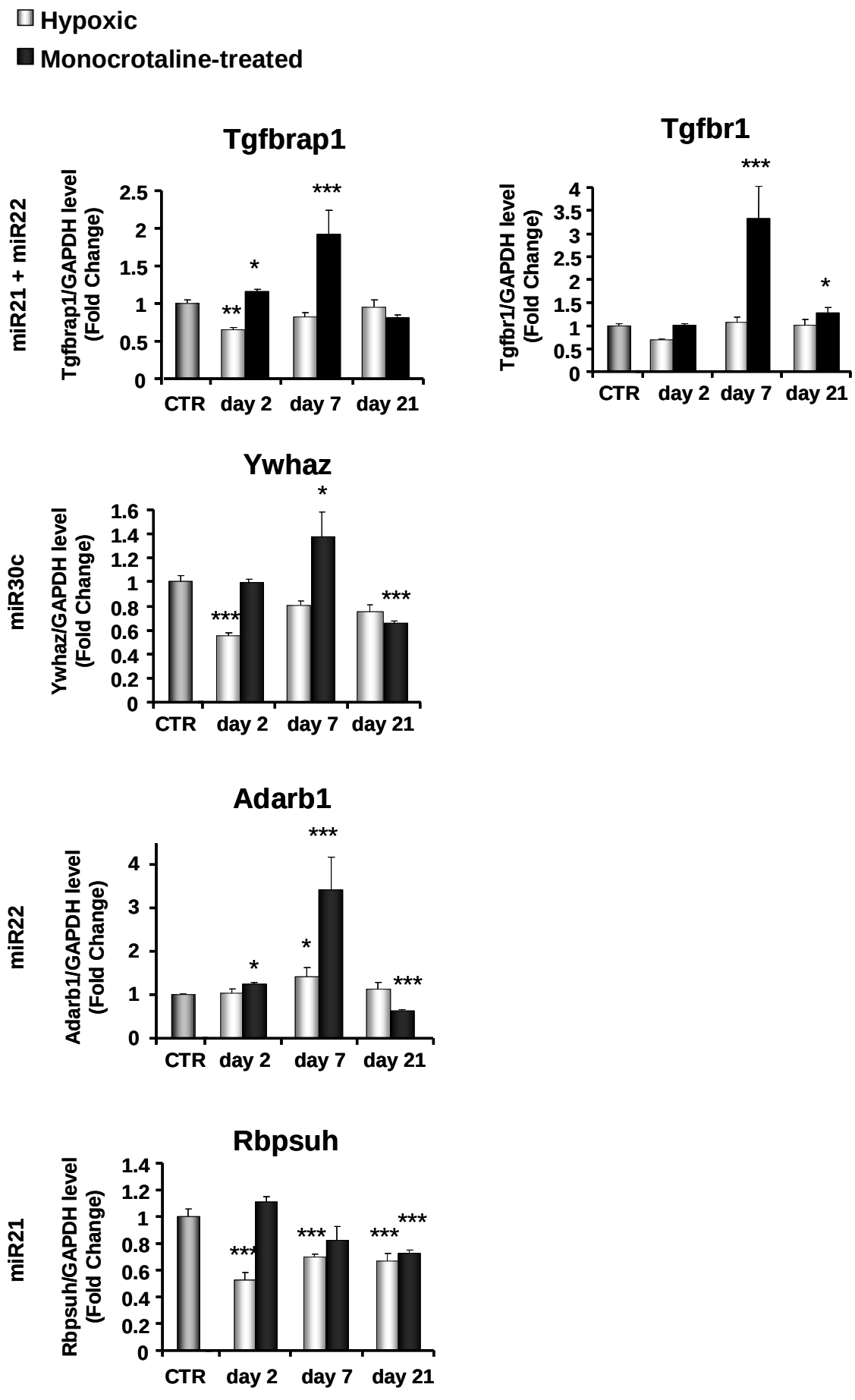
Hypoxic
Monocrotaline-treated
Tgfbrap1
miR21 + miR22
Tgfbrap1/GAPDH level (Fold Change)
2.5
2
1.5
1
0.5
0
**
*
***
CTR
day 2
day 7
day 21
Tgfbr1
Tgfbr1/GAPDH level (Fold Change)
4
3.5
3
2.5
2
1.5
1
0.5
0
***
*
CTR
day 2
day 7
day 21
Ywhaz
miR30c
Ywhaz/GAPDH level (Fold Change)
1.6
1.4
1.2
1
0.8
0.6
0.4
0.2
0
***
*
***
CTR
day 2
day 7
day 21
Adarb1
miR22
Adarb1/GAPDH level (Fold Change)
4
3
2
1
0
*
*
***
***
CTR
day 2
day 7
day 21
Rbpsuh
miR21
Rbpsuh/GAPDH level (Fold Change)
1.4
1.2
1
0.8
0.6
0.4
0.2
0
***
***
***
CTR
day 2
day 7
day 21

Figure 3-9 Assessment of miRNA target mRNA levels in rat lung following hypoxic and monocrotaline injuries. Total RNA was extracted from lung samples of hypoxic (light grey bars) and monocrotaline-treated (black bars) male rats. cDNA was prepared and mRNA levels were tested in triplicate by TaqMan® Real-Time PCR and plotted as fold change versus control samples. Results were normalized to GAPDH values. The miRNAs that possess predicted seed sequences for each target are indicated. Data are expressed as mean ± SEM and analyzed by two way ANOVA followed by Bonferroni's post-hoc test. *P<0.05, **P<0.01, ***P<0.001 compared to CTR rats. N = 5/group.

3.2.10 Analysis of TGFBR1 Expression in Stimulated and Hypoxic- Treated Rat Cells

Next, we assessed the expression level of this target in the rat PASMCs stimulated with TGF-*beta* and BMP4 previously analyzed for miRNA expression. *TGFBR1* was significantly up-regulated after TGF-*beta* stimulation and significantly down-regulated after BMP4 stimulation, an expression profile consistent with profile of miR-22 and miR-21, its potential regulators (i.e. down-regulated by TGF-*beta* and up-regulated by BMP4 stimulation) (Figure 3-11A). However, *TGFBR1* was not dysregulated in 24 h hypoxic PAFs (Figure 3-11B).

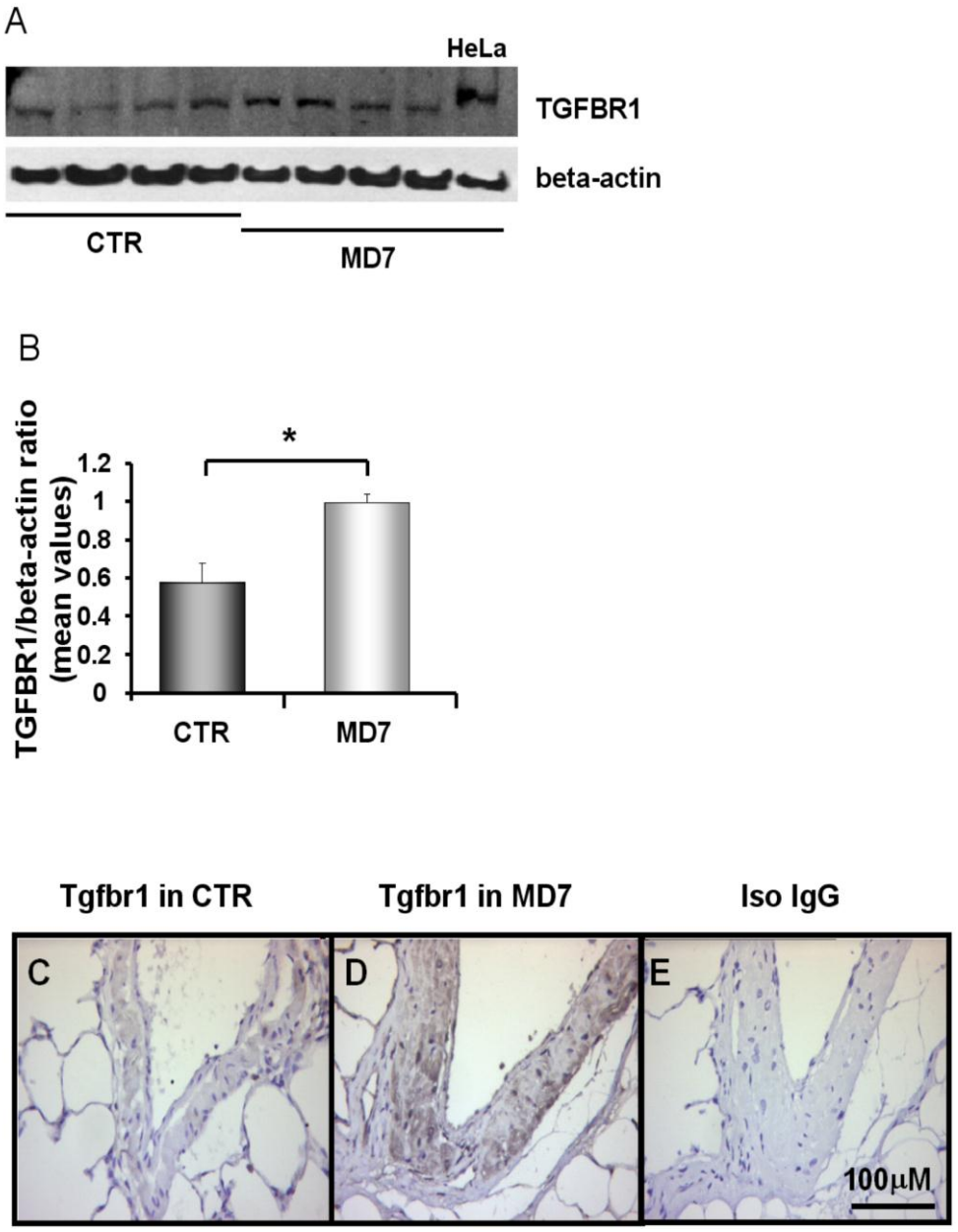

Figure 3-10 Assessment of TGFBR1 protein expression level in total rat lung protein extracts and its localization in rat lung paraffin sections. (A) TGFBR1 expression level was quantified by western blot analysis in proteins extracted from lung samples of monocrotaline-treated male rats on day 7 (MD7) and control (CTR) rats. Four samples were tested for each group, and the intensity of the western blot bands was measured using specific software (Scion Image software). The resulting quantification bars are represented in the graph (B), with the monocrotaline day 7 group represented by the light gray bar. Data are expressed as mean ± SEM and analyzed by unpaired t-test. *P<0.05 compared to CTR rats.TGFBR1 was localized in lung paraffin sections using an immunohistochemistry assay. (C) TGFBR1 staining in CTR rat lungs. (D) TGFBR1 staining in lungs after monocrotaline exposure for 7 days (MD7). (E) Lung stained with a nonimmune isotype-IgG CTR antibody. Scale bar = 100 μm.

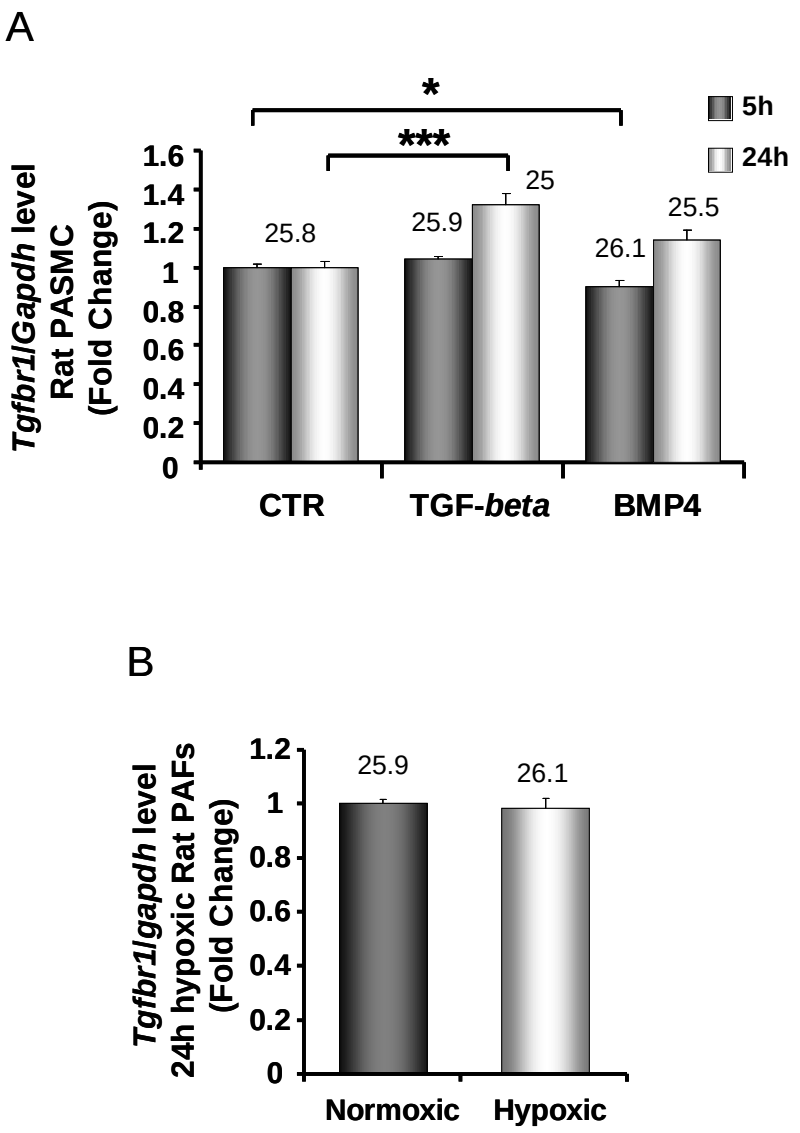

Figure 3-11 Tgfbr1 expression in stimulated and hypoxic rat cells. The expression level of *Tgfbr1* was assessed by TaqMan® Real-Time PCR in rat PASMCs stimulated with TGF-*beta* and BMP4 for 5 and 24 h (A), and in rat PAFs exposed to hypoxia for 24 h. Samples were tested in triplicate. Results were normalized to GAPDH values. Raw Ct values for the target gene are indicated above each column. For statistical analysis: (A) Data are expressed as mean ± SEM and analyzed by one way ANOVA followed by Bonferroni's post-hoc test. *P<0.05, ***P<0.001 compared to CTR rats. N = 3/group. (B) An unpaired t-test was conducted, but no significant dysregulation was identified. N = 6/group.

3.2.11 miRNA Expression in Hypoxic Mice

The identified dysregulation of specific miRNAs in two different rat models of PAH and the similar changes observed in targets potentially involved in the development of PAH suggest a potentially important role for miRNAs in the development of this pathology. To prove the conserved character of this dysregulation, we next analyzed the expression level of our miRNAs of interest in WT male mice exposed to hypoxia for 14 days. Total RNA (including miRNA) was extracted from the whole lung of 10 weeks old normoxic and hypoxic mice and TaqMan® Real-Time PCR experiments were performed. The analysis of these data confirmed the dysregulation identified in the rat models. In fact, we observed a significant down-regulation of miR-22, miR-30c and let-7a, while miR-21 and let-7f did not show any dysregulation (Figure 3-12). The only differentially regulated miRNA was miR-451. Although miR-451 was substantially up-regulated in both the rats PAH models, we couldn't observe any dysregulation in 14 days hypoxic male mice (Figure 3-12). MiR-322, a rat specific miRNA, was not analyzed in these samples.

3.2.12 miRNA Dysregulation in Human Hypoxic Cells

To verify whether the dysregulation of specific miRNAs could be identified in human samples, human fetal PAFs and human PAECs were exposed to chronic hypoxia for 24 h and then assessed by TaqMan® Real-Time PCR for the expression of the miRNA group identified in the rat study. The analysis of human PAFs showed a significant dysregulation of all the five miRNAs down-regulated in rats (even miR-21 in this case resulted significantly dysregulated after the hypoxic treatment), while in hypoxic PAECs only miR-30c resulted modestly down-regulated (Figure 3-13A and B**).** MiR-451, undetectable in PAFs, showed no significant changes in PAECs (Figure 3-13A and B). MiR-322, (rat specific) was not analyzed in human samples.

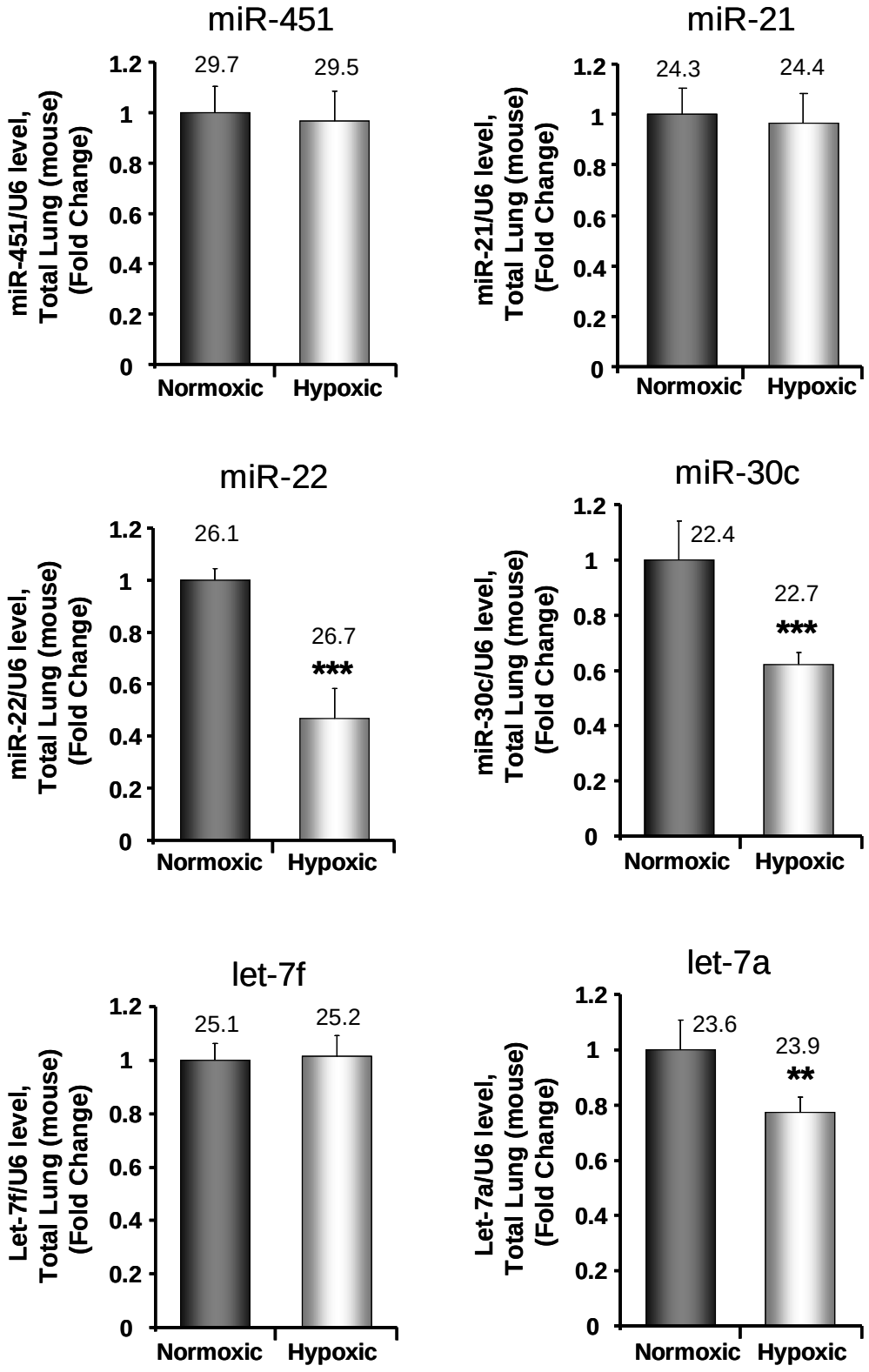

Figure 3-12 miRNa expression in hypoxic mice. TaqMan® Real-Time PCR analysis of normoxic and 14 days hypoxic WT male mice. Total RNA was extracted from the lung of normoxic (dark grey bars) or hypoxic (light grey bars) 10 weeks old male mice. 6 mice/group were analyzed. Every sample was tested in triplicate. Results were normalized to U6 values and expressed as relative fold change, with an arbitrary value of 1 assigned to the control group. Raw Ct values for the target miRNAs are indicated above each column. For statistical analysis, an unpaired t-test was conducted. **P<0.01, ***P<0.001 compared to normoxic mice.

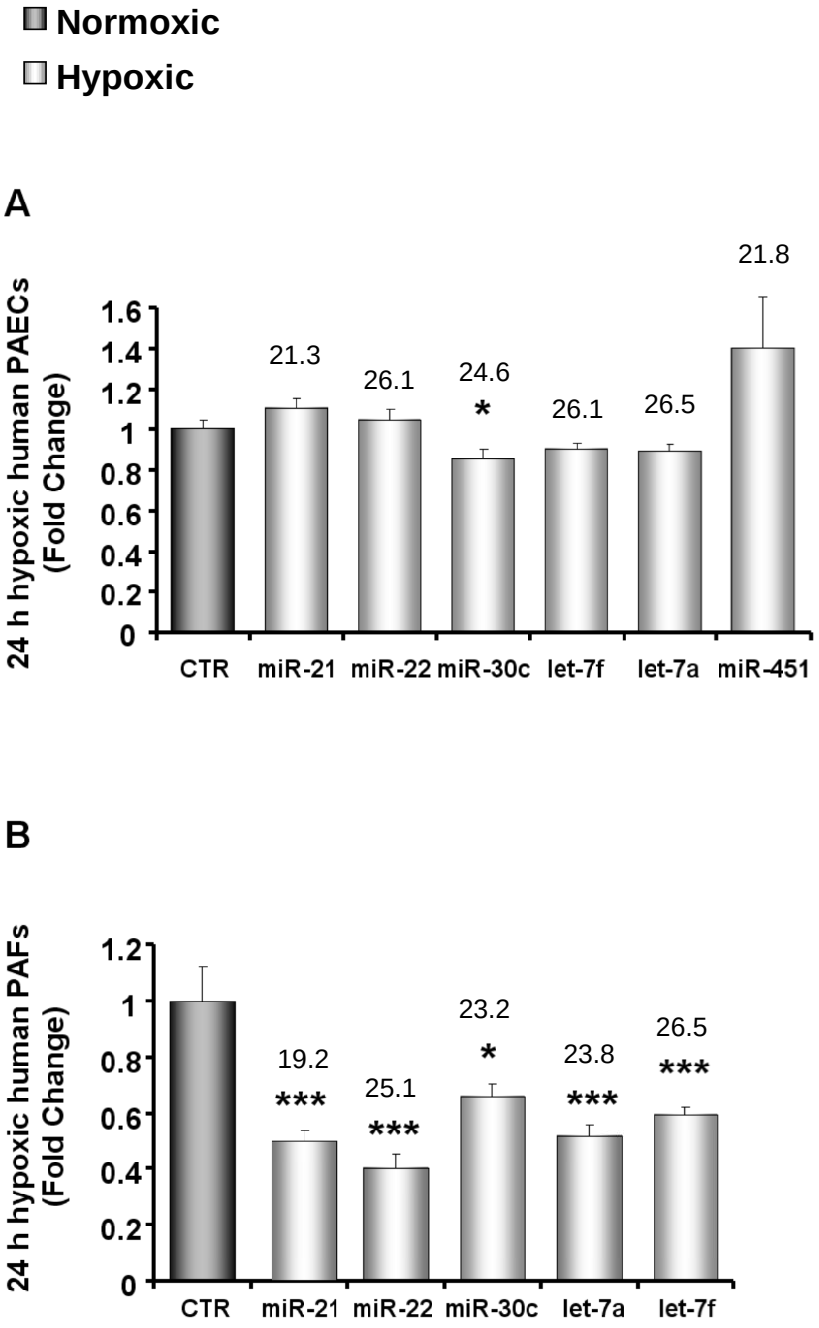

Figure 3-13 miRNA expression is regulated by hypoxia *in vitro* in human cells. (A and B) TaqMan® Real-Time PCR analysis of hypoxic fetal human PAECs (A) and human PAFs (B) showing the expression level of miR-21, miR-22, miR-30c and let-7f after 24 h of stimulation. These experiments were performed with total RNA extracted from both the control and the hypoxic cells. Samples were tested in triplicate. Results were normalized to Rnu-48 values and expressed as relative fold change, with an arbitrary value of 1 assigned to the control group. Raw Ct values for the target miRNAs are indicated above each column. For statistical analysis, an unpaired t-test was conducted. *P<0.05, ***P<0.001 compared to CTR. N = 6/group.

3.2.13 Expression Level of miR-22 and miR-451 in Idiopathic Pulmonary Arterial Hypertension Patients

Considering the high level of dysregulation observed in male rats both *in vivo* and *in vitro* for miR-451 and miR-22, the effect of both TGF-*beta* and BMP4 on their expression level, and the correlation between miR-22 dysregulation and *TGFBR1* expression previously shown in the rat study, we next analyzed total RNA extracted from paraffin-embedded lungs of patients with IPAH and HPAH and unaffected controls in order to assess the dysregulation of these two miRNAs in the human pathology. A significant down-regulation of miR-22 was observed, while miR-451 was not altered (Figure 3-14A and B).

3.2.14 Expression Level of miR-22 and miR-451 in PASMCs Obtained From Patients with a Mutation in the BMPR2 Gene

We next analysed RNA extracted from PASMCs isolated from patients with HPAH and in particular with an identified mutation in the *BMPR2* gene. The analysis of these samples in comparison with cells obtained from unaffected controls completely concurred with previous results, showing a significant down-regulation of miR-22 and no alteration of miR-451 expression level (Figure 3-15A and B). Taken together, the analyzed human samples suggest a conserved dysregulation of miR-22 across species, and a selective dysregulation of miR-451 in rat models of this pathology.

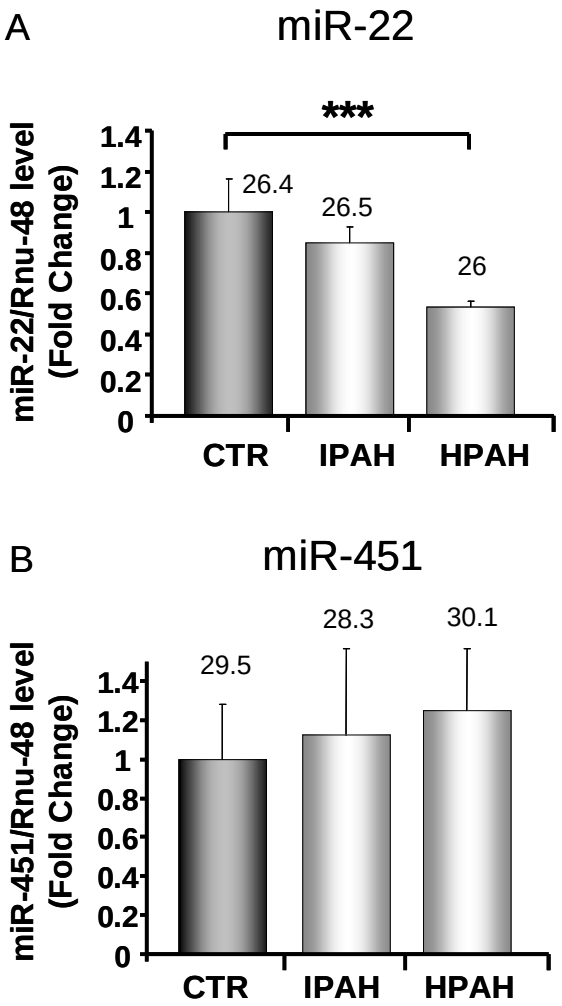

Figure 3-14 miR-22 and miR-451 expression level in PAH patients. TaqMan® Real-Time PCR analysis of miR-22 (A) and miR-451 (B) expression level in paraffin-embedded human lungs of patients with idiopathic and heritable PAH and controls (CTRs). Samples were analyzed in triplicate, normalized to Rnu-48 values and expressed as relative fold change, with an arbitrary value of 1 assigned to the CTR group. Raw Ct values for the target miRNAs are indicated above each column. Data are expressed as mean ± SEM and analyzed by two way ANOVA followed by Bonferroni's post-hoc test. ***P<0.001 compared to CTR.

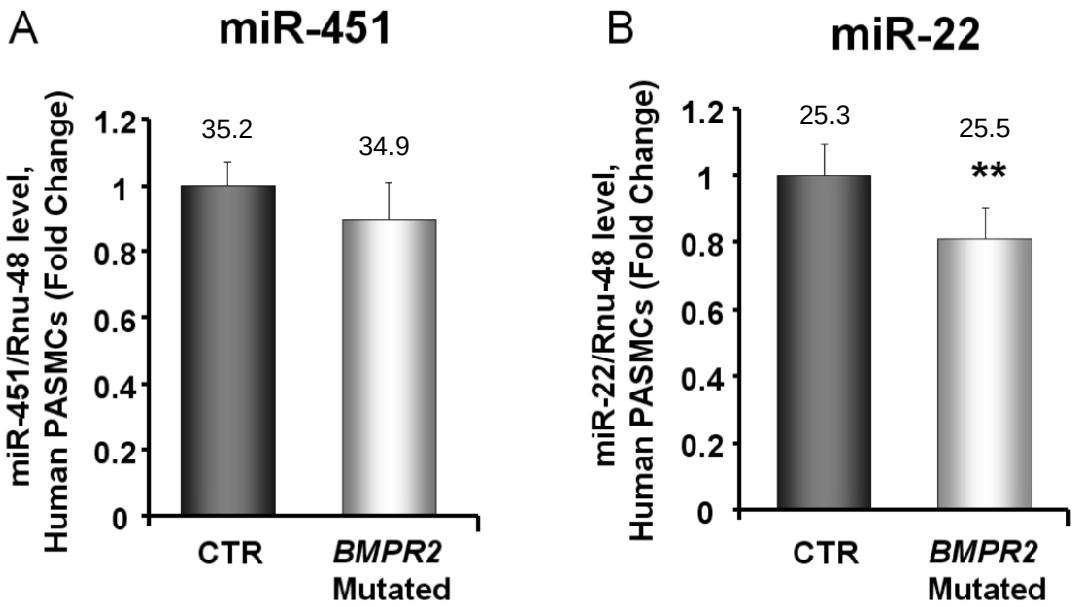

Figure 3-15 Analysis of miR-451 and miR-22 in PASMCs isolated from PAH patients known to harbour a mutation in *BMPR2*. TaqMan® Real-Time PCR analysis of miR-451 (A) and miR-22 (B) expression in human PASMCs. Total RNA was extracted from PASMCs of HPAH patients with a mutation in the *BMPR2* gene. Passage 4 primary cells were used. Samples were tested in triplicate. Results were normalized to Rnu-48 and expressed as relative fold change, with an arbitrary value of 1 assigned to the control group. Raw Ct values for the target miRNAs are indicated above each column. For statistical analysis, an unpaired t-test was conducted. **P<0.01 compared to CTR. N = 5/group.

3.3 Discussion

Target gene dysregulation mediated by miRNA in the progression of several diseases is becoming increasingly relevant (Erson and Petty 2008; Zhang 2008; Small and Olson 2011). Here, we profiled miRNA signatures in the WT lung and compared them longitudinally with rats exposed to either chronic hypoxia or monocrotaline injuries at 2, 7, and 21 days. We show that a small subset of miRNAs is significantly changed (i.e. miR-21, miR-22, miR-30c, let-7f, let-7a, miR-322, and miR-451). These miRNA profiles were validated by TaqMan® Real-Time PCR to confirm the microarray result, and their dysregulation was also mimicked in *in vitro* models involving exposure of rat PAFs, rat PASMCs, human PAFs, and human PAECs to hypoxia, or exposure of rat PASMCs to TGF-*beta* or BMPs. While some differences were observed across species or conditions of analysis (i.e. miR-451 dysregulation was observed in rat, but not in mouse and human samples), we observed some clear profile of miRNA in all the experiments performed. A clear example of this is represented by miR-22 expression, substantially decreased in rat and mouse PAH models but also in human pathological samples and in cells exposed to TGF-*beta* and BMP4.

By using bioinformatics analysis, we also predicted the target sequences for the dysregulated miRNAs identified. A number of predicted targets were regulated in a manner consistent with the miRNA dysregulation pattern. Moreover, a preliminary analysis of targets of the down-regulated miRNAs (i.e., miR-21, miR-22, and miR-30c) and targets of the up-regulated miRNAs (i.e., miR-451 and miR-322) showed the presence of several proteins in common, an indication of the potential complex regulation of such targets *in vivo*. This could explain why the expression level of several targets did not always correlate perfectly with the modulation of a single miRNA. More experiments will be necessary to correlate directly miRNA dysregulation and targets expression level. In particular, a luciferase assay (performed by cloning the seed sequence for a miRNA of interest at the end of the gene coding for the luciferase gene) will allow us to show if the dysregulation of a specific miRNA is able to modify directly *in vitro* the expression of luciferase.

Hypoxia and monocrotaline-injection induced consistent changes in miR-451, miR-322 and to some extent miR-30c and let-7f. let-7a, miR-21 and miR-22 were regulated differently between the two models. This suggests that hypoxia- and monocrotaline-induced PAH share some common elements relating to miRNA regulation but also differential regulation. Such differential regulation is not entirely unexpected as the result of the diverse pathobiology induced by hypoxia and monocrotaline (Wilson, Segall et al. 1989; Hessel, Steendijk et al. 2006; Stenmark, Fagan et al. 2006; Stenmark, Meyrick et al. 2009; Firth, Mandel et al. 2010). Monocrotaline challenge mainly targets the pulmonary vascular endothelium and triggers an inflammatory process, especially monocyte recruitment, both of which play an important role in the course of human PAH (Ono and Voelkel 1991; Voelkel and Tuder 1995; Voelkel and Tuder 2000). The course of the development of PAH is also different in each model, as is well-known and confirmed in the present study. Hypoxia stimulates changes in medial, adventitial, and endothelial layers of the pulmonary artery; however, hypoxia leads to less inflammation than monocrotaline. The underlying pathobiology in both models leads to differences at protein level. For example, by using a proteomic approach, it has recently been shown that in the hypoxic model, proteins of the nitric oxide, carbon monoxide, and vascular endothelial growth factor pathways are significantly increased (Laudi, Steudel et al. 2007). In the monocrotaline model, proteins involved in serotonin synthesis, the enhanced unfolded protein response, and intracellular chloride channels are significantly elevated (Laudi, Steudel et al. 2007). Dysregulation of BMP and TGF-*beta* signaling occurs in both the hypoxic and monocrotaline models of PAH, but not exactly in the same way. In fact, the monocrotaline rat model appears to be more clearly regulated by TGF-*beta* than the hypoxic rat model (Long, Crosby et al. 2009). Specifically, a reduced lung expression of BMPR2 is observed in both the models, while a reduced BMP signaling (via the downstream Smad1/5 pathway) and an increased TGF-*beta* signaling (with increased Smad3 phosphorylation and increased expression of TGF-*beta* target genes) have pronounced effects only in the monocrotaline model (Long, Crosby et al. 2009).

Interestingly, responsive elements for SMAD3 (GTCTGGCCT) and SMAD4 (GTCTAGTCT) have recently been identified in the promoter region of miR-451 (Gal, Pandi et al. 2008). Thus, activation of TGF-*beta* signaling could be responsible for the increased expression of miR-451 observed in our study in rats pathological samples and in

particular in the monocrotaline model, where the TGF-*beta* signaling increase is more evident, as previously discussed (Long, Crosby et al. 2009). In fact, the stimulation of rat PASMCs with TGF-*beta* resulted in a significant and early up-regulation of this miRNA (after 5 h), while levels comparable with the untreated cells were observed after 24 h. Despite the increase number of studies on miRNA role in different systems, the function of this miRNA is still quite poorly understood. In particular, miR-451 has been proven to play a central role in erythropoiesis regulation through at least two different direct targets, *YWHAZ*, an intracellular regulator of cytokine signaling, and GATA-1, a critical hematopoietic transcription factor (Dore, Amigo et al. 2008; Patrick, Zhang et al. 2010). Moreover, mice deficient for miR-451 display a reduction in hematrocrit, an erythroid differentiation defect, and ineffective erythropoiesis in response to oxidative stress (Patrick, Zhang et al. 2010). Concerning the action of this miRNA on YWHAZ, it is interesting to notice that here we include the same protein in the list of targets of miR-30c, down-regulated in the *in vivo* rat study and in our *in vitro* stimulations. MiR-451 has also been recently studied for its potential involvement in the pathobiology of glioblastoma through its capacity of regulating the LKB1/AMPK pathway in response to altered energy availability (Godlewski, Bronisz et al. 2010; Godlewski, Nowicki et al. 2010), but its role in other pathological models has never been evaluated. Here we show like a substantial increase (up to 20 times) of this miRNA can be observed in both the analyzed rat models and in particular in the monocrotaline model after 7 days from the treatment. However, no significant changes can be identified in 14 days hypoxic male mice or in human samples obtained from patients with idiopathic or familial PAH, suggesting a specific role for this miRNA in the rat pathology. It is also interesting to notice that this miRNA is so significantly up-regulated in both the rat models despite the down-regulation of the expression level of *DICER*, essential for the maturation of a pre-miRNA in its final form, observed *in vivo* in the hypoxic model. Recent studies showed that the maturation of this specific miRNA is *DICER*-independent but involves a biogenesis pathway that uses AGO2 catalytic activity. MiR-451 levels are therefore refractory to *DICER* loss of function or dysregulation (Cheloufi, Dos Santos et al. 2010; Cifuentes, Xue et al. 2010; Yang and Lai 2010; Yang, Maurin et al. 2010). More experiments will be necessary in order to define the role of miR-451 in the hypoxic and monocrotaline-induced pathology in rats and confirm if this highly significant dysregulation can be considered specific of this species. In particular, *in situ* analysis will be important to localize in lung

sections miR-451 expression, while the analysis of KO animals will allow observing the effect of miR-451 depletion on PAH development.

As previously mentioned, the stimulation of PASMCs resulted as expected in a significant up-regulation of miR-451, but also the other miRNAs identified in the *in vivo* rat study responded to the stimulation in a compatible way with our previous observations. In fact, the TGF-*beta* stimulation was able to induce the down-regulation of miR-21, miR-22, miR-30c, let-7f and let-7a in our experiments, mimicking our *in vivo* observations. On the contrary, rat cells stimulated with BMP4 showed the significant up-regulation of the same miRNAs in a time-dependent manner. These results suggest the involvement of the TGF-*beta* super-family in the regulation of this group of miRNAs.

If some of the miRNAs analyzed in this study showed a significant dysregulation only in specific models or in particular conditions (e.g. miR-451 or miR-21), others were consistently altered in all the analyzed samples, suggesting a conserved role and regulation in rat, mouse and human PAH. MiR-22 for example displayed a characteristic down-regulation in the models evaluated. The involvement and importance of this miRNA in disease pathogenesis is becoming increasing well documented. For example, recent studies show evidences of a mutual regulation between miR-22 and the tumor suppressor PTEN, a lipid phosphatase involved in the regulation of the cell cycle. PTEN was identified as a direct target of this miRNA (Bar and Dikstein 2010). In particular, in cardiomyocytes miR-22 up-regulation, and consequent PTEN down-regulation, significantly increases cell size and markedly influences the expression of hypotrophic markers, suggesting a role for miR-22 in cardiomyocytes hypertrophy (Xu, Song et al. 2011). Moreover, through direct repression of both the c-Myc binding protein and the obligate c-Myc binding factor Max, miR-22 was recently shown to be able to regulate the activity of this oncogenic transcription factor, with effects on cell proliferation (Xiong, Du et al. 2010).
Here, we show that miR-22 is significantly down-regulated after exposure to hypoxia or monocrotaline injection, even if at different time points as previously mentioned. Monocrotaline can rapidly (after 2 days) induce a reduction in miR-22 expression, but no changes are observed at 7 and 21 days, while miR-22 dysregulation in hypoxic rats become significant after 7 days of exposition and reach its maximum level after 21

days. Thus, if a direct effect of this miRNA on c-Myc family members could be proved also in our models, a relevant role for miR-22 in the vascular cell proliferation observed in PAH could be hypothesized, at least partially through its involvement in the regulation of this pathway. Future experiments will clarify this aspect of miR-22 activity. In this study we decided to focus our attention on another miR-22 target, TGFBR1 (also known as ALK-5), a member of the TGF-*beta* super-family already known for its dysregulation in IPAH patients and for being involved in the progression of the pathology induced by monocrotaline (Morty, Nejman et al. 2007; Zaiman, Podowski et al. 2008; Long, Crosby et al. 2009; Thomas, Docx et al. 2009) (Chapter 1, Section 1.2.4.1). Several studies have demonstrated that vascular cells and lung tissues isolated from patients with IPAH exhibit elevated TGFBR1 signaling, with induction of cell proliferation. This favors muscularization and subsequent remodeling of the small pulmonary arterioles (Richter, Yeager et al. 2004; Castanares, Redondo-Horcajo et al. 2007; Thomas, Docx et al. 2009). Moreover, the use of TGFBR1 inhibitors (able to decrease the TGF-*beta*/Smad3 activity) can prevent the development of monocrotaline-induced PAH in rats, suggesting that strategies to inhibit TGFBR1 signaling may have therapeutic benefit on the progression of this pathology (Zaiman, Podowski et al. 2008; Long, Crosby et al. 2009; Thomas, Docx et al. 2009). However, the mechanism implicated in TGFBR1 dysregulation has not been fully elucidated, suggesting the involvement of other elements. The negative regulation of miR-22 on this target could therefore have a precise role in the regulation of the TGFBR1-mediated TGF-*beta* pathway. Here we show that TGF-*beta* stimulation of PASMCs is able to induce the down-regulation of miR-22, resulting in the up-regulation of *TGFBR1*, while BMP4 stimulation has an opposite effect on both the miRNA and the target. PAFs exposed to hypoxia for 24 h were significantly down-regulated for miR-22 expression, but did not show any dysregulation of this target. A 3' UTR luciferase reporter assay would need to be performed to verify the direct effect of miR-22 dysregulation on *TGFBR1* expression *in vitro*. Also, for this and other miRNAs, it will be critical to define the potential effect of miRNA modulation in disease prevention. In the future, it will be important to generate reliable methods to deliver miRNA therapeutics to the lung efficiently and selectively. This might require new strategies to modulate the tropism of a gene delivery system (e.g. viruses) and to generate selective agents and cells.

Here, we have focused on those miRNAs showing the largest changes after the onset of injury. However, recent studies have shown that even subtle changes in miRNA expression can lead to large changes in phenotype (Baek, Villén et al. 2008; Selbach, Schwanhäusser et al. 2008). Thus, the large changes we have observed in miRNAs in this study are likely to strongly affect the cell biology and pathobiology associated with the development of PAH.

In summary we have reported the global miRNA profiles of rat lungs after exposure to hypoxia and monocrotaline injury, and proved that the dysregulation of specific miRNAs is conserved in mouse models and PAH-affected patients. This highlights the potential importance of miRNA in disease progression and possible targets (either the miRNAs themselves or their mRNA targets) for future therapeutic intervention.

4. MiR-143 and miRNA-145 Expression in Pulmonary Arterial Hypertension: Evidence from Mouse Models and Patient Samples

4.1 Introduction

Several recent studies have assessed the direct role of miRNAs in vascular inflammation and in the development of vascular pathologies (Ji, Cheng et al. 2007; Urbich, Kuehbacher et al. 2008; Zhang 2009; Kartha and Subramanian 2010). In this chapter we evaluated the role of miR-143 and miR-145, already known for being abundantly expressed in the vessel wall (Cheng, Liu et al. 2009), in the development of PAH.

MiR-143 and miR-145 are transcribed in cluster as a long pri-miRNA coded on human chromosome 5 (≈ 1.7 Kb) and on mouse chromosome 18 (≈ 1.4 Kb) (Figure 4-1). The analysis of the promoter of this transcript revealed the presence of a cardiovascular specific enhancer, highly conserved from human to opossum, located between -3328 and -3056 bp upstream of the gene. This region contains a serum response factor (SRF) binding site, known as CArG box (Xin, Small et al. 2009; Rangrez, Massy et al. 2011). Cordes et al. and Boettger et al. recently analyzed the expression profile of miR-143 and miR-145 during mouse development. In agreement with the presence of a cardiovascular specific enhancer, both the groups observed, in the mouse embryo, a specific expression of the cluster in the heart, vascular and visceral SMCs. However, during late fetal and postnatal development, miR-143/145 expression was decreased in the heart but still high in vascular and visceral SMCs, suggesting a role for these miRNAs in the regulation of this cells type in the adult. In fact, in the postnatal organism, VSMCs are highly plastic and are able to modulate their phenotype in response to specific environmental stimuli, switching from a differentiated (known as contractile) to a dedifferentiated (called synthetic) state, required for cell proliferation and migration (Sobue, Hayashi et al. 1999). VSMCs acquire a synthetic state during angiogenesis, but is also in a variety of proliferative cardiovascular diseases such as atherosclerosis and hypertension, in which it leads to vascular occlusion (Owens, Kumar et al. 2004). The role of miR-143 and miR-145 was mainly assessed through the pharmacological or genetic ablation of a single miRNA or the whole cluster *in vitro* and

in vivo, although the results observed were sometimes controversial. *In vitro*, antagomiR-mediated inhibition of miR-145 expression blocked the ability of myocardin (myocd), a potent SRF co-activator, to convert fibroblasts into VSMCs, with only a little effect of miR-143 knock-down. Moreover, the up-regulation of miR-145 (but not miR-143) in neural crest stem cells was sufficient to induce the conversion of ≈75% of cells into VSMCs (Cordes, Sheehy et al. 2009). *In vivo*, abnormalities in the vessel wall of the aorta and other arteries, noticeably thinner than those of WT animals, were observed in miR-145 and miR-143/145 double KO mice. These changes were ascribed to a reduction in the cell size of VSMCs isolated from mutated mice, due to a decreased number of actin-based stress fiber, characteristic of fully differentiated SMCs, identified in the cytoplasm of these cells. This result suggests a central role of miR-145 in the modulation of cytoskeletal assembly (Xin, Small et al. 2009). However, while Boettger et al. reported a severe reduction in the number of differentiated VSMCs in KO mice, Xin et al. could not observe any difference in the expression level of markers of smooth muscle cell differentiation between WT and miR-145 deleted cells, concluding that miR-145, and to a lesser extent miR-143, are required for the production of normal actin stress fibers but not for SMC differentiation *per se* (Boettger, Beetz et al. 2009; Xin, Small et al. 2009). Also, Xin et al. reported, in miR-145 KO mice subjected to carotid artery ligation, the nearly abolished formation of neointima, abundantly observed in WT animals (Xin, Small et al. 2009). On the contrary, Cheng et al. study showed that adenoviral-mediated over-expression of miR-145 inhibits neointima formation in the carotid of rats in response to balloon injury (Cheng, Liu et al. 2009). Although embryonic KO and post-natal knock-down/over-expression of a sequence of interest can definitely have different consequences on cell differentiation/proliferation, these controversial results complicate the identification of a specific role for miR-143/miR-145 cluster in VSMCs plasticity. However, despite the communal regulation of these two miRNAs, it is important to notice that selective modulation of miR-145 (but not miR-143) is sufficient for the observation of abnormalities in the vasculature and pathological phenotypes, suggesting a predominant role for this miRNA in SMC regulation.

Several targets for miR-143 and miR-145 have already been validated *in vitro* and *in vivo*, and they are mostly involved in VSMCs differentiation (Figure 4-2). In particular, it is interesting to notice that despite the lack of sequence homology between miR-143

and miR-145, these miRNAs are often predicted to target the same genes (Xin, Small et al. 2009). The validated targets include kruppel-like factor 4 and 5 (KLF4 and 5), which are positive regulators of smooth muscle proliferation (Figure 4-2) (Cordes, Sheehy et al. 2009), but are also able to up-regulate SM *alpha*-actin in specific cell types (Adam, Regan et al. 2000); angiotensin converting enzyme (ACE), which converts circulating angiotensin I into its active form angiotensin II, a major regulator of the contractile phenotype of VSMCs (Boettger, Beetz et al. 2009); E twenty-six (ETS)-like transcription factor 1 (Elk-1), a competitor of myocd (Figure 4-2) (Cordes, Sheehy et al. 2009). Myocd itself is regulated by miR-143 and miR-145, and its induction is observed in response to their up-regulation (Figure 4-2) (Cordes, Sheehy et al. 2009).

Very recently, the mechanism behind miR-143/145 regulation has been partially clarified through the observation that agonists within the TGF-*beta* super-family are able to regulate miR-143/145 cluster via a Smad-dependent pathway. In fact, both TGF-*beta* and BMP4, already known for their capacity to promote the contractile phenotype in VSMCs, can activate transcription of miR-143/145 cluster through the CArG box present in its promoter, although this induction is mediated by distinct SRF coactivators, Myocd and Myocd-related transcription factor A (MRTF-A) respectively (Davis-Dusenbery, Chan et al. 2011; Long and Miano 2011) (Figure 4-3).

In the previous chapter we did not observe any dyregulation of miR-145 expression in the lung of male hypoxic or monocrotaline-injected rats when assessed by TaqMan® Real-Time PCR (Caruso, MacLean et al. 2010) but we did not assess the expression of this miRNA in mouse or human models, nor did we further investigate miR-145 more in detail in either rat model. MiR-143 expression was never evaluated in that study (Caruso, MacLean et al. 2010).

Here, in consideration of the reported importance of miR-145/143 in smooth muscle cell biology (Cheng, Liu et al. 2009; Cordes, Sheehy et al. 2009; Zhang 2009; Rangrez, Massy et al. 2011), coupled with the importance of this cellular compartment in the etiology of PAH, we examined the expression and function of miR-145 and miR-143 in the development of PAH. In this study, we employed mouse models and human samples derived from patients with either IPAH or HPAH as well as control human lung. We show that both these miRNAs are significantly up-regulated in female mice in

response to chronic hypoxia and that genetic ablation of miR-145 alone is protective against the development of PAH in this animal model. Further, both miR-143 and miR-145 are up-regulated in mice heterozygous for a truncating *BMPR2* mutation. In human tissues we show elevation of pre- and mature forms of miR-145 and miR-143 in lung and isolated PASMCs obtained from PAH patients with a mutation in the *BMPR2* gene compared to controls. In consideration of the protective role of miR-145 observed in hypoxic mice, we propose a critical role for this miRNA in the development of PAH and identify miR-145 as a potential new target for therapeutic intervention.

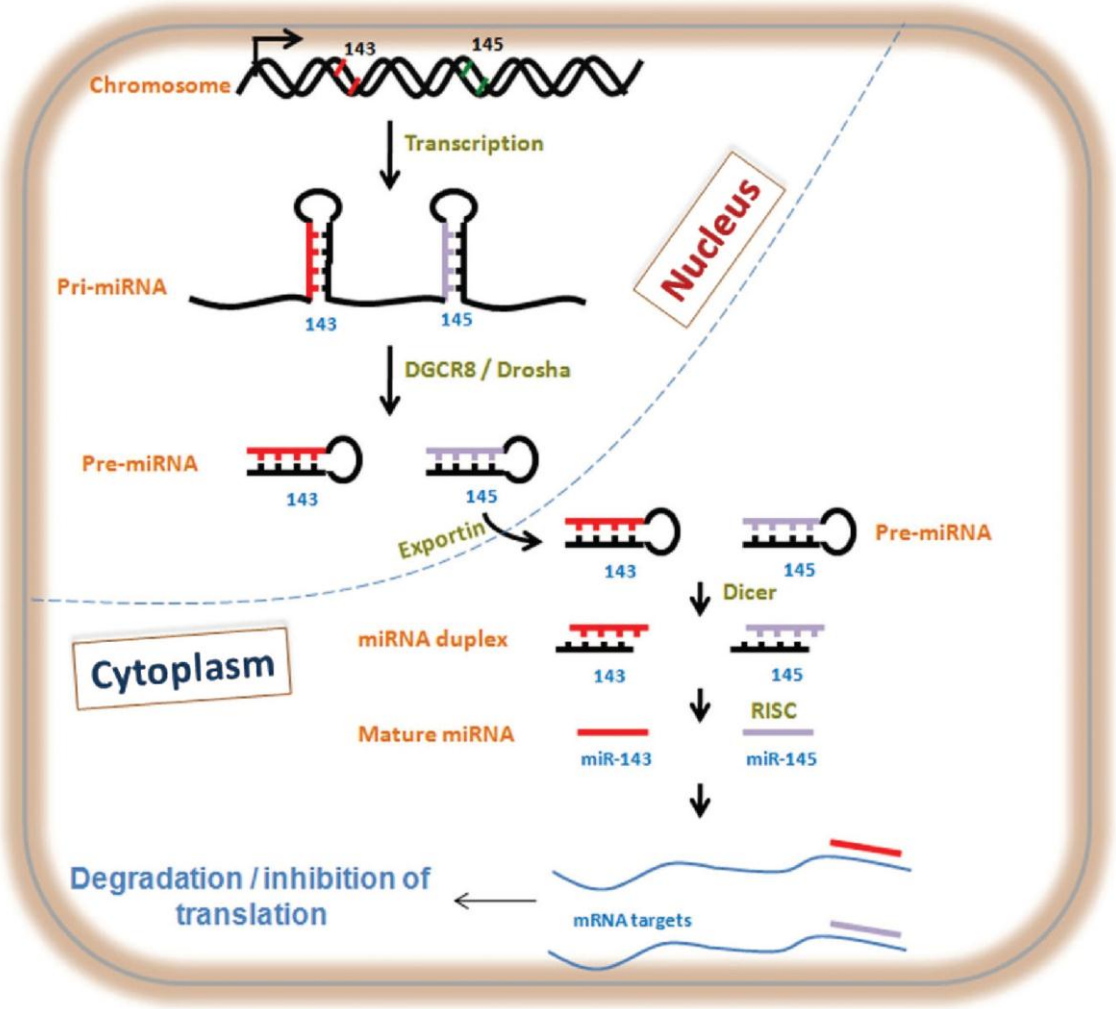

Figure 4-1 Biogenesis of miR-143 and miR-145. miR-143 and miR-145 are co-transcribed as a single pri-miRNA. This long precursor is then processed to obtain 2 mature miRNAs as described in Chapter 1 (Sections 1.3.3.3-1.3.3.6). Reproduced from (Rangrez, Massy et al. 2011).

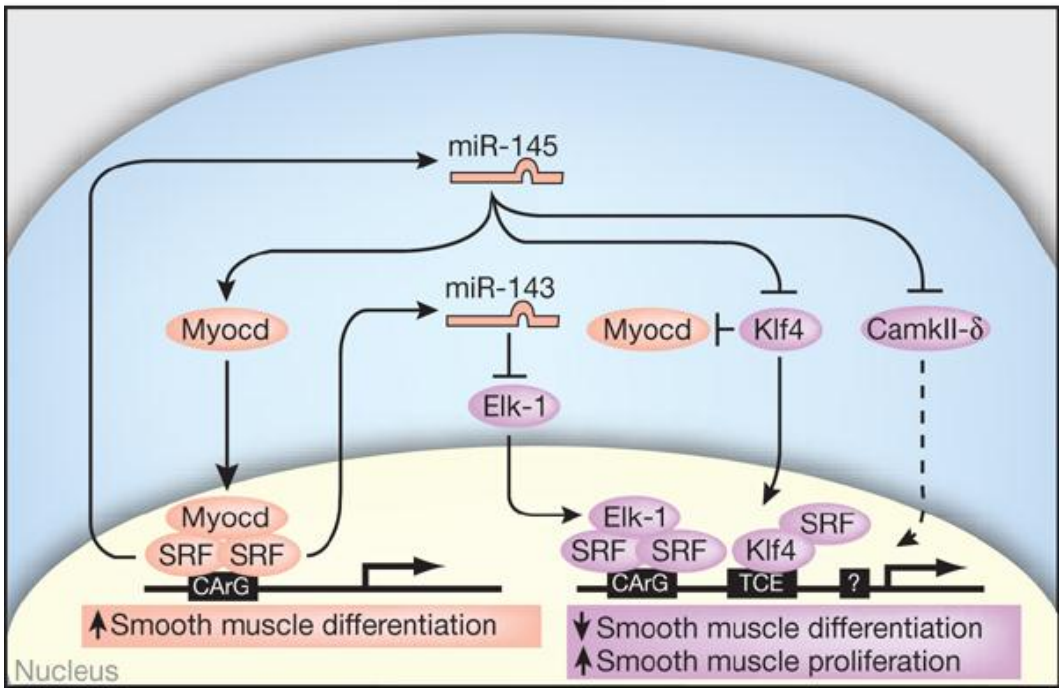

Figure 4-2 miR-143 and miR-145 regulation of smooth muscle cell proliferation and differentiation. miR-143 and miR-145 can repress multiple factors that normally promote the less differentiated, more proliferative smooth muscle phenotype (lavender). These factors include Klf4 and Elk-1, which both interact with SRF and can also repress Myocd. miR-145 can also induce Myocd activity to promote the more differentiated smooth muscle phenotype (peach). Dashed lines indicate indirect effects. Reproduced from (Cordes, Sheehy et al. 2009).

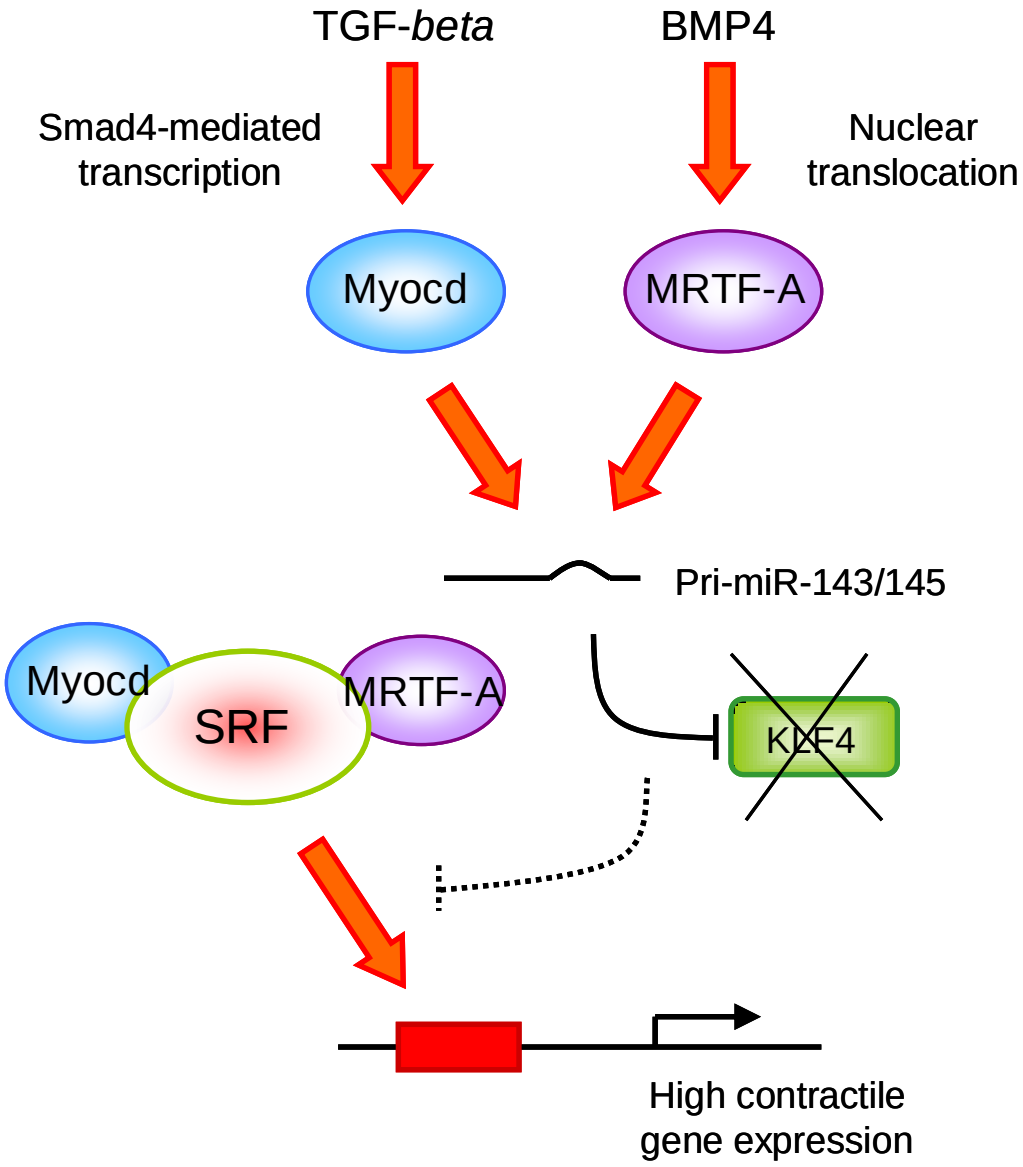

Figure 4-3 Schematic representation of BMP and TGF-*beta* induction of pri-miR-143/145. TGF-*beta* and BMP4 can activate transcription of miR-143/145 cluster through the CArG box present in its promoter. In particular, TGF-*beta* induction if Smad4 dependent and it is mediated by Myocd, whereas BMP4 can stimulate miR-143/145 transcription through MRTF-A. Mature miR-145 can therefore repress KLF4 expression allowing enhanced binding of Myocd/ or MRTF-A/SRF complexes to the CArG boxes of contractile genes and increase contractile gene expression. Adapted from (Davis-Dusenbery, Chan et al. 2011).

4.2 Results

4.2.1 Expression and Regulation of miR-143 and miR-145 in WT Hypoxic Mice

In chapter 3 we reported that miR-145 is not altered in the RNA extracted from whole lung samples of male rats treated with hypoxia or monocrotaline and compared to controls in a longitudinal study (Caruso, MacLean et al. 2010). However, due to the importance of miR-145 and miR-143 in vascular smooth muscle cell biology (Cheng, Liu et al. 2009; Zhang 2009), and their reported dysregulation in acute vascular remodeling and neointima formation (Boettger, Beetz et al. 2009; Cheng, Liu et al. 2009; Elia, Quintavalle et al. 2009), we decided to assess the expression of both these miRNAs in female and male WT mice exposed to chronic hypoxia, in order to establish their role in a different animal model of PAH and also identify a potential gender difference. In fact both idiopathic and familial forms of PAH predominantly affect women through an unknown mechanism (the ratio of females to males in the human pathology is 1.9:1, Chapter 1, Section 1.2.1) and it has been recently observed that female gender predisposes SERT+ mice to the development of PAH with a critical role played by 17*beta* oestradiol in this process (White, Dempsie et al. 2011; White, Loughlin et al. 2011). Our analysis showed a significant up-regulation of miR-143 and miR-145 in response to 14 days of chronic hypoxia in female, but not male mice (Figure 4-4A and B). For the purpose of subsequent experiments, we therefore focused on female mice. Next, the expression level of miR-143 and miR-145 was assessed in the RNA extracted from the spleen, the kidney and the brain of female WT mice exposed to chronic hypoxia for 14 days, in order to understand if the dysregulation of these miRNAs in this animal model of PAH is lung specific or characteristic of all the organs. These experiments showed no alteration of miR-145 in these tissues, while miR-143 was slightly up-regulated only in the kidney of the treated mice but stable in spleen and brain (Figure 4-5). Thus, miR-145 and miR-143 are expressed in smooth muscle cells in the lung of mice and their up-regulation after 14 days of chronic hypoxia is mainly lung specific.

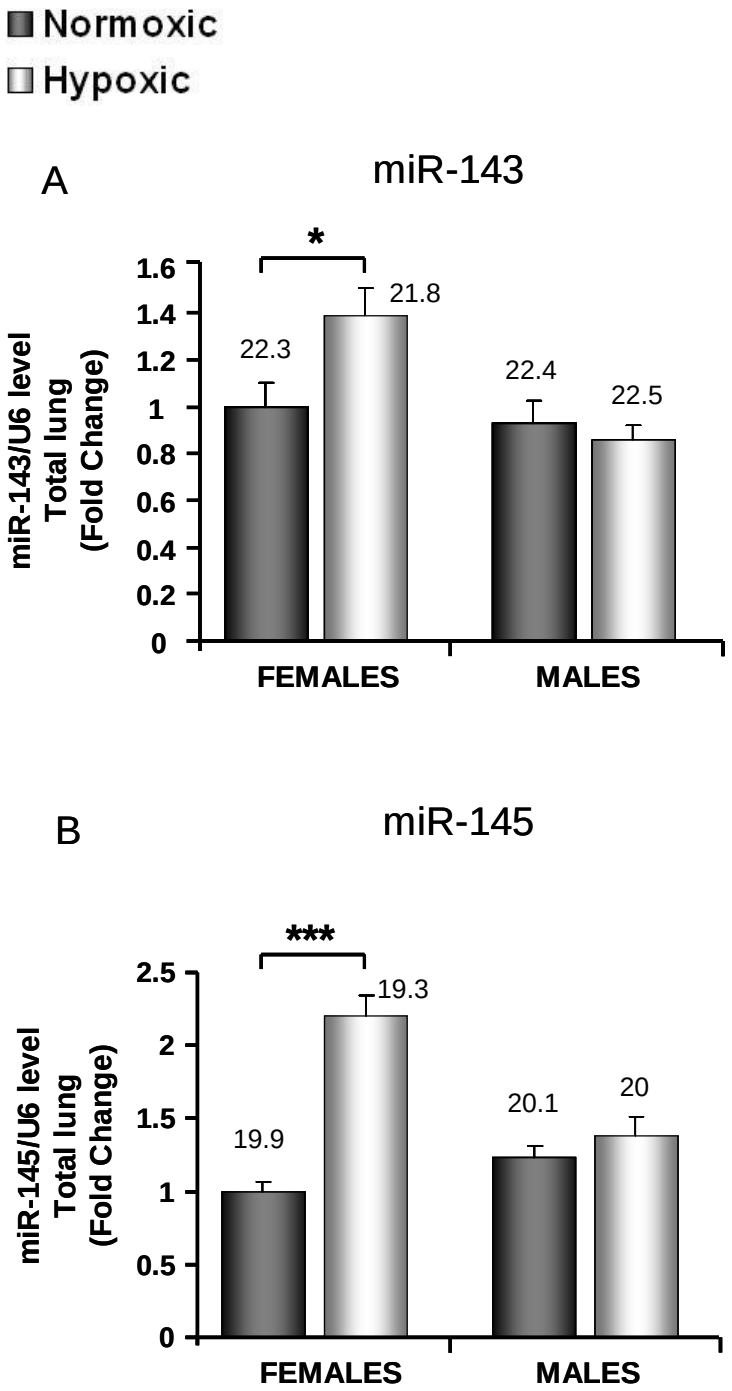

Figure 4-4 miR-143 (A) and miR-145 (B) expression in female and male WT mice exposed to chronic hypoxic for 14 days. Total RNA was extracted from the lung of normoxic (dark grey bars) and hypoxic (light grey bars) female and male mice at the age of 10 weeks. Samples were tested in triplicate. Results were normalized to U6 values and expressed as relative fold change, with an arbitrary value of 1 assigned to the normoxic female group. Raw Ct values for the target miRNAs are indicated above each column. Data are expressed as mean ± SEM and analysed by one way ANOVA followed by Bonferroni's post-hoc test. *P<0.05, ***P<0.001 compared to normoxic mice. N = 3/group.

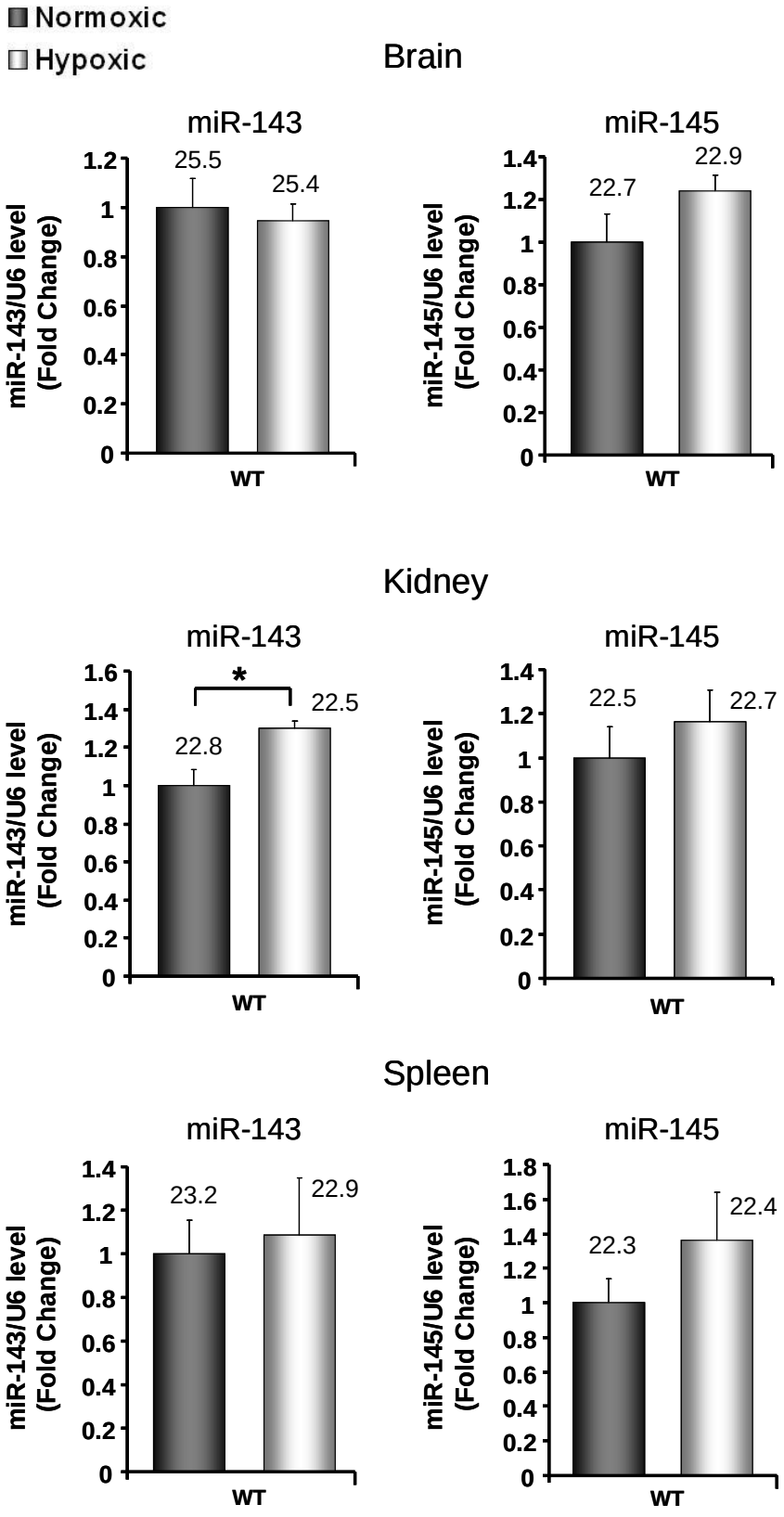

Figure 4-5 miR-143 and miR-145 expression in the brain, kidney and spleen of hypoxic WT female mice. Total RNA was extracted from each organ and tested in triplicate by TaqMan® Real-Time PCR. Raw Ct values for the target miRNAs are indicated above each column. Data were analyzed using an unpaired t-test. *P<0.05 compared to normoxic mice. N = 4/group.

4.2.2 Characterization of miR-143 and miR-145 Expression in miR-145-/- Mice and Quantification of the Development of PAH in This Model in Comparison to Controls

Based on the up-regulation of miR-145 in hypoxic mice, we next evaluated the effect of miR-145 ablation on the development of PAH and assessed the expression level of miR-143 in this animal model. 8 weeks old miR-145-/- mice and WT control age-matched mice were exposed to chronic hypoxia or maintained in normoxic conditions for 14 days and analyzed for the development of PAH using a series of *in vivo* measurements. Homozygous miR-145 KO mice were viable at birth and did not display any obvious disorder in normal conditions, indicating that this miRNA is not crucial for development. The absence of miR-145 expression in the KO animals used in the study was confirmed by TaqMan® Real-Time PCR and *in situ* hybridization (Figure 4-6A and B). In agreement with our previous experiment, WT control mice exposed to hypoxia showed a significant increase in miR-145 expression in comparison with normoxic animals (Figure 4-6A). Since miR-145 is transcribed in its pri- form clustered with miR-143, we also analyzed WT and KO animals for the expression of this miRNA under both normoxic and hypoxic conditions to ensure that miR-143 levels were not substantially altered in the lung following genetic ablation of miR-145 and in response to hypoxic insult. TaqMan® Real-Time PCR analysis of miR-143 expression showed the up-regulation of this miRNA in WT hypoxic mice in comparison with normoxic animals (Figure 4-7). However, although a down-regulation of miR-143 was identified in normoxic mice depleted for miR-145, no differences in its expression level were observed between WT and miR-145 -/- animals in response to hypoxia (Figure 4-7), suggesting that the genetic ablation of miR-145 does not influence miR-143 regulation in pathological conditions. Thus, any change in the development of PAH in miR-145 -/- mice in response to hypoxia is specific to the selective loss of miR-145. In consideration of this, *in situ* hybridization was performed to localize miR-145 within the lung of control mice since this has not previously been evaluated. We observed positive staining for this miRNA within the smooth muscle layer of vessels and bronchi in the lungs of WT mice (Figure 4-8).

We next quantified the development of PAH in WT and miR-145 -/- mice. It has been recently reported how the genetic ablation of miR-145 (and to a lesser extent of miR-143) is able in mice to determine an alteration in the structure of the aorta that show a thinner wall than the WT (Xin, Small et al. 2009). This abnormality is due to a reduction in cell size of VSMCs identified in KO animals in comparison with WT, reduction caused by the dramatic decrease of the number of actin-based stress fibers (characteristic of completely differentiated cells) observed in KO VSMCs. Here, we show like the KO of miR-145 alone is sufficient to determine a significant reduction of the mean systemic arterial pressure (SAP), confirming that the ablation of this miRNA can induce a widespread alteration in the wall formation of the vasculature due to its involvement in VSMCs proliferation and differentiation (Figure 4-9A, Table 4-1). However, both in WT and KO mice the exposition to chronic hypoxia doesn't determine any alteration in SAP as showed in previous studies (Morecroft, Dempsie et al. 2007; Mair, MacLean et al. 2008; Morecroft, Doyle et al. 2011) (Figure 4-9A, Table 4-1). Moreover, in WT mice, we observed a significant and expected increase in systolic right ventricular pressure (sRVP) and right ventricular hypertrophy (RVH) (Figure 4-10A and B, Table 4-1 and Table 4-2) whereas miR-145-/- animals displayed no increase in these parameters (Figure 4-10A and B, Table 4-1 and Table 4-2). Interestingly, there was no difference in baseline systolic RVP or RVH between wild type and miR-145 -/- mice but a different response to the hypoxic insult (Figure 4-10A and B, Table 4-1 and Table 4-2). No changes in heart rate (HR) were reported (Figure 4-9B, Table 4-1). Histological analysis showed the presence of pulmonary vascular remodeling in small PAs of WT animals following exposure to hypoxia but this was reduced in lungs harvested from miR-145 KO animals, a finding confirmed by quantitative scoring (Figure 4-11A and B). Therefore, genetic ablation of miR-145 was able alone to protect mice against the development of PAH in response to hypoxia without any compensatory effect on miR-143 expression.

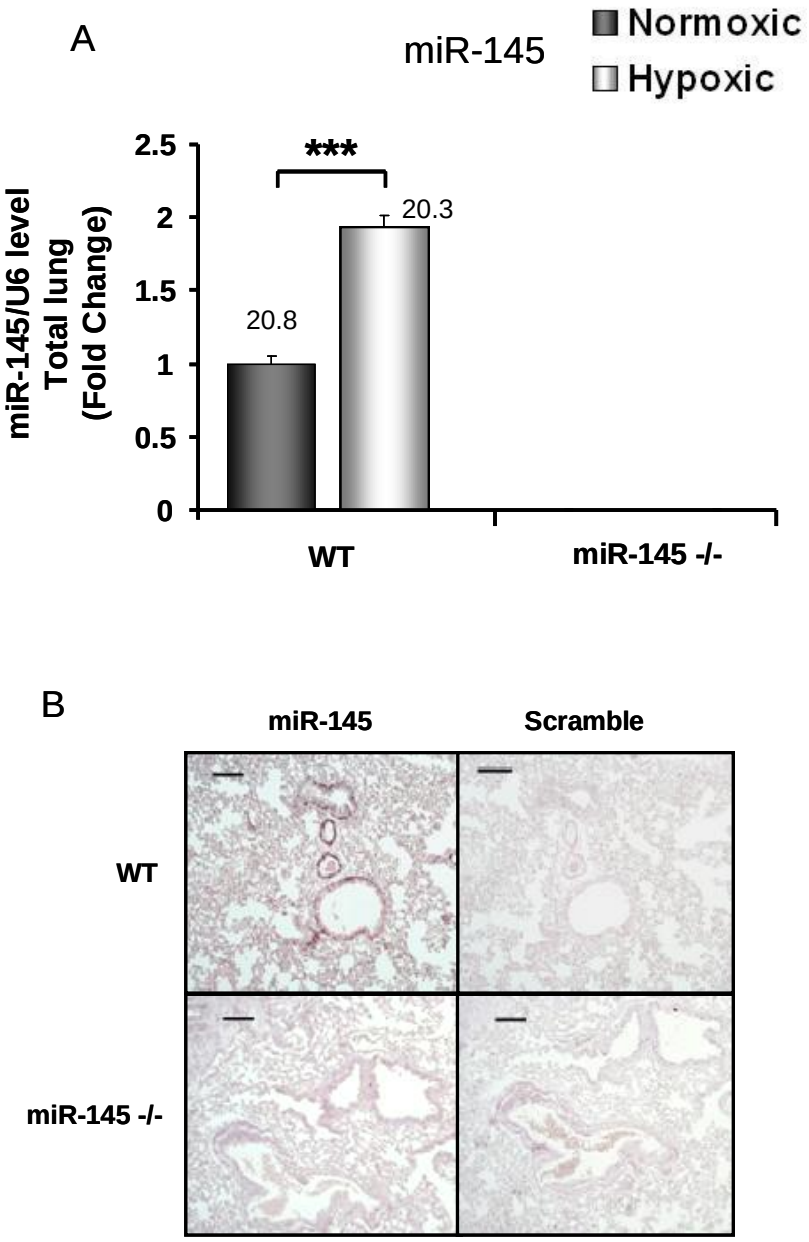

Figure 4-6 Analysis of miR-145 expression in miR-145 -/- female mice in comparison with WT mice. miR-145 genetic ablation in 10 weeks old, KO mice was confirmed in the lung by TaqMan® Real-Time PCR (A) and *in situ* analysis (B). In (A) data are expressed as mean ± SEM and analysed by two way ANOVA followed by Bonferroni's post-hoc test. ***P<0.001 compared to normoxic mice. Raw Ct values for the target miRNAs are indicated above each column. N = 6/group. In (B) images all x100 magnification, scale bars = 100 μm.

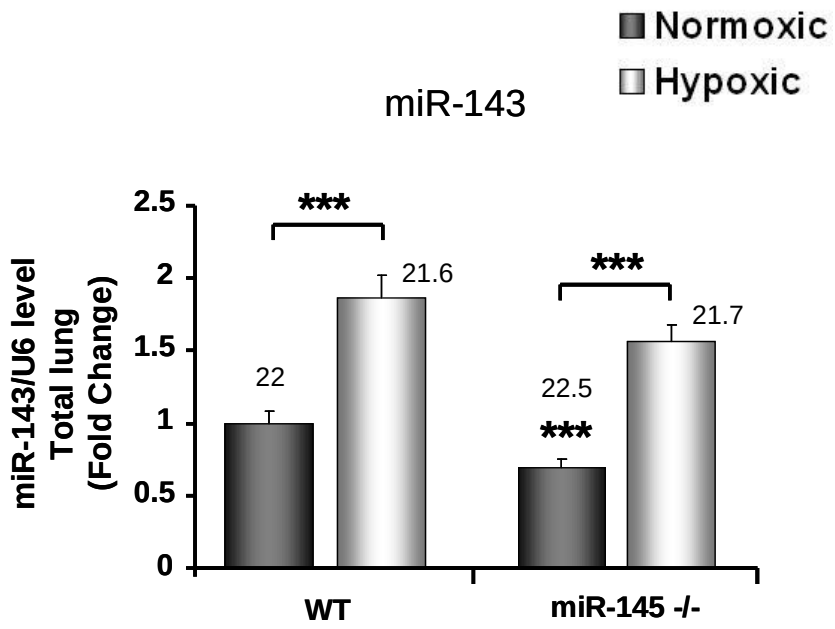

Figure 4-7 miR-143 expression in WT and miR-145 -/- female mice in response to hypoxia. TaqMan® Real-Time PCR analysis of normoxic and 14 days hypoxic WT and KO mice. Total RNA was extracted from the lung of normoxic (dark grey bars) or hypoxic (light grey bars) 10 week old mice. 6 mice/group were analyzed. Samples were tested in triplicate. Results were normalized to U6 values and expressed as relative fold change, with an arbitrary value of 1 assigned to the control group. Raw Ct values for the target miRNAs are indicated above each column. Data were analyzed using a two-way ANOVA followed by Bonferroni's post-hoc test. ***p<0.001 compared to normoxic samples.

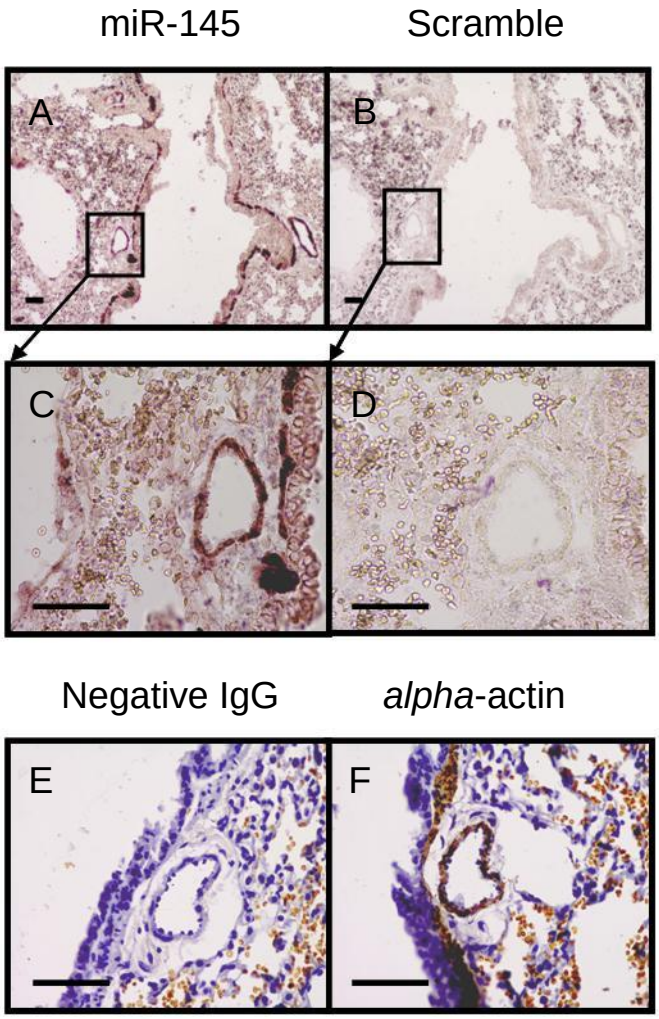

Figure 4-8 miR-145 localization in mouse lung sections. (A-F) *In situ* hybridization showing miR-145 localization in mouse lung. Paraffin sections were rehydrated and incubated with an anti-miR-145 (A, C) or scramble probe (B, D) as negative control. For co-localization, *alpha*-actin was detected in the same samples using an immunohistochemistry assay (F), with non-immune isotype-IgG antibody as negative control (E). Images x100 (A, B) or x400 (C-F) magnification, scale bars = 50 μm.

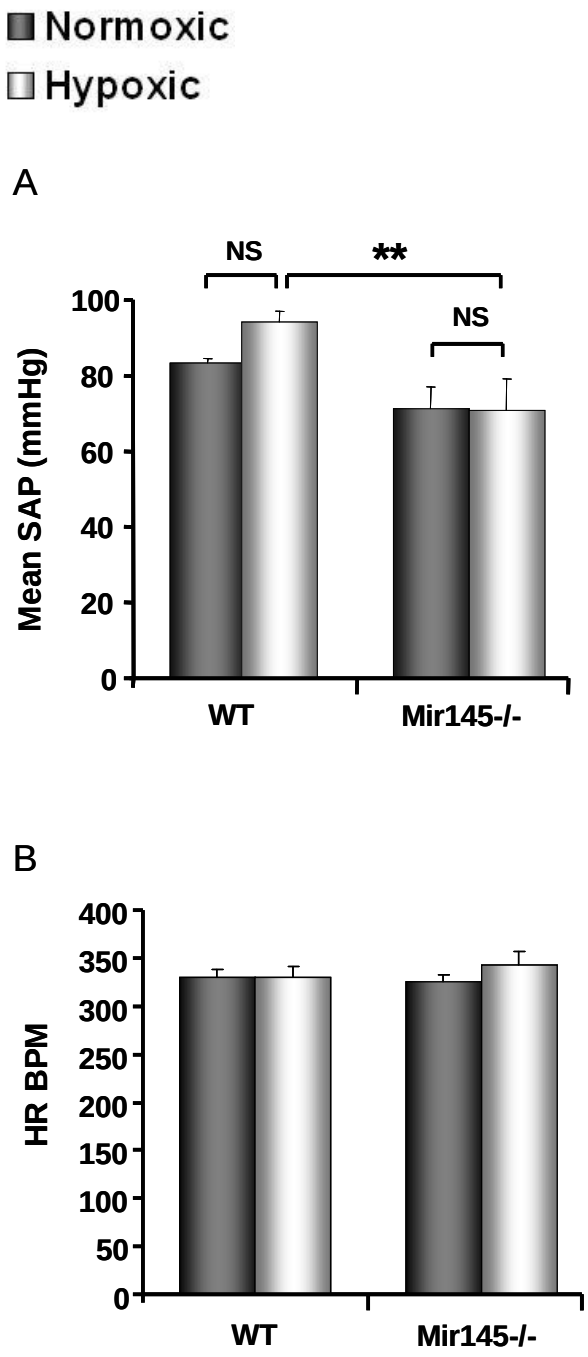

Figure 4-9 Assessment of systemic arterial pressure (SAP, A, n = 6–9) and heart rate (HR, B, n=8-10) in WT and miR-145 -/- mice, normoxic and hypoxic. 10 weeks old female mice were assessed. Data were analyzed using a two-way ANOVA followed by Bonferroni's post-hoc test. **p<0.005 compared to WT hypoxic mice.

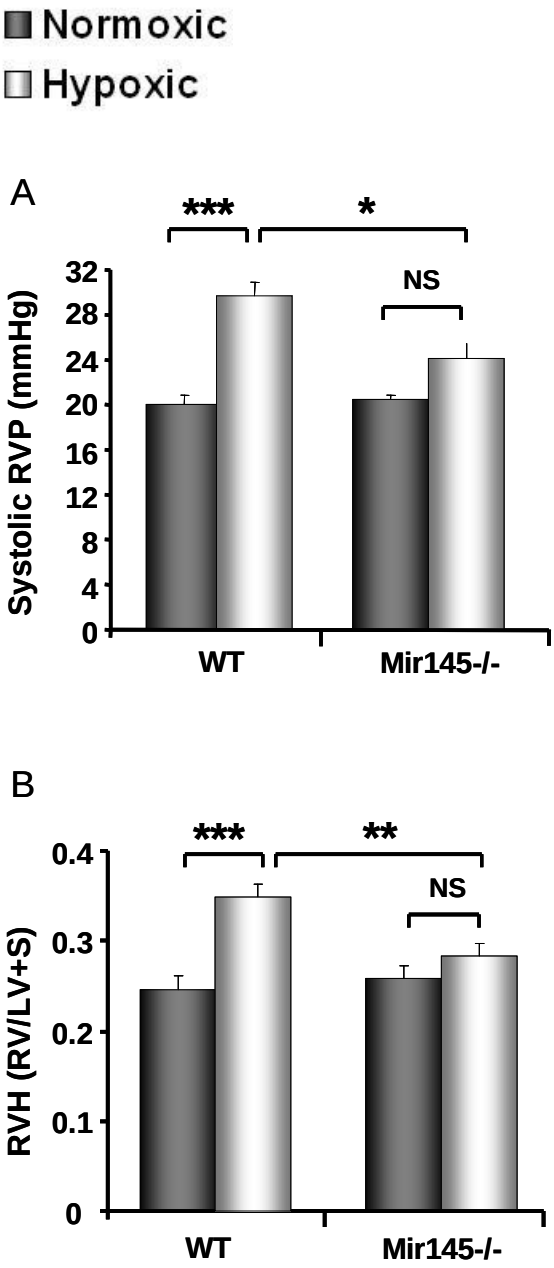

Figure 4-10 Effect of miR-145 genetic ablation on PAH development in mice. Assessment of sRVP (A, n = 9–10) and RVH (B, n = 9–10) in 10 weeks old female WT and miR-145 -/- mice, normoxic or exposed to chronic hypoxia for 14 days. Data were analyzed using a two-way ANOVA followed by Bonferroni's post-hoc test. *P<0.05, **P<0.01, ***P<0.001 compared to normoxic mice or WT hypoxic mice as indicated. NS = non-significant change.

Parameter	WT Normoxic	WT hypoxic	KO Normoxic	KO Hypoxic
sRVP, mmHg	20.00 ± 0.80	29.71± 1.16***	21.21± 0.61	24.07± 1.38†
SAP, mmHg	83.22 ± 1.55	94.01± 2.91	71.34± 8.14**	70.92 ± 5.59**
Heart rate, bpm	329.42 ± 8.92	329.18 ± 12.66	325.88 ± 6.67	342.08 ± 14.78

Table 4-1 Haemodynamics in WT and miR-145 -/- mice, normoxic and hypoxic. Systolic right ventricular pressure (sRVP), systemic systolic arterial pressure (SAP) and heart rate measurements in normoxic and chronically hypoxic female WT and miR-145 -/- mice. **P<0.005, ***P<0.001 compared to WT normoxic mice; †P<0.01 compared to WT hypoxic mice; Data expressed as mean + SEM. n=9-10.

Group	RV (mg)	LV+S (mg)	RV/LV+S
WT Normoxic	22.06 ± 1.13	85.12 ± 1.24	0.26 ± 0.015
WT Hypoxic	25.71 ± 0.84	73.69 ± 1.77	0.35 ± 0.012***
miR-145 -/- Normoxic	18.60 ± 1.25	69.74 ± 3.08	0.27 ± 0.014
miR-145 -/- Hypoxic	19.21 ± 0.85	68.63 ± 1.92	0.28 ± 0.014††

Table 4-2 Ventricle weight in WT and miR-145 -/- mice. Right ventricle (RV) weight, left ventricle plus septum (LV+S) weight and RV/LV+S ratio. ***P<0.001 compared to WT normoxic mice; ††P<0.005 compared to WT hypoxic mice. Data expressed as mean + SEM. *N* = 9-10.

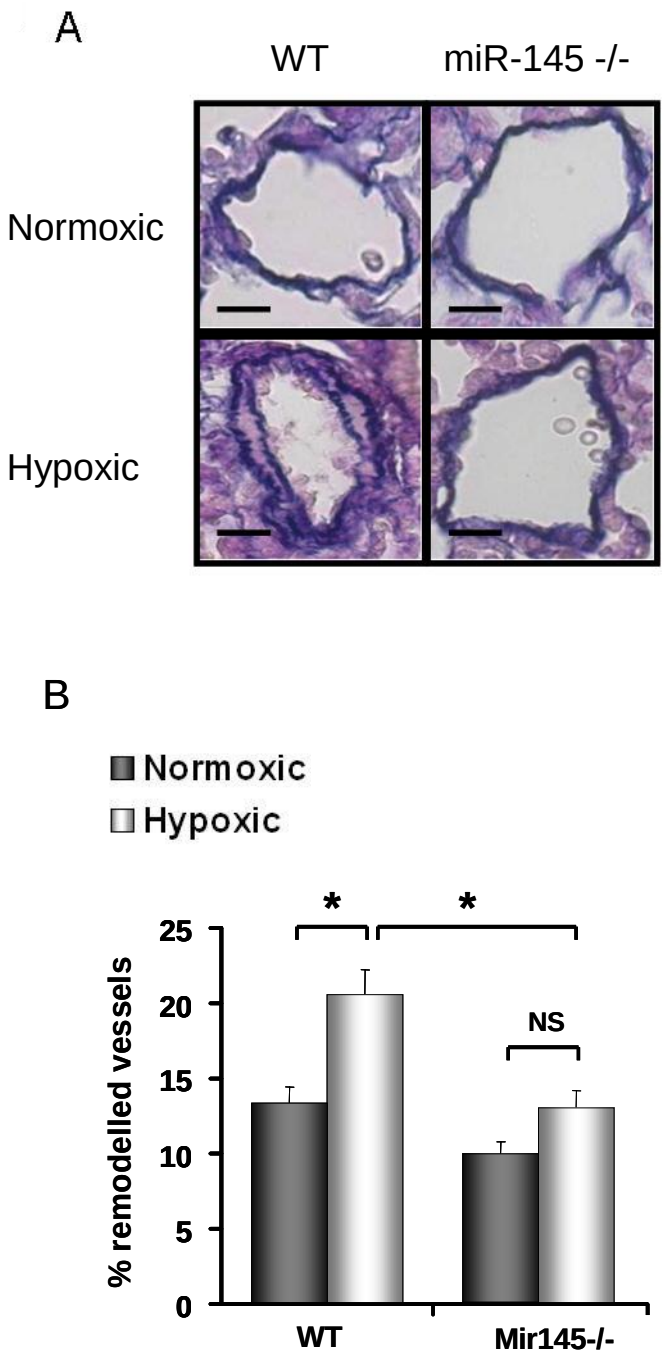

Figure 4-11 Effect of miR-145 genetic ablation on vessel remodelling in mice. (A) Representative PAs stained with elastic-Van Gieson. Images all x40 magnification, scale bars = 20 μm. (B) Pulmonary arterial remodelling from normoxic and hypoxic WT and miR-145 -/- female mice (n = 5/group). Mice were subjected to chronic hypoxia for 14 days and analyzed at 10 weeks of age. Lung sections (5 sections/group) were stained with Elastin-Van Gieson and microscopically assessed in a blanded fashion. Pulmonary arteries (≤ 80 microns external diameter) were considered muscolarized if they possessed a distinct double elastic lamina for at least half the diameter of the vessel cross section. Approximately 150 arteries from each sagittal lung section were assessed. Data were analyzed using a two-way ANOVA followed by Bonferroni's post-hoc test. *$p<0.05$ compared to normoxic mice or WT hypoxic mice as indicated. NS = non-significant change.

4.2.3 miR-145 Expression in the Right Ventricle and the Left Ventricle Plus Septum of WT Hypoxic Mice

Considering the reduction in RVH observed in miR-145 KO mice, we also evaluated miR-145 expression in the right ventricle and the left ventricle plus septum of WT and miR-145 -/- mice exposed to chronic hypoxia for 14 days. The analysis of the KO mice confirmed the absence of miR-145 expression in these tissues, while in WT mice we observed a significant up-regulation of this miRNA in comparison with normoxic animals (Figure 4-12A and B), suggesting that miR-145 could be not only indirectly (because of its involvement in vascular remodelling) (Cheng, Liu et al. 2009) but also directly involved in the RVH characteristic of this animal model.

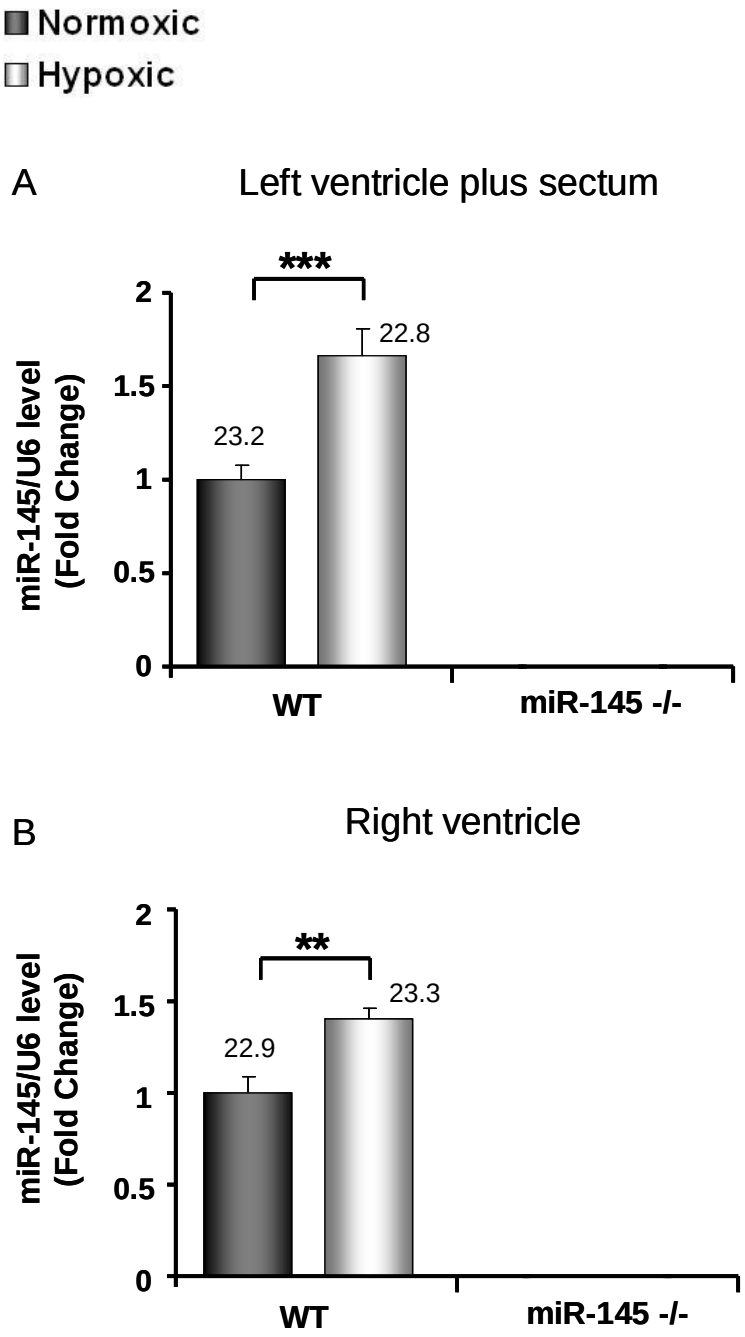

Figure 4-12 miR-145 expression in the left ventricle plus septum (A) and the right ventricle (B) of WT and miR-145 -/- female mice. Total RNA was extracted from the left ventricle plus septum (A) or the right ventricle (B) of normoxic (dark grey bars) or 14 days hypoxic (light grey bars) 10 week old mice. 6 mice/group were analyzed. Every sample was tested in triplicate. Results were normalized to U6 values and expressed as relative fold change, with an arbitrary value of 1 assigned to the control group. Raw Ct values for the target miRNAs are indicated above each column. Data were analyzed using a two-way ANOVA followed by Bonferroni's post-hoc test. **p<0.005, ***p<0.001 compared to wt normoxic mice.

4.2.4 Analysis of miR-145 Targets in the Total Lung of miR-145 KO Mice in Comparison with Control Animals

In order to verify the effect of miR-145 genetic ablation on gene and protein expression, several miR-145 gene targets, already validated in literature (Section 4.1) or identified using TargetScan and PicTar prediction algorithms and selected for their involvement in PAH were analyzed by TaqMan® Real-Time PCR and western blot in total lung of WT and miR-145 KO animals. As for Chapter 3, *GAPDH* was selected as housekeeping gene after evaluation of its stability in hypoxia. Representative results are showed for *KLF4* and *KLF5* analysis (Figure 4-13). The selected targets included *KLF4* and *KLF5*, both involved in SMCs proliferation and differentiation, *ACE*, which converts circulating angiotensin I into its active form angiotensin II, major regulator of the contractile phenotype of VSMCs, *Myocd*, a potent SRF co-activator involved in VSMCs differentiation, and also *SMAD4* and *SMAD5*, members of the TGF-*beta* super-family (Chapter 1, Section 1.2.4.1), not validated to date in the literature. Analysis of RNA revealed a significant up-regulation of both *SMAD4* and *SMAD5* in miR-145 -/- normoxic mice in comparison with WT normoxic mice but no changes were observed in WT mice in response to hypoxia (Figure 4-14A and B). ACE and Myocd were down-regulated in WT mice in response to hypoxia (result compatible with miR-145 up-regulation in these samples), but no increase in their expression was observed in KO mice in comparison with WT, in contrast with previous observations (Boettger, Beetz et al. 2009; Cordes, Sheehy et al. 2009) (Figure 4-14C and D). *KLF4* was elevated both in normoxic and hypoxic miR-145 -/- mice in comparison with WT while *KLF5* expression was significantly up-regulated in WT hypoxic versus miR-145 -/- hypoxic mice (Figure 4-14E and F), suggesting that the genetic ablation of miR-145 has an effect on the expression of these two genes in particular in response to chronic hypoxia, responsible in WT mice of altered proliferation of PASMCs. The western blot analysis of KLF4 protein expression in WT and KO animals in hypoxic conditions confirmed the significant up-regulation of this target, whereas no significant changes were observed in nomoxia (Figure 4-15). On the contrary, KLF5 was not significantly up-regulated in the same samples both in normoxic and hypoxic conditions (Figure 4-15).

A **GAPDH Ct values in KLF5 analysis (total lung)**

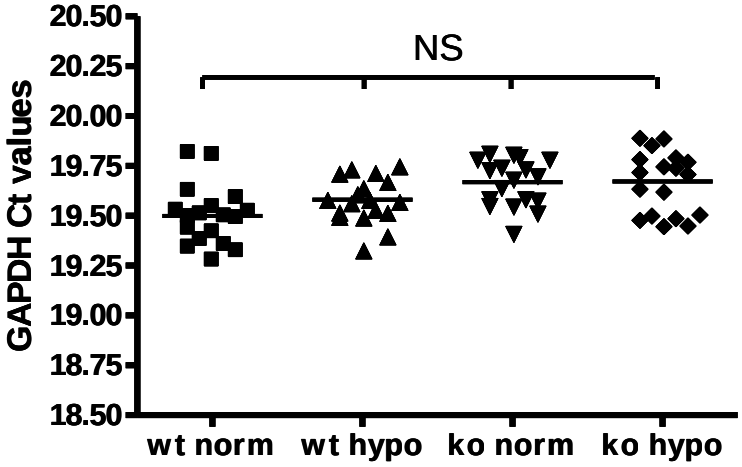

B **GAPDH Ct values in KLF4 analysis (total lung)**

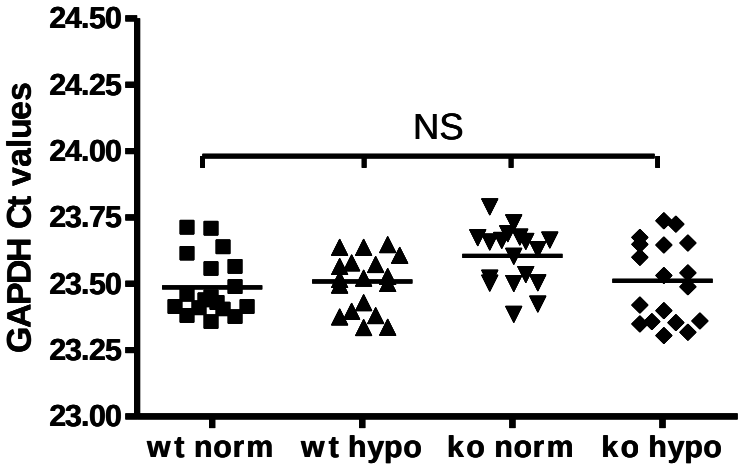

Figure 4-13 GAPDH row Ct values in hypoxic mice, WT and miR-145 KO, in comparison with normoxic mice. GAPDH expression level was evaluated in hypoxic mice and compared with normoxic animals in order to assess weather hypoxia can induce its expression as previously reported. Raw data are indicated for each sample analyzed in triplicate by TaqMan® Real-Time PCR, with a lane representing the mean value for each group.

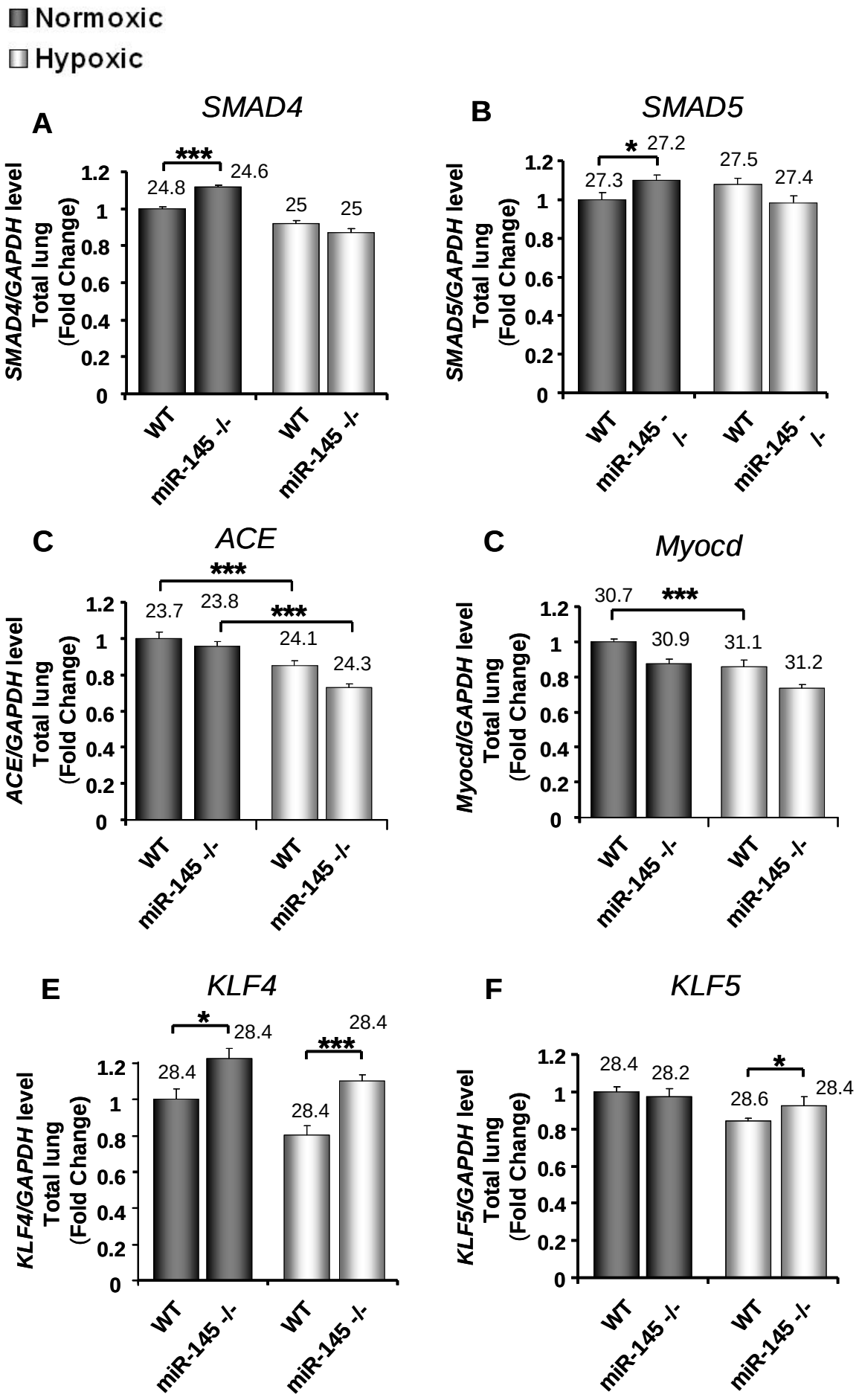
Normoxic
Hypoxic
A
SMAD4
SMAD4/GAPDH level Total lung (Fold Change)
***
24.8
24.6
25
25
B
SMAD5
SMAD5/GAPDH level Total lung (Fold Change)
*
27.3
27.2
27.5
27.4
C
ACE
ACE/GAPDH level Total lung (Fold Change)
***
***
23.7
23.8
24.1
24.3
C
Myocd
Myocd/GAPDH level Total lung (Fold Change)
***
30.7
30.9
31.1
31.2
E
KLF4
KLF4/GAPDH level Total lung (Fold Change)
*
***
28.4
28.4
28.4
28.4
F
KLF5
KLF5/GAPDH level Total lung (Fold Change)
*
28.4
28.2
28.6
28.4
WT
miR-145 -/-

Figure 4-14 Analysis of miR-145 selected targets. The expression level of SMAD4 (A), SMAD5 (B), ACE (C), Myocd (D), KLF4 (E) and KLF5 (F) was assessed by TaqMan® Real-Time PCR in the total lung of WT and miR-145 -/- female mice, normoxic and 14 days hypoxic. Samples were tested in triplicate. Results were normalized to GAPDH values and expressed as relative fold change, with an arbitrary value of 1 assigned to the control group. Raw Ct values for the target genes are indicated above each column. Data were analyzed using a two-way ANOVA followed by Bonferroni's post-hoc test. *p<0.05, ***p<0.001 as indicated. N = 6/group.

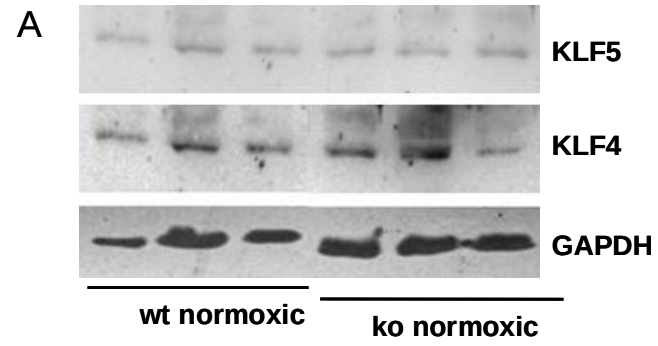
A
KLF5
KLF4
GAPDH
wt normoxic
ko normoxic

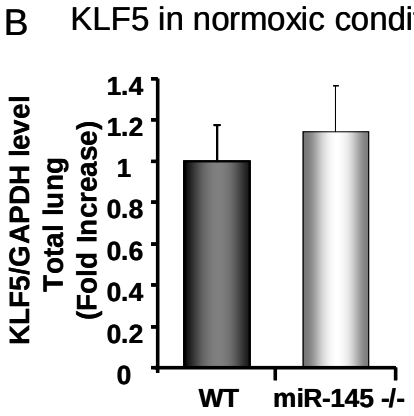
B KLF5 in normoxic conditions
KLF5/GAPDH level
Total lung
(Fold Increase)
1.4
1.2
1
0.8
0.6
0.4
0.2
0
WT
miR-145 -/-

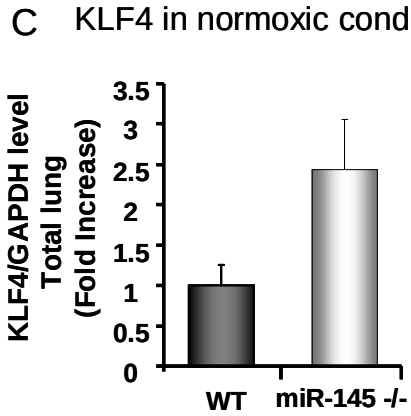
C KLF4 in normoxic conditions
KLF4/GAPDH level
Total lung
(Fold Increase)
3.5
3
2.5
2
1.5
1
0.5
0
WT
miR-145 -/-

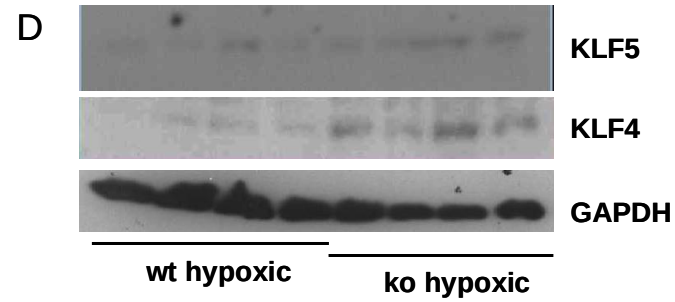
D
KLF5
KLF4
GAPDH
wt hypoxic
ko hypoxic

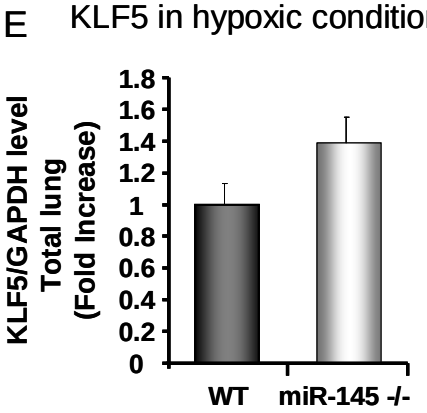
E KLF5 in hypoxic conditions
KLF5/GAPDH level
Total lung
(Fold Increase)
1.8
1.6
1.4
1.2
1
0.8
0.6
0.4
0.2
0
WT
miR-145 -/-

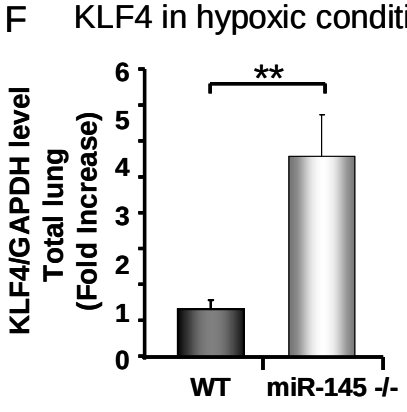
F KLF4 in hypoxic conditions
**
KLF4/GAPDH level
Total lung
(Fold Increase)
6
5
4
3
2
1
0
WT
miR-145 -/-

Figure 4-15 Analysis of KLF4 and KLF5 protein expression level in WT and miR-145 -/- hypoxic female mice. (A, D) The expression level of KLF4 and KLF5 was assessed by western blot in the total lung of WT and miR-145 -/- mice exposed to chronic hypoxia for 14 days. 4 mice/group were analyzed, and the intensity of the western blot bands was measured using a specific software (Scion Image software). The resulting quantification bars are represented in graphs in B, C, E and F. Results were normalized to GAPDH values and expressed as fold increase, with an arbitrary value of 1 assigned to the WT group. Data were analyzed using an unpaired t-test. **p<0.005 compared to wt mice.

4.2.5 MiR-145 and miR-143 in Human PAH

We next assessed whether miR-145 and miR-143 are dysregulated in patients with PAH and examined their expression levels in the lung of patients with IPAH and HPAH in comparison with control lung tissue. Although miR-145 KO alone had a protective effect against the development of PAH in hypoxic mice without any compensatory effect on miR-143 expression, we decided to evaluate also miR-143 expression in PAH patients, in consideration of the up-regulation of this miRNA observed in hypoxic female mice. We first extracted miRNAs from paraffin-embedded lung sections. Compared to controls, both miR-143 and miR-145 were significantly elevated in both HPAH and IPAH samples (Figure 4-16A and B). We next used *in situ* hybridization to localize expression of miR-145 and miR-143 in human lungs selected from the above patients (Figure 4-17 and Figure 4-18). In concordance with analysis of the mouse lung, expression of miR-145 and miR-143 in control lung sections was confined to smooth muscle cells, including both vascular and bronchiolar lineages (Figure 4-17 and Figure 4-18). PAH is characterized by the development of both constrictive and complex arterial lesions involving the pre- and intra-acinar pulmonary arteries. In patients with IPAH and HPAH, both these miRNAs were expressed by arterial smooth muscle cells and observed within the muscular component of constrictive lesions and complex vascular lesions wherever present (Figure 4-17 and Figure 4-18). Mir-145 and miR-143 positive cells were also observed in pre- and intra-acinar arteries with increased thickness and muscularization (Figure 4-17 and Figure 4-18). In addition, newly muscularized arterioles at the level of alveolar ducts expressed abundant levels of both these miRNAs. Although *in situ* localization is not quantitative, we also observed vessels with extensive remodeling where neotintimal SMC has notably reduced levels of miR-145 compared to SMCs resident within the medial layer (Figure 4-17C), accordingly with previous observations (Cheng, Liu et al. 2009; Cordes, Sheehy et al. 2009). Since the growth and characteristics of SMCs isolated from patients with *BMPR2* mutations are fundamentally different to those isolated from patients without germline mutations, we used human primary cells in culture to assess the effect of *BMPR2* mutations on miR-145 and miR-143 regulation. We therefore cultured primary human PASMCs obtained from PAH patients and quantified the expression of our miRNAs of interest at the pre-miRNA and mature miRNA level. The pri- form of both

miR-145 and miR-143 was undetectable, possibly because pri-miRNA transcripts are rapidly processed into their mature forms. miR-145 and miR-143 resulted significantly elevated in cells derived from patients with known *BMPR2* mutations compared to unaffected controls (Figure 4-19A and B and Figure 4-20A and B) in the pre- and the mature forms. We next performed northern blot analysis to confirm and quantify the differential levels of the mature miR-145 and miR-143 in the same samples. In concordance with the Real-Time PCR analysis, miR-145 and miR-143 were significantly elevated in the RNA extracted from patients with mutations in *BMPR2* compared to non-mutated control PASMCs (Figure 4-19C and D and Figure 4-20C and D). Therefore, we can conclude that basal levels of miR-145 and miR-143 are elevated in patients with germline *BMPR2* mutations.

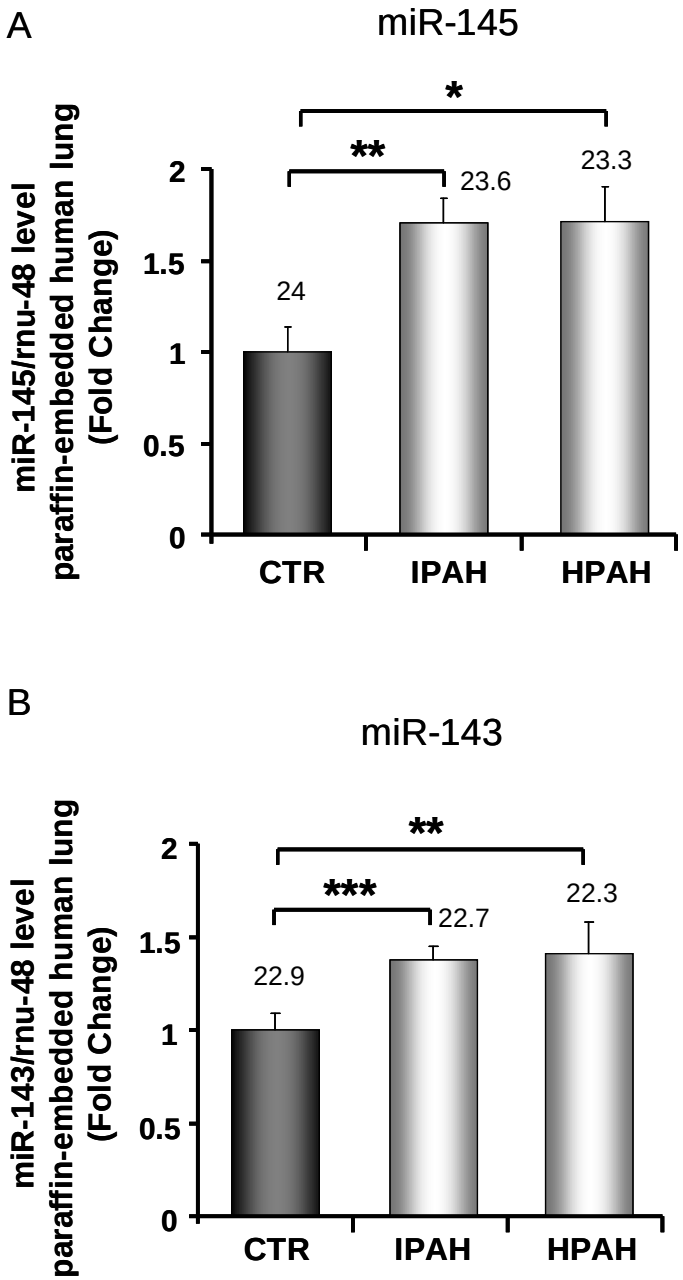

Figure 4-16 Assessment of miR-145 and miR-143 expression level in IPAH and HPAH human lung. TaqMan® Real-Time PCR analysis of RNA extracted from paraffin-embedded human lungs of IPAH (n = 6), HPAH (n = 5) and control patients (n = 6) showing the expression level of miR-145 (A) and miR-143 (B). All samples were tested in triplicate and normalized to Rnu-48 values and expressed as relative fold change, with an arbitrary value of 1 assigned to the control group. Raw Ct values for the target miRNAs are indicated above each column. Data were analyzed using a one-way ANOVA followed by Bonferroni's post-hoc test. *p<0.05, **p<0.005, ***p<0.001 compared to CTR group.

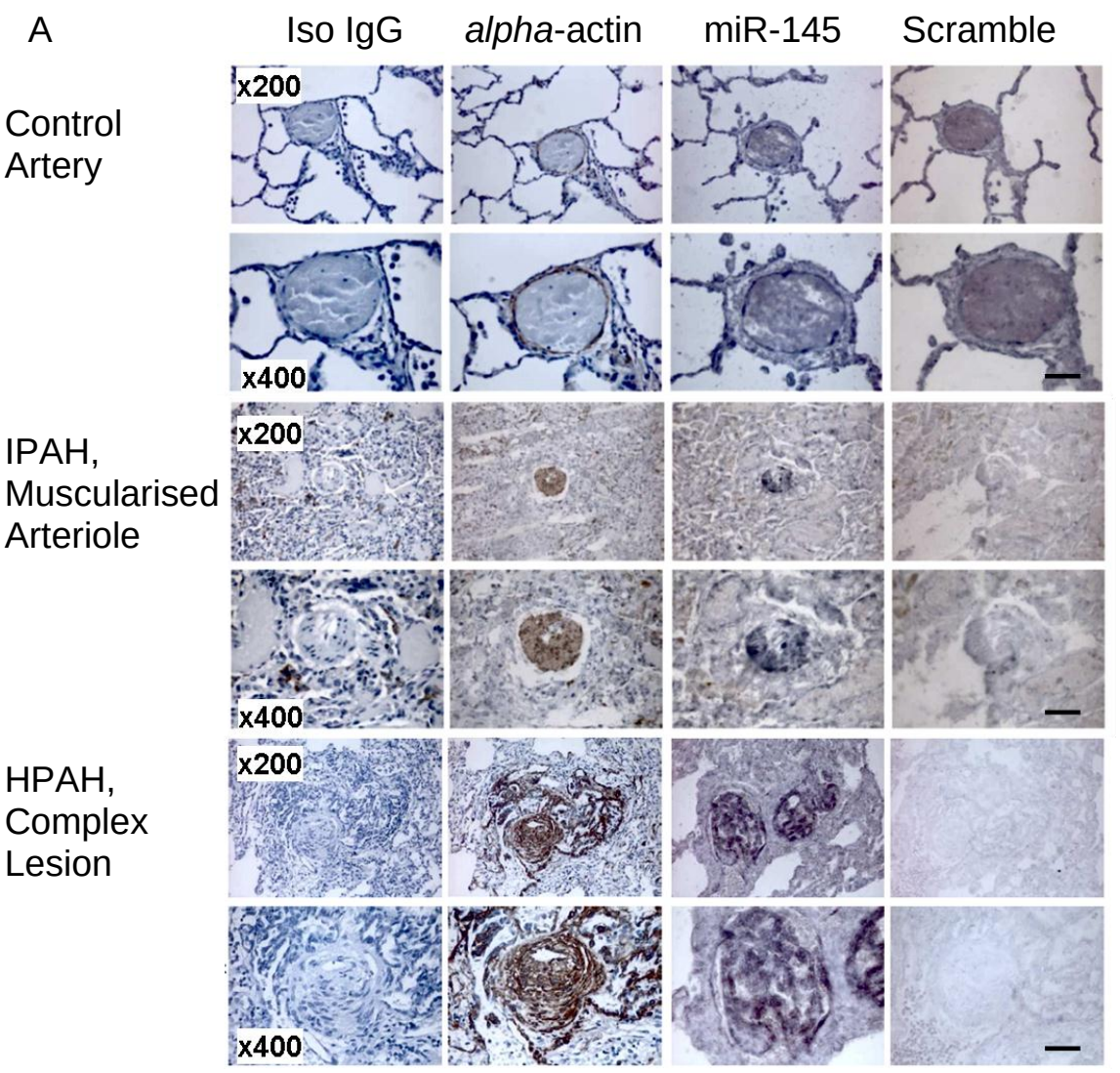
A
Iso IgG
alpha-actin
miR-145
Scramble
Control Artery
IPAH, Muscularised Arteriole
HPAH, Complex Lesion
x200
x400

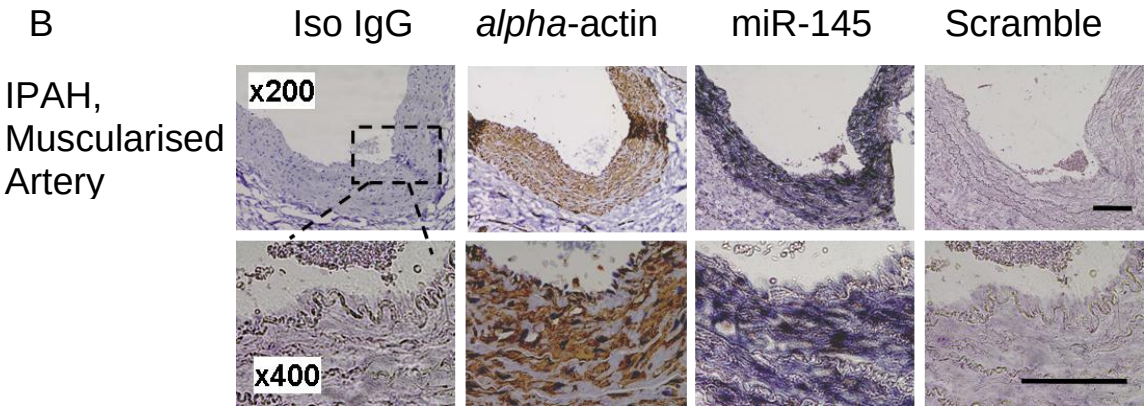
B
Iso IgG
alpha-actin
miR-145
Scramble
IPAH, Muscularised Artery
x200
x400

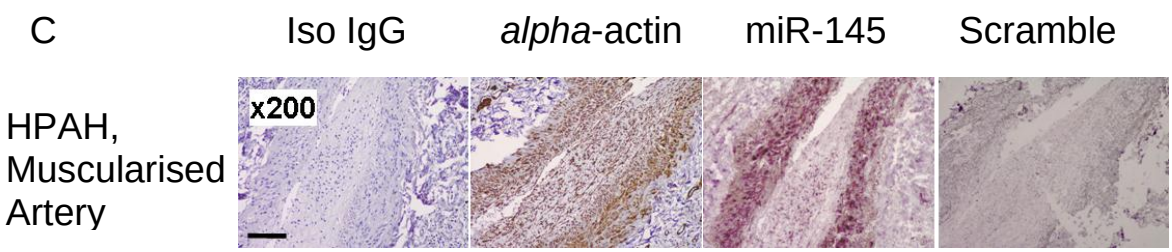

Figure 4-17 *In situ* analysis of miR-145 expression in paraffin sections obtained from the same samples used in figure 4.14. (A, B, C) Arteries of different sizes and different examples of lesions are shown. A scramble probe was used as negative control. For co-localization, *alpha*-actin was detected in the same samples using immunohistochemistry on serial sections, with non-immune isotype-IgG antibody as negative control. Images demonstrate increased expression of *alpha*-actin and miR-145 in a typical complex lesion and in newly muscularized arterioles and arteries. (A) scale bars = 50 μm, (B) scale bars = 100 μm. (C) miR-145 detection in the neointimal lesion of HPAH patients. Images show a decreased expression of *alpha*-actin and miR-145 in the neointima formation of big arteries in comparison with SMCs resident within the medial layer. Scale bars = 100 μm.

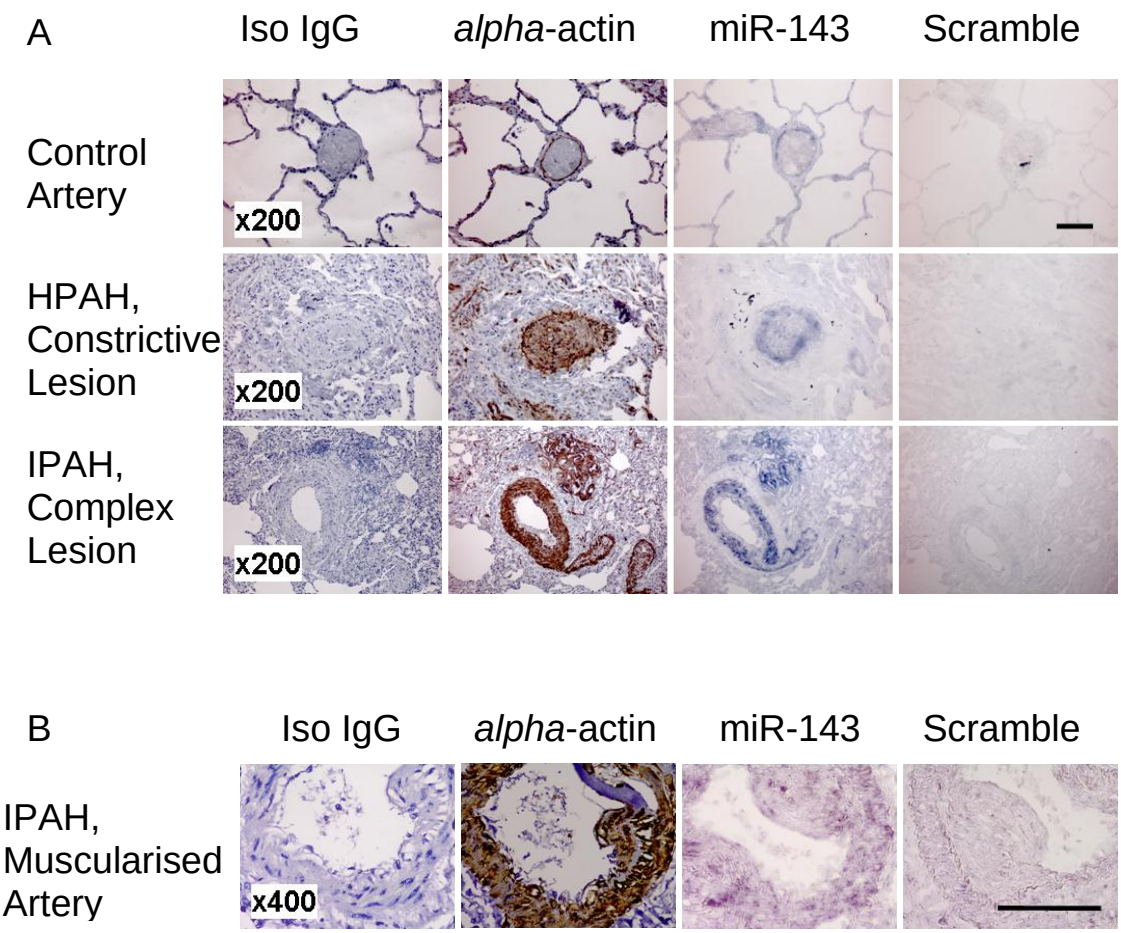

Figure 4-18 *In situ* analysis of miR-143 expression in paraffin sections obtained from the same samples used in Figure 4.14. (A, B) Arteries of different sizes and different examples of lesions are shown. A scramble probe was used as negative control. For co-localization, *alpha*-actin was detected in the same samples using immunohistochemistry on serial sections, with non-immune isotype-IgG antibody as negative control. Images demonstrate increased expression of *alpha*-actin and miR-145 in a typical complex lesion and in a newly muscularized arteriole. (A) scale bar = 50 μm, (B) scale bars = 100 μm.

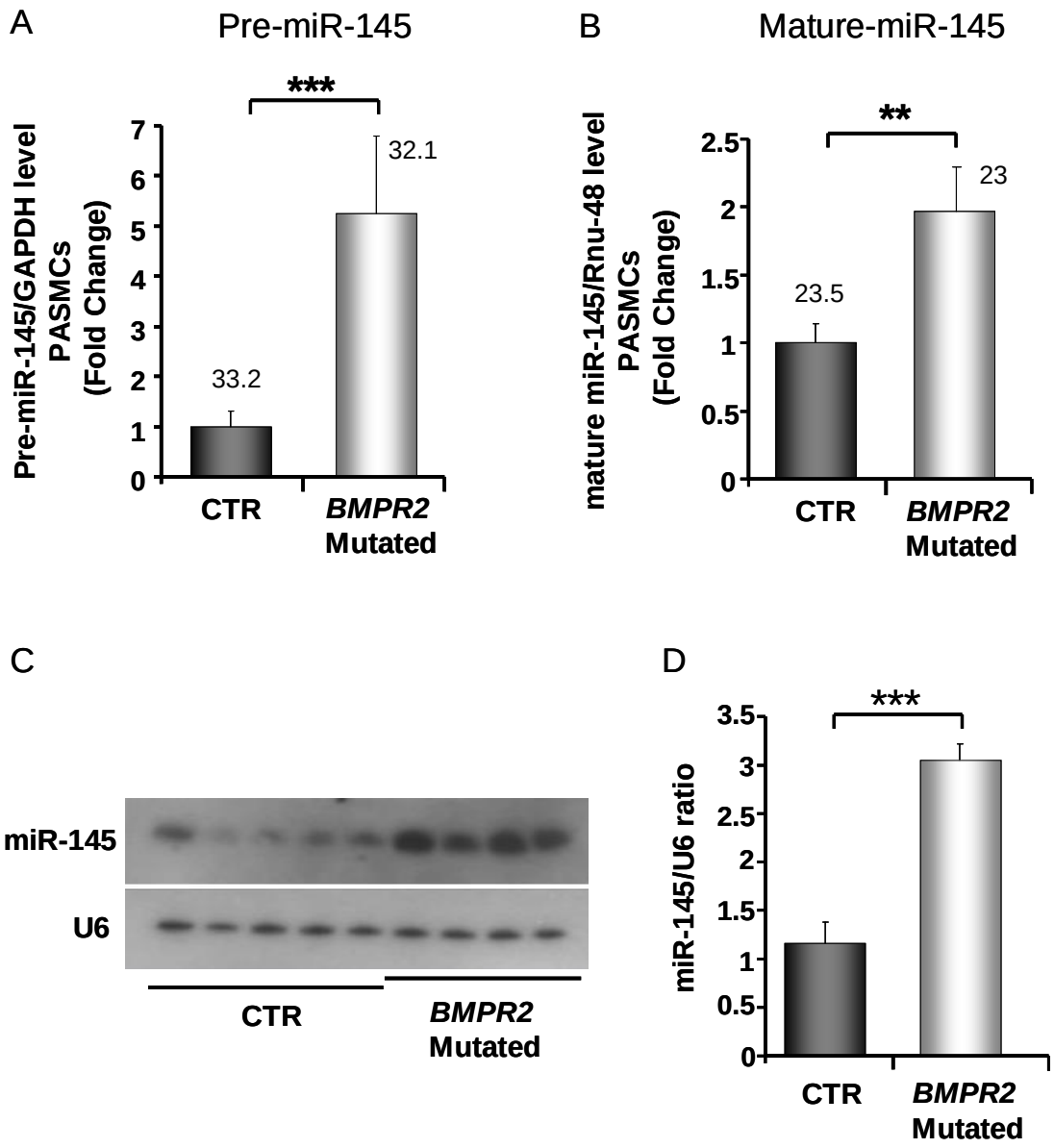

Figure 4-19 Analysis of miR-145 in human *BMPR2* mutated PASMCs. (A, B) TaqMan® Real-Time PCR analysis of miR-145 expression in human PASMCs. Total RNA was extracted from PASMCs of HPAH patients with a mutation in the *BMPR2* gene. Passage 4 primary cells were used. cDNA was analyzed in triplicate for pre- (A) and mature-miR-145 expression (B) in comparison with unaffected controls. Results were normalized to GAPDH for the pre- and Rnu-48 for the mature-miR-145 and expressed as relative fold change, with an arbitrary value of 1 assigned to the control group. Raw Ct values for the target miRNAs are indicated above each column. Data were analyzed using an unpaired t-test. **p<0.005, ***p<0.001 compared to control samples. (C, D) The same total RNA extracted from WT and *BMPR2* mutated cells was also used for northern blot analysis in order to confirm the TaqMan® Real-Time PCR results. The blot quantification (D) was performed with Scion Image software (www.scioncorp.com): band intensities of the miRNA of interest were established and normalized to the relative U6 signal. Data were analyzed using an unpaired t-test. ***p<0.001 compared to control samples.

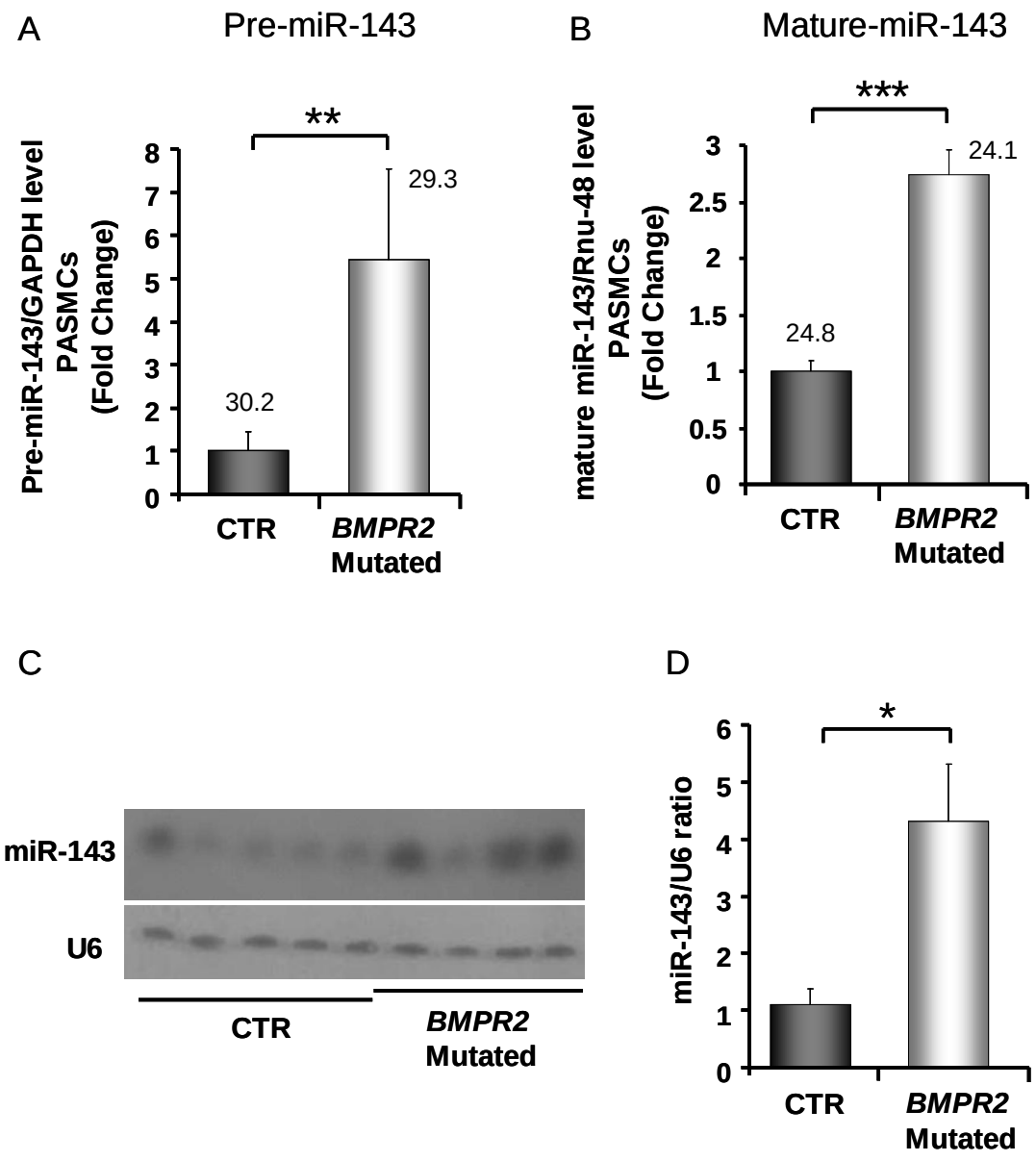

Figure 4-20 Analysis of miR-143 in human *BMPR2* mutated PASMCs. (A, B) TaqMan® Real-Time PCR analysis of miR-143 expression in human PASMCs. Total RNA was extracted from PASMCs of HPAH patients with a mutation in the *BMPR2* gene. Passage 4 primary cells were used. cDNA was analyzed in triplicate for pre- (A) and mature-miR-143 expression (B) in comparison with unaffected controls. Results were normalized to GAPDH for the pre- and Rnu-48 for the mature-miR-143 and expressed as relative fold change, with an arbitrary value of 1 assigned to the control group. Raw Ct values for the target miRNAs are indicated above each column. Data were analyzed using an unpaired t-test. **p<0.005, ***p<0.001 compared to control samples. (C, D) The same total RNA extracted from WT and *BMPR2* mutated cells was also used for northern blot analysis in order to confirm the TaqMan® Real-Time PCR results. The blot quantification (D) was performed with Scion Image software (www.scioncorp.com): band intensities of the miRNA of interest were established and normalized to the relative U6 signal. Data were analyzed using an unpaired t-test. *p<0.05 compared to control samples.

4.2.6 miR-145 and miR-143 Expression in BMPR2 R899X mice

Considering the dysregulation observed in miR-145 and miR-143 expression level in human PASMCs isolated from HPAH patients harbouring a mutation in the *BMPR2* gene, we evaluated the effect of a truncating *BMPR2* mutation on miR-145 and miR-143 expression in heterozygous R899X +/- mice. West et al. recently reported these mice, which harbor a mutation in the *BMPR2* gene tail domain, develop PAH and significant vascular remodeling (West, Harral et al. 2008). RNA was extracted from the whole lung of 6 month old mice and analyzed by TaqMan® Real-Time PCR and northern blot for miR-145 and miR-143 expression. This revealed a significant up-regulation of both these miRNAs in mutated mice compared to controls (Figure 4-21). *In situ* localization if miR-145 in paraffin lung sections confirmed positive staining within the smooth muscle layer of pulmonary vessels and bronchi of both wt and *BMPR2* mutated mice, with strong staining observed in mutated animals (Figure 4-22).

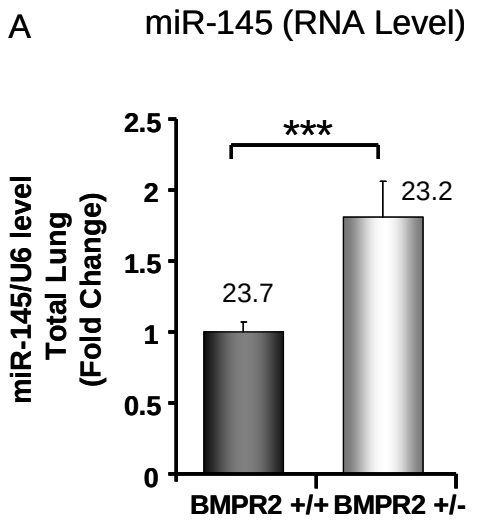
A
miR-145 (RNA Level)
***
23.7
23.2
miR-145/U6 level
Total Lung
(Fold Change)
2.5
2
1.5
1
0.5
0
BMPR2 +/+
BMPR2 +/-

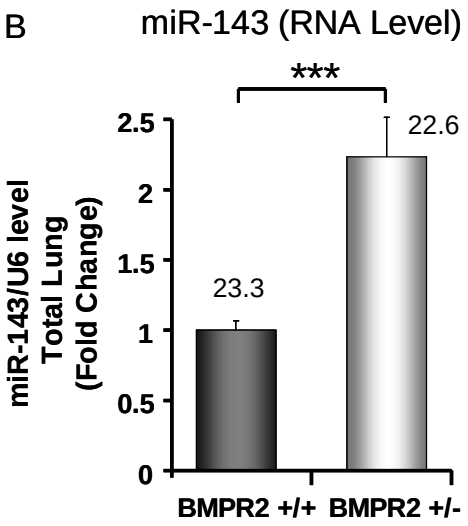
B
miR-143 (RNA Level)
***
23.3
22.6
miR-143/U6 level
Total Lung
(Fold Change)
2.5
2
1.5
1
0.5
0
BMPR2 +/+
BMPR2 +/-

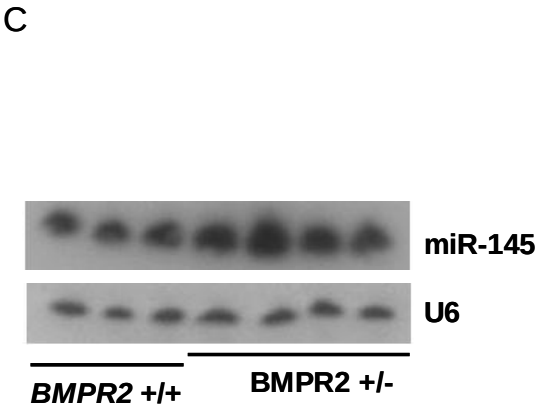
C
miR-145
U6
BMPR2 +/+
BMPR2 +/-

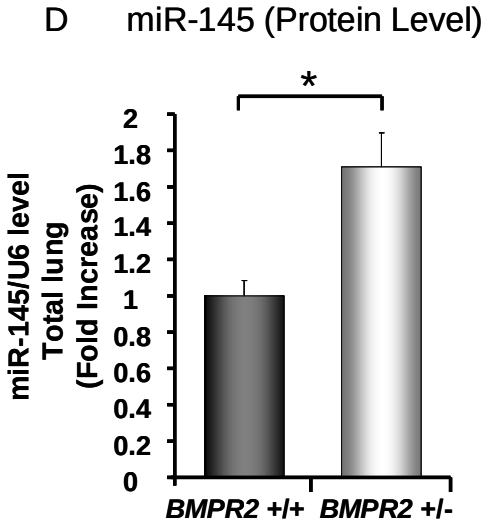
D
miR-145 (Protein Level)
*
miR-145/U6 level
Total lung
(Fold Increase)
2
1.8
1.6
1.4
1.2
1
0.8
0.6
0.4
0.2
0
BMPR2 +/+
BMPR2 +/-

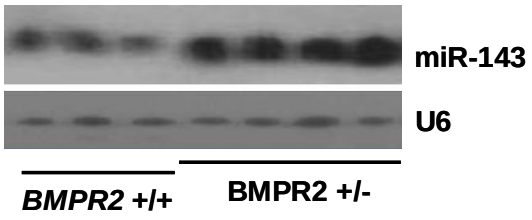
E
miR-143
U6
BMPR2 +/+
BMPR2 +/-

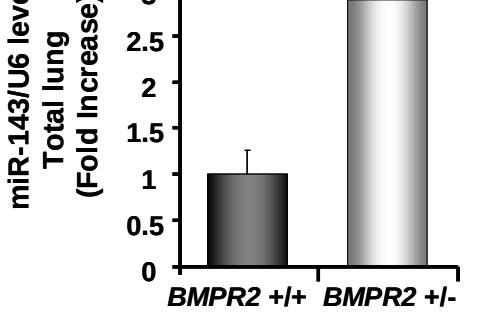
F
miR-143 (Protein Level)
***
miR-143/U6 level
Total lung
(Fold Increase)
4
3.5
3
2.5
2
1.5
1
0.5
0
BMPR2 +/+
BMPR2 +/-

Figure 4-21 miR-145 and miR-143 expression in WT and *BMPR2* R899X mice. RNA was extracted from the total lung of 3 WT mice and 4 animals heterozygous for a nonsense mutation in the *BMPR2* gene, and tested in triplicate for miR-145 (A) and miR-143 (B) expression by TaqMan® Real-Time PCR and northern blot (C-F). Real-Time PCR results were normalized to U6 expression and analyzed using an unpaired t-test. ***p<0.001 compared to *BMPR2* +/+ mice. Blots quantification (D, F) was performed with Scion Image software (www.scioncorp.com). Results were normalized to U6 values and expressed as fold increase, with an arbitrary value of 1 assigned to the *BMPR2* +/+ group. Raw Ct values for the target miRNAs are indicated above each column. Results were analyzed using an unpaired t-test. ***p<0.001, *p<0.05 compared to *BMPR2* +/+ mice.

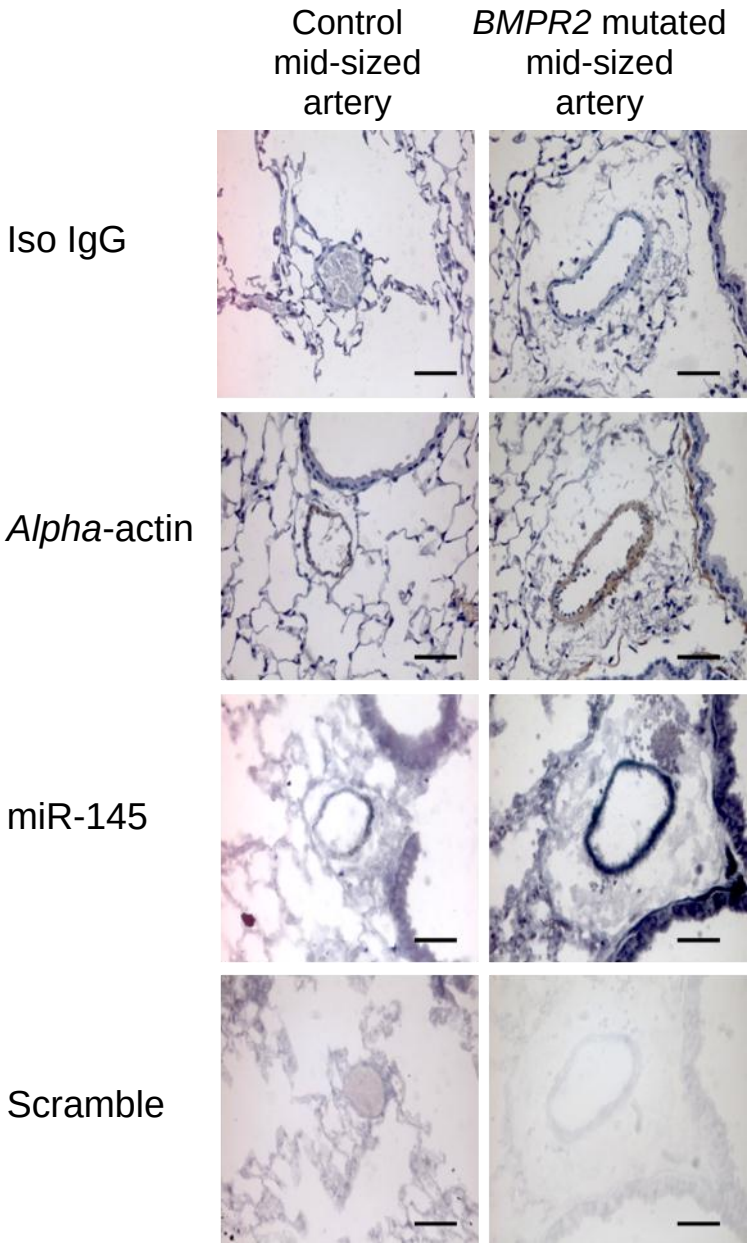

Figure 4-22 miR-145 localization in WT and *BMPR2* R899X mouse lung. *In situ* hybridization showing miR-145 localization in the lung of the animals used for the experiments showed in Figure 4.15. Paraffin sections were rehydrated and incubated with an anti-miR-145 or scramble probe as negative control. For co-localization, *alpha*-actin was detected in the same samples using an immunohistochemistry assay, with non-immune isotype-IgG antibody as negative control. Images x200 magnification, scale bars = 50 μm.

4.2.7 Effect of BMPR2 Down-Regulation on miR-143 and miR-145 Expression in Human PASMCs

Davis-Dusembery et al. recently reported that BMP4 is able to induce the expression of the miR-143/145 cluster through the CArG box present in its promoter (Section 4.1) (Davis-Dusenbery, Chan et al. 2011). However, we reported the up-regulation of both these miRNAs in systems characterized by an impairment of the BMP signaling due to mutations in the type II receptor *BMPR2*. For this reason we decided to evaluate *in vitro* the effect of a siRNA-mediated knock-down of *BMPR2* on miR-143 and miR-145 expression level in human WT PASMCs. Cells were therefore transfected with a short interfering (si) sequence, able to target and down-regulate specifically *BMPR2*, or with a siScramble as negative control. RNA was extracted from these samples and from untreated cells after 72 h for comparison. The efficacy of the down-regulation of *BMPR2* was assessed through TaqMan® Real-Time PCR analysis (Figure 4-23A). In agreement with our previous findings, the down-regulation of *BMPR2* induced the significant up-regulation of both miR-143 and miR-145, whereas no changes were observed in untreated or siScramble-treated cells (Figure 4-23B and C).

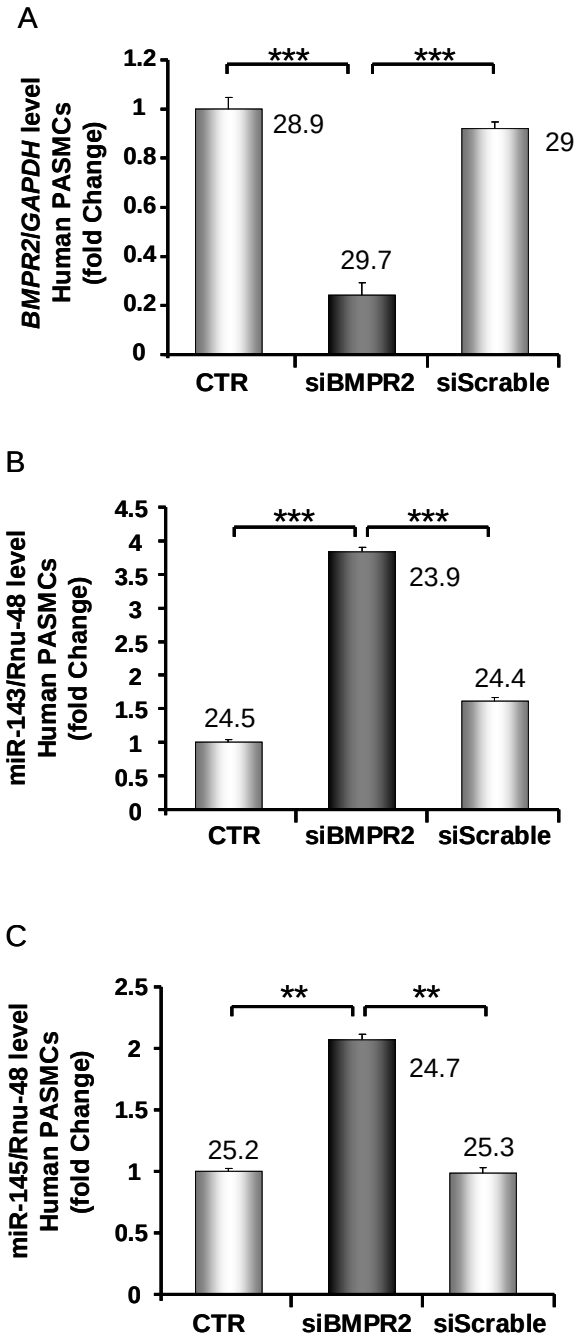

Figure 4-23 miR-143 and miR-145 up-regulation in human PASMCs down-regulated for *BMPR2* expression via a siRNA. Primary human PASMCs were transfected with a siRNA able to target and repress specifically *BMPR2* expression or with a siScramble as a negative control. Total RNA was extracted after 72 h from these samples and untreated cells for comparison and tested in triplicate. The efficiency of *BMPR2* down-regulation was evaluated by TaqMan® Real-Time PCR (A). miR-143 (B) and miR-145 (C) expression were also assessed in the same samples. All Samples were tested in triplicate. Results were normalized to GAPDH for *BMPR2* and Rnu-48 for miR-143 and miR-145 and expressed as relative fold change, with an arbitrary value of 1 assigned to the control group. Raw Ct values for the target miRNAs and gene are indicated above each column. Data were analyzed using a one-way ANOVA followed by Bonferroni's post-hoc test. **p<0.005, ***p<0.001 compared to CTR or si-Scramble group as indicated.

4.3 Discussion

In this chapter we describe the expression and regulation of miR-145 and miR-143 in the lung under normal physiology and in response to hypoxic injury. We show that these two miRNAs are mainly expressed in the SMC compartment both in lungs taken from mice subjected to normoxic or hypoxic conditions as well as in human lungs from control subjects and patients with either HPAH or IPAH. In the hypoxic mouse model we show elevation of miR-143 and miR-145 levels in total lung and in the heart of female animals compared to controls with no dysregulation in other organs such as brain, spleen and kidney. These observations suggest that miR-143/145 deregulation in response to hypoxia is specific of the cardiovascular system.

We also hypothesize an essential role for miR-145 (but potentially not miR-143) in the development of PAH. Recently, several studies pointed out not only the specific smooth muscle localization of these miRNAs, but also their fundamental role in the differentiation of this cell type (Rangrez, Massy et al. 2011). In particular, miR-145 has been identified as the most abundant miRNA in normal arteries and in differentiated VSMCs (Cheng, Liu et al. 2009). Considering the central role of PASMCs remodeling in the small peripheral, normally non-muscular PAs during the development of PAH, we decided to evaluate the effect of the ablation of this miRNA in mice exposed to hypoxia. In particular, we used KO mice deleted for the sequence coding for miR-145 but able to express miR-143, transcribed in the same precursor. This is relevant since a recent study showed how the introduction of miR-145, but not miR-143, into neural crest stem cells was sufficient to guide 75% of cells into the VSMC lineage within only 24 hours (Cordes, Sheehy et al. 2009). Also, antagomiR-mediated inhibition of miR-145 expression blocked the ability of myocd to convert fibroblasts into VSMCs, with only a little effect of miR-143 knock-down (Cordes, Sheehy et al. 2009). A different study demonstrated that reintroduction of miR-145, but not miR-143, into vascular SMC rescues the reduction in SMC marker expression in Dicer KO vascular SMCs (Albinsson, Suarez et al. 2010). These observations suggest a predominant role of miR-145 in SMCs differentiation, leading us to use a single miR-145 -/- in this study in order to evaluate its role in the development of PAH. A functional analysis of the vasculature of miR-145 -/- mice revealed a reduced response to hypoxia: when these mice were exposed to

hypoxia for two weeks, systolic pressure did not show a significant rise as in WT mice. A similar result was obtained for right ventricular hypertrophy. In addition, the percentage of remodeled vessels was significantly reduced in the KO animals, suggesting a protective role for miR-145 ablation in PAH development. This occurred in the absence of any modulation of miR-143, thus confirming the importance of miR-145 alone in the development of PAH. A different *in vivo* study very recently conducted by our group proved that the antagomiR-mediated substantial down-regulation of miR-145 (but not miR-143) also has a protective effect against the development of PAH in hypoxic mice, confirming what we show in this Chapter (data not shown).

mRNA analysis of the expression of some predicted targets confirmed in some cases their up-regulation in miR-145 ablated samples, both in normoxic and hypoxic conditions, whereas other targets did not present the expected regulation in KO mice. This is the case of ACE, down-regulated in miR-145 -/- samples, although it was possible to observe its significant down-regulation in WT hypoxic mice, characterized by the up-regulation of miR-145. It is important to remember that the capacity of miR-145 to regulate the expression of this specific target has been previously reported (Boettger, Beetz et al. 2009). In particular, Boettger et al. recently showed the up-regulation of ACE in VSMCs of miR-143/145 depleted mice and explained, at least in part, with this observation the shift from the contractile to the synthetic phenotype observed in these mutant mice. This finding could not be confirmed in our miR-145 KO mice, since no up-regulation in ACE expression was observed, both in normoxic and hypoxic conditions, in the total lung. A western blot analysis will clarify in the future if such a regulation occurs at protein level, whereas the analysis of the PAs will be important to evaluate in a more specific way the effect of miR-145 ablation on the vasculature. On the other hand, both *KLF4* and *KLF5* were significantly up-regulated in KO mice exposed to chronic hypoxia at mRNA and protein level, suggesting a direct role for these targets in the protective effect against the development of PAH observed in these mutant mice. Future experiments will be conducted to assess the effect of KLF4/KLF5 manipulation on PAH development. A different case is represented by myocd, since the up-regulation of this factor was previously reported as a consequence of miR-143 and miR-145 induction, suggesting its role as an indirect targets of these miRNAs (Cordes, Sheehy et al. 2009). Moreover, myocd plays an important role in the TGF-*beta*-mediated induction of the miR-143/145 cluster, as

recently reported (Davis-Dusenbery, Chan et al. 2011). However, we could not observe any up-regulation of myocd in WT hypoxic mice, nor a significant down-regulation in the KO animals. These findings suggest that in our system miR-143/145 induction is not myocd-mediated and that myocd itself is not influenced by the deregulation of this cluster. A western blot analysis of myocd protein expression level and the analysis of PAs will be necessary to confirm this hypothesis. Immunohistochemistry assays will also be important to localize myocd expression. As future work, a microarray based analysis of mRNA expression could be important to have a global view of the effects of miR-145 genetic ablation on gene regulation. In particular, such a study could be conducted using total lung but more conveniently PAs in order to assess directly the component of the pulmonary vasculature involved in PAH development. Moreover, luciferase assays performed *in vitro* on PASMCs will further confirm the direct effect of miR-145 manipulation on the expression of specific genes in our system.

Moreover, we have demonstrated significant up-regulation of both miR-143 and miR-145 in HPAH and IPAH patients and in particular in *BMPR2* mutated PASMCs extracted from HPAH patients. A similar level of up-regulation of the cluster was also identified in mice carrying a mutation in this gene. This conserved dysregulation suggests the presence of a link between the regulation of miR-143 and miR-145 and the TGF-*beta* super-family, already involved in the maturation process of other miRNAs including miR-21, through the interaction of SMADs with DROSHA during the second step of miRNA biogenesis (Davis, Hilyard et al. 2008) (Chapter 1, Section 1.3.3.4). Very recently, this link has been proved with the observation that both TGF-*beta* and BMP4 are able to activate transcription of miR-143/145 cluster through the CArG box present in its promoter, but with a different mechanism. In fact, MRTF-A results essential for BMP4-dependent induction of the cluster, while TGF-*beta* enhance miR-143/145 expression inducing SRF and myocd expression, as already mentioned (Davis-Dusenbery, Chan et al. 2011; Long and Miano 2011). However, since the BMP signaling is impaired in the presence of mutations in the *BMPR2* gene, our findings do not correlate well with this theory. Our observations of an up-regulation of miR-143 and miR-145 in *BMPR2*-mutated human cells and mouse models was also confirmed *in vitro*, since a similar dysregulation of these two miRNAs was induced in human PASMCs by the down-regulation of *BMPR2* expression, obtained via a siRNA able to inhibit specifically the expression of this gene. More experiments will be necessary to

elucidate further the role of the TGF-*beta* super-family in the regulation of the miR-143/145 cluster (particularly *in vivo*) and to identify the effector of their up-regulation in mice exposed to chronic hypoxia and PAH patients, including for example stimulations *in vitro* with different members of the TGF-*beta* super-family to evaluate their effect on miR-143 and miR-145 expression or vice-versa specific-inhibition, *in vitro* and *in vivo*, of these elements.

Localization studies revealed miR-143 and miR-145 expression both in medial and neointimal SMCs of complex lesions. Interestingly, consistently with the up-regulation of these two miRNAs observed in the total lung of the analyzed PAH patients, the *in situ* localization of miR-143 and miR-145 in the vessels of IPAH and HPAH patients showed their abundant expression in hypertrophied arteries, pulmonary vascular lesions and newly muscularized arterioles. However, lower expression of miR-145 was observed in neointima formation in comparison with medial hypertrophy and adventitial thickening and with newly muscularized arterioles. The lack of neointimal expression of this miRNA is consistent with the presence of a dedifferentiated mesenchymal cell in this area of the vessel. It has been reported that lack of miR-145 profoundly impedes the development of a neointima in the mouse carotid injury model due to diminished migratory activity of SMCs (Xin, Small et al. 2009). However, it is important to notice that the mouse hypoxic model is a model of distal muscularization of the pulmonary circulation, rather than neointima formation, and for this reason it does not represent the ideal model to evaluate this aspect. For this reason, it will be necessary in the future to evaluate more extensively this aspect in human pathological samples in comparison with unaffected controls. Nevertheless, taken together our findings and results in the systemic circulation suggest that inhibition of miR-145 may perturb both the process of muscularization and neointima formation.

It is also important to note that a miR-145 up-regulation in the PASMCs obtained from IPAH patients has been recently marked in another study (Courboulin, Paulin et al. 2011), confirming our findings. However, in that study the focus was on the role of miR-204 in PAH, without further analysis of miR-145 expression and regulation. Dysregulation of several miRNAs in the pathological samples (animal or human) in PAH is now clear, each miRNA having potentially many hundreds of potential gene targets.

This defines a complex situation, with several pathways and cell types potentially involved, all important but not necessarily regulated at the same time or at the same level. The manipulation of individual miRNAs, however, such as miR-145 here, or miR-204 (Courboulin, Paulin et al. 2011), appears to exert a substantial impact on the development of PAH. For this reason, our study also highlights the potential for miR-145 down-regulation as a novel therapeutic approach for PAH. Strategies to achieve this may require selective delivery to the pulmonary system to avoid potentially deleterious effects of down-regulation of miR-145 in the peripheral vasculature, considering that a significant reduction of SAP was observed in mice genetically depleted for this miRNA. Our *in situ* studies in mouse and human show almost exclusive expression of miR-145 in the smooth muscle cells of the lung and within vascular lesions associated with PAH, hence strategies to delivery selectively within the lung are attractive.

Taken together, this study demonstrates an essential role for miR-145 in the development of PAH through remodeling associated with the SMC compartment and association of elevated miR-145 levels in patients with mutations in the *BMPR2* receptor.

5. MiR-21 Expression in Pulmonary Arterial Hypertension: Evidence from Mouse Models and Patient Samples

5.1 Introduction

miR-21 is a miRNA highly expressed in the cardiovascular system (Cheng, Ji et al. 2007; Ji, Cheng et al. 2007), and its role in different human pathologies has been studied in detail in the last years. Here we will evaluate the role of this miRNA in the development of PAH.

miR-21 was one of the first miRNAs identified in the human genome, and it shows a strong evolutionary conservation across a wide range of vertebrate species (Cai, Hagedorn et al. 2004). miR-21 is encoded by a single gene that in *Homo sapiens* is located on chromosome 17 (and on chromosome 10 and 21 in rat and mouse respectively) (Figure 5-1), where it overlaps with the protein-coding gene *VMP1* (vacuole membrane protein-1, also known as *TMEM49*, transmembrane protein-49) (Selcuklu, Donoghue et al. 2009). However, it has been demonstrated that the 3433 nt long pri-miR-21 is independently transcribed from a conserved promoter localized within an intron of the overlapping protein-coding gene (Fujita, Ito et al. 2008).

Unlike miR-143 and miR-145, selectively expressed in SMCs, miR-21 is universally expressed in mammal organs such as lung, heart and spleen, and also in different cells types including fibroblasts, endothelial and smooth muscle cells (Lagos-Quintana, Rauhut et al. 2002). The function of miR-21 in cancer has been evaluated in several studies, and its over-expression has been observed in the majority of cancer types analyzed, including glioblastoma (Chan, Krichevsky et al. 2005), lung cancer (Yanaihara, Caplen et al. 2006; Hatley, Patrick et al. 2010), prostate cancer (Volinia, Calin et al. 2006), pancreas (Lee, Gusev et al. 2007) and breast cancer (Iorio, Ferracin et al. 2005). In particular, the over-expression of miR-21 in primary breast cancer is correlated with advanced clinical stage and poor prognosis (Yan, Huang et al. 2008). These observations lead to the conclusion that this miRNA has oncogenic activity and can be classed as an “oncomir”.

More recently, the role of miR-21 in cardiovascular biology and disease has been evaluated. Ji et al. reported in rats a fivefold increase of the expression level of this miRNA in balloon-injured arteries compared with normal control vessels, and miR-21 knock-down substantially inhibited neointimal lesion formation (Ji, Cheng et al. 2007). Moreover, they observed that inhibition of miR-21 significantly decreased proliferation of VSMCs *in vitro* (Ji, Cheng et al. 2007). Since neointimal formation is a common pathological characteristic of diverse proliferative cardiovascular disorders including atherosclerosis, coronary heart disease and PAH, this observation includes miR-21 in the list of miRNAs potentially involved directly in the development of such pathologies.

More controversial are the results reported so far about miR-21 involvement in cardiac hypertrophy and heart failure. In several studies the significant up-regulation of this miRNA in hypertrophic animal hearts was observed (van Rooij, Sutherland et al. 2006; Cheng, Ji et al. 2007; Sayed, Hong et al. 2007). However, whereas Thum et al. reported that the antagomiR-mediated depletion of miR-21 prevents cardiac hypertrophy and fibrosis in response to pressure overload induced by transaortic constriction (TAC), Patrick et al. could not confirm this result in mice pharmacologically or genetically depleted for miR-21 expression (Thum, Gross et al. 2008; Patrick, Montgomery et al. 2010), suggesting a role for this miRNA more difficult to clarify. In addition to this, observations concerning miR-21 role in angiogenesis are also quite controversial. In fact, in human prostate cancer cells over-expression of miR-21 induced tumor angiogenesis increasing the expression of HIF-1*alpha* (Hypoxia-Inducible Factor 1 *alpha*) and VEGF (Liu, Li et al. 2011), whereas a recent study reported an impaired angiogenesis and a reduced endothelial cell proliferation and migration in response to miR-21 over-expression (Sabatel, Malvaux et al. 2011). These findings are probably due to different roles played by this miRNA in different cells types.

Several targets of miR-21 negative regulation have been identified so far. Among them, the tumor suppressors phosphatase and tensin homolog (PTEN), and programmed cell death 4 (PDCD4). PTEN is expressed in cardiomyocytes but also in vascular cells where it modulates cell survival/apoptosis, hypertrophy and contractility (Oudit, Sun et al. 2004; Ji, Cheng et al. 2007), whereas PDCD4, already known as a tumor suppressor gene (Lankat-Buttgereit and Goke 2009), has been recently involved in cardiovascular

biology by regulating apoptosis mechanisms in vascular smooth muscle cells and cardiac cells (Cheng, Liu et al. 2009; Lin, Liu et al. 2009).

As we reported in Chapter 4 about miR-143 and miR-145, BMPs and TGF-*beta* (Chapter 1, Section 1.2.4.1) can stimulate the expression of miR-21. In this case this stimulation occurs at a post-transcriptional level since ligand-specific SMAD proteins can interact with the DROSHA microprocessor subunit p68 to induce pre-miRNA accumulation. In PASMCs, this stimulation negatively regulates way the expression of PDCD4 as a result of miR-21 induction, causing the increase of different SMC markers including SMA, calponin and Sm22*alpha*. We can therefore conclude that TGF-*beta* and BMPs induce a contractile phenotype in SMCs via the increase of miR-21 (Davis, Hilyard et al. 2008).

In Chapter 3 we showed that miR-21 is significantly down-regulated in male rats injected with the pneumotoxic alkaloid monocrotaline, but levels do not change in response to chronic hypoxia in rats (Chapter 3, Section 3.2.2). Also, rat PAFs and PASMCs exposed to hypoxia for 24 h did not present any dysregulation of miR-21, whereas this miRNA was significantly down-regulated in human hypoxic PAFs, suggesting that miR-21 could be differentially regulated in different species or cell types (Caruso, MacLean et al. 2010). For this reason, considering that we had not analyzed miR-21 expression in mouse models of PAH, we evaluated in detail miR-21 expression in mouse models of PAH and in human samples derived from patients with either IPAH or HPAH as well as in control human lung. Here, we show that miR-21 is significantly up-regulated in female mice in response to chronic hypoxia and that genetic ablation of miR-21 can induce an exaggerated hypoxia-induced PAH. Further, we show the down-regulation of miR-21 in the total lung of idiopathic and heritable PAH patients, whereas in PASMCs isolated from PAH patients with a mutation in the *BMPR2* gene miR-21 is up-regulated in its pri-form, does not change in its pre-precursor and it is down-regulated in its mature form. This suggests that the regulation of miR-21 expression occurs at a post-transcriptional step. Also, both TGF-*beta* and BMP4 can induce *in vitro* miR-21 expression, but the expression of this miRNA is decreased in cells down-regulated for *BMPR2*. However, the observation that miR-21 is not dysregulated in the total lung of mice harboring a truncating mutation in the *BMPR2* gene suggests that miR-21 regulation could be complex and different in different species.

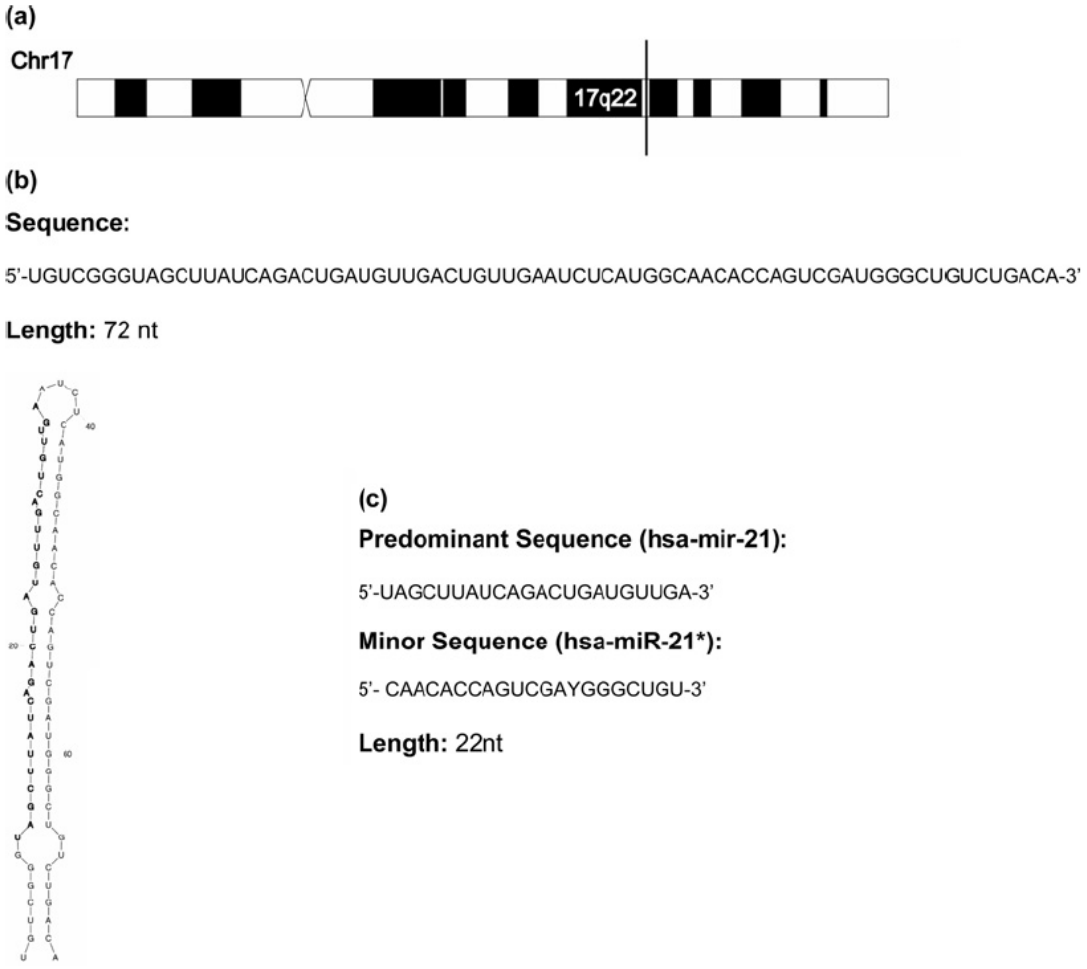

Figure 5-1 miR-21 location and structure. (A) miR-21 location on human chromosome 17. (B) pre-miR-21 sequence and stem-loop structure. Mature miR-21 sequence is shown in bold. (C) mature miR-21 sequence. Both the guide strand (predominant) and the passenger strand (minor) (Chapter 1, Section 1.3.3.2) are shown. adapted from (Selcuklu, Donoghue et al. 2009).

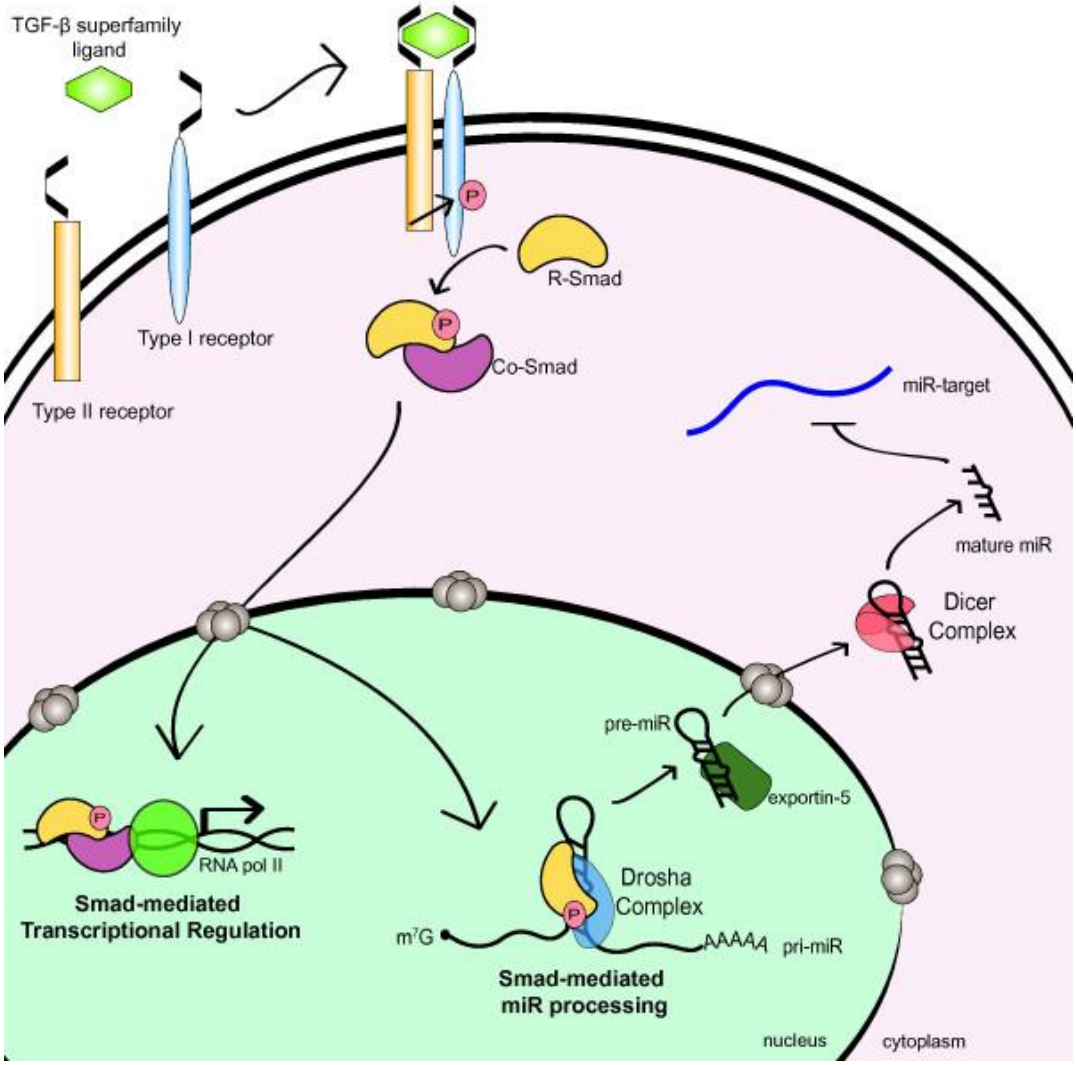

Figure 5-2 Schematic representation of BMP and TGF-*beta* induction of pre-miR-21. TGF-*beta* and BMP signaling stimulates the production of pre-miR-21 by inducing the formation of a complex comprising R-Smads, Pri-miR-21 and members of the microprocessor complex such as Drosha and p68. Reproduced from (Davis and Hata 2009).

5.2 Results

5.2.1 Expression and Regulation of miR-21 in WT Hypoxic Mice

In Chapter 3 we reported that miR-21 is not dysregulated in WT male rats exposed to chronic hypoxia (Caruso, MacLean et al. 2010). However, considering the gender specific up-regulation of miR-145 observed in response to hypoxia (proper of female mice only) in the mouse study described in Chapter 4, we decided to analyze miR-21 expression level in male and female WT mice exposed to chronic hypoxia for 14 days. The decision to investigate more in detail the expression pattern of this miRNA in the hypoxic mouse model of PAH was also due to the significant down-regulation of miR-21 observed in rats injected with monocrotaline and also in human PAFs exposed to chronic hypoxia for 24 h, described in Chapter 3 (Sections 3.2.2 and 3.2.4) (Caruso, MacLean et al. 2010). As observed for miR-143 and miR-145 (Chapter 4, Section 4.2.1), our analysis showed a significant up-regulation of miR-21 in response to 14 days of chronic hypoxia in female, but not male mice (Figure 4-4). For the purpose of subsequent experiments, we therefore focused on female mice.

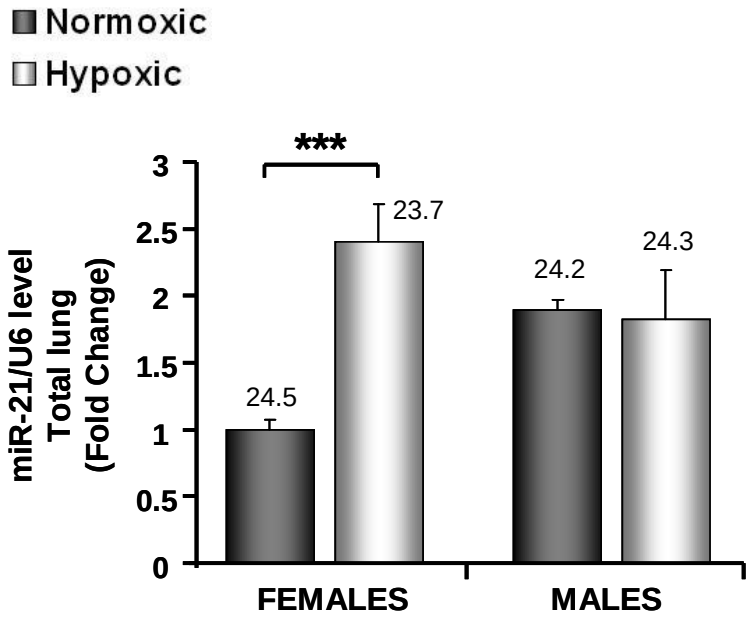

Figure 5-3 miR-21 expression in female and male WT mice exposed to chronic hypoxic for 14 days. Total RNA was extracted from the lung of normoxic (dark grey bars) and hypoxic (light grey bars) female and male mice at the age of 10 weeks. Samples were tested in triplicate. Results were normalized to U6 values and expressed as relative fold change, with an arbitrary value of 1 assigned to the female normoxic group. Raw Ct values for the target miRNA are indicated above each column. Data are expressed as mean ± SEM and analysed by one way ANOVA followed by Bonferroni's post-hoc test. ***P<0.001 compared to female normoxic mice. N = 3/group.

5.2.2 Quantification of the Development of PAH miR-21 -/- Mice in Comparison with Controls

Based on the up-regulation of miR-21 in hypoxic female mice, we next evaluated the effect of miR-21 genetic ablation on the development of PAH. 8 weeks old miR-21 -/- mice and control age-matched mice were exposed to chronic hypoxia or maintained in normoxic conditions for 14 days and analyzed for the development of PAH using a series of *in vivo* measurements. As already reported from Patrick et al. (Patrick, Montgomery et al. 2010), homozygous miR-21 KO mice were viable at birth and did not display any obvious disorder in normal conditions, indicating that this miRNA is not crucial for development. The absence of miR-21 expression in the KO animals used in the study was confirmed by TaqMan® Real-Time PCR in the total lung, PA, right ventricle (RV) and left ventricle plus septum (LV + S) (Figure 5-4A and B and Figure 5-5A and B). In agreement with our previous experiment, WT female mice exposed to chronic hypoxia showed a significant increase in miR-21 expression in the total lung in comparison with normoxic animals (Figure 5-4A). To understand more in detail miR-21 regulation in WT mice in response to hypoxia we also analyzed miR-21 expression in PA, RV and LV + S. miR-21 resulted more up-regulated in the PA than in the total lung (Figure 5-4A and B), and also significantly dysregulated in the RV but not in the LV + S, suggesting that alterations in the expression level of this miRNA could be proper only of the ventricle affected by hypertrophy in PAH (Figure 5-5A and B).

We next quantified the development of PAH in WT and miR-21 -/- mice. No changes in HR or mean SAP were reported between normoxic/hypoxic or WO/KO mice (Figure 4-9A and B and Table 5-1). As expected, we observed a significant increase in sRVP and RVH in WT normoxic mice in comparison with hypoxic (Figure 4-10A and B, Table 5-1 and Table 5-2). However, miR-21 KO mice exposed to hypoxia presented a worsen sRVP in comparison with WT mice (Figure 4-10A and Table 5-1). No differences in baseline sRVP between WT and miR-145 -/- in normoxia were identified but a significant increase was mrasured in hypoxia (Figure 4-10A and Table 5-1). RVH increased at the same level in WT and KO mice in response to hypoxia but a significant increase was identified in hypoxic WT versus hypoxic KO animals (Figure 4-10B and Table 5-2). Histological analysis showed the presence of pulmonary vascular remodelling in small PAs of WT animals following exposure to hypoxia and this was

worsen in lungs harvested from miR-21 KO animals, a finding confirmed by quantitative scoring (Figure 4-11A and B). Also, we observed a significant increase of pulmonary vascular remodelling in normoxic WT versus normoxic KO animals and in hypoxic WT versus hypoxic KO mice, suggesting that the genetic depletion of miR-21 can induce vascular remodelling also in normoxic conditions (Figure 4-11). Therefore, genetic ablation of miR-21 induced in mice more severe haemodynamic measurements.

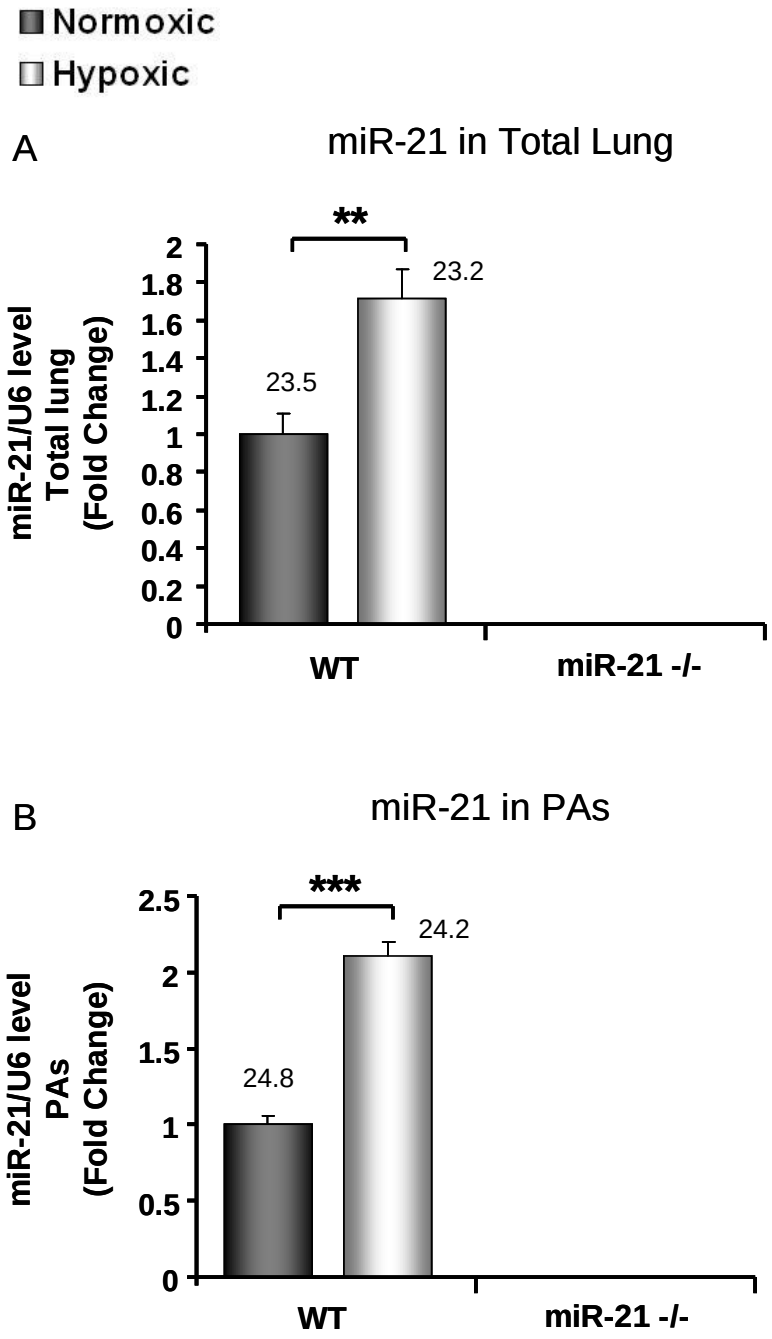

Figure 5-4 Analysis of miR-21 expression in total lung and PA isolated from miR-21 -/- female mice or WT female mice. miR-21 expression was assessed in the total lung (A) and the PA (B) of WT and KO 10 weeks old female mice, normoxic or exposed to chronic hypoxia for 14 days. Samples were tested in triplicate. Analysis of KO samples confirmed miR-21 genetic ablation in the tissues. Results were normalized to U6 values and expressed as relative fold change, with an arbitrary value of 1 assigned to the WT normoxic group. Raw Ct values for the target miRNA are indicated above each column. Data are expressed as mean ± SEM and analysed by two way ANOVA followed by Bonferroni's post-hoc test. ***P<0.001 compared to normoxic mice. N = 6/group.

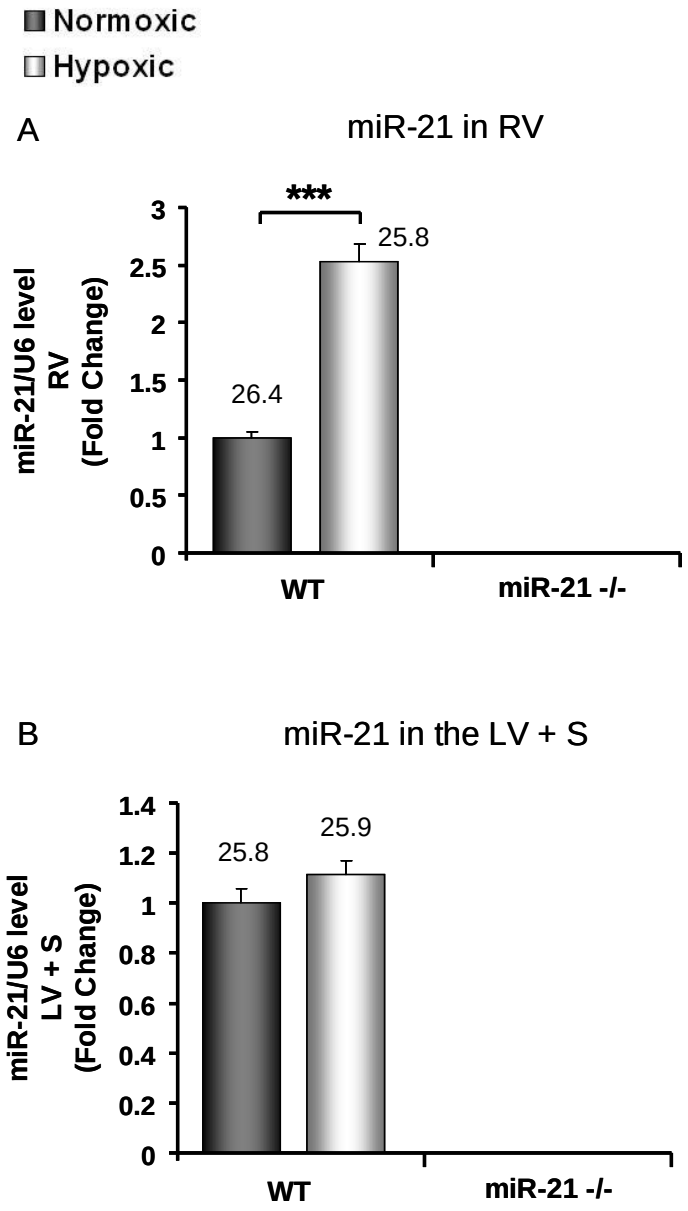

Figure 5-5 Analysis of miR-21 expression in the RV and the LV + S isolated from miR-21 -/- female mice or WT female mice. miR-21 expression was assessed in the RV (A) and the LV + S (B) of WT and KO 10 weeks old female mice, normoxic or exposed to chronic hypoxia for 14 days. Samples were tested in triplicate. Analysis of KO samples confirmed miR-21 genetic ablation in the tissues. Results were normalized to U6 values and expressed as relative fold change, with an arbitrary value of 1 assigned to the WT normoxic group. Raw Ct values for the target miRNA are indicated above each column. Data are expressed as mean ± SEM and analysed by two way ANOVA followed by Bonferroni's post-hoc test. ***P<0.001 compared to normoxic mice. N = 6/group.

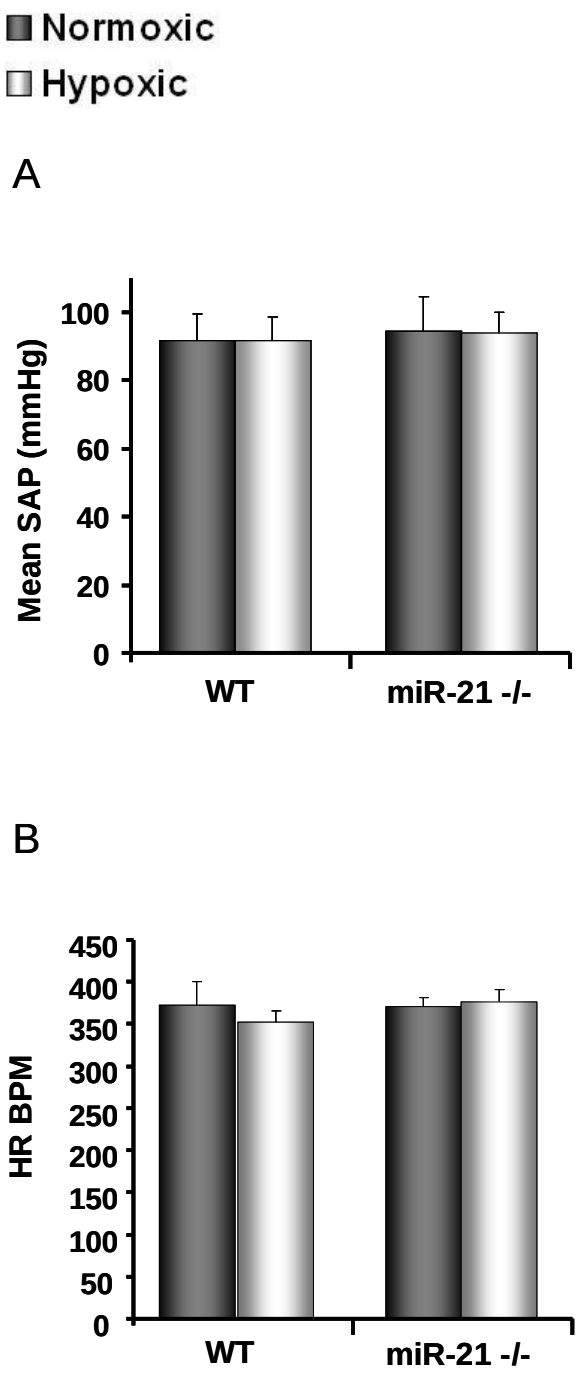

Figure 5-6 Assessment of systemic arterial pressure (SAP, A, n = 6–9) and heart rate (HR, B, n=8-10) in WT and miR-21 -/- mice, normoxic and hypoxic. 10 weeks old female mice, normoxic (dark grey bars) and hypoxic (light grey bars) were assessed. Data were analyzed using a two-way ANOVA followed by Bonferroni's post-hoc test, but no significant differences were observed.

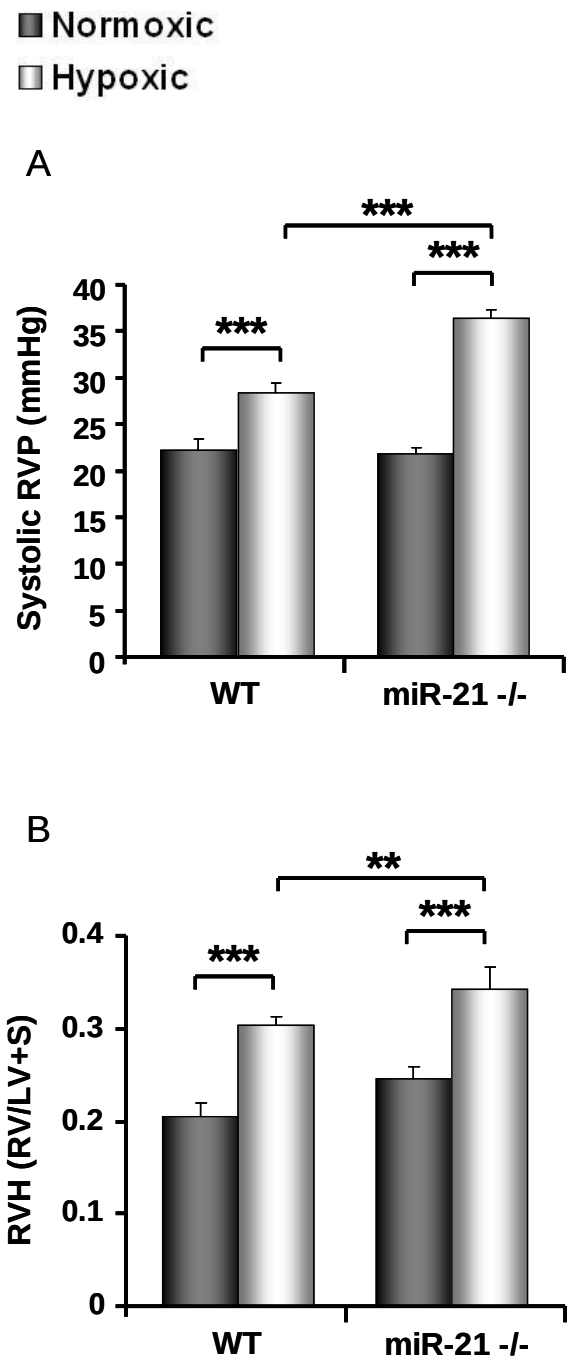

Figure 5-7 Effect of miR-21 genetic ablation on PAH development in mice. Assessment of sRVP (A, n = 9–12) and RVH (B, n = 9–10) in 10 weeks old female WT and miR-145 -/- mice, normoxic (dark grey bars) or exposed to chronic hypoxia for 14 days (light grey bars). Data were analyzed using a two-way ANOVA followed by Bonferroni's post-hoc test. *P<0.05, **P<0.01, ***P<0.001 compared to normoxic mice or WT hypoxic mice as indicated.

Parameter	WT Normoxic	WT hypoxic	KO Normoxic	KO Hypoxic
sRVP, mmHg	22.21± 1.18	28.41 ± 1.07***	21.75 ± 0.78	36.36 ± 0.10†††§§§
SAP, mmHg	91.80 ± 7.68	91.70 ± 6.68	94.24 ± 10.18	93.84 ± 5.80
Heart rate, bpm	371.78 ± 28.72	352.45 ± 13.10	370.3 ± 11.06	375.85 ± 14.96

Table 5-1 Haemodynamics in WT and miR-21 -/- mice, normoxic and hypoxic. Systolic right ventricular pressure (sRVP), systemic systolic arterial pressure (SAP) and heart rate measurements in normoxic and chronically hypoxic female WT and miR-21 -/- mice. ***P<0.001 compared to WT normoxic mice; §§§P<0.001 compared to miR-21 -/- mice; †††P<0.001 compared to WT hypoxic mice; Data expressed as mean + SEM. n=6-10.

Group	RV (mg)	LV+S (mg)	RV/LV+S
WT Normoxic	19.27± 1.41	94.26 ± 4.08	0.20 ± 0.013
WT Hypoxic	33.62 ± 1.82	113.31 ± 6.23	0.30 ± 0.010***
miR-21 -/- Normoxic	21.15 ± 0.88	85.81 ± 2.44	0.25 ± 0.010
miR-21 -/- Hypoxic	35.92 ± 0.85	115.96 ± 8.46	0.34 ± 0.025††§§§

Table 5-2 Ventricle weight in WT and miR-21 -/- mice. Right ventricle (RV) weight, left ventricle plus septum (LV+S) weight and RV/LV+S ratio. ***P<0.001 compared to WT normoxic mice; §§§P<0.001 compared to miR-21 -/- mice; ††P<0.005 compared to WT hypoxic mice; Data expressed as mean + SEM. n=9-10.

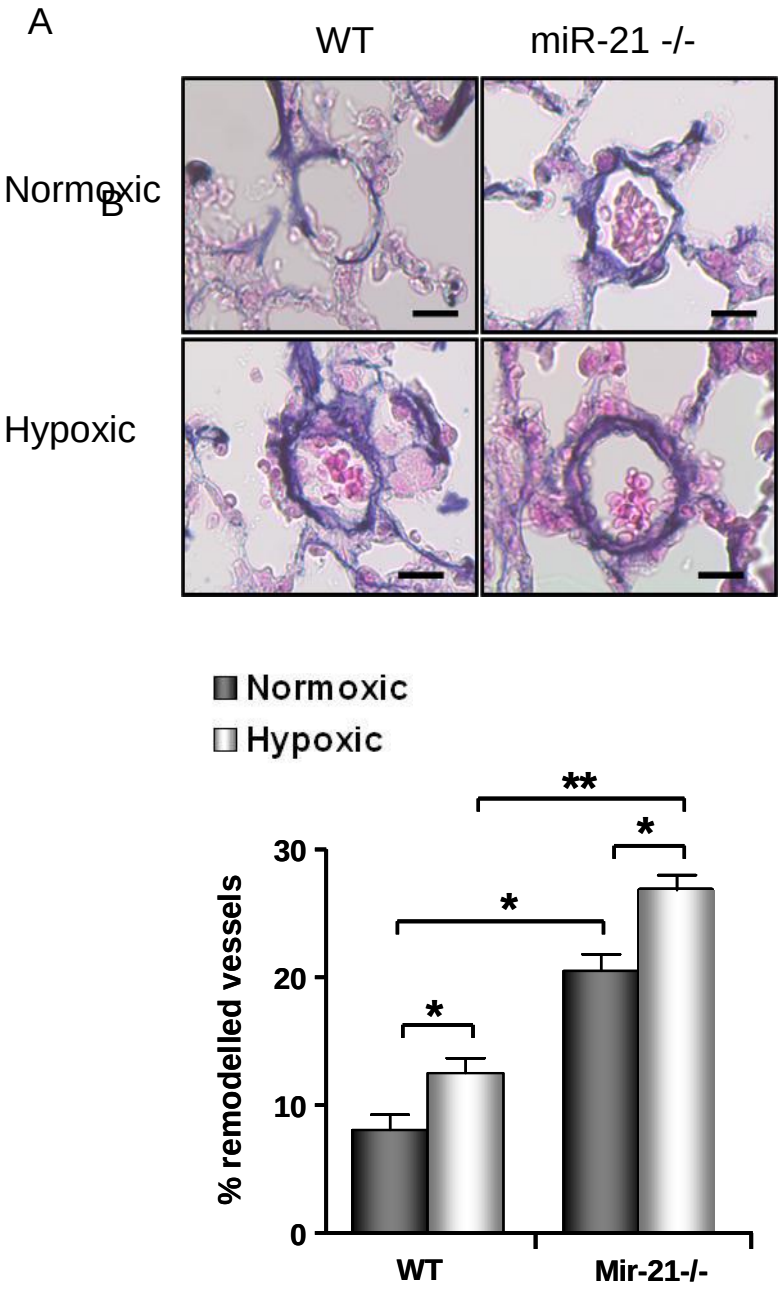

Figure 5-8 Effect of miR-21 genetic ablation on vessel remodelling in mice. (A) Representative PAs stained with elastic-Van Gieson. Images all x40 magnification, scale bars = 20 μm. (B) Pulmonary arterial remodeling from normoxic and hypoxic WT and miR-21 -/- female mice (n = 5/group). Mice were subjected to chronic hypoxia for 14 days and analyzed at 10 weeks of age. . Lung sections (5 sections/group) were stained with Elastin-Van Gieson and microscopically assessed in a blanded fashion. Pulmonary arteries (≤ 80 microns external diameter) were considered muscolarized if they possessed a distinct double elastic lamina for at least half the diameter of the vessel cross section. Approximately 150 arteries from each sagittal lung section were assessed. Data were analyzed using a two-way ANOVA followed by Bonferroni's post-hoc test. *p<0.05, **P<0.01 compared to normoxic mice or WT hypoxic mice as indicated.

5.2.3 MiR-21 in Human PAH

In consideration of the down-regulation of miR-21 observed in human PAFs exposed to hypoxia for 24 h, we next evaluated whether miR-21 is dysregulated in patients with PAH and examined its expression level in the lung of patients with IPAH and HPAH in comparison with control lung tissue. We first extracted miRNA from paraffin-embedded lungs. Compared to controls, miR-21 was significantly down-regulated in both HPAH and IPAH samples (Figure 5-9). After that, we cultured primary human PASMCs obtained from HPAH patients and quantified the expression of our miRNA of interest at the pri-, pre- and mature miRNA level (Figure 5-10A, B and C). It is interesting to notice that the pri- form of miR-21 was up-regulated in *BMPR2* mutated cells in comparison with WT (Figure 5-10A), the pre-form was not deregulated (Figure 5-10B) whereas the mature form resulted significantly down-regulated (Figure 5-10C), suggesting that two different mechanisms of miRNA dysregulation could act at the same time, at transcriptional and post-transcriptional level.

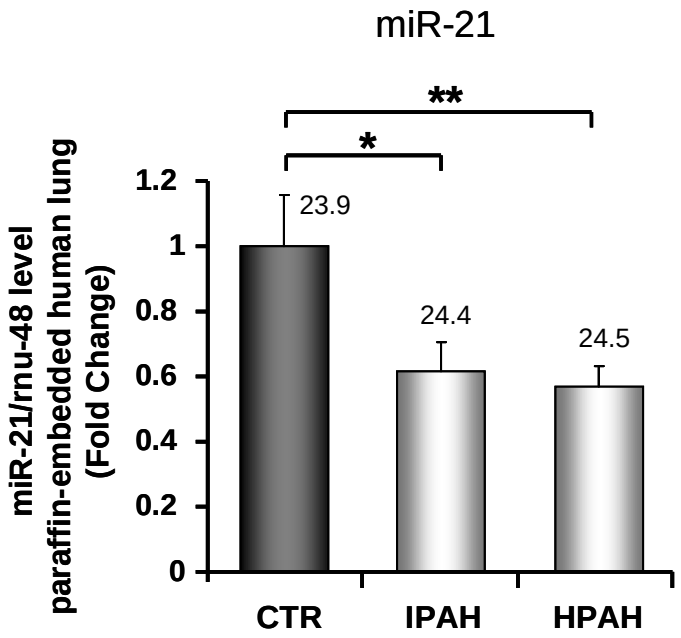

Figure 5-9 Assessment of miR-21 expression level in IPAH and HPAH human lung. TaqMan® Real-Time PCR analysis of RNA extracted from paraffin-embedded human lungs of IPAH (n = 6), HPAH (n = 5) and control patients (n = 6) showing the expression level of miR-21. All samples were normalized to Rnu-48 values and expressed as relative fold change, with an arbitrary value of 1 assigned to the control group. Raw Ct values for the target miRNA are indicated above each column. Data were analyzed using a one-way ANOVA followed by Bonferroni's post-hoc test. *$p<0.05$, **$p<0.005$ compared to CTR group.

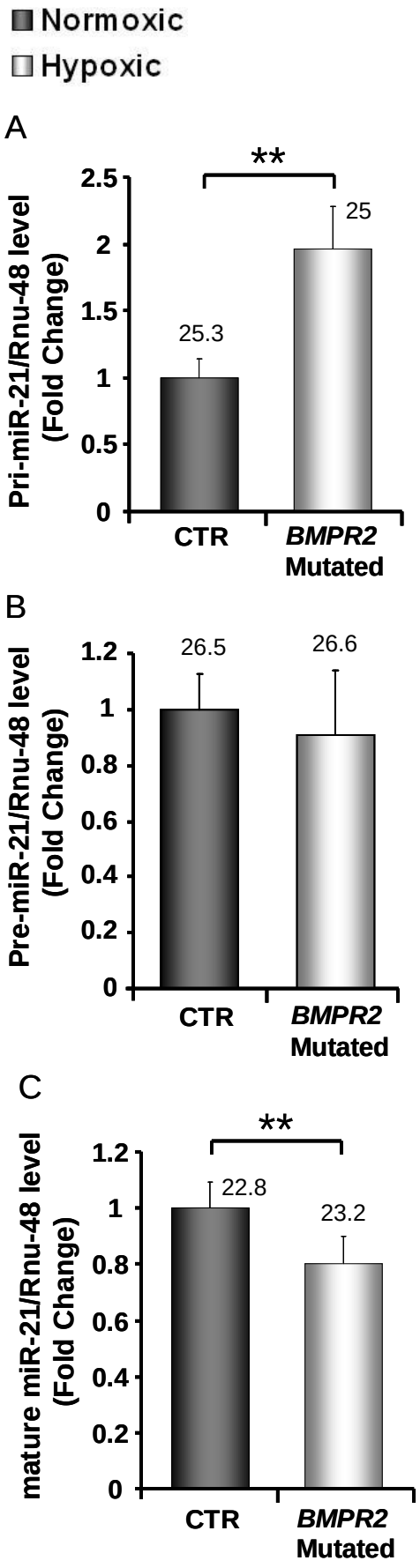
Normoxic
Hypoxic
A
**
Pri-miR-21/Rnu-48 level (Fold Change)
2.5
2
1.5
1
0.5
0
25.3
25
CTR
BMPR2 Mutated
B
Pre-miR-21/Rnu-48 level (Fold Change)
1.2
1
0.8
0.6
0.4
0.2
0
26.5
26.6
CTR
BMPR2 Mutated
C
**
mature miR-21/Rnu-48 level (Fold Change)
1.2
1
0.8
0.6
0.4
0.2
0
22.8
23.2
CTR
BMPR2 Mutated

Figure 5-10 Analysis of miR-21 expression level in human *BMPR2* mutated PASMCs. (A, B) TaqMan® Real-Time PCR analysis of miR-21 expression in human PASMCs. Total RNA was extracted from PASMCs of HPAH patients with a mutation in the *BMPR2* gene. Passage 4 primary cells were used. cDNA was analyzed for pri- pre- and mature-miR-21 expression in comparison with unaffected controls. Results were normalized to GAPDH for the pre- and Rnu-48 for the mature-miR-145 and expressed as relative fold change, with an arbitrary value of 1 assigned to the control group. Raw Ct values for the target miRNA are indicated above each column. Data were analyzed using an unpaired t-test. **p<0.005 compared to control samples.

5.2.4 miR-21 Expression in BMPR2 R899X mice

Considering the dysregulation observed in miR-21 expression level in human PASMCs isolated from HPAH patients harbouring a mutation in the *BMPR2* gene, we evaluated the effect of a truncating *BMPR2* mutation on miR-21 expression in heterozygous R899X +/- mice. RNA was extracted from the whole lung of 6 month old mice and analyzed by TaqMan® Reat-Time PCR. However miR-21 did not change, suggesting that a deregulation of miR-21 in response to an impaired BMPs signaling could be proper of human samples or PASMCs specific, and therefore difficult to detect in the whole lung (Figure 5-11).

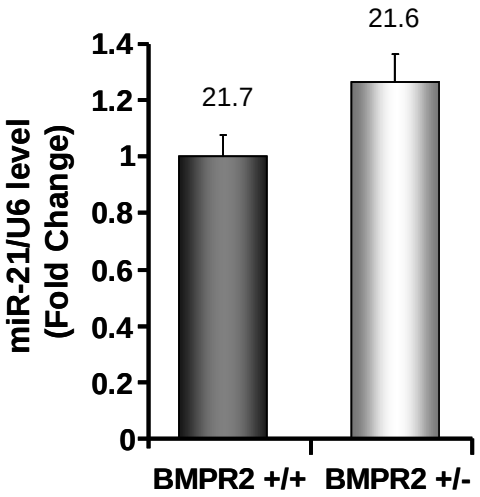

Figure 5-11 miR-21 expression in WT and *BMPR2* R899X mice. RNA was extracted from the total lung of WT mice and animals heterozygous for a mutation in the *BMPR2* gene, and assessed for miR-21 expression by TaqMan® Real-Time PCR. Values were normalized to U6 expression and data were analyzed using an unpaired t-test. Raw Ct values for the target miRNA are indicated above each column. No statistically significant differences were observed between the groups.

5.2.5 Effect of BMPR2 Down-Regulation on miR-21 Expression in Human PASMCs

Davis et al. recently demonstrated that BMP4 can induce the expression of miR-21. This stimulation occurs at a post-transcriptional level since ligand-specific SMAD proteins can interact with the DROSHA microprocessor subunit p68 to induce pre-miRNA accumulation (Section 5.1) (Davis, Hilyard et al. 2008). Here we reported the down-regulation of miR-21 miRNAs in human PASMCs harboring a mutation in the *BMPR2* gene, a systems characterized by an impairment of the BMP signaling (Section 5.2.3). However, no changes where observed in mice with a truncating mutation in the same gene (Section 5.2.4). To have a confirmation of our results in human samples, we next evaluated the effect of a siRNA-mediated knock-down of *BMPR2* on miR-21 expression level in human WT PASMCs *in vitro*. As previously reported in Chapter 4 (Section 4.2.7), cells were transfected with a si-RNA able to target and down-regulate specifically *BMPR2*, or with a siScramble as negative control. RNA was extracted from these samples and from untreated cells after 72 h for comparison. The efficacy of the down-regulation of *BMPR2* was assessed through TaqMan® Real-Time PCR analysis (Figure 5-12A). In agreement with our previous findings, the down-regulation of *BMPR2* induced the significant down-regulation of miR-21, whereas no changes were observed in untreated or siScramble-treated cells (Figure 5-12B).

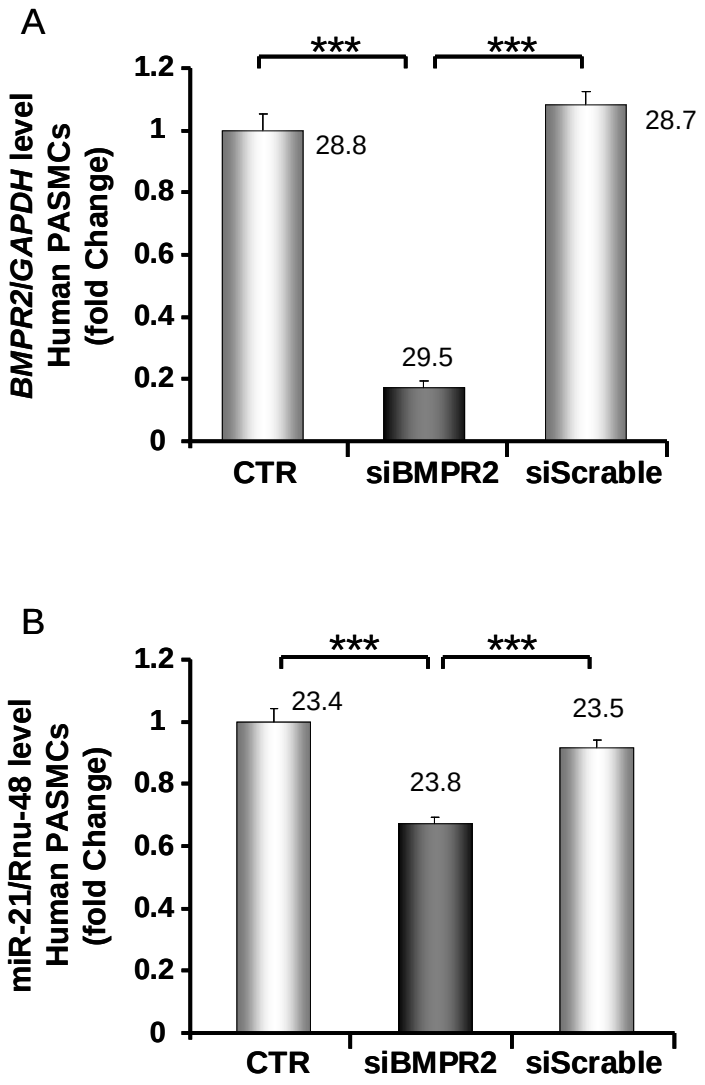

Figure 5-12 miR-21 down-regulation in human PASMCs down-regulated for *BMPR2* expression via a siRNA. Primary human PASMCs were transfected with a siRNA able to target and repress specifically *BMPR2* expression or with a siScramble as a negative control. Total RNA was extracted after 72 h from these samples and untreated cells for comparison. The efficiency of *BMPR2* down-regulation was evaluated by TaqMan® Real-Time PCR (A). miR-21 (B) expression was also assessed in the same samples. Results were normalized to GAPDH for *BMPR2* and Rnu-48 for miR-21 and expressed as relative fold change, with an arbitrary value of 1 assigned to the control group. Raw Ct values for the target miRNA and gene are indicated above each column. Data were analyzed using a one-way ANOVA followed by Bonferroni's post-hoc test. **p<0.005, ***p<0.001 compared to CTR or si-Scramble group as indicated.

5.3 Discussion

In this chapter we assess the expression and regulation of miR-21 in the cardiovascular system in response to hypoxic injury and also in pathological samples. In the hypoxic mouse model we show elevation of miR-21 expression level in total lung of female (but not male) animals compared to controls. This miRNA was also significantly over-expressed in PAs and in the right ventricle, with no changes observed in the left ventricle. The expression of miR-21 in other organs still needs to be evaluated in order to understand if this deregulation is specific of the cardiovascular system.

We also evaluated the role of miR-21 in the development of PAH. Recently, different studies reported the involvement of this miRNA in cardiac hypertrophy and heart failure, showing the up-regulation of miR-21 in hypertrophic animal hearts (van Rooij, Sutherland et al. 2006; Cheng, Ji et al. 2007; Sayed, Hong et al. 2007). Also, Ji et al. reported in rats a substantial increase of the expression level of this miRNA in balloon-injured arteries compared with normal control vessels, then showing an inhibition in neointima lesion formation in response to a miR-21 knock-down (Ji, Cheng et al. 2007). These observations led us to hypothesize an involvement of miR-21 also In the development of PAH, characterized by cell proliferation, neointima formation and RVH (Chapter 1, Section 1.2.2). We therefore decided to evaluate the effect of the genetic ablation of this miRNA in mice exposed to chronic hypoxia. Previous studies conducted on miR-21-depleted mice have given controversial results. In fact, whereas Thum et al. reported that the antagomiR-mediated depletion of miR-21 prevents cardiac hypertrophy and fibrosis in response to pressure overload induced by TAC, Patrick et al. could not confirm this result in mice pharmacologically or genetically depleted for miR-21 expression (Thum, Gross et al. 2008; Patrick, Montgomery et al. 2010). Two very recent studies have been conducted so far to analyze the effect of such a depletion on the lung and the pulmonary vasculature. In agreement with our data, Pullamsetti et al. and Yang et al. reported a significant increase of miR-21 expression in mice exposed to chronic hypoxia and then analyzed the effect of an antagomiR-mediated down-regulation of miR-21 on hypoxia-induced PAH (Pullamsetti, Doebele et al. 2011; Yang, Banerjee et al. 2012). In particular, Pullamsetti et al. observed that this treatment was able to significantly lower the hypoxia-induced increase in sRVP in

comparison with placebo-treated mice, whereas no changes were reported on RVH and percentage of remodelled vessels (Pullamsetti, Doebele et al. 2011). Yang et al. on the contrary reported the significant reduction of RVH and percentage of remodelled vessels in antimiR-treated mice (Yang, Banerjee et al. 2012). These observations completely disagree with our findings. In fact, here we show that a functional analysis of the vasculature of miR-21 -/- mice revealed a worsened response to hypoxia: when these mice were exposed to hypoxia for two weeks, both sRVP and RVH resulted drastically increased in comparison with WT animals exposed to the same conditions. Also, the percentage of remodeled vessels was significantly increased in the KO animals, strongly suggesting a negative effect of miR-21 genetic ablation on PAH development. A more exhaustive analysis of miR-21 expression in the cardiovascular system revealed a significant up-regulation of this miRNA also in the PAs of female WT hypoxic mice. Interestingly, in these mice miR-21 was significantly up-regulated in the right ventricle but not in the left ventricle plus septum, suggesting a hypothetical direct involvement of this miRNA in the RVH reported. However, the mechanism responsible for the worsen phenotype observed in KO mice in response to hypoxia still need to be identified and also the differences observed between Pullamsetti et al. and Yang et al. studies (Pullamsetti, Doebele et al. 2011; Yang, Banerjee et al. 2012) and our findings still need to be clarified. These will require more extensive studies, although some hypotheses can be formulated about this second point. First of all, it is important to note that embryonic KO and post-natal knock-down can have very different consequences considering that in the second case the development of the treated animal is not influenced by the manipulation of the expression of the genomic sequence of interest. Moreover, pharmacological ablation results in the down-regulation of the target sequence, with a basal expression still detectable. Finally, no mention of the gender of the mice used for the experiments can be found in both the Pullamsetti et al. and the Yang et al. studies (Pullamsetti, Doebele et al. 2011; Yang, Banerjee et al. 2012). Considering the differential regulation of miR-21 in response to hypoxia observed in female and male mice (Section 5.2.1), this information could be important to understand their results.

It is important to mention that our *in vivo* study still needs to be completed, since no targets have been analyzed so far. The analysis of predicted/validated targets expression in lung, PA, RV and LV will give important information on the pathways

involved in the process. Regarding this, it is interesting to note that very recently new targets of miR-21 in the vasculature have been identified in several members of the DOCK (dedicator of cytokinesis) family (Kang, Davis-Dusenbery et al. 2011), previously involved in the regulation of cell motility and cytoskeletal assembly in particular in the nervous system (Miyamoto and Yamauchi 2010). This study demonstrate that miR-21 mediated down-regulation of DOCKs is critical for the promotion of the contractile phenotype induced by BMP4 stimulation (Kang, Davis-Dusenbery et al. 2011). It will be therefore interesting to evaluate DOCKs expression in response to hypoxia and in miR-21 -/- mice. Also, since unlike miR-143 and miR-145, miR-21 is universally expressed in mammal organs and cell types, *in situ* localization of this miRNA in the vasculature of normoxic and hypoxic mice will give important information about the specific cell types involved in miR-21 deregulation.

In this chapter we also analyze miR-21 expression in human pathological samples. In particular, we demonstrate significant down-regulation of miR-21 in HPAH and IPAH patients and also in *BMPR2* mutated PASMCs extracted from HPAH patients. As previously mentioned, and in agreement with our observations, the TGF-*beta* super-family has been already involved in the maturation process of specific miRNAs (including miR-21), through the interaction of SMADs with Drosha complex during the second step of miRNA biogenesis (Davis, Hilyard et al. 2008) (Chapter 1, Section 1.3.3.4). Our observations of a down-regulation of miR-21 in *BMPR2*-mutated human cells was also confirmed *in vitro*, since a similar dysregulation of this miRNA was induced in human PASMCs by the down-regulation of *BMPR2* expression, obtained via a siRNA able to inhibit specifically the expression of this non-coding gene. However no changes in miR-21 expression were observed in mice carrying a mutation in this gene. It is important to mention that a recent study also reported a significant reduction in miR-21 expression in human PAECs down-regulated for *BMPR2* expression, although no significant changes were observed in human PASMCs (Drake, Zygmunt et al. 2011). Further studies will be necessary to understand if the differences in miR-21 regulation observed in the two species can be correlated with the differences in PAH observed between the mouse model and the human pathology. For example, the exposure of mouse vascular cells to hypoxia could be important to confirm the up-regulation observed *in vivo* in these conditions. It is important to remember that in chapter 3 we reported the down-regulation of miR-21 in human PAFs exposed to chronic hypoxia for

24 h, confirming the dysregulation of this miRNA observed in human pathological samples in this chapter, whereas no changes were observed in PAECs. The analysis of PASMCs will complete that study. Moreover, the stimulation of both mouse and human cells with different members of the TGF-*beta* super-family will consent the identification of differential responses. Also, it is important to note that the analysis of *BMPR2* mutated human PASMCs revealed the significant down-regulation of the mature miR-21, whereas the pri- form was up-regulated. Since the pri- is the first precursor of a miRNA, directly transcribed from the DNA, this finding could suggest the presence, in human samples, of two different types of regulation: one transcriptional, resulting in the accumulation of the first precursor, and one post-transciptional, leading to the down-regulation of the mature miRNA. If the post-transcriptional regulation could be identified in the already reported effect of BMPs on miR-21 expression (with a reduced amount of mature miRNA in case of an impairment of the BMP signaling due to *BMPR2* mutations), the transcriptional regulator of miR-21 in this system still need to be identified. Mouse models of PAH could present different types of regulations, or it could be hypothesized that the transcriptional regulation could be predominant in mouse model. An exhaustive analysis of pri- and pre-miR-21 in the hypoxic mouse model will be fundamental to clarify this aspect. Also, as already mentioned, in Section 5.2.1 we show that miR-21 up-regulation in response to hypoxia can be observed only in female mice with no effects of this treatment on males. Moreover, hypoxic male rats exposed to chronic hypoxia did not present any dysregulation in miR-21 expression, as reported in Chapter 3 (Section 3.2.2). The identification of the differences in miRNA and target expression between female and male mice, WT and miR-21 -/-, in response to hypoxia will give us many answers about the role played by gender in miR-21 deregulation in PAH. Also, it will be interesting to evaluate the effect of the genetic depletion of miR-21 on older mice, normally characterized by a more severe phenotype. In fact, as already reported for other animal models of PAH (MacLean, Deuchar et al. 2004), 5-6 months old mice could develop spontaneously the pathology or show a dramatic increase of sRVP and RVH in response to chronic hypoxia. Concerning the results obtained from the analysis of human samples, a detailed analysis of miR-21 expression also in PAECs and PAFs isolated from PAH patients, with or without mutations in the *BMPR2* gene, will let us understand if the dysregulation observed in the total lung is specific of PASMCs or proper of all the cell types implicated in PAH. All these studies will be necessary to

further evaluate the role of miR-21 in the development of this pathology and understand the differences observed between the mouse model and human samples.

Nevertheless, our preliminary observations about miR-21 dysregulation in PAH confirm a role for this miRNA in the development of this pathology, suggesting the possibility of a novel therapeutic approach in the future. Also, the identification of a specific miRNA expression profile could be used as a new efficient way to obtain an early diagnosis with substantial benefits for patients.

6. General Discussion

Pulmonary arterial hypertension (PAH) is a complex, multifactorial pathology, rare but severe. It is characterized by high pulmonary artery pressure, vascular remodelling and right ventricular hypertrophy, and if untreated it culminates in right heart failure within 3 years (Eddahibi, Morrell et al. 2002; Jeffery and Morrell 2002). The etiology of PAH is not entirely understood, but a genetic component is known to contribute. Members of the TGF-*beta* super-family are major candidates since mutations in the gene encoding for a BMPs receptor (*BMPR2*) have been identified in 80% of families characterized by affected members (Machado, Aldred et al. 2006), and also 15-40% of patients with IPAH are carriers of similar genetic abnormalities (Thomson, Machado et al. 2000). In particular, the expression of *BMPR2* is reduced in the pulmonary vasculature of HPAH patients carrying a mutation but also in IPAH patients in whom no mutation have been identified, suggesting a central role of *BMPR2* in the pathogenesis of this pathology also in non-carriers.

Also the serotonin system has been implicated in the pathobiology of PAH. In fact, several studies identified the serotonin transporter SERT as another genetic risk factor for the development of this pathology. In particular, an increased expression of the this gene has been observed in IPAH patients (Eddahibi, Humbert et al. 2001) and mice over-expressing SERT (SERT+) were reported to exhibit an enhanced RVP and vascular remodelling, and to develop an exaggerated PAH in response to hypoxia (MacLean, Deuchar et al. 2004).

A more exhaustive knowledge of the regulation of these genes will be important to increase our current understanding of PAH and possibly improve the prognosis of patients, since all the treatments available at the moment can only provide a symptomatic relief (Chapter 1). For this reason, in this project we decided to evaluate the role played by miRNAs in the development of PAH. MiRNAs are small non-coding RNAs able to negatively regulate gene expression by binding to the 3'UTR of their specific target mRNAs, thereby promoting their degradation or inhibiting their translation. Biogenesis, activity and contribution of miRNAs to the development of several pathologies were outlined in Chapter 1.

The first part of this study (Chapter 3), published in 2010, was the first to report the significant dysregulation of specific miRNAs in rat models with correlation in human pathological samples. Considering the complete lack of information about this topic at that time, we decided to evaluate globally miRNA expression in hypoxic and monocrotaline-injected rats as starting point. For this reason we performed a microarray based analysis of miRNA expression, assessing in total 350 different miRNAs at three different time points (2, 7 and 21 days) after the hypoxic/monocrotaline treatment. For the identification of the most dysregulated miRNAs, a basal microarray signal intensity of 500 arbitrary units (AU) was chosen, as recommended by LC Sciences, commissioned to perform the experiment. This choice has been taken considering the scanner's lower limit of detection and the efficiency of hybridization of the probes used, and it allowed us to consider only the most reliable data obtained. Of course it is important to take into account that specific miRNAs, expressed at low level but still relevant for the development of the pathology, could be excluded in this way from further analysis. This was the case of miR-204, poorly expressed in our samples and therefore excluded from our study but recently implicated in the development of PAH (Courboulin, Paulin et al. 2011). It is also possible that some miRNAs are expressed at a low level since specific of the vasculature, and therefore their concentration is diluted when assessed in the total lung. Aware of this, we decided to use these stringent criteria for a first screening in order to avoid experimental noise and select a manageable number of dysregulated miRNAs to be carried forward for further investigations. A lower cut-off value could be chosen in the future to re-analyze the data including a wider group of miRNAs. Using the threshold of 500 AU, we selected a group of seven miRNAs significantly altered in the hypoxic and/or the monocrotaline rat model (i.e. miR-21, miR-22, miR-30c, miR-451, miR-322, let-7a and let-7f) and their expression was validated by TaqMan® Real-Time PCR. The alteration of these miRNAs was also confirmed *in vitro* in rat PASMCs and PAFs exposed to chronic hypoxia, and a similar regulation was also observed in human cells. It is interesting to note that in agreement with the significant down-regulation of Dicer observed in the hypoxic models and at the latest time point of the monocrotaline model, the majority of miRNAs significantly dysregulated in the microarray was down-regulated, suggesting that the process of miRNA maturation is impaired in these models. It will be therefore important in the future to evaluate the effects on miRNA dysregulation of Dicer manipulation *in vivo*.

Considering that the hypoxic and the monocrotaline rat models are well established animal models for the study of PAH but they do not completely represent the human pathology as explained in Chapter 1, we considered fundamental to investigate also human pathological samples and cells. In particular we focused our attention on miR-451, up-regulated in a substantial way in both the models and especially in monocrotaline-treated rats, and miR-22, consistently down-regulated in all the rat pathological samples tested, *in vivo* and *in vitro*. The results obtained gave us the confirmation that miRNA regulation can be complex and not always conserved between different species. In fact, we could observe a dysregulation of miR-22 compatible with what observed in rats, whereas miR-451 did not show any alteration in human pathological samples. Despite this and in consideration of the remarkable up-regulation observed in rats, an in vivo study is currently in progress to evaluate the effects of the genetic and pharmacological ablation of this miRNA on the development of PAH. The analysis of the other miRNAs identified in the study in the same human samples will be important as next step of this study to have a clearer view of the similarities between the hypoxic and the monocrotaline rat model and the human disease. A careful evaluation of the differences could contribute to explain those differences identified in the pathogenesis of PAH between species and also between different models within the same species. The analysis of different animal models, more recently introduced for the study of PAH (e.g. the sugen 5416 rat model, Chapter 1, Section 1.2.3) could also confirm the dysregulation of defined miRNAs.

In Chapter 3 we also used bioinformatics prediction algorithms to identify predicted target mRNAs of our miRNAs of interest. Several databases are currently available for this purpose, based on the most updated knowledge of miRNA biology. However, it is important to remember that the very rapid development of this field dictates a continuous improvement in these algorithms. An evident consequence of this is represented by the exclusion of *BMPR2* from the list of targets validated in the rat model. In fact this enzyme, whose expression in altered in patients also in the absence of specific mutations, has been identified as a target of miR-21 (Qin, Zhao et al. 2009), but it was not reported in any databases when this study was conducted. TaqMan® Real-Time PCR analysis of *BMPR2* mRNA levels *in vivo* and *in vitro* will be important to evaluate if its expression correlates with miR-21 alteration, although Long et al.

already reported the significant down-regulation of *BMPR2* in monocrotaline-treated rats, characterized by a decreased expression of miR-21 (Long, Crosby et al. 2009). Therefore *BMPR2* regulation does not seem to correlate well with miR-21 expression level, at least in monocrotaline-injected rats. In Chapter 5 we reported how the down-regulation of *BMPR2* results in a decreased expression of this miRNA, suggesting that this receptor can influence miR-21 regulation through the interaction of SMADs with DROSHA complex during the second step of miRNA biogenesis, as previously reported (Davis, Hilyard et al. 2008). If miR-21 should be proved to be able to regulate *BMPR2* expression in turn, the presence of a regulatory loop could be suggested, but further experiments will be necessary to evaluate this hypothesis. First of all, it will be important to analyze in the siBMPR2 samples not only the mature form, but also the miR-21 precursors in order to identify the step of miRNA maturation affected by the BMP signaling. This is particularly important in consideration of what observed in BMPR2 mutated PASMCs isolated from PAH patients. In those samples, as showed in Chapter 5, we observed an up-regulation of pri-miR-21 and a down-regulation of the mature form, suggesting that both a transcriptional and a post-transcriptional regulation of this miRNA take place in patients. After that, the si-mediated down-regulation of specific members of the TGF-beta super-family, including receptors like Alk1 and Alk5, but also different Smads (Smad2-3 and Smad1-5-8) will let us identify the factors involved in the process.

However, it is important to note that only male rats have been analyzed in Chapter 3, and an *in vivo* study involving female animals will be fundamental in the future, taking account of the differences observed between female and male hypoxic mice in Chapter 4 and Chapter 5. Gender in relation with miRNA expression could be an interesting topic to evaluate in detail in animal models and PAH affected patients, considering that it has been well reported from different epidemiological studies how this pathology is more frequent in women, with an incidence of both IPAH and HPAH up to three-fold higher in female patients (Humbert, Sitbon et al. 2006; Peacock, Murphy et al. 2007; Thenappan, Shah et al. 2007). Moreover, well established experimental models of PAH could not provide insight into this phenomenon, and paradoxically several of them exhibit male susceptibility, making the situation controversial and difficult to interpret (Rabinovitch, Gamble et al. 1981; Miller, Hislop et al. 2005; Hansmann, Wagner et al. 2007; Said, Hamidi et al. 2007). Both in Chapter 4

and Chapter 5 we show how miRNA regulation, in the same conditions, can be different between female and male mice exposed to chronic hypoxia, and this could be useful to clarify this aspect of PAH biology. An extensive evaluation of female hypoxic/monocrotaline-treated rats and male hypoxic (WT or KO for specific miRNAs) mice will give us important information about this topic.

Relating to target analysis, no luciferase assays have been conducted so far to confirm the existence of a direct link between the dysregulation of a specific miRNA and the alteration of the expression of a gene, although both in Chapter 3 and Chapter 4 several targets evaluated by TaqMan® Real-Time PCR and western blot were dysregulated in a way compatible with miRNA expression. The alteration *in vitro* of a specific miRNA followed by the transfection of cells with a construct coding for a luciferase gene modified to carry at its 3'UTR seed sequences compatible with that miRNA will definitely prove that the dysregulation observed *in vivo* is due to the action of the miRNA itself. It is also important to consider that the computational approaches for miRNA target prediction via bioinformatics algorithms used in Chapter 3, based on the tendency of miRNAs to form complete base pairings to a target mRNA at miRNA nucleotides 2–8 (the seed region), do not consent to identify all those targets that do not conform to the seed theory, and have therefore evident limitations. For this reason, new methods have been developed in the last few years to improve targets identification. One of them was described in the Orom et al. study (Orom and Lund 2007) and used by Kang et al. to identify miR-21 targets within the DOCK family (Kang, Davis-Dusenbery et al. 2011). Briefly, this method is based on the use of synthetic miRNA duplexes carrying a biotin group attached to the 3'-end of the sense strand. These duplexes are then transfected into a cell type of interest, where the tagged miRNA sense strands incorporate into miRISC complexes and associate with endogenous target mRNAs. The miRNA–mRNA complexes are captured on streptavidin beads and analyzed (Orom and Lund 2007). This method could be used in the future to identify novel targets of our miRNAs of interest.

The study conducted in Chapter 3 proved us that miRNAs are significantly dysregulated in PAH and gave us important information about what happens in the lung in terms of coding and non-coding gene expression at different stages after the hypoxic and monocrotaline insult. However, it also let us understands the limitations of such a

study. In fact, although miRNAs normally work in families or groups to influence in a cooperative way the expression of a target, the simultaneous analysis of the effect of several miRNAs on gene expression can become extremely complex, expensive and time consuming, since each miRNA is normally reported to have several thousands of predicted target sequences. A microarray based mRNA study similar to that conducted in Chapter 3 for miRNA expression could be a solution, but it is important to consider the cost of such and assay and also the importance to validate the data obtained with a TaqMan® Real-Time PCR analysis of the selected genes, considering the high rate of false positive and false negative assigned to this kind of experiment. Moreover, the data obtained from such a global alteration of miRNA expression could be very difficult to interpret, especially if the field has been poorly studied. For this reason, in Chapter 4 and Chapter 5 we decided to focus our attention on miR-143/145 cluster and miR-21 respectively. A TaqMan® Real-Time PCR analysis of the expression of these miRNAs in the total lung of WT mice exposed to chronic hypoxia showed a selective up-regulation in females.

To evaluate the effect of the genetic ablation of miR-145 or miR-21 on PAH development, we exposed to chronic hypoxia mice deleted for these genes. In both cases the result was relevant. In fact, miR-145 genetic ablation resulted significantly protective against the development of this pathology, reducing sRVP, RVH and percentage of remodelled vessels. As reported before (Boettger, Beetz et al. 2009; Xin, Small et al. 2009), SAP was reduced in KO mice, normoxic or hypoxic, making the possibility to obtain lung specific ablation of miR-145 to reduce the systemic effects attractive. The effect of miR-145 ablation on the vasculature, and in particular on the muscular component, described in detail in Chapter 4, had already been evaluated in previous studies (Boettger, Beetz et al. 2009; Xin, Small et al. 2009), but our study is the first to examine specifically the implications of this genetic modification on PAH. Our group also evaluated the effect of pharmacological ablation of this miRNA using an antimiR (data not shown), obtaining a similar result. This is particularly relevant since pharmacological ablation could be used on patients as therapeutic approach. For this reason we decided to evaluate the expression of miR-143 and miR-143 also in pathological human samples, in order to understand if a similar regulation can be identified in mice models and patients. In Chapter 4 we report the significant up-regulation of miR-143 and miR-145 in the total lung of heritable and idiopathic PAH

affected patients, and also in PASMCs extracted from patients harboring a mutation in the *BMPR2* gene, therefore confirming in human samples a dysregulation similar to that observed in hypoxic WT mice. For this reason it is possible to hypothesize that a pharmacological inhibition of miR-145 could have a positive effect on the prognosis of patients, although an extensive sperimentation will be necessary to prove it. First of all, an *in vivo* study will be conducted to evaluate if the pharmacological ablation of miR-145 is also able to reverse PAH in mice already exposed to hypoxia. This type of study, called "rescue study" will clarify if such a treatment can only prevent the onset of PAH or also reverse it in animals (ans eventually patients) already affected.

A correlation between *BMPR2* and miR-143/145 expression have been also observed in further experiments. In fact, mice heterozygous for a truncating mutation in this gene showed a significant up-regulation of the cluster in normoxic conditions, and an *in vitro* down-regulation of *BMPR2*, performed on human PASMCs, had the same consequence. These results appear interesting but in contrast with the recent observation that members of the TGF-*beta* super-family can induce miR-143 and miR-145 expression (Davis-Dusenbery, Chan et al. 2011; Long and Miano 2011). If this mechanism would be fundamentally involved in the regulation of these miRNAs in our system, an impairment of the BMP signaling, induced by a *BMPR2* down-regulation, should result in their down-regulation instead. An explanation for this still need to be identified and will required more experiments focused on the role played by different members of the TGF-*beta* super-family in this system. For example could be hypothesized that in case of an impairment of the BMP signaling via BMPR2, a different type of regulation is activated in the cell to complement this function. Also, since not only BMP4 but also TGF-*beta* has been reported to up-regulate miR-143 and miR-145 (Davis-Dusenbery, Chan et al. 2011; Long and Miano 2011), it could be hypothesized that not the BMP impairment but the subsequent increase of the TGF-beta signaling observed in PAH could be responsible for this miRNA dysreguation. An in vitro manipulation of receptors (i.e. Alk5) or effectors (i.e. Smad2 and Smad3) of the TGF-beta signaling will be necessary to validate this theory.

Also, considering the attractive possibility to use in the future the pharmacological ablation of miR-145 as a therapy for PAH patients, the gender difference in miR-145 expression reported at the beginning of Chapter 4 will need to be further esamined. In

fact, we observed that 2 months old hypoxic female mice are characterized by miR-145 up-regulation, with no dysregulation observed in males. Since older mice develop a more severe PAH in response to hypoxia, it will be important to analyze miR-145 expression level also in 5-6 months old mice, both female and male, in order to understand if this differential expression can still be observed. Moreover, we have proved that the genetic (Chapter 4) and pharmacological (not shown) ablation of miR-145 is protective in female mice against the development of PAH, but a similar study will have to be conducted in males, ideally at 2 and 5-6 months of age, to prove is a similar effect occours. Finally, since a mixture of female and male patients have been currently analyzed for miR-145 expression, it will be important as further step to improve the number of patients assessed in order to have a separate analysis of female and male samples. This part in particular will be challenging, considering the low number of affected patients and available human samples.

Similarly to what we reported in Chapter 4, miR-21 genetic ablation showed a significant effect on PAH development, as reported in Chapter 5. In this case however, the lack of expression of this miRNA resulted in an exaggerated PAH in response to hypoxia, characterized by an increased sRVP, RVH and higher number of remodelled vessels. This study still need to be completed with the analysis of predicted targets, but the results obtained so far are in contrast with the observations reported very recently from two studies (Pullamsetti, Doebele et al. 2011; Yang, Banerjee et al. 2012). They both describe like the pharmacological ablation of miR-21 can induce a significant decrease in sRVP or RVH and percentage of remodeled vessels (in Pullamsetti et al. study and Yang et al. study respectively), with a protective effect against the development of PAH (Pullamsetti, Doebele et al. 2011; Yang, Banerjee et al. 2012). As mentioned in Chapter 5, these differences could be attributed to the use of an antagomiR sequence, different from a genetic ablation, but definitely need to be clarified in the future.

Since as mentioned before only 2 months old mice have been assessed in this study, but older mice normally develop a more severe form of PAH, it will be interesting to see the effects of miR-21 genetic ablation on 5-6 months older mice. As it has been observed for SERT mice, these animals could in fact develop PAH spontaneously, without any hypoxic insult. Moreover, also in this case the gender issue will have to be

further evaluated to see if also male mice KO for miR-21 develop a more severe form of PAH in response to hypoxia.

To make the situation more complex, the analysis of WT hypoxic mice, characterized by an over-expression of miR-21, at least in females, is in contrast with the results obtained from the assessment of human pathological samples, where a down-regulation of miR-21 was observed. These findings seem to suggest a differential regulation of miR-21 in different species, as already reported for miR-451 in Chapter 3. A more extensive analysis of mouse and human samples will be necessary to confirm this hypothesis, but if this should be confirmed miR-21 manipulation as therapeutic approach could become complex. However, it is important to remember that the hypoxic mouse model, well established and often used for the study of PAH, is an acute but not chronic model of the pathology, unlike human PAH, whereas we observed a miR-21 decreased expression in the chronic monocrotaline rat model. A genetic or pharmacologic ablation of this miRNA in this animal model could be important to determine the effect on PAH in a chronic system characterized by a regulation of miR-21 similar to that observed in human samples. Also, as mentioned before in this chapter, a comprehensive analysis of miR-145 precursors in mouse models and human samples will be fundamental in the future to evaluate if a transcriptional or post-transcriptional regulation of miR-21 can be observed and if this regulation is conserved across species or is different between mouse models and patients.

The data reported in this thesis support the hypothesis that the modulation of specific miRNAs could have important clinical applications. Such a possibility has been already tested in few recent studies. For example, after reporting the capacity of a chemically-synthesized inhibitor of miR-208 to suppress pathological cardiac remodelling in a model of heart failure induced by chronic high blood pressure (Montgomery, Hullinger et al. 2011), the preclinical-stage biopharmaceutical company Miragen™ Therapeutics has announced the intention to start in 2012, in collaboration with Servier, a research, development and commercialization programme for this drug candidate, with potential potent beneficial effects for patients suffering from heart failure. Moreover, the clinical-stage biopharmaceutical company Santaris Pharma A/S presented in November 2011 new data from a Phase 2a trial showing that a four-week

monotherapy treatment with miravirsen, a miRNA-targeted drug able to inhibit miR-122, provided robust dose-dependent and prolonged Hepatitis C virus (HCV) reduction in infected patients, that was maintained for more than four weeks beyond the end of therapy. These are only two representative examples of the potential of miRNA use in clinical applications.

In summary, the main observations of this thesis include the identification of a specific group of miRNAs dysregulated in different animal models of PAH but also in human pathological samples; the confirmation *in vitro* of those alterations observed *in vivo*; a comparison of miRNA regulation in different species, sometimes highly conserved but also different in specific cases; the evaluation *in vivo* of the effects of a genetic ablation of specific miRNAs on the development of PAH, never tested before.

In conclusion, I have demonstrated for the first time the direct involvement of a specific group of miRNAs in the development of PAH, presenting the possibility, in a more distant future, to introduce the use of a miRNA-based therapy for the treatment of this fatal pathology.

7. References

Aaronson, P. I., T. P. Robertson, et al. (2002). "Endothelium-derived mediators and hypoxic pulmonary vasoconstriction." Respir Physiol Neurobiol **132**(1): 107-120.

Abenhaim, L., Y. Moride, et al. (1996). "Appetite-suppressant drugs and the risk of primary pulmonary hypertension. International Primary Pulmonary Hypertension Study Group." N Engl J Med **335**(9): 609-616.

Adam, P. J., C. P. Regan, et al. (2000). "Positive- and negative-acting Kruppel-like transcription factors bind a transforming growth factor beta control element required for expression of the smooth muscle cell differentiation marker SM22alpha in vivo." J Biol Chem **275**(48): 37798-37806.

Ahmed, F., H. R. Ansari, et al. (2009). "Prediction of guide strand of microRNAs from its sequence and secondary structure." BMC Bioinformatics **10**: 105.

Albinsson, S., Y. Suarez, et al. (2010). "MicroRNAs are necessary for vascular smooth muscle growth, differentiation, and function." Arterioscler Thromb Vasc Biol **30**(6): 1118-1126.

Ambros, V. (2004). "The functions of animal microRNAs." Nature **431**(7006): 350-355.

Ambros, V., B. Bartel, et al. (2003). "A uniform system for microRNA annotation." RNA **9**(3): 277-279.

Ambs, S., R. L. Prueitt, et al. (2008). "Genomic profiling of microRNA and messenger RNA reveals deregulated microRNA expression in prostate cancer." Cancer Res **68**(15): 6162-6170.

Ameshima, S., H. Golpon, et al. (2003). "Peroxisome proliferator-activated receptor gamma (PPARgamma) expression is decreased in pulmonary hypertension and affects endothelial cell growth." Circ Res **92**(10): 1162-1169.

Aramburu, J., K. Drews-Elger, et al. (2006). "Regulation of the hypertonic stress response and other cellular functions by the Rel-like transcription factor NFAT5." Biochem Pharmacol **72**(11): 1597-1604.

Archer, S. L., X. C. Wu, et al. (2004). "Preferential expression and function of voltage-gated, O2-sensitive K+ channels in resistance pulmonary arteries explains regional heterogeneity in hypoxic pulmonary vasoconstriction: ionic diversity in smooth muscle cells." Circ Res **95**(3): 308-318.

Atkinson, C., S. Stewart, et al. (2002). "Primary pulmonary hypertension is associated with reduced pulmonary vascular expression of type II bone morphogenetic protein receptor." Circulation **105**(14): 1672-1678.

Baber, S. R., W. Deng, et al. (2007). "Intratracheal mesenchymal stem cell administration attenuates monocrotaline-induced pulmonary hypertension and endothelial dysfunction." Am J Physiol Heart Circ Physiol **292**(2): H1120-1128.

Badesch, D. B., S. H. Abman, et al. (2004). "Medical therapy for pulmonary arterial hypertension: ACCP evidence-based clinical practice guidelines." Chest **126**(1 Suppl): 35S-62S.

Badesch, D. B., S. H. Abman, et al. (2007). "Medical therapy for pulmonary arterial hypertension: updated ACCP evidence-based clinical practice guidelines." Chest **131**(6): 1917-1928.

Badesch, D. B., H. C. Champion, et al. (2009). "Diagnosis and assessment of pulmonary arterial hypertension." J Am Coll Cardiol **54**(1 Suppl): S55-66.

Badesch, D. B., J. Feldman, et al. (2011). "ARIES-3: Ambrisentan Therapy in a Diverse Population of Patients with Pulmonary Hypertension." Cardiovasc Ther.

Badesch, D. B., V. F. Tapson, et al. (2000). "Continuous intravenous epoprostenol for pulmonary hypertension due to the scleroderma spectrum of disease. A randomized, controlled trial." Ann Intern Med **132**(6): 425-434.

Baek, D., J. Villén, et al. (2008). "The impact of microRNAs on protein output." Nature **455**(7209): 64-71.

Bagga, S., J. Bracht, et al. (2005). "Regulation by let-7 and lin-4 miRNAs results in target mRNA degradation." Cell **122**(4): 553-563.

Bar, N. and R. Dikstein (2010). "miR-22 forms a regulatory loop in PTEN/AKT pathway and modulates signaling kinetics." PLoS One **5**(5): e10859.

Barnes, P. J. and S. F. Liu (1995). "Regulation of pulmonary vascular tone." Pharmacol Rev **47**(1): 87-131.

Barst, R. J., L. J. Rubin, et al. (1996). "A comparison of continuous intravenous epoprostenol (prostacyclin) with conventional therapy for primary pulmonary hypertension. The Primary Pulmonary Hypertension Study Group." N Engl J Med **334**(5): 296-302.

Bartel, D. P. (2004). "MicroRNAs: genomics, biogenesis, mechanism, and function." Cell **116**(2): 281-297.

Bartel, D. P. (2009). "MicroRNAs: target recognition and regulatory functions." Cell **136**(2): 215-233.

Beall, A. C. and T. H. Rosenquist (1990). "Smooth muscle cells of neural crest origin form the aorticopulmonary septum in the avian embryo." Anat Rec **226**(3): 360-366.

Behm-Ansmant, I., J. Rehwinkel, et al. (2006). "mRNA degradation by miRNAs and GW182 requires both CCR4:NOT deadenylase and DCP1:DCP2 decapping complexes." Genes Dev **20**(14): 1885-1898.

Berezikov, E., W. J. Chung, et al. (2007). "Mammalian mirtron genes." Mol Cell **28**(2): 328-336.

Beringer, M. and M. V. Rodnina (2007). "The ribosomal peptidyl transferase." Mol Cell **26**(3): 311-321.

Bernstein, E., S. Y. Kim, et al. (2003). "Dicer is essential for mouse development." Nat Genet **35**(3): 215-217.

Bhatia, S., R. P. Frantz, et al. (2003). "Immediate and long-term hemodynamic and clinical effects of sildenafil in patients with pulmonary arterial hypertension receiving vasodilator therapy." Mayo Clin Proc **78**(10): 1207-1213.

Bhattacharyya, S. N., R. Habermacher, et al. (2006). "Relief of microRNA-mediated translational repression in human cells subjected to stress." Cell **125**(6): 1111-1124.

Black, S. M., E. Mata-Greenwood, et al. (2003). "Emergence of smooth muscle cell endothelin B-mediated vasoconstriction in lambs with experimental congenital heart disease and increased pulmonary blood flow." Circulation **108**(13): 1646-1654.

Boettger, T., N. Beetz, et al. (2009). "Acquisition of the contractile phenotype by murine arterial smooth muscle cells depends on the Mir143/145 gene cluster." J Clin Invest **119**(9): 2634-2647.

Bohnsack, M. T., K. Czaplinski, et al. (2004). "Exportin 5 is a RanGTP-dependent dsRNA-binding protein that mediates nuclear export of pre-miRNAs." RNA **10**(2): 185-191.

Boland, A., F. Tritschler, et al. (2010). "Crystal structure and ligand binding of the MID domain of a eukaryotic Argonaute protein." EMBO Rep **11**(7): 522-527.

Borchert, G. M., W. Lanier, et al. (2006). "RNA polymerase III transcribes human microRNAs." Nat Struct Mol Biol **13**(12): 1097-1101.

Bortolin-Cavaille, M. L., M. Dance, et al. (2009). "C19MC microRNAs are processed from introns of large Pol-II, non-protein-coding transcripts." Nucleic Acids Res **37**(10): 3464-3473.

Boyd, S. D. (2008). "Everything you wanted to know about small RNA but were afraid to ask." Lab Invest **88**(6): 569-578.

Breitling, R., P. Armengaud, et al. (2004). "Rank products: a simple, yet powerful, new method to detect differentially regulated genes in replicated microarray experiments." FEBS Lett **573**(1-3): 83-92.

Brengues, M., D. Teixeira, et al. (2005). "Movement of eukaryotic mRNAs between polysomes and cytoplasmic processing bodies." Science **310**(5747): 486-489.

Brennecke, J., A. A. Aravin, et al. (2007). "Discrete small RNA-generating loci as master regulators of transposon activity in Drosophila." Cell **128**(6): 1089-1103.

Brennecke, J., A. Stark, et al. (2005). "Principles of microRNA-target recognition." PLoS Biol **3**(3): e85.

Brock, M., M. Trenkmann, et al. (2009). "Interleukin-6 modulates the expression of the bone morphogenic protein receptor type II through a novel STAT3-microRNA cluster 17/92 pathway." Circ Res **104**(10): 1184-1191.

Brower-Toland, B., S. D. Findley, et al. (2007). "Drosophila PIWI associates with chromatin and interacts directly with HP1a." Genes Dev **21**(18): 2300-2311.

Brusselmans, K., V. Compernolle, et al. (2003). "Heterozygous deficiency of hypoxia-inducible factor-2alpha protects mice against pulmonary hypertension and right ventricular dysfunction during prolonged hypoxia." J Clin Invest **111**(10): 1519-1527.

Burke, D. L., M. G. Frid, et al. (2009). "Sustained hypoxia promotes the development of a pulmonary artery-specific chronic inflammatory microenvironment." Am J Physiol Lung Cell Mol Physiol **297**(2): L238-250.

Cai, X., C. H. Hagedorn, et al. (2004). "Human microRNAs are processed from capped, polyadenylated transcripts that can also function as mRNAs." RNA **10**(12): 1957-1966.

Calin, G. A. and C. M. Croce (2006). "MicroRNA signatures in human cancers." Nat Rev Cancer **6**(11): 857-866.

Calin, G. A., C. D. Dumitru, et al. (2002). "Frequent deletions and down-regulation of micro- RNA genes miR15 and miR16 at 13q14 in chronic lymphocytic leukemia." Proc Natl Acad Sci U S A **99**(24): 15524-15529.

Calin, G. A., M. Ferracin, et al. (2005). "A MicroRNA signature associated with prognosis and progression in chronic lymphocytic leukemia." N Engl J Med **353**(17): 1793-1801.

Callis, T. E., K. Pandya, et al. (2009). "MicroRNA-208a is a regulator of cardiac hypertrophy and conduction in mice." J Clin Invest **119**(9): 2772-2786.

Caruso, P., M. R. MacLean, et al. (2010). "Dynamic changes in lung microRNA profiles during the development of pulmonary hypertension due to chronic hypoxia and monocrotaline." Arterioscler Thromb Vasc Biol **30**(4): 716-723.

Carvalho, R. L., F. Itoh, et al. (2007). "Compensatory signalling induced in the yolk sac vasculature by deletion of TGFbeta receptors in mice." J Cell Sci **120**(Pt 24): 4269-4277.

Castanares, C., M. Redondo-Horcajo, et al. (2007). "Signaling by ALK5 mediates TGF-beta-induced ET-1 expression in endothelial cells: a role for migration and proliferation." J Cell Sci **120**(Pt 7): 1256-1266.

Chan, J. A., A. M. Krichevsky, et al. (2005). "MicroRNA-21 is an antiapoptotic factor in human glioblastoma cells." Cancer Res **65**(14): 6029-6033.

Chang, T. C., D. Yu, et al. (2008). "Widespread microRNA repression by Myc contributes to tumorigenesis." Nat Genet **40**(1): 43-50.

Chatterjee, S. and H. Grosshans (2009). "Active turnover modulates mature microRNA activity in Caenorhabditis elegans." Nature **461**(7263): 546-549.

Cheloufi, S., C. O. Dos Santos, et al. (2010). "A dicer-independent miRNA biogenesis pathway that requires Ago catalysis." Nature **465**(7298): 584-589.

Chen, C., D. A. Ridzon, et al. (2005). "Real-time quantification of microRNAs by stem-loop RT-PCR." Nucleic Acids Res **33**(20): e179.

Chen, J. F., E. M. Mandel, et al. (2006). "The role of microRNA-1 and microRNA-133 in skeletal muscle proliferation and differentiation." Nat Genet **38**(2): 228-233.

Chen, J. F., E. P. Murchison, et al. (2008). "Targeted deletion of Dicer in the heart leads to dilated cardiomyopathy and heart failure." Proc Natl Acad Sci U S A **105**(6): 2111-2116.

Chen, X. (2009). "Small RNAs and their roles in plant development." Annu Rev Cell Dev Biol **25**: 21-44.

Chen, X., Y. Ba, et al. (2008). "Characterization of microRNAs in serum: a novel class of biomarkers for diagnosis of cancer and other diseases." Cell Res **18**(10): 997-1006.

Cheng, Y., R. Ji, et al. (2007). "MicroRNAs are aberrantly expressed in hypertrophic heart: do they play a role in cardiac hypertrophy?" Am J Pathol **170**(6): 1831-1840.

Cheng, Y., X. Liu, et al. (2009). "MicroRNA-145, a novel smooth muscle cell phenotypic marker and modulator, controls vascular neointimal lesion formation." Circ Res **105**(2): 158-166.

Cheng, Y., X. Liu, et al. (2009). "MicroRNA-21 protects against the H(2)O(2)-induced injury on cardiac myocytes via its target gene PDCD4." J Mol Cell Cardiol **47**(1): 5-14.

Chinetti, G., S. Griglio, et al. (1998). "Activation of proliferator-activated receptors alpha and gamma induces apoptosis of human monocyte-derived macrophages." J Biol Chem **273**(40): 25573-25580.

Chiosea, S., E. Jelezcova, et al. (2007). "Overexpression of Dicer in precursor lesions of lung adenocarcinoma." Cancer Res **67**(5): 2345-2350.

Christman, B. W., C. D. McPherson, et al. (1992). "An imbalance between the excretion of thromboxane and prostacyclin metabolites in pulmonary hypertension." N Engl J Med **327**(2): 70-75.

Chung, W. J., K. Okamura, et al. (2008). "Endogenous RNA interference provides a somatic defense against Drosophila transposons." Curr Biol **18**(11): 795-802.

Cifuentes, D., H. Xue, et al. (2010). "A Novel miRNA Processing Pathway Independent of Dicer Requires Argonaute2 Catalytic Activity." Science **328**(5986): 1694-1698.

Cikos, S., A. Bukovska, et al. (2007). "Relative quantification of mRNA: comparison of methods currently used for real-time PCR data analysis." BMC Mol Biol **8**: 113.

Cimmino, A., G. A. Calin, et al. (2005). "miR-15 and miR-16 induce apoptosis by targeting BCL2." Proc Natl Acad Sci U S A **102**(39): 13944-13949.

Comroe, J. H., Jr. (1966). "The main functions of the pulmonary circulation." Circulation **33**(1): 146-158.

Condorelli, G., M. V. G. Latronico, et al. (2010). "microRNAs in heart disease: putative novel therapeutic targets?" European Heart Journal.

Connolly, M. J. and P. I. Aaronson (2011). "Key role of the RhoA/Rho kinase system in pulmonary hypertension." Pulm Pharmacol Ther **24**(1): 1-14.

Conte, N., E. Charafe-Jauffret, et al. (2002). "Carcinogenesis and translational controls: TACC1 is down-regulated in human cancers and associates with mRNA regulators." Oncogene **21**(36): 5619-5630.

Corbin, J. D., A. Beasley, et al. (2005). "High lung PDE5: a strong basis for treating pulmonary hypertension with PDE5 inhibitors." Biochem Biophys Res Commun **334**(3): 930-938.

Cordes, K. R., N. T. Sheehy, et al. (2009). "miR-145 and miR-143 regulate smooth muscle cell fate and plasticity." Nature **460**(7256): 705-710.

Costa, F. F. (2008). "Non-coding RNAs, epigenetics and complexity." Gene **410**(1): 9-17.

Courboulin, A., R. Paulin, et al. (2011). "Role for miR-204 in human pulmonary arterial hypertension." J Exp Med **208**(3): 535-548.

Cowan, K. N., A. Heilbut, et al. (2000). "Complete reversal of fatal pulmonary hypertension in rats by a serine elastase inhibitor." Nat Med **6**(6): 698-702.

Croce, C. M. (2009). "Causes and consequences of microRNA dysregulation in cancer." Nature Reviews Genetics **10**(10): 704-714.

Csiszar, A., N. Labinskyy, et al. (2009). "Resveratrol prevents monocrotaline-induced pulmonary hypertension in rats." Hypertension **54**(3): 668-675.

Cullen, B. R. (2003). "Nuclear RNA export." J Cell Sci **116**(Pt 4): 587-597.

Cummins, J. M., Y. He, et al. (2006). "The colorectal microRNAome." Proc Natl Acad Sci U S A **103**(10): 3687-3692.

Czech, B., C. D. Malone, et al. (2008). "An endogenous small interfering RNA pathway in Drosophila." Nature **453**(7196): 798-802.

D'Alonzo, G. E., R. J. Barst, et al. (1991). "Survival in patients with primary pulmonary hypertension. Results from a national prospective registry." Ann Intern Med **115**(5): 343-349.

David, L., C. Mallet, et al. (2007). "Identification of BMP9 and BMP10 as functional activators of the orphan activin receptor-like kinase 1 (ALK1) in endothelial cells." Blood **109**(5): 1953-1961.

Davie, N., S. J. Haleen, et al. (2002). "ET(A) and ET(B) receptors modulate the proliferation of human pulmonary artery smooth muscle cells." Am J Respir Crit Care Med **165**(3): 398-405.

Davies, R. J. and N. W. Morrell (2008). "Molecular mechanisms of pulmonary arterial hypertension: role of mutations in the bone morphogenetic protein type II receptor." Chest **134**(6): 1271-1277.

Davis-Dusenbery, B. N., M. C. Chan, et al. (2011). "Downregulation of KLF4 by MIR-143/145 is critical for modulation of vascular smooth muscle cell phenotype by TGF-{beta} and BMP." J Biol Chem.

Davis, B. N. and A. Hata (2009). "Regulation of MicroRNA Biogenesis: A miRiad of mechanisms." Cell Commun Signal **7**: 18.

Davis, B. N., A. C. Hilyard, et al. (2008). "SMAD proteins control DROSHA-mediated microRNA maturation." Nature **454**(7200): 56-61.

Deng, G., S. A. Curriden, et al. (1996). "Is plasminogen activator inhibitor-1 the molecular switch that governs urokinase receptor-mediated cell adhesion and release?" J Cell Biol **134**(6): 1563-1571.

Denli, A. M., B. B. Tops, et al. (2004). "Processing of primary microRNAs by the Microprocessor complex." Nature **432**(7014): 231-235.

Derynck, R. and Y. E. Zhang (2003). "Smad-dependent and Smad-independent pathways in TGF-beta family signalling." Nature **425**(6958): 577-584.

Dewachter, L., S. Adnot, et al. (2009). "Bone morphogenetic protein signalling in heritable versus idiopathic pulmonary hypertension." Eur Respir J **34**(5): 1100-1110.

Diebold, I., D. Kraicun, et al. (2008). "The 'PAI-1 paradox' in vascular remodeling." Thromb Haemost **100**(6): 984-991.

Doench, J. G. and P. A. Sharp (2004). "Specificity of microRNA target selection in translational repression." Genes Dev **18**(5): 504-511.

Dore, L. C., J. D. Amigo, et al. (2008). "A GATA-1-regulated microRNA locus essential for erythropoiesis." Proc Natl Acad Sci U S A **105**(9): 3333-3338.

Drake, K. M., D. Zygmunt, et al. (2011). "Altered microRNA Processing in Heritable Pulmonary Arterial Hypertension: an Important Role for Smad-8." Am J Respir Crit Care Med.

Duan, W., J. H. Chan, et al. (2005). "Inhaled p38alpha mitogen-activated protein kinase antisense oligonucleotide attenuates asthma in mice." Am J Respir Crit Care Med **171**(6): 571-578.

Dumitrascu, R., S. Koebrich, et al. (2008). "Characterization of a murine model of monocrotaline pyrrole-induced acute lung injury." BMC Pulm Med **8**: 25.

Dupuis, J., C. A. Goresky, et al. (1996). "Pulmonary clearance of circulating endothelin-1 in dogs in vivo: exclusive role of ETB receptors." J Appl Physiol **81**(4): 1510-1515.

Ebert, M. S., J. R. Neilson, et al. (2007). "MicroRNA sponges: competitive inhibitors of small RNAs in mammalian cells." Nat Methods **4**(9): 721-726.

Ebert, M. S. and P. A. Sharp (2010). "Emerging roles for natural microRNA sponges." Curr Biol **20**(19): R858-861.

Eddahibi, S., A. Chaouat, et al. (2003). "Polymorphism of the serotonin transporter gene and pulmonary hypertension in chronic obstructive pulmonary disease." Circulation **108**(15): 1839-1844.

Eddahibi, S., N. Hanoun, et al. (2000). "Attenuated hypoxic pulmonary hypertension in mice lacking the 5-hydroxytryptamine transporter gene." J Clin Invest **105**(11): 1555-1562.

Eddahibi, S., M. Humbert, et al. (2001). "Serotonin transporter overexpression is responsible for pulmonary artery smooth muscle hyperplasia in primary pulmonary hypertension." J Clin Invest **108**(8): 1141-1150.

Eddahibi, S., N. Morrell, et al. (2002). "Pathobiology of pulmonary arterial hypertension." Eur Respir J **20**(6): 1559-1572.

Eickelberg, O. and R. E. Morty (2007). "Transforming growth factor beta/bone morphogenic protein signaling in pulmonary arterial hypertension: remodeling revisited." Trends Cardiovasc Med **17**(8): 263-269.

Elia, L., M. Quintavalle, et al. (2009). "The knockout of miR-143 and -145 alters smooth muscle cell maintenance and vascular homeostasis in mice: correlates with human disease." Cell Death Differ **16**(12): 1590-1598.

Erson, A. E. and E. M. Petty (2008). "MicroRNAs in development and disease." Clin Genet **74**(4): 296-306.

Esau, C. C. (2008). "Inhibition of microRNA with antisense oligonucleotides." Methods **44**(1): 55-60.

Estrada, K. D. and N. C. Chesler (2009). "Collagen-related gene and protein expression changes in the lung in response to chronic hypoxia." Biomech Model Mechanobiol **8**(4): 263-272.

Eulalio, A., E. Huntzinger, et al. (2008). "GW182 interaction with Argonaute is essential for miRNA-mediated translational repression and mRNA decay." Nat Struct Mol Biol **15**(4): 346-353.

Evans, A. M., H. J. Cobban, et al. (1999). "ET(A) receptors are the primary mediators of myofilament calcium sensitization induced by ET-1 in rat pulmonary artery smooth muscle: a tyrosine kinase independent pathway." Br J Pharmacol **127**(1): 153-160.

Feinberg, M. W., M. Watanabe, et al. (2004). "Transforming growth factor-beta1 inhibition of vascular smooth muscle cell activation is mediated via Smad3." J Biol Chem **279**(16): 16388-16393.

Feng, X. H. and R. Derynck (2005). "Specificity and versatility in tgf-beta signaling through Smads." Annu Rev Cell Dev Biol **21**: 659-693.

Fichtlscherer, S., S. De Rosa, et al. (2010). "Circulating microRNAs in patients with coronary artery disease." Circ Res **107**(5): 677-684.

Filipowicz, W., S. N. Bhattacharyya, et al. (2008). "Mechanisms of post-transcriptional regulation by microRNAs: are the answers in sight?" Nat Rev Genet **9**(2): 102-114.

Fire, A., S. Xu, et al. (1998). "Potent and specific genetic interference by double-stranded RNA in Caenorhabditis elegans." Nature **391**(6669): 806-811.

Firth, A. L., J. Mandel, et al. (2010). "Idiopathic pulmonary arterial hypertension." Dis Model Mech **3**(5-6): 268-273.

Franco-Zorrilla, J. M., A. Valli, et al. (2007). "Target mimicry provides a new mechanism for regulation of microRNA activity." Nat Genet **39**(8): 1033-1037.

Frid, M. G., E. P. Moiseeva, et al. (1994). "Multiple phenotypically distinct smooth muscle cell populations exist in the adult and developing bovine pulmonary arterial media in vivo." Circ Res **75**(4): 669-681.

Fujita, S., T. Ito, et al. (2008). "miR-21 Gene expression triggered by AP-1 is sustained through a double-negative feedback mechanism." J Mol Biol **378**(3): 492-504.

Fukuroda, T., M. Nishikibe, et al. (1992). "Analysis of responses to endothelins in isolated porcine blood vessels by using a novel endothelin antagonist, BQ-153." Life Sci **50**(15): PL107-112.

Gaine, S. P. and L. J. Rubin (1998). "Primary pulmonary hypertension." Lancet **352**(9129): 719-725.

Gal, H., G. Pandi, et al. (2008). "MIR-451 and Imatinib mesylate inhibit tumor growth of Glioblastoma stem cells." Biochemical and Biophysical Research Communications **376**(1): 86-90.

Galie, N., H. A. Ghofrani, et al. (2005). "Sildenafil citrate therapy for pulmonary arterial hypertension." N Engl J Med **353**(20): 2148-2157.

Galie, N., A. L. Hinderliter, et al. (2003). "Effects of the oral endothelin-receptor antagonist bosentan on echocardiographic and doppler measures in patients with pulmonary arterial hypertension." J Am Coll Cardiol **41**(8): 1380-1386.

Galie, N., A. Torbicki, et al. (2004). "Guidelines on diagnosis and treatment of pulmonary arterial hypertension. The Task Force on Diagnosis and Treatment of Pulmonary Arterial Hypertension of the European Society of Cardiology." Eur Heart J **25**(24): 2243-2278.

Galie, N., G. Ussia, et al. (1995). "Role of pharmacologic tests in the treatment of primary pulmonary hypertension." Am J Cardiol **75**(3): 55A-62A.

Gentner, B., G. Schira, et al. (2009). "Stable knockdown of microRNA in vivo by lentiviral vectors." Nat Methods **6**(1): 63-66.

Ghildiyal, M., H. Seitz, et al. (2008). "Endogenous siRNAs derived from transposons and mRNAs in Drosophila somatic cells." Science **320**(5879): 1077-1081.

Ghofrani, H. A. and F. Grimminger (2009). "Modulating cGMP to treat lung diseases." Handb Exp Pharmacol(191): 469-483.

Ghofrani, H. A., I. H. Osterloh, et al. (2006). "Sildenafil: from angina to erectile dysfunction to pulmonary hypertension and beyond." Nat Rev Drug Discov **5**(8): 689-702.

Giaid, A. and D. Saleh (1995). "Reduced expression of endothelial nitric oxide synthase in the lungs of patients with pulmonary hypertension." N Engl J Med **333**(4): 214-221.

Giaid, A., M. Yanagisawa, et al. (1993). "Expression of endothelin-1 in the lungs of patients with pulmonary hypertension." N Engl J Med **328**(24): 1732-1739.

Gilad, S., E. Meiri, et al. (2008). "Serum microRNAs are promising novel biomarkers." PLoS One **3**(9): e3148.

Giraldez, A. J., Y. Mishima, et al. (2006). "Zebrafish MiR-430 promotes deadenylation and clearance of maternal mRNAs." Science **312**(5770): 75-79.

Girard, A., R. Sachidanandam, et al. (2006). "A germline-specific class of small RNAs binds mammalian Piwi proteins." Nature **442**(7099): 199-202.

Girgis, R. E., A. E. Frost, et al. (2007). "Selective endothelin A receptor antagonism with sitaxsentan for pulmonary arterial hypertension associated with connective tissue disease." Ann Rheum Dis **66**(11): 1467-1472.

Godlewski, J., A. Bronisz, et al. (2010). "microRNA-451: A conditional switch controlling glioma cell proliferation and migration." Cell Cycle **9**(14): 2742-2748.

Godlewski, J., M. O. Nowicki, et al. (2010). "MicroRNA-451 Regulates LKB1/AMPK Signaling and Allows Adaptation to Metabolic Stress in Glioma Cells." Molecular Cell **37**(5): 620-632.

Goumans, M. J. and C. Mummery (2000). "Functional analysis of the TGFbeta receptor/Smad pathway through gene ablation in mice." Int J Dev Biol **44**(3): 253-265.

Goumans, M. J., G. Valdimarsdottir, et al. (2003). "Activin receptor-like kinase (ALK)1 is an antagonistic mediator of lateral TGFbeta/ALK5 signaling." Mol Cell **12**(4): 817-828.

Goumans, M. J., G. Valdimarsdottir, et al. (2002). "Balancing the activation state of the endothelium via two distinct TGF-beta type I receptors." EMBO J **21**(7): 1743-1753.

Graven, K. K., R. F. Troxler, et al. (1994). "Regulation of endothelial cell glyceraldehyde-3-phosphate dehydrogenase expression by hypoxia." J Biol Chem **269**(39): 24446-24453.

Gregor, M. and Janig (1977). "Effects of sytemic hypoxia and hypercapnia on cutaneous and muscle vasoconstrictor neurones to the cat's hindlimb." Pflugers Arch **368**(1-2): 71-81.

Gregory, R. I., T. P. Chendrimada, et al. (2005). "Human RISC couples microRNA biogenesis and posttranscriptional gene silencing." Cell **123**(4): 631-640.

Gregory, R. I. and R. Shiekhattar (2005). "MicroRNA biogenesis and cancer." Cancer Res **65**(9): 3509-3512.

Gregory, R. I., K. P. Yan, et al. (2004). "The Microprocessor complex mediates the genesis of microRNAs." Nature **432**(7014): 235-240.

Grewal, S. I. (2010). "RNAi-dependent formation of heterochromatin and its diverse functions." Curr Opin Genet Dev **20**(2): 134-141.

Griffiths-Jones, S. (2007). "Annotating noncoding RNA genes." Annu Rev Genomics Hum Genet **8**: 279-298.

Griffiths-Jones, S. (2010). "miRBase: microRNA sequences and annotation." Curr Protoc Bioinformatics **Chapter 12**: Unit 12 19 11-10.

Griffiths-Jones, S., R. J. Grocock, et al. (2006). "miRBase: microRNA sequences, targets and gene nomenclature." Nucleic Acids Res **34**(Database issue): D140-144.

Griffiths-Jones, S., H. K. Saini, et al. (2008). "miRBase: tools for microRNA genomics." Nucleic Acids Res **36**(Database issue): D154-158.

Grishok, A., A. E. Pasquinelli, et al. (2001). "Genes and mechanisms related to RNA interference regulate expression of the small temporal RNAs that control C. elegans developmental timing." Cell **106**(1): 23-34.

Guglin, M. and H. Khan (2010). "Pulmonary hypertension in heart failure." J Card Fail **16**(6): 461-474.

Guignabert, C., M. Izikki, et al. (2006). "Transgenic mice overexpressing the 5-hydroxytryptamine transporter gene in smooth muscle develop pulmonary hypertension." Circ Res **98**(10): 1323-1330.

Gunawardane, L. S., K. Saito, et al. (2007). "A slicer-mediated mechanism for repeat-associated siRNA 5' end formation in Drosophila." Science **315**(5818): 1587-1590.

Guo, H., N. T. Ingolia, et al. (2010). "Mammalian microRNAs predominantly act to decrease target mRNA levels." Nature **466**(7308): 835-840.

Guo, L. and Z. Lu (2010). "The fate of miRNA* strand through evolutionary analysis: implication for degradation as merely carrier strand or potential regulatory molecule?" PLoS One **5**(6): e11387.

Guo, S. and K. J. Kemphues (1995). "par-1, a gene required for establishing polarity in C. elegans embryos, encodes a putative Ser/Thr kinase that is asymmetrically distributed." Cell **81**(4): 611-620.

Gwizdek, C., B. Ossareh-Nazari, et al. (2003). "Exportin-5 mediates nuclear export of minihelix-containing RNAs." J Biol Chem **278**(8): 5505-5508.

Haase, A. D., L. Jaskiewicz, et al. (2005). "TRBP, a regulator of cellular PKR and HIV-1 virus expression, interacts with Dicer and functions in RNA silencing." EMBO Rep **6**(10): 961-967.

Hahn, M. W. and G. A. Wray (2002). "The g-value paradox." Evol Dev **4**(2): 73-75.

Hall, S. M., A. A. Hislop, et al. (2000). "Prenatal origins of human intrapulmonary arteries: formation and smooth muscle maturation." Am J Respir Cell Mol Biol **23**(2): 194-203.

Hamilton, A. J. and D. C. Baulcombe (1999). "A species of small antisense RNA in posttranscriptional gene silencing in plants." Science **286**(5441): 950-952.

Han, J., Y. Lee, et al. (2004). "The Drosha-DGCR8 complex in primary microRNA processing." Genes Dev **18**(24): 3016-3027.

Han, J., Y. Lee, et al. (2006). "Molecular basis for the recognition of primary microRNAs by the Drosha-DGCR8 complex." Cell **125**(5): 887-901.

Hansmann, G., V. A. de Jesus Perez, et al. (2008). "An antiproliferative BMP-2/PPARgamma/apoE axis in human and murine SMCs and its role in pulmonary hypertension." J Clin Invest **118**(5): 1846-1857.

Hansmann, G., R. A. Wagner, et al. (2007). "Pulmonary arterial hypertension is linked to insulin resistance and reversed by peroxisome proliferator-activated receptor-gamma activation." Circulation **115**(10): 1275-1284.

Harrison, R. E., J. A. Flanagan, et al. (2003). "Molecular and functional analysis identifies ALK-1 as the predominant cause of pulmonary hypertension related to hereditary haemorrhagic telangiectasia." J Med Genet **40**(12): 865-871.

Hassoun, P. M., L. Mouthon, et al. (2009). "Inflammation, growth factors, and pulmonary vascular remodeling." J Am Coll Cardiol **54**(1 Suppl): S10-19.

Hatley, M. E., D. M. Patrick, et al. (2010). "Modulation of K-Ras-dependent lung tumorigenesis by MicroRNA-21." Cancer Cell **18**(3): 282-293.

Hayashi, H., S. Abdollah, et al. (1997). "The MAD-related protein Smad7 associates with the TGFbeta receptor and functions as an antagonist of TGFbeta signaling." Cell **89**(7): 1165-1173.

Heneghan, H. M., N. Miller, et al. (2010). "Circulating microRNAs as novel minimally invasive biomarkers for breast cancer." Ann Surg **251**(3): 499-505.

Herr, A. J., M. B. Jensen, et al. (2005). "RNA polymerase IV directs silencing of endogenous DNA." Science **308**(5718): 118-120.

Hessel, M. H., P. Steendijk, et al. (2006). "Characterization of right ventricular function after monocrotaline-induced pulmonary hypertension in the intact rat." Am J Physiol Heart Circ Physiol **291**(5): H2424-2430.

Highland, K. B., C. Strange, et al. (2003). "Treatment of pulmonary arterial hypertension: a preliminary decision analysis." Chest **124**(6): 2087-2092.

Hirose, S., Y. Hosoda, et al. (2000). "Expression of vascular endothelial growth factor and its receptors correlates closely with formation of the plexiform lesion in human pulmonary hypertension." Pathol Int **50**(6): 472-479.

Hislop, A. and L. Reid (1978). "Normal structure and dimensions of the pulmonary arteries in the rat." J Anat **125**(Pt 1): 71-83.

Hislop, A. A. and C. M. Pierce (2000). "Growth of the vascular tree." Paediatr Respir Rev **1**(4): 321-327.

Hoeper, M. M., H. Leuchte, et al. (2006). "Combining inhaled iloprost with bosentan in patients with idiopathic pulmonary arterial hypertension." Eur Respir J **28**(4): 691-694.

Hoeper, M. M., M. Schwarze, et al. (2000). "Long-term treatment of primary pulmonary hypertension with aerosolized iloprost, a prostacyclin analogue." N Engl J Med **342**(25): 1866-1870.

Holden, W. E. and E. McCall (1984). "Hypoxia-induced contractions of porcine pulmonary artery strips depend on intact endothelium." Exp Lung Res **7**(2): 101-112.

Hollnagel, A., V. Oehlmann, et al. (1999). "Id genes are direct targets of bone morphogenetic protein induction in embryonic stem cells." J Biol Chem **274**(28): 19838-19845.

Hori, S., Y. Komatsu, et al. (1992). "Distinct tissue distribution and cellular localization of two messenger ribonucleic acids encoding different subtypes of rat endothelin receptors." Endocrinology **130**(4): 1885-1895.

Hsu, H. H., W. J. Ko, et al. (2009). "Simvastatin ameliorates established pulmonary hypertension through a heme oxygenase-1 dependent pathway in rats." Respir Res **10**: 32.

Huang, W., R. T. Yen, et al. (1996). "Morphometry of the human pulmonary vasculature." J Appl Physiol **81**(5): 2123-2133.

Huang, Z., D. Huang, et al. (2010). "Plasma microRNAs are promising novel biomarkers for early detection of colorectal cancer." Int J Cancer **127**(1): 118-126.

Hughes, J. M. (1975). "Lung gas tensions and active regulation of ventilation/perfusion ratios in health and disease." Br J Dis Chest **69**: 153-170.

Humbert, M. (2010). "Pulmonary arterial hypertension and chronic thromboembolic pulmonary hypertension: pathophysiology." Eur Respir Rev **19**(115): 59-63.

Humbert, M., R. J. Barst, et al. (2004). "Combination of bosentan with epoprostenol in pulmonary arterial hypertension: BREATHE-2." Eur Respir J **24**(3): 353-359.

Humbert, M., N. W. Morrell, et al. (2004). "Cellular and molecular pathobiology of pulmonary arterial hypertension." J Am Coll Cardiol **43**(12 Suppl S): 13S-24S.

Humbert, M., O. Sitbon, et al. (2006). "Pulmonary arterial hypertension in France: results from a national registry." Am J Respir Crit Care Med **173**(9): 1023-1030.

Humphreys, D. T., B. J. Westman, et al. (2005). "MicroRNAs control translation initiation by inhibiting eukaryotic initiation factor 4E/cap and poly(A) tail function." Proc Natl Acad Sci U S A **102**(47): 16961-16966.

Ichimura, T., J. Uchiyama, et al. (1995). "Identification of the site of interaction of the 14-3-3 protein with phosphorylated tryptophan hydroxylase." J Biol Chem **270**(48): 28515-28518.

Imamura, T., M. Takase, et al. (1997). "Smad6 inhibits signalling by the TGF-beta superfamily." Nature **389**(6651): 622-626.

Iorio, M. V., M. Ferracin, et al. (2005). "MicroRNA gene expression deregulation in human breast cancer." Cancer Res **65**(16): 7065-7070.

Ivey, K. N., A. Muth, et al. (2008). "MicroRNA regulation of cell lineages in mouse and human embryonic stem cells." Cell Stem Cell **2**(3): 219-229.

Jackson, R. J. and N. Standart (2007). "How do microRNAs regulate gene expression?" Sci STKE **2007**(367): re1.

Jankov, R. P., C. Kantores, et al. (2006). "Endothelin-1 inhibits apoptosis of pulmonary arterial smooth muscle in the neonatal rat." Pediatr Res **60**(3): 245-251.

Jeffery, T. K. and N. W. Morrell (2002). "Molecular and cellular basis of pulmonary vascular remodeling in pulmonary hypertension." Prog Cardiovasc Dis **45**(3): 173-202.

Ji, R., Y. Cheng, et al. (2007). "MicroRNA expression signature and antisense-mediated depletion reveal an essential role of MicroRNA in vascular neointimal lesion formation." Circ Res **100**(11): 1579-1588.

Ji, X., R. Takahashi, et al. (2009). "Plasma miR-208 as a biomarker of myocardial injury." Clin Chem **55**(11): 1944-1949.

Jiang, C., A. T. Ting, et al. (1998). "PPAR-gamma agonists inhibit production of monocyte inflammatory cytokines." Nature **391**(6662): 82-86.

Jiang, Z. L., G. S. Kassab, et al. (1994). "Diameter-defined Strahler system and connectivity matrix of the pulmonary arterial tree." J Appl Physiol **76**(2): 882-892.

Jinek, M. and J. A. Doudna (2009). "A three-dimensional view of the molecular machinery of RNA interference." Nature **457**(7228): 405-412.

Johnson, J. A., C. L. Vnencak-Jones, et al. (2009). "Copy-number variation in BMPR2 is not associated with the pathogenesis of pulmonary arterial hypertension." BMC Med Genet **10**: 58.

Jones-Rhoades, M. W., D. P. Bartel, et al. (2006). "MicroRNAS and their regulatory roles in plants." Annu Rev Plant Biol **57**: 19-53.

Kahvejian, A., Y. V. Svitkin, et al. (2005). "Mammalian poly(A)-binding protein is a eukaryotic translation initiation factor, which acts via multiple mechanisms." Genes Dev **19**(1): 104-113.

Kai, Z. S. and A. E. Pasquinelli (2010). "MicroRNA assassins: factors that regulate the disappearance of miRNAs." Nat Struct Mol Biol **17**(1): 5-10.

Kang, H., B. N. Davis-Dusenbery, et al. (2011). "Bone morphogenetic protein 4 promotes vascular smooth muscle contractility by activating miR-21, which downregulates expression of the family of Dedicator of Cytokinesis (DOCK) proteins." J Biol Chem.

Kartha, R. V. and S. Subramanian (2010). "MicroRNAs in cardiovascular diseases: biology and potential clinical applications." J Cardiovasc Transl Res **3**(3): 256-270.

Karube, Y., H. Tanaka, et al. (2005). "Reduced expression of Dicer associated with poor prognosis in lung cancer patients." Cancer Sci **96**(2): 111-115.

Kay, J. M., P. Harris, et al. (1967). "Pulmonary hypertension produced in rats by ingestion of Crotalaria spectabilis seeds." Thorax **22**(2): 176-179.

Kayser, S. R. (2005). "Combination drug therapy in the management of pulmonary arterial hypertension." Prog Cardiovasc Nurs **20**(4): 177-182.

Kazazian, H. H., Jr. (2004). "Mobile elements: drivers of genome evolution." Science **303**(5664): 1626-1632.

Khvorova, A., A. Reynolds, et al. (2003). "Functional siRNAs and miRNAs exhibit strand bias." Cell **115**(2): 209-216.

Kim, J., A. Krichevsky, et al. (2004). "Identification of many microRNAs that copurify with polyribosomes in mammalian neurons." Proc Natl Acad Sci U S A **101**(1): 360-365.

Kim, V. N., J. Han, et al. (2009). "Biogenesis of small RNAs in animals." Nat Rev Mol Cell Biol **10**(2): 126-139.

Kim, Y. K. and V. N. Kim (2007). "Processing of intronic microRNAs." EMBO J **26**(3): 775-783.

Kinch, L. N. and N. V. Grishin (2009). "The human Ago2 MC region does not contain an eIF4E-like mRNA cap binding motif." Biol Direct **4**: 2.

Kiriakidou, M., G. S. Tan, et al. (2007). "An mRNA m7G cap binding-like motif within human Ago2 represses translation." Cell **129**(6): 1141-1151.

Klinger, J. R., R. J. Oudiz, et al. (2011). "Long-term pulmonary hemodynamic effects of ambrisentan in pulmonary arterial hypertension." Am J Cardiol **108**(2): 302-307.

Kramer, M. S. and D. A. Lane (1998). "Aminorex, dexfenfluramine, and primary pulmonary hypertension." J Clin Epidemiol **51**(4): 361-364.

Krutzfeldt, J., N. Rajewsky, et al. (2005). "Silencing of microRNAs in vivo with 'antagomirs'." Nature **438**(7068): 685-689.

Kuehbacher, A., C. Urbich, et al. (2007). "Role of Dicer and Drosha for endothelial microRNA expression and angiogenesis." Circ Res **101**(1): 59-68.

Kulkarni, M., S. Ozgur, et al. (2010). "On track with P-bodies." Biochem Soc Trans **38**(Pt 1): 242-251.

Kuramochi-Miyagawa, S., T. Watanabe, et al. (2008). "DNA methylation of retrotransposon genes is regulated by Piwi family members MILI and MIWI2 in murine fetal testes." Genes Dev **22**(7): 908-917.

Kuwabara, Y., K. Ono, et al. (2011). "Increased microRNA-1 and microRNA-133a levels in serum of patients with cardiovascular disease indicate myocardial damage." Circ Cardiovasc Genet **4**(4): 446-454.

Kuzmiak, H. A. and L. E. Maquat (2006). "Applying nonsense-mediated mRNA decay research to the clinic: progress and challenges." Trends Mol Med **12**(7): 306-316.

Lagna, G., P. H. Nguyen, et al. (2006). "BMP-dependent activation of caspase-9 and caspase-8 mediates apoptosis in pulmonary artery smooth muscle cells." Am J Physiol Lung Cell Mol Physiol **291**(5): L1059-1067.

Lagos-Quintana, M., R. Rauhut, et al. (2001). "Identification of novel genes coding for small expressed RNAs." Science **294**(5543): 853-858.

Lagos-Quintana, M., R. Rauhut, et al. (2002). "Identification of tissue-specific microRNAs from mouse." Curr Biol **12**(9): 735-739.

Lane, K. B., R. D. Machado, et al. (2000). "Heterozygous germline mutations in BMPR2, encoding a TGF-beta receptor, cause familial primary pulmonary hypertension." Nat Genet **26**(1): 81-84.

Lankat-Buttgereit, B. and R. Goke (2009). "The tumour suppressor Pdcd4: recent advances in the elucidation of function and regulation." Biol Cell **101**(6): 309-317.

Lasorella, A., T. Uo, et al. (2001). "Id proteins at the cross-road of development and cancer." Oncogene **20**(58): 8326-8333.

Laudi, S., W. Steudel, et al. (2007). "Comparison of lung proteome profiles in two rodent models of pulmonary arterial hypertension." Proteomics **7**(14): 2469-2478.

Lawrie, C. H., S. Gal, et al. (2008). "Detection of elevated levels of tumour-associated microRNAs in serum of patients with diffuse large B-cell lymphoma." Br J Haematol **141**(5): 672-675.

Lee, E. J., Y. Gusev, et al. (2007). "Expression profiling identifies microRNA signature in pancreatic cancer." Int J Cancer **120**(5): 1046-1054.

Lee, R. C., R. L. Feinbaum, et al. (1993). "The C. elegans heterochronic gene lin-4 encodes small RNAs with antisense complementarity to lin-14." Cell **75**(5): 843-854.

Lee, S. J., C. Jiko, et al. (2011). "Selective nuclear export mechanism of small RNAs." Curr Opin Struct Biol **21**(1): 101-108.

Lee, Y., C. Ahn, et al. (2003). "The nuclear RNase III Drosha initiates microRNA processing." Nature **425**(6956): 415-419.

Lee, Y., I. Hur, et al. (2006). "The role of PACT in the RNA silencing pathway." EMBO J **25**(3): 522-532.

Lee, Y., K. Jeon, et al. (2002). "MicroRNA maturation: stepwise processing and subcellular localization." EMBO J **21**(17): 4663-4670.

Lee, Y., M. Kim, et al. (2004). "MicroRNA genes are transcribed by RNA polymerase II." EMBO J **23**(20): 4051-4060.

Lee, Y. S., K. Nakahara, et al. (2004). "Distinct roles for Drosophila Dicer-1 and Dicer-2 in the siRNA/miRNA silencing pathways." Cell **117**(1): 69-81.

Lei, E. P. and P. A. Silver (2002). "Protein and RNA export from the nucleus." Dev Cell **2**(3): 261-272.

Lewis, B. P., C. B. Burge, et al. (2005). "Conserved seed pairing, often flanked by adenosines, indicates that thousands of human genes are microRNA targets." Cell **120**(1): 15-20.

Lewis, B. P., I. H. Shih, et al. (2003). "Prediction of mammalian microRNA targets." Cell **115**(7): 787-798.

Li, W., B. J. Dunmore, et al. (2010). "Bone morphogenetic protein type II receptor mutations causing protein misfolding in heritable pulmonary arterial hypertension." Proc Am Thorac Soc **7**(6): 395-398.

Lim, L. P., M. E. Glasner, et al. (2003). "Vertebrate microRNA genes." Science **299**(5612): 1540.

Lim, L. P., N. C. Lau, et al. (2005). "Microarray analysis shows that some microRNAs downregulate large numbers of target mRNAs." Nature **433**(7027): 769-773.

Lin, Y., X. Liu, et al. (2009). "Involvement of MicroRNAs in hydrogen peroxide-mediated gene regulation and cellular injury response in vascular smooth muscle cells." J Biol Chem **284**(12): 7903-7913.

Liu, J., M. A. Carmell, et al. (2004). "Argonaute2 is the catalytic engine of mammalian RNAi." Science **305**(5689): 1437-1441.

Liu, J., M. A. Valencia-Sanchez, et al. (2005). "MicroRNA-dependent localization of targeted mRNAs to mammalian P-bodies." Nat Cell Biol **7**(7): 719-723.

Liu, L. Z., C. Li, et al. (2011). "MiR-21 induced angiogenesis through AKT and ERK activation and HIF-1alpha expression." PLoS One **6**(4): e19139.

Liu, N., A. H. Williams, et al. (2007). "An intragenic MEF2-dependent enhancer directs muscle-specific expression of microRNAs 1 and 133." Proc Natl Acad Sci U S A **104**(52): 20844-20849.

Liu, Y., W. Ren, et al. (2009). "Serotonin induces Rho/ROCK-dependent activation of Smads 1/5/8 in pulmonary artery smooth muscle cells." FASEB J **23**(7): 2299-2306.

Livak, K. J. and T. D. Schmittgen (2001). "Analysis of relative gene expression data using real-time quantitative PCR and the 2(-Delta Delta C(T)) Method." Methods **25**(4): 402-408.

Lodes, M. J., M. Caraballo, et al. (2009). "Detection of cancer with serum miRNAs on an oligonucleotide microarray." PLoS One **4**(7): e6229.

Lomakin, I. B., C. U. Hellen, et al. (2000). "Physical association of eukaryotic initiation factor 4G (eIF4G) with eIF4A strongly enhances binding of eIF4G to the internal ribosomal entry site of encephalomyocarditis virus and is required for internal initiation of translation." Mol Cell Biol **20**(16): 6019-6029.

Long, L., A. Crosby, et al. (2009). "Altered bone morphogenetic protein and transforming growth factor-beta signaling in rat models of pulmonary hypertension: potential for activin receptor-like kinase-5 inhibition in prevention and progression of disease." Circulation **119**(4): 566-576.

Long, L., M. R. MacLean, et al. (2006). "Serotonin increases susceptibility to pulmonary hypertension in BMPR2-deficient mice." Circ Res **98**(6): 818-827.

Long, X. and J. M. Miano (2011). "TGF{beta}1 utilizes distinct pathways for the transcriptional activation of microRNA 143/145 in human coronary artery smooth muscle cells." J Biol Chem.

Lu, J., G. Getz, et al. (2005). "MicroRNA expression profiles classify human cancers." Nature **435**(7043): 834-838.

Lujambio, A., G. A. Calin, et al. (2008). "A microRNA DNA methylation signature for human cancer metastasis." Proc Natl Acad Sci U S A **105**(36): 13556-13561.

Lund, E., S. Guttinger, et al. (2004). "Nuclear export of microRNA precursors." Science **303**(5654): 95-98.

Machado, R. D., M. A. Aldred, et al. (2006). "Mutations of the TGF-beta type II receptor BMPR2 in pulmonary arterial hypertension." Hum Mutat **27**(2): 121-132.

MacLean, M. R., G. A. Deuchar, et al. (2004). "Overexpression of the 5-hydroxytryptamine transporter gene: effect on pulmonary hemodynamics and hypoxia-induced pulmonary hypertension." Circulation **109**(17): 2150-2155.

MacLean, M. R., P. Herve, et al. (2000). "5-hydroxytryptamine and the pulmonary circulation: receptors, transporters and relevance to pulmonary arterial hypertension." Br J Pharmacol **131**(2): 161-168.

Macrae, I. J., K. Zhou, et al. (2006). "Structural basis for double-stranded RNA processing by Dicer." Science **311**(5758): 195-198.

Mair, K. M., M. R. MacLean, et al. (2008). "Novel interactions between the 5-HT transporter, 5-HT1B receptors and Rho kinase in vivo and in pulmonary fibroblasts." Br J Pharmacol **155**(4): 606-616.

Malone, C. D. and G. J. Hannon (2009). "Small RNAs as guardians of the genome." Cell **136**(4): 656-668.

Mandegar, M., Y. C. Fung, et al. (2004). "Cellular and molecular mechanisms of pulmonary vascular remodeling: role in the development of pulmonary hypertension." Microvasc Res **68**(2): 75-103.

Mandegar, M. and J. X. Yuan (2002). "Role of K+ channels in pulmonary hypertension." Vascul Pharmacol **38**(1): 25-33.

Marshall, C. and B. E. Marshall (1992). "Hypoxic pulmonary vasoconstriction is not endothelium dependent." Proc Soc Exp Biol Med **201**(3): 267-270.

Martello, G., A. Rosato, et al. (2010). "A MicroRNA targeting dicer for metastasis control." Cell **141**(7): 1195-1207.

Masri, F. A., W. Xu, et al. (2007). "Hyperproliferative apoptosis-resistant endothelial cells in idiopathic pulmonary arterial hypertension." Am J Physiol Lung Cell Mol Physiol **293**(3): L548-554.

Mathai, S. C., R. E. Girgis, et al. (2007). "Addition of sildenafil to bosentan monotherapy in pulmonary arterial hypertension." Eur Respir J **29**(3): 469-475.

Mauban, J. R., C. V. Remillard, et al. (2005). "Hypoxic pulmonary vasoconstriction: role of ion channels." J Appl Physiol **98**(1): 415-420.

McCulloch, K. M., C. C. Docherty, et al. (1996). "EndothelinB receptor-mediated contraction in human pulmonary resistance arteries." Br J Pharmacol **119**(6): 1125-1130.

McCulloch, K. M., F. E. Kempsill, et al. (2000). "Regional distribution of potassium currents in the rabbit pulmonary arterial circulation." Exp Physiol **85**(5): 487-496.

McLaughlin, V. V., O. Sitbon, et al. (2005). "Survival with first-line bosentan in patients with primary pulmonary hypertension." Eur Respir J **25**(2): 244-249.

McMurtry, I. F., K. Abe, et al. (2010). "Rho kinase-mediated vasoconstriction in pulmonary hypertension." Adv Exp Med Biol **661**: 299-308.

McMurtry, I. F., A. B. Davidson, et al. (1976). "Inhibition of hypoxic pulmonary vasoconstriction by calcium antagonists in isolated rat lungs." Circ Res **38**(2): 99-104.

McMurtry, M. S., R. Moudgil, et al. (2007). "Overexpression of human bone morphogenetic protein receptor 2 does not ameliorate monocrotaline pulmonary arterial hypertension." Am J Physiol Lung Cell Mol Physiol **292**(4): L872-878.

Meister, G., M. Landthaler, et al. (2004). "Human Argonaute2 mediates RNA cleavage targeted by miRNAs and siRNAs." Mol Cell **15**(2): 185-197.

Melo, S. A., C. Moutinho, et al. (2010). "A genetic defect in exportin-5 traps precursor microRNAs in the nucleus of cancer cells." Cancer Cell **18**(4): 303-315.

Meyrick, B. O. and E. A. Perkett (1989). "The sequence of cellular and hemodynamic changes of chronic pulmonary hypertension induced by hypoxia and other stimuli." Am Rev Respir Dis **140**(5): 1486-1489.

Michelakis, E., W. Tymchak, et al. (2002). "Oral sildenafil is an effective and specific pulmonary vasodilator in patients with pulmonary arterial hypertension: comparison with inhaled nitric oxide." Circulation **105**(20): 2398-2403.

Michelakis, E. D., W. Tymchak, et al. (2003). "Long-term treatment with oral sildenafil is safe and improves functional capacity and hemodynamics in patients with pulmonary arterial hypertension." Circulation **108**(17): 2066-2069.

Miller, A. A., A. A. Hislop, et al. (2005). "Deletion of the eNOS gene has a greater impact on the pulmonary circulation of male than female mice." Am J Physiol Lung Cell Mol Physiol **289**(2): L299-306.

Mitani, Y., A. Mutlu, et al. (2002). "Dexfenfluramine protects against pulmonary hypertension in rats." J Appl Physiol **93**(5): 1770-1778.

Mitchell, P. S., R. K. Parkin, et al. (2008). "Circulating microRNAs as stable blood-based markers for cancer detection." Proc Natl Acad Sci U S A **105**(30): 10513-10518.

Miyamoto, S., N. Nagaya, et al. (2000). "Clinical correlates and prognostic significance of six-minute walk test in patients with primary pulmonary hypertension. Comparison with cardiopulmonary exercise testing." Am J Respir Crit Care Med **161**(2 Pt 1): 487-492.

Miyamoto, Y. and J. Yamauchi (2010). "Cellular signaling of Dock family proteins in neural function." Cell Signal **22**(2): 175-182.

Miyazono, K. and K. Miyazawa (2002). "Id: a target of BMP signaling." Sci STKE **2002**(151): pe40.

Moncada, S. and A. Higgs (1993). "The L-arginine-nitric oxide pathway." N Engl J Med **329**(27): 2002-2012.

Montani, D., L. Savale, et al. (2010). "Long-term response to calcium-channel blockers in non-idiopathic pulmonary arterial hypertension." Eur Heart J **31**(15): 1898-1907.

Montgomery, R. L., T. G. Hullinger, et al. (2011). "Therapeutic inhibition of miR-208a improves cardiac function and survival during heart failure." Circulation **124**(14): 1537-1547.

Morecroft, I., Y. Dempsie, et al. (2007). "Effect of tryptophan hydroxylase 1 deficiency on the development of hypoxia-induced pulmonary hypertension." Hypertension **49**(1): 232-236.

Morecroft, I., B. Doyle, et al. (2011). "Mice lacking the Raf-1 kinase inhibitor protein exhibit exaggerated hypoxia-induced pulmonary hypertension." Br J Pharmacol **163**(5): 948-963.

Morecroft, I., L. Pang, et al. (2010). "In vivo effects of a combined 5-HT1B receptor/SERT antagonist in experimental pulmonary hypertension." Cardiovasc Res **85**(3): 593-603.

Morgan, T., J. Lauri, et al. (2004). "Effect of different antihypertensive drug classes on central aortic pressure." Am J Hypertens **17**(2): 118-123.

Morrell, N. W. (2010). "Genetics of pulmonary arterial hypertension: do the molecular findings have translational value?" F1000 Biol Rep **2**.

Morrell, N. W. (2010). "Role of bone morphogenetic protein receptors in the development of pulmonary arterial hypertension." Adv Exp Med Biol **661**: 251-264.

Morrell, N. W., S. Adnot, et al. (2009). "Cellular and molecular basis of pulmonary arterial hypertension." J Am Coll Cardiol **54**(1 Suppl): S20-31.

Morty, R. E., B. Nejman, et al. (2007). "Dysregulated bone morphogenetic protein signaling in monocrotaline-induced pulmonary arterial hypertension." Arterioscler Thromb Vasc Biol **27**(5): 1072-1078.

Morty, R. E., B. Nejman, et al. (2007). "Dysregulated Bone Morphogenetic Protein Signaling in Monocrotaline-Induced Pulmonary Arterial Hypertension." Arteriosclerosis, Thrombosis, and Vascular Biology **27**(5): 1072-1078.

Moudgil, R., E. D. Michelakis, et al. (2005). "Hypoxic pulmonary vasoconstriction." J Appl Physiol **98**(1): 390-403.

Murchison, E. P. and G. J. Hannon (2004). "miRNAs on the move: miRNA biogenesis and the RNAi machinery." Curr Opin Cell Biol **16**(3): 223-229.

Murray, J. F. (2010). "The structure and function of the lung." Int J Tuberc Lung Dis **14**(4): 391-396.

Napoli, C., C. Lemieux, et al. (1990). "Introduction of a Chimeric Chalcone Synthase Gene into Petunia Results in Reversible Co-Suppression of Homologous Genes in trans." Plant Cell **2**(4): 279-289.

Nauser, T. D. and S. W. Stites (2001). "Diagnosis and treatment of pulmonary hypertension." Am Fam Physician **63**(9): 1789-1798.

Nelson, P. T., A. G. Hatzigeorgiou, et al. (2004). "miRNP:mRNA association in polyribosomes in a human neuronal cell line." RNA **10**(3): 387-394.

Newman, J. H., R. C. Trembath, et al. (2004). "Genetic basis of pulmonary arterial hypertension: current understanding and future directions." J Am Coll Cardiol **43**(12 Suppl S): 33S-39S.

Newman, J. H., L. Wheeler, et al. (2001). "Mutation in the gene for bone morphogenetic protein receptor II as a cause of primary pulmonary hypertension in a large kindred." N Engl J Med **345**(5): 319-324.

Nissen, P., J. Hansen, et al. (2000). "The structural basis of ribosome activity in peptide bond synthesis." Science **289**(5481): 920-930.

Nottrott, S., M. J. Simard, et al. (2006). "Human let-7a miRNA blocks protein production on actively translating polyribosomes." Nat Struct Mol Biol **13**(12): 1108-1114.

O'Donnell, K. A., E. A. Wentzel, et al. (2005). "c-Myc-regulated microRNAs modulate E2F1 expression." Nature **435**(7043): 839-843.

Okamura, K., W. J. Chung, et al. (2008). "The Drosophila hairpin RNA pathway generates endogenous short interfering RNAs." Nature **453**(7196): 803-806.

Okamura, K., J. W. Hagen, et al. (2007). "The mirtron pathway generates microRNA-class regulatory RNAs in Drosophila." Cell **130**(1): 89-100.

Olschewski, H., G. Simonneau, et al. (2002). "Inhaled iloprost for severe pulmonary hypertension." N Engl J Med **347**(5): 322-329.

Olsen, P. H. and V. Ambros (1999). "The lin-4 regulatory RNA controls developmental timing in Caenorhabditis elegans by blocking LIN-14 protein synthesis after the initiation of translation." Dev Biol **216**(2): 671-680.

Ono, S. and N. F. Voelkel (1991). "PAF antagonists inhibit monocrotaline-induced lung injury and pulmonary hypertension." J Appl Physiol **71**(6): 2483-2492.

Opitz, C. F., R. Wensel, et al. (2005). "Clinical efficacy and survival with first-line inhaled iloprost therapy in patients with idiopathic pulmonary arterial hypertension." Eur Heart J **26**(18): 1895-1902.

Orom, U. A., S. Kauppinen, et al. (2006). "LNA-modified oligonucleotides mediate specific inhibition of microRNA function." Gene **372**: 137-141.

Orom, U. A. and A. H. Lund (2007). "Isolation of microRNA targets using biotinylated synthetic microRNAs." Methods **43**(2): 162-165.

Otsuka, G., R. Agah, et al. (2006). "Transforming growth factor beta 1 induces neointima formation through plasminogen activator inhibitor-1-dependent pathways." Arterioscler Thromb Vasc Biol **26**(4): 737-743.

Otsuka, G., A. Stempien-Otero, et al. (2007). "Mechanisms of TGF-beta1-induced intimal growth: plasminogen-independent activities of plasminogen activator inhibitor-1 and heterogeneous origin of intimal cells." Circ Res **100**(9): 1300-1307.

Oudit, G. Y., H. Sun, et al. (2004). "The role of phosphoinositide-3 kinase and PTEN in cardiovascular physiology and disease." J Mol Cell Cardiol **37**(2): 449-471.

Oudiz, R. J., N. Galie, et al. (2009). "Long-term ambrisentan therapy for the treatment of pulmonary arterial hypertension." J Am Coll Cardiol **54**(21): 1971-1981.

Owens, G. K. (2007). "Molecular control of vascular smooth muscle cell differentiation and phenotypic plasticity." Novartis Found Symp **283**: 174-191; discussion 191-173, 238-141.

Owens, G. K., M. S. Kumar, et al. (2004). "Molecular regulation of vascular smooth muscle cell differentiation in development and disease." Physiol Rev **84**(3): 767-801.

Packer, A. N., Y. Xing, et al. (2008). "The bifunctional microRNA miR-9/miR-9* regulates REST and CoREST and is downregulated in Huntington's disease." J Neurosci **28**(53): 14341-14346.

Padgett, R. A., P. J. Grabowski, et al. (1986). "Splicing of messenger RNA precursors." Annu Rev Biochem **55**: 1119-1150.

Partanen, J., M. S. Nieminen, et al. (1993). "Death in a patient with primary pulmonary hypertension after 20 mg of nifedipine." N Engl J Med **329**(11): 812; author reply 812-813.

Pasquinelli, A. E., B. J. Reinhart, et al. (2000). "Conservation of the sequence and temporal expression of let-7 heterochronic regulatory RNA." Nature **408**(6808): 86-89.

Patrick, D. M., R. L. Montgomery, et al. (2010). "Stress-dependent cardiac remodeling occurs in the absence of microRNA-21 in mice." J Clin Invest **120**(11): 3912-3916.

Patrick, D. M., C. C. Zhang, et al. (2010). "Defective erythroid differentiation in miR-451 mutant mice mediated by 14-3-3 " Genes & Development **24**(15): 1614-1619.

Paul, G. A., J. S. Gibbs, et al. (2005). "Bosentan decreases the plasma concentration of sildenafil when coprescribed in pulmonary hypertension." Br J Clin Pharmacol **60**(1): 107-112.

Peacock, A. J., K. E. Dawes, et al. (1992). "Endothelin-1 and endothelin-3 induce chemotaxis and replication of pulmonary artery fibroblasts." Am J Respir Cell Mol Biol **7**(5): 492-499.

Peacock, A. J., N. F. Murphy, et al. (2007). "An epidemiological study of pulmonary arterial hypertension." Eur Respir J **30**(1): 104-109.

Peng, Y., Q. Kang, et al. (2004). "Inhibitor of DNA binding/differentiation helix-loop-helix proteins mediate bone morphogenetic protein-induced osteoblast differentiation of mesenchymal stem cells." J Biol Chem **279**(31): 32941-32949.

Petersen, C. P., M. E. Bordeleau, et al. (2006). "Short RNAs repress translation after initiation in mammalian cells." Mol Cell **21**(4): 533-542.

Pillai, R. S., S. N. Bhattacharyya, et al. (2005). "Inhibition of translational initiation by Let-7 MicroRNA in human cells." Science **309**(5740): 1573-1576.

Poliseno, L., L. Salmena, et al. (2010). "A coding-independent function of gene and pseudogene mRNAs regulates tumour biology." Nature **465**(7301): 1033-1038.

Pozeg, Z. I., E. D. Michelakis, et al. (2003). "In vivo gene transfer of the O2-sensitive potassium channel Kv1.5 reduces pulmonary hypertension and restores hypoxic pulmonary vasoconstriction in chronically hypoxic rats." Circulation **107**(15): 2037-2044.

Pullamsetti, S. S., C. Doebele, et al. (2011). "Inhibition of microRNA-17 Improves Lung and Heart Function in Experimental Pulmonary Hypertension." Am J Respir Crit Care Med.

Pullamsetti, S. S., R. Savai, et al. (2011). "Inflammation, immunological reaction and role of infection in pulmonary hypertension." Clin Microbiol Infect **17**(1): 7-14.

Qin, S. and C. Zhang (2011). "MicroRNAs in vascular disease." J Cardiovasc Pharmacol **57**(1): 8-12.

Qin, W., B. Zhao, et al. (2009). "BMPRII is a direct target of miR-21." Acta Biochim Biophys Sin (Shanghai) **41**(7): 618-623.

Rabinovitch, M. (2008). "Molecular pathogenesis of pulmonary arterial hypertension." J Clin Invest **118**(7): 2372-2379.

Rabinovitch, M., W. J. Gamble, et al. (1981). "Age and sex influence on pulmonary hypertension of chronic hypoxia and on recovery." Am J Physiol **240**(1): H62-72.

RajBhandary, U. L. and C. Kohrer (2006). "Early days of tRNA research: discovery, function, purification and sequence analysis." J Biosci **31**(4): 439-451.

Rangrez, A. Y., Z. A. Massy, et al. (2011). "miR-143 and miR-145: molecular keys to switch the phenotype of vascular smooth muscle cells." Circ Cardiovasc Genet **4**(2): 197-205.

Rao, P. K., R. M. Kumar, et al. (2006). "Myogenic factors that regulate expression of muscle-specific microRNAs." Proc Natl Acad Sci U S A **103**(23): 8721-8726.

Rao, P. K., Y. Toyama, et al. (2009). "Loss of cardiac microRNA-mediated regulation leads to dilated cardiomyopathy and heart failure." Circ Res **105**(6): 585-594.

Rehwinkel, J., P. Natalin, et al. (2006). "Genome-wide analysis of mRNAs regulated by Drosha and Argonaute proteins in Drosophila melanogaster." Mol Cell Biol **26**(8): 2965-2975.

Reiner, A., D. Yekutieli, et al. (2003). "Identifying differentially expressed genes using false discovery rate controlling procedures." Bioinformatics **19**(3): 368-375.

Reinhart, B. J. and D. P. Bartel (2002). "Small RNAs correspond to centromere heterochromatic repeats." Science **297**(5588): 1831.

Reinhart, B. J., F. J. Slack, et al. (2000). "The 21-nucleotide let-7 RNA regulates developmental timing in Caenorhabditis elegans." Nature **403**(6772): 901-906.

Reynolds, A. M., M. D. Holmes, et al. (2011). "Targeted gene delivery of BMPR-2 attenuates pulmonary hypertension." Eur Respir J.

Reynolds, A. M., W. Xia, et al. (2007). "Bone morphogenetic protein type 2 receptor gene therapy attenuates hypoxic pulmonary hypertension." Am J Physiol Lung Cell Mol Physiol **292**(5): L1182-1192.

Rhoades, M. W., B. J. Reinhart, et al. (2002). "Prediction of plant microRNA targets." Cell **110**(4): 513-520.

Rich, S., D. R. Dantzker, et al. (1987). "Primary pulmonary hypertension. A national prospective study." Ann Intern Med **107**(2): 216-223.

Rich, S. and E. Kaufmann (1991). "High dose titration of calcium channel blocking agents for primary pulmonary hypertension: guidelines for short-term drug testing." J Am Coll Cardiol **18**(5): 1323-1327.

Rich, S., E. Kaufmann, et al. (1992). "The effect of high doses of calcium-channel blockers on survival in primary pulmonary hypertension." N Engl J Med **327**(2): 76-81.

Richter, A., M. E. Yeager, et al. (2004). "Impaired transforming growth factor-beta signaling in idiopathic pulmonary arterial hypertension." Am J Respir Crit Care Med **170**(12): 1340-1348.

Rodnina, M. V., M. Beringer, et al. (2007). "How ribosomes make peptide bonds." Trends Biochem Sci **32**(1): 20-26.

Roest Crollius, H., O. Jaillon, et al. (2000). "Estimate of human gene number provided by genome-wide analysis using Tetraodon nigroviridis DNA sequence." Nat Genet **25**(2): 235-238.

Rosenkranz, S. and E. Erdmann (2008). "[World Conference 2008 in Dana Point: important developments in the field of pulmonary hypertension]." Dtsch Med Wochenschr **133 Suppl 6**: S165-166.

Roth, R. A., L. A. Dotzlaf, et al. (1981). "Effect of monocrotaline ingestion on liver, kidney, and lung of rats." Toxicol Appl Pharmacol **60**(2): 193-203.

Rothman, R. B., M. A. Ayestas, et al. (1999). "Aminorex, fenfluramine, and chlorphentermine are serotonin transporter substrates. Implications for primary pulmonary hypertension." Circulation **100**(8): 869-875.

Rubin, L. J. (1999). "Cellular and molecular mechanisms responsible for the pathogenesis of primary pulmonary hypertension." Pediatr Pulmonol Suppl **18**: 194-197.

Rubin, L. J., D. B. Badesch, et al. (2002). "Bosentan therapy for pulmonary arterial hypertension." N Engl J Med **346**(12): 896-903.

Rubin, L. J., J. Mendoza, et al. (1990). "Treatment of primary pulmonary hypertension with continuous intravenous prostacyclin (epoprostenol). Results of a randomized trial." Ann Intern Med **112**(7): 485-491.

Ruby, J. G., C. H. Jan, et al. (2007). "Intronic microRNA precursors that bypass Drosha processing." Nature **448**(7149): 83-86.

Ruzinova, M. B. and R. Benezra (2003). "Id proteins in development, cell cycle and cancer." Trends Cell Biol **13**(8): 410-418.

Sabatel, C., L. Malvaux, et al. (2011). "MicroRNA-21 exhibits antiangiogenic function by targeting RhoB expression in endothelial cells." PLoS One **6**(2): e16979.

Said, H. M., C. Hagemann, et al. (2007). "GAPDH is not regulated in human glioblastoma under hypoxic conditions." BMC Mol Biol **8**: 55.

Said, H. M., B. Polat, et al. (2009). "Absence of GAPDH regulation in tumor-cells of different origin under hypoxic conditions in - vitro." BMC Res Notes **2**: 8.

Said, S. I., S. A. Hamidi, et al. (2007). "Moderate pulmonary arterial hypertension in male mice lacking the vasoactive intestinal peptide gene." Circulation **115**(10): 1260-1268.

Sakao, S., K. Tatsumi, et al. (2009). "Endothelial cells and pulmonary arterial hypertension: apoptosis, proliferation, interaction and transdifferentiation." Respir Res **10**: 95.

Samarakoon, R. and P. J. Higgins (2008). "Integration of non-SMAD and SMAD signaling in TGF-beta1-induced plasminogen activator inhibitor type-1 gene expression in vascular smooth muscle cells." Thromb Haemost **100**(6): 976-983.

Sandoval, J., A. Torbicki, et al. (2011). "Safety and efficacy of sitaxsentan 50 and 100 mg in patients with pulmonary arterial hypertension." Pulm Pharmacol Ther.

Sastry, B. K., C. Narasimhan, et al. (2004). "Clinical efficacy of sildenafil in primary pulmonary hypertension: a randomized, placebo-controlled, double-blind, crossover study." J Am Coll Cardiol **43**(7): 1149-1153.

Sato, K., M. Oka, et al. (1995). "Effects of separate and combined ETA and ETB blockade on ET-1-induced constriction in perfused rat lungs." Am J Physiol **269**(5 Pt 1): L668-672.

Sayed, D., C. Hong, et al. (2007). "MicroRNAs play an essential role in the development of cardiac hypertrophy." Circ Res **100**(3): 416-424.

Schanen, B. C. and X. Li (2011). "Transcriptional regulation of mammalian miRNA genes." Genomics **97**(1): 1-6.

Schermuly, R. T., K. P. Kreisselmeier, et al. (2004). "Chronic sildenafil treatment inhibits monocrotaline-induced pulmonary hypertension in rats." Am J Respir Crit Care Med **169**(1): 39-45.

Scherr, M., L. Venturini, et al. (2007). "Lentivirus-mediated antagomir expression for specific inhibition of miRNA function." Nucleic Acids Res **35**(22): e149.

Schmitter, D., J. Filkowski, et al. (2006). "Effects of Dicer and Argonaute down-regulation on mRNA levels in human HEK293 cells." Nucleic Acids Res **34**(17): 4801-4815.

Schwarz, D. S., G. Hutvagner, et al. (2003). "Asymmetry in the assembly of the RNAi enzyme complex." Cell **115**(2): 199-208.

Seggerson, K., L. Tang, et al. (2002). "Two genetic circuits repress the Caenorhabditis elegans heterochronic gene lin-28 after translation initiation." Dev Biol **243**(2): 215-225.

Selbach, M., B. Schwanhäusser, et al. (2008). "Widespread changes in protein synthesis induced by microRNAs." Nature **455**(7209): 58-63.

Selcuklu, S. D., M. T. Donoghue, et al. (2009). "miR-21 as a key regulator of oncogenic processes." Biochem Soc Trans **37**(Pt 4): 918-925.

Sheth, U. and R. Parker (2003). "Decapping and decay of messenger RNA occur in cytoplasmic processing bodies." Science **300**(5620): 805-808.

Shi, Y. and J. Massague (2003). "Mechanisms of TGF-beta signaling from cell membrane to the nucleus." Cell **113**(6): 685-700.

Shichiri, M., H. Kato, et al. (1997). "Endothelin-1 as an autocrine/paracrine apoptosis survival factor for endothelial cells." Hypertension **30**(5): 1198-1203.

Shirotani, M., Y. Yui, et al. (1991). "U-61,431F, a stable prostacyclin analogue, inhibits the proliferation of bovine vascular smooth muscle cells with little antiproliferative effect on endothelial cells." Prostaglandins **41**(2): 97-110.

Simonneau, G., R. J. Barst, et al. (2002). "Continuous subcutaneous infusion of treprostinil, a prostacyclin analogue, in patients with pulmonary arterial hypertension: a double-blind, randomized, placebo-controlled trial." Am J Respir Crit Care Med **165**(6): 800-804.

Simonneau, G., N. Galie, et al. (2004). "Clinical classification of pulmonary hypertension." J Am Coll Cardiol **43**(12 Suppl S): 5S-12S.

Simonneau, G., I. M. Robbins, et al. (2009). "Updated clinical classification of pulmonary hypertension." J Am Coll Cardiol **54**(1 Suppl): S43-54.

Siomi, M. C., K. Sato, et al. (2011). "PIWI-interacting small RNAs: the vanguard of genome defence." Nat Rev Mol Cell Biol **12**(4): 246-258.

Sitbon, O., M. Humbert, et al. (1998). "Inhaled nitric oxide as a screening agent for safely identifying responders to oral calcium-channel blockers in primary pulmonary hypertension." Eur Respir J **12**(2): 265-270.

Sitbon, O., M. Humbert, et al. (2005). "Long-term response to calcium channel blockers in idiopathic pulmonary arterial hypertension." Circulation **111**(23): 3105-3111.

Small, E. M. and E. N. Olson (2011). "Pervasive roles of microRNAs in cardiovascular biology." Nature **469**(7330): 336-342.

Smith, C. M. and J. A. Steitz (1997). "Sno storm in the nucleolus: new roles for myriad small RNPs." Cell **89**(5): 669-672.

Sobolewski, A., K. B. Jourdan, et al. (2004). "Mechanism of cicaprost-induced desensitization in rat pulmonary artery smooth muscle cells involves a PKA-mediated inhibition of adenylyl cyclase." Am J Physiol Lung Cell Mol Physiol **287**(2): L352-359.

Sobue, K., K. Hayashi, et al. (1999). "Expressional regulation of smooth muscle cell-specific genes in association with phenotypic modulation." Mol Cell Biochem **190**(1-2): 105-118.

Soll, D. and U. L. RajBhandary (2006). "The genetic code - thawing the 'frozen accident'." J Biosci **31**(4): 459-463.

Song, J. J., J. Liu, et al. (2003). "The crystal structure of the Argonaute2 PAZ domain reveals an RNA binding motif in RNAi effector complexes." Nat Struct Biol **10**(12): 1026-1032.

Stenmark, K. R., K. A. Fagan, et al. (2006). "Hypoxia-induced pulmonary vascular remodeling: cellular and molecular mechanisms." Circ Res **99**(7): 675-691.

Stenmark, K. R., B. Meyrick, et al. (2009). "Animal models of pulmonary arterial hypertension: the hope for etiological discovery and pharmacological cure." AJP: Lung Cellular and Molecular Physiology **297**(6): L1013-L1032.

Sun, X. H., N. G. Copeland, et al. (1991). "Id proteins Id1 and Id2 selectively inhibit DNA binding by one class of helix-loop-helix proteins." Mol Cell Biol **11**(11): 5603-5611.

Suzuki, Y., K. Montagne, et al. (2008). "BMPs promote proliferation and migration of endothelial cells via stimulation of VEGF-A/VEGFR2 and angiopoietin-1/Tie2 signalling." J Biochem **143**(2): 199-206.

Sztrymf, B., F. Coulet, et al. (2008). "Clinical outcomes of pulmonary arterial hypertension in carriers of BMPR2 mutation." Am J Respir Crit Care Med **177**(12): 1377-1383.

Taft, R. J., M. Pheasant, et al. (2007). "The relationship between non-protein-coding DNA and eukaryotic complexity." Bioessays **29**(3): 288-299.

Tam, O. H., A. A. Aravin, et al. (2008). "Pseudogene-derived small interfering RNAs regulate gene expression in mouse oocytes." Nature **453**(7194): 534-538.

Tanaka, M., K. Oikawa, et al. (2009). "Down-regulation of miR-92 in human plasma is a novel marker for acute leukemia patients." PLoS One **4**(5): e5532.

Tantini, B., A. Manes, et al. (2005). "Antiproliferative effect of sildenafil on human pulmonary artery smooth muscle cells." Basic Res Cardiol **100**(2): 131-138.

Taraseviciene-Stewart, L., Y. Kasahara, et al. (2001). "Inhibition of the VEGF receptor 2 combined with chronic hypoxia causes cell death-dependent pulmonary endothelial cell proliferation and severe pulmonary hypertension." FASEB J **15**(2): 427-438.

Teichert-Kuliszewska, K., M. J. Kutryk, et al. (2006). "Bone morphogenetic protein receptor-2 signaling promotes pulmonary arterial endothelial cell survival: implications for loss-of-function mutations in the pathogenesis of pulmonary hypertension." Circ Res **98**(2): 209-217.

Teixeira, D., U. Sheth, et al. (2005). "Processing bodies require RNA for assembly and contain nontranslating mRNAs." RNA **11**(4): 371-382.

ten Dijke, P., O. Korchynskyi, et al. (2003). "Controlling cell fate by bone morphogenetic protein receptors." Mol Cell Endocrinol **211**(1-2): 105-113.

Thenappan, T., S. J. Shah, et al. (2007). "A USA-based registry for pulmonary arterial hypertension: 1982-2006." Eur Respir J **30**(6): 1103-1110.

Thomas, M., C. Docx, et al. (2009). "Activin-Like Kinase 5 (ALK5) Mediates Abnormal Proliferation of Vascular Smooth Muscle Cells from Patients with Familial Pulmonary Arterial Hypertension and Is Involved in the Progression of Experimental Pulmonary Arterial Hypertension Induced by Monocrotaline." The American Journal of Pathology **174**(2): 380-389.

Thomson, J. R., R. D. Machado, et al. (2000). "Sporadic primary pulmonary hypertension is associated with germline mutations of the gene encoding BMPR-II, a receptor member of the TGF-beta family." J Med Genet **37**(10): 741-745.

Thum, T., C. Gross, et al. (2008). "MicroRNA-21 contributes to myocardial disease by stimulating MAP kinase signalling in fibroblasts." Nature **456**(7224): 980-984.

Tijsterman, M. and R. H. Plasterk (2004). "Dicers at RISC; the mechanism of RNAi." Cell **117**(1): 1-3.

Tokumaru, S., M. Suzuki, et al. (2008). "let-7 regulates Dicer expression and constitutes a negative feedback loop." Carcinogenesis **29**(11): 2073-2077.

Topkara, V. K. and D. L. Mann (2011). "Role of microRNAs in cardiac remodeling and heart failure." Cardiovasc Drugs Ther **25**(2): 171-182.

Tsubouchi, Y., H. Sano, et al. (2000). "Inhibition of human lung cancer cell growth by the peroxisome proliferator-activated receptor-gamma agonists through induction of apoptosis." Biochem Biophys Res Commun **270**(2): 400-405.

Tsunetsugu-Yokota, Y. and T. Yamamoto (2010). "Mammalian MicroRNAs: Post-Transcriptional Gene Regulation in RNA Virus Infection and Therapeutic Applications." Front Microbiol **1**: 108.

Tuder, R. M., S. H. Abman, et al. (2009). "Development and pathology of pulmonary hypertension." J Am Coll Cardiol **54**(1 Suppl): S3-9.

Tuder, R. M., C. D. Cool, et al. (1999). "Prostacyclin synthase expression is decreased in lungs from patients with severe pulmonary hypertension." Am J Respir Crit Care Med **159**(6): 1925-1932.

Tuder, R. M., B. Groves, et al. (1994). "Exuberant endothelial cell growth and elements of inflammation are present in plexiform lesions of pulmonary hypertension." Am J Pathol **144**(2): 275-285.

Urbich, C., A. Kuehbacher, et al. (2008). "Role of microRNAs in vascular diseases, inflammation, and angiogenesis." Cardiovasc Res **79**(4): 581-588.

Valadi, H., K. Ekstrom, et al. (2007). "Exosome-mediated transfer of mRNAs and microRNAs is a novel mechanism of genetic exchange between cells." Nat Cell Biol **9**(6): 654-659.

Valdimarsdottir, G., M. J. Goumans, et al. (2002). "Stimulation of Id1 expression by bone morphogenetic protein is sufficient and necessary for bone morphogenetic protein-induced activation of endothelial cells." Circulation **106**(17): 2263-2270.

Valencia-Sanchez, M. A., J. Liu, et al. (2006). "Control of translation and mRNA degradation by miRNAs and siRNAs." Genes Dev **20**(5): 515-524.

van Almen, G. C., W. Verhesen, et al. (2011). "MicroRNA-18 and microRNA-19 regulate CTGF and TSP-1 expression in age-related heart failure." Aging Cell.

van der Krol, A. R., L. A. Mur, et al. (1990). "Flavonoid genes in petunia: addition of a limited number of gene copies may lead to a suppression of gene expression." Plant Cell **2**(4): 291-299.

van Niel, G., I. Porto-Carreiro, et al. (2006). "Exosomes: a common pathway for a specialized function." J Biochem **140**(1): 13-21.

van Rooij, E., L. B. Sutherland, et al. (2006). "A signature pattern of stress-responsive microRNAs that can evoke cardiac hypertrophy and heart failure." Proc Natl Acad Sci U S A **103**(48): 18255-18260.

van Rooij, E., L. B. Sutherland, et al. (2007). "Control of stress-dependent cardiac growth and gene expression by a microRNA." Science **316**(5824): 575-579.

van Rooij, E., L. B. Sutherland, et al. (2008). "Dysregulation of microRNAs after myocardial infarction reveals a role of miR-29 in cardiac fibrosis." Proc Natl Acad Sci U S A **105**(35): 13027-13032.

Varol, N., E. Konac, et al. (2010). "The realm of microRNAs in cancers." Molecular Biology Reports **38**(2): 1079-1089.

Verdel, A., S. Jia, et al. (2004). "RNAi-mediated targeting of heterochromatin by the RITS complex." Science **303**(5658): 672-676.

Voelkel, N. F. and C. Cool (2004). "Pathology of pulmonary hypertension." Cardiol Clin **22**(3): 343-351, v.

Voelkel, N. F. and R. M. Tuder (1995). "Cellular and molecular mechanisms in the pathogenesis of severe pulmonary hypertension." Eur Respir J **8**(12): 2129-2138.

Voelkel, N. F. and R. M. Tuder (2000). "Hypoxia-induced pulmonary vascular remodeling: a model for what human disease?" J Clin Invest **106**(6): 733-738.

Voinnet, O. (2009). "Origin, biogenesis, and activity of plant microRNAs." Cell **136**(4): 669-687.

Volinia, S., G. A. Calin, et al. (2006). "A microRNA expression signature of human solid tumors defines cancer gene targets." Proc Natl Acad Sci U S A **103**(7): 2257-2261.

Volpe, T., V. Schramke, et al. (2003). "RNA interference is required for normal centromere function in fission yeast." Chromosome Res **11**(2): 137-146.

Wang, J., J. Chen, et al. (2009). "MicroRNAs in plasma of pancreatic ductal adenocarcinoma patients as novel blood-based biomarkers of disease." Cancer Prev Res (Phila) **2**(9): 807-813.

Wang, X., X. Xu, et al. (2011). "Dynamic mechanisms for pre-miRNA binding and export by Exportin-5." RNA **17**(8): 1511-1528.

Wang, Y., G. Sheng, et al. (2008). "Structure of the guide-strand-containing argonaute silencing complex." Nature **456**(7219): 209-213.

Wang, Y., T. Weng, et al. (2007). "Identification of rat lung-specific microRNAs by micoRNA microarray: valuable discoveries for the facilitation of lung research." BMC Genomics **8**: 29.

Watanabe, H., A. Fujiyama, et al. (2004). "DNA sequence and comparative analysis of chimpanzee chromosome 22." Nature **429**(6990): 382-388.

Watanabe, T., Y. Totoki, et al. (2008). "Endogenous siRNAs from naturally formed dsRNAs regulate transcripts in mouse oocytes." Nature **453**(7194): 539-543.

Waypa, G. B. and P. T. Schumacker (2005). "Hypoxic pulmonary vasoconstriction: redox events in oxygen sensing." J Appl Physiol **98**(1): 404-414.

Welsh, D. J., M. Harnett, et al. (2004). "Proliferation and signaling in fibroblasts: role of 5-hydroxytryptamine2A receptor and transporter." Am J Respir Crit Care Med **170**(3): 252-259.

West, J., J. Harral, et al. (2008). "Mice expressing BMPR2R899X transgene in smooth muscle develop pulmonary vascular lesions." Am J Physiol Lung Cell Mol Physiol **295**(5): L744-755.

Wharton, J., J. W. Strange, et al. (2005). "Antiproliferative effects of phosphodiesterase type 5 inhibition in human pulmonary artery cells." Am J Respir Crit Care Med **172**(1): 105-113.

White, K., Y. Dempsie, et al. (2011). "The serotonin transporter, gender, and 17beta oestradiol in the development of pulmonary arterial hypertension." Cardiovasc Res **90**(2): 373-382.

White, K., L. Loughlin, et al. (2011). "Serotonin transporter, sex, and hypoxia: microarray analysis in the pulmonary arteries of mice identifies genes with relevance to human PAH." Physiol Genomics **43**(8): 417-437.

Wightman, B., I. Ha, et al. (1993). "Posttranscriptional regulation of the heterochronic gene lin-14 by lin-4 mediates temporal pattern formation in C. elegans." Cell **75**(5): 855-862.

Wilkins, M. R., G. A. Paul, et al. (2005). "Sildenafil versus Endothelin Receptor Antagonist for Pulmonary Hypertension (SERAPH) study." Am J Respir Crit Care Med **171**(11): 1292-1297.

Willers, E. D., J. H. Newman, et al. (2006). "Serotonin transporter polymorphisms in familial and idiopathic pulmonary arterial hypertension." Am J Respir Crit Care Med **173**(7): 798-802.

Wilson, D. W., H. J. Segall, et al. (1989). "Progressive inflammatory and structural changes in the pulmonary vasculature of monocrotaline-treated rats." Microvasc Res **38**(1): 57-80.

Wilson, D. W., H. J. Segall, et al. (1992). "Mechanisms and pathology of monocrotaline pulmonary toxicity." Crit Rev Toxicol **22**(5-6): 307-325.

Winge, I., J. A. McKinney, et al. (2008). "Activation and stabilization of human tryptophan hydroxylase 2 by phosphorylation and 14-3-3 binding." Biochem J **410**(1): 195-204.

Wu, E., C. Thivierge, et al. (2010). "Pervasive and cooperative deadenylation of 3'UTRs by embryonic microRNA families." Mol Cell **40**(4): 558-570.

Wu, H., H. Xu, et al. (2000). "Human RNase III is a 160-kDa protein involved in preribosomal RNA processing." J Biol Chem **275**(47): 36957-36965.

Wu, L., J. Fan, et al. (2006). "MicroRNAs direct rapid deadenylation of mRNA." Proc Natl Acad Sci U S A **103**(11): 4034-4039.

Xie, Z. and X. Qi (2008). "Diverse small RNA-directed silencing pathways in plants." Biochim Biophys Acta **1779**(11): 720-724.

Xin, M., E. M. Small, et al. (2009). "MicroRNAs miR-143 and miR-145 modulate cytoskeletal dynamics and responsiveness of smooth muscle cells to injury." Genes Dev **23**(18): 2166-2178.

Xiong, J., Q. Du, et al. (2010). "Tumor-suppressive microRNA-22 inhibits the transcription of E-box-containing c-Myc target genes by silencing c-Myc binding protein." Oncogene **29**(35): 4980-4988.

Xu, X. D., X. W. Song, et al. (2011). "Attenuation of microRNA-22 derepressed PTEN to effectively protect rat cardiomyocytes from hypertrophy." J Cell Physiol.

Yan, L. X., X. F. Huang, et al. (2008). "MicroRNA miR-21 overexpression in human breast cancer is associated with advanced clinical stage, lymph node metastasis and patient poor prognosis." RNA **14**(11): 2348-2360.

Yanaihara, N., N. Caplen, et al. (2006). "Unique microRNA molecular profiles in lung cancer diagnosis and prognosis." Cancer Cell **9**(3): 189-198.

Yang, H., W. Kong, et al. (2008). "MicroRNA expression profiling in human ovarian cancer: miR-214 induces cell survival and cisplatin resistance by targeting PTEN." Cancer Res **68**(2): 425-433.

Yang, J.-S. and E. C. Lai (2010). "Dicer-independent, Ago2-mediated microRNA biogenesis in vertebrates." Cell Cycle **9**(22): 4455-4460.

Yang, J. S., T. Maurin, et al. (2010). "Conserved vertebrate mir-451 provides a platform for Dicer-independent, Ago2-mediated microRNA biogenesis." Proceedings of the National Academy of Sciences **107**(34): 15163-15168.

Yang, J. S., M. D. Phillips, et al. (2011). "Widespread regulatory activity of vertebrate microRNA* species." RNA **17**(2): 312-326.

Yang, S., S. Banerjee, et al. (2012). "miR-21 regulates chronic hypoxia induced pulmonary vascular remodeling." Am J Physiol Lung Cell Mol Physiol.

Yang, X., L. Long, et al. (2005). "Dysfunctional Smad signaling contributes to abnormal smooth muscle cell proliferation in familial pulmonary arterial hypertension." Circ Res **96**(10): 1053-1063.

Yi, R., Y. Qin, et al. (2003). "Exportin-5 mediates the nuclear export of pre-microRNAs and short hairpin RNAs." Genes Dev **17**(24): 3011-3016.

Yuan, J. X., A. M. Aldinger, et al. (1998). "Dysfunctional voltage-gated K+ channels in pulmonary artery smooth muscle cells of patients with primary pulmonary hypertension." Circulation **98**(14): 1400-1406.

Zaiman, A. L., M. Podowski, et al. (2008). "Role of the TGF- /Alk5 Signaling Pathway in Monocrotaline-induced Pulmonary Hypertension." American Journal of Respiratory and Critical Care Medicine **177**(8): 896-905.

Zeng, Y. and B. R. Cullen (2004). "Structural requirements for pre-microRNA binding and nuclear export by Exportin 5." Nucleic Acids Res **32**(16): 4776-4785.

Zhang, C. (2008). "MicroRNAs: role in cardiovascular biology and disease." Clin Sci (Lond) **114**(12): 699-706.

Zhang, C. (2009). "MicroRNA-145 in vascular smooth muscle cell biology: a new therapeutic target for vascular disease." Cell Cycle **8**(21): 3469-3473.

Zhang, L., S. Volinia, et al. (2008). "Genomic and epigenetic alterations deregulate microRNA expression in human epithelial ovarian cancer." Proc Natl Acad Sci U S A **105**(19): 7004-7009.

Zhang, S., I. Fantozzi, et al. (2003). "Bone morphogenetic proteins induce apoptosis in human pulmonary vascular smooth muscle cells." Am J Physiol Lung Cell Mol Physiol **285**(3): L740-754.

Zhao, Y., E. Samal, et al. (2005). "Serum response factor regulates a muscle-specific microRNA that targets Hand2 during cardiogenesis." Nature **436**(7048): 214-220.

Zhong, H. and J. W. Simons (1999). "Direct comparison of GAPDH, beta-actin, cyclophilin, and 28S rRNA as internal standards for quantifying RNA levels under hypoxia." Biochem Biophys Res Commun **259**(3): 523-526.